U.S. DEPARTMENT OF COMMERCE
National Technical Information Service

PB-281 582

Development of a Mathematical Basis for Relating Sludge Properties to FGD-Scrubber Operating Variables

Radian Corp, Austin, Tex

Prepared for

Industrial Environmental Research Lab, Research Triangle Park, N C

Apr 78

PB 281 582

EPA
U.S. Environmental Protection Agency
Office of Research and Development
Industrial Environmental Research
Laboratory
Research Triangle Park, North Carolina 27711

EPA-600/7-78-072
April 1978

DEVELOPMENT OF A MATHEMATICAL BASIS FOR RELATING SLUDGE PROPERTIES TO FGD-SCRUBBER OPERATING VARIABLES

Interagency
Energy-Environment
Research and Development
Program Report

REPRODUCED BY
NATIONAL TECHNICAL
INFORMATION SERVICE
U. S. DEPARTMENT OF COMMERCE
SPRINGFIELD, VA. 22161

RESEARCH REPORTING SERIES

Research reports of the Office of Research and Development, U.S. Environmental Protection Agency, have been grouped into nine series. These nine broad categories were established to facilitate further development and application of environmental technology. Elimination of traditional grouping was consciously planned to foster technology transfer and a maximum interface in related fields. The nine series are:

1. Environmental Health Effects Research
2. Environmental Protection Technology
3. Ecological Research
4. Environmental Monitoring
5. Socioeconomic Environmental Studies
6. Scientific and Technical Assessment Reports (STAR)
7. Interagency Energy-Environment Research and Development
8. "Special" Reports
9. Miscellaneous Reports

This report has been assigned to the INTERAGENCY ENERGY-ENVIRONMENT RESEARCH AND DEVELOPMENT series. Reports in this series result from the effort funded under the 17-agency Federal Energy/Environment Research and Development Program. These studies relate to EPA's mission to protect the public health and welfare from adverse effects of pollutants associated with energy systems. The goal of the Program is to assure the rapid development of domestic energy supplies in an environmentally-compatible manner by providing the necessary environmental data and control technology. Investigations include analyses of the transport of energy-related pollutants and their health and ecological effects; assessments of, and development of, control technologies for energy systems; and integrated assessments of a wide range of energy-related environmental issues.

REVIEW NOTICE

This report has been reviewed by the participating Federal Agencies, and approved for publication. Approval does not signify that the contents necessarily reflect the views and policies of the Government, nor does mention of trade names or commercial products constitute endorsement or recommendation for use.

This document is available to the public through the National Technical Information Service, Springfield, Virginia 22161.

TECHNICAL REPORT DATA

(Please read Instructions on the reverse before completing)

1. REPORT NO. EPA-600/7-78-072	2.	3. RECIPIENT'S ACCESSION NO. PB281582
4. TITLE AND SUBTITLE Development of a Mathematical Basis for Relating Sludge Properties to FGD-Scrubber Operating Variables		5. REPORT DATE April 1978 6. PERFORMING ORGANIZATION CODE
7. AUTHOR(S) J. L. Phillips, J. C. Terry, K. A. Wilde, G. P. Behrens, P. S. Lowell, J. L. Skloss, and K. W. Luke		8. PERFORMING ORGANIZATION REPORT NO.
9. PERFORMING ORGANIZATION NAME AND ADDRESS Radian Corporation 8500 Shoal Creek Boulevard Austin, Texas 78766		10. PROGRAM ELEMENT NO. EHE624 11. CONTRACT/GRANT NO. 68-02-2608, Task 11
12. SPONSORING AGENCY NAME AND ADDRESS EPA, Office of Research and Development Industrial Environmental Research Laboratory Research Triangle Park, NC 27711		13. TYPE OF REPORT AND PERIOD COVERED Task Final; Through 1/78 14. SPONSORING AGENCY CODE EPA/600/13

15. SUPPLEMENTARY NOTES IERL-RTP project officer is Robert H. Borgwardt, Mail Drop 65, 919/541-2234.

16. ABSTRACT The report gives results of research to investigate prospects for increasing the size of calcium sulfite sludge particles in flue gas desulfurization systems. The approach included four work packages: a literature survey and development of a mathematical basis for predicting calcium sulfite sludge distribution; a computer solution of the size distribution model to determine parameter sensitivity; a literature survey and screening of analytical methods for measuring settling rate, settled density, and particle size distribution; and planning a test program to investigate parameters not available from previous work to verify the size distribution model. The crystal population balance concept was introduced into the mathematical basis for predicting particle size distribution of calcium sulfite sludge. Relationships were derived that required nucleation and crystal growth rate expressions which must be obtained from experimental data. Available pilot and full-scale scrubber data were used to increase the usefulness of the theoretical model. The relationship derived was solved for a specific process configuration. An approximate solution was obtained assuming that crystal size distribution does not change in the scrubber. A computer routine was written to permit convenient parameter sensitivity studies using the size distribution model.

17. KEY WORDS AND DOCUMENT ANALYSIS

a. DESCRIPTORS		b. IDENTIFIERS/OPEN ENDED TERMS	c. COSATI Field/Group	
Air Pollution	Properties	Air Pollution Control	13B	14B
Flue Gases	Mathematical Models	Stationary Sources	21B	
Desulfurization		Particulate	07A, 07D	12A
Gas Scrubbing	Measurement		13H	
Calcium Sulfites	Crystal Growth		07B	20B
Sludge	Density			
Settling	Nucleation			

18. DISTRIBUTION STATEMENT Unlimited	19. SECURITY CLASS *(This Report)* Unclassified	21. NO. OF PAGES 372
	20. SECURITY CLASS *(This page)* Unclassified	22. PRICE PCA16/MFA01

A Form 2220-1 (9-73)

i

EPA-600/7-78-072
April 1978

DEVELOPMENT OF A MATHEMATICAL BASIS FOR RELATING SLUDGE PROPERTIES TO FGD-SCRUBBER OPERATING VARIABLES

by

J.L. Phillips, J.C. Terry, K.C. Wilde,
G.P. Behrens, P.S. Lowell, J.L. Skloss, and K.W. Luke

Radian Corporation
8500 Shoal Creek Boulevard
Austin, Texas 78766

Contract No. 68-02-2608
Task 11
Program Element No. EHE624

EPA Project Officer: Robert H. Borgwardt

Industrial Environmental Research Laboratory
Office of Energy, Minerals, and Industry
Research Triangle Park, N.C. 27711

Prepared for

U.S. ENVIRONMENTAL PROTECTION AGENCY
Office of Research and Development
Washington, D.C. 20460

CONTENTS

Section		Page
1	Introduction and Summary	1
2	Conclusions	3
3	Recommendations	4
4	Continuous Crystallization Theory	6
Mathematical Basis	6
Nucleation Rate	7
Growth Rate	9
Material Balances	9
5	Modeling the Calcium Sulfite Crystal Size Distribution (CSD)	11
The "Typical" Process Arrangement	11
The Scrubber/Hold Tank Equations	11
The Hold Tank/Clarifier Model	14
Parameter Sensitivity Study	16
6	Analytical Methods for Sludge Quality	22
Settling Rate and Settled Density	22
Crystal Size Distribution	26
7	Test Plan	30
Objectives	30
Test Sequence and Operating Conditions	31
Analytical Requirements	34
NOMENCLATURE	37
REFERENCES	39
APPENDIX A - AN APPROACH TO PREDICTING CALCIUM SULFITE CRYSTAL SIZE DISTRIBUTION IN LIME/LIMESTONE WET SCRUBBING SYSTEMS (Technical Note #200-187-11-1)	A-i
APPENDIX B - AN ANALYSIS OF CRYSTALLIZATION DYNAMICS AND PARAMETER SENSITIVITY IN LIME/LIMESTONE WET SCRUBBING SYSTEMS (Technical Note #200-187-11-3)	B-i
APPENDIX C - STANDARD METHODS DEVELOPMENT FOR THE DETERMINATION OF SLUDGE QUALITY (Technical Note #200-187-11-2)	C-i

CONTENTS (continued)

Section Page

APPENDIX D - COMPARISON OF METHODS FOR MEASURING THE PARTICLE SIZE DISTRIBUTION OF SMALL PARTICLES (Technical Note #200-187-11-5).............................. D-i

APPENDIX E - TEST PLAN DOCUMENT (Technical Note #200-187-11-4)... E-i

FIGURES

Figure		Page
5-1	Process Flow Sheet for a Lime or Limestone Scrubbing System	12
5-2	Simplified Crystallization Model	15
5-3	Mass Average Crystal Size and Relative Saturation Versus Solids Residence Time (Hold Tank Volume) at Constant SO_2 Removal, 10 Weight Percent Solids	19
5-4	Mass Average Crystal Size and Calcium Sulfite Relative Saturation Weight Percent Versus Solids in Clarifier Feed W_{CF} at Constant SO_2 Removal and Hold Tank Volume	20
6-1	Photomicrograph of Sludge Platelets Taken from Limestone Scrubber, 200X	23
6-2	Photomicrograph of Sludge Granules Taken from Lime Scrubber, 200X	24
6-3	Settling Rates of Sludges Versus Weight % Solids at 25°C and 50°C	25
6-4	Sludge Granules from Lime Scrubber: Cumulative Percent of Particles Versus Diameter	27
6-5	Sludge Platelets from Limestone Scrubber: Cumulative Percent of Particles Versus Width	28
7-1	Size Distribution Data for Limestone Scrubber Slurry. (Coulter Counter) n(L) versus L	35

TABLES

Table		Page
5-1	Sample Print Out for Simplified Hold Tank/Clarifier Model	18
7-1	Phase I - Test Schedule	32
7-2	Phase II - Test Schedule	33

SECTION 1

INTRODUCTION AND SUMMARY

Sludge disposal represents a significant operating cost in most applications of lime/limestone or dual alkali scrubbing processes. In systems where calcium sulfite is the major product, the waste sludge generally settles slowly and has a low settled density. The objectives of this work are to examine prospects for increasing the average particle size of calcium sulfite produced in these SO_2 removal systems in order to improve settling rate and settled density and ultimately to be able to correlate sludge quality with design and operating conditions.

The approach taken to meet this objective includes four work packages:

- literature survey and development of a mathematical basis for predicting the sulfite size distribution,
- computer solution of the size distribution model to determine parameter sensitivity,
- literature survey and screening of analytical methods for measuring settling rate, settled density, and particle size distribution, and
- planning a test program to investigate parameters expected to improve settling rate and settled density by increasing the average particle size.

Section 3 of this report describes a mathematical basis for predicting the size distribution of calcium sulfite crystals produced in lime/limestone scrubbing systems. The crystal population balance concept is introduced and size distribution relationships are derived. This approach requires nucleation and crystal growth rate expressions. These must be obtained from experimental data. Expected forms for these rate expressions were selected from the literature. Experimental data from pilot and full-scale scrubbers were used where applicable to increase the usefulness of the theoretical development.

The relationships derived in Section 3 are solved for a specific process configuration in Section 4. An approximate solution to the problem was obtained by assuming that the crystal size distribution does not change in the scrubber. This assumption is expected to be realistic for supersaturated scrubber operation. It may not apply to operations where scrubber alkalinity is buffered by dissolution of calcium sulfite. A computer routine was written to permit convenient parameter sensitivity studies using the size distribution model. Size distributions were predicted that were in order of magnitude agreement with experimental measurements.

Verification of the crystal size distribution model requires further experimental data. Analytical methods are discussed in Section 5. Potential methods for measuring calcium sulfite size distribution, settling rate, and settled density were selected based on a literature survey. Reproducible settling rate and settling density methods are described. Four size distribution techniques were compared. Manual counting by optical microscope was in good agreement with micromesh sieve data. Two instrumental techniques, the Coulter Counter and Micromeritics Sedigraph, showed much smaller size distributions than the microscope or sieves. Further work will be necessary to select the best method.

A pilot-scale test program is described in Section 6 of this report. The approach and objectives are based on the literature survey and size distribution model. Major emphasis is placed on identifying calcium sulfite nucleation sources in an operating pilot unit. Tests are described which will aid in quantifying rate parameters used in the crystal size distribution model.

SECTION 2

CONCLUSIONS

A model has been developed to predict the crystal size distribution of calcium sulfite produced in limestone wet scrubbing systems. The model computes size distributions comparable to those observed in operating scrubber systems. The present model may not apply as well to lime systems, but the approach used here can be adapted as necessary data are obtained.

The model has been used to examine the sensitivity of the product crystal size distribution to changes in process variables. Prospects for improving the size distribution depend on further investigation of nucleation kinetics in the system. Changes in hold tank size or slurry solids content may lead to an increase or decrease in crystal size, depending on the specific form of the nucleation and growth rate expressions. The present growth rate expression is based on a fair amount of experimental data for limestone systems. No definite correlations relating nucleation phenomena to design and operating conditions were found in the present data, however.

Several methods for measuring the size distribution of scrubber sludge were compared. Two instrumental methods indicated much finer size distributions than the optical microscope or micromesh sieves. Additional work needs to be done to resolve observed differences in results for the crystal size distribution measurement.

Since the behavior of the crystal size distribution depends on the nucleation rate expressions, the test program developed in this work needs to be pursued at the RTP laboratory pilot unit. The proposed tests are intended to provide more information about sources and rates of nucleation in the system. The model developed here can be used both to interpret experimental results and to predict favorable operating conditions for other process configurations.

SECTION 3

RECOMMENDATIONS

The CSD data suggests two mechanisms for particle generation in FGD scrubber systems. The optical microscope and micromesh sieve CSD curves on a number basis suggest that particle breakage or attrition is the major or at least a significant mechanism for new particle generation. The Coulter Counter and Micromeritics Sedigraph CSD curves are consistent with particle generation by nucleation. The Coulter Counter and Micromeritics Sedigraph methods also indicate much finer crystal size distributions than the optical microscope and micromesh sieves. Additional work is recommended to resolve these observed differences. Areas which should be investigated are effects of sample preparation, background noise in the instrumental methods, use of scanning electron micrographs, and multiple magnification overlap techniques with the optical microscope.

More bench and pilot scale work is needed to define both nucleation and growth rate parameters. We recommend that the test plan document produced during this program be pursued at the RTP laboratory pilot unit. Crystal size distributions must be measured to have useful data. The bench and pilot unit data should be correlated with the model. The computer program should be used as a subroutine of widely available nonlinear curve-fitting programs. Then rate parameters can be deduced from crystal size distributions and total solids concentration.

The model should be extended to include growth rate-size relations intermediate between constant and linear in particle size. Incorporation of the model into complete SO_2 scrubbing system simulations should be explored.

Scrubber dissolution of fines could be examined as a possibility of increased sludge particle size. Further definition of this aspect will require considerably more work, both experimental and modeling. Since dissolution is much faster than precipitation, its study on a pilot scale may not be feasible. The best approach may be bench scale dissolution rate studies to provide data for resolution of the present model's problems with the dissolution case.

The basis of hold tank sizing should be reexamined. The present model provides a better basis for system design than conventional methods. Although rate parameters in the model are not yet known, a better use of available information should be possible.

SECTION 4

CONTINUOUS CRYSTALLIZATION THEORY

The objective of this program is ultimately to be able to correlate waste sludge quality of lime/limestone scrubbing processes with design and operating conditions. It is assumed that the size distribution of calcium sulfite crystals can be adequately used to predict sludge quality for most systems. While settling rates and settled density are also of interest in equipment design, the crystal size distribution is more easily related to process conditions. In this discussion, the term "calcium sulfite" also includes any coprecipitated sulfate.

MATHEMATICAL BASIS

The size distribution of crystals leaving a scrubbing system is determined by the relative rates of nucleation and growth sustained in the process vessels and by the residence time characteristics of these vessels. Prediction of the crystal size distribution requires:

- a nucleation (crystal birth-death) rate expression,
- a growth rate expression,
- a description of the environment in the process vessels, and
- a description of the process streams.

A simultaneous solution of the crystal population balance and process material balances is required for a complete description of the process.

The mathematical approach used in this work to describe calcium sulfite crystallization is based primarily on the particle balance concepts of Randolph and Larson (1). The first step is to define a crystal size distribution function, n(L) (meter^{-4}), such that $n(L)\Delta L$ is equal to the number of crystals in the size range L to $L + \Delta L$ per unit volume of slurry. It is assumed that a single characteristic dimension, L, can be used to describe a crystal. The crystal population balance states that:

> Rate of accumulation of crystals of size L per unit volume of slurry is equal to the net input of crystals of size L via convection plus the net input via growth plus the net generation of crystals of size L via other mechanism (e.g., breakage).

Application of this principle to a well-mixed process vessel leads to a mathematical statement of the problem:

$$\frac{d(Rn)}{dL} - n\Sigma\frac{1}{T_j} + D(L) = \sum\frac{n_i}{T_i} + B(L) \qquad (4\text{-}1)$$

where the T's are time constants equal to the vessel volume divided by inlet (i's) and outlet (j's) stream flow rates, R(L) is the crystal growth rate, D(L) and B(L) are crystal death and birth functions other than nucleation and n(L) is the size distribution defined above. The nucleation rate, B_o ($\text{meter}^{-3}\text{sec}^{-1}$) is equal to the limit of the product nR as L approaches zero,

$$B_o = \lim_{L \to 0} n(L)R(L) \qquad (4\text{-}2)$$

Tne nucleation rate, B_o, enters the solution of Equation (4-1) as a boundary condition. The terms B(L) an D(L) will be assumed to be negligible for the time being. Details of the derivation of Equation (4-1) are given in Appendix A.

Solution of Equation (4-1) requires a description of B_o and R(L) for all conditions in the process volume V. This information is normally contained in nucleation and growth rate correlations based on experimental data. A detailed literature survey was conducted to determine the most appropriate form for these correlations.

NUCLEATION RATE

Recent literature pertaining to nucleation in continuous crystallization processes has focused on the mechanism and kinetics of "secondary" nucleation. This is defined as the formation of new crystals of negligible size in the presence of a suspension of existing seed crystals of the same solute. Secondary nucleation is generally thought to be the most important source of new crystals in processes where a substantial slurry density is maintained. Secondary nucleation is also known to occur at much lower supersaturations than those necessary to produce new crystals from a clear solution.

There is some disagreement among investigators as to the exact mechanisms of secondary nucleation. Some feel that "micro-attrition" or physical removal of microscopic particles occurs while others hypothesize that nuclei merely form from the solution near or at the surface of seed crystals. Judging from reported experimental results, the following variables are most important in fixing the secondary nucleation rate for a given crystallizer situation:

- temperature,
- supersaturation,
- slurry solids content, and
- factors affecting the energy of collisions or liquid shear at the crystal surface in the system (e.g., impeller speed and material, crystal size).

More detailed discussion of variable effects on secondary nucleation is presented in Appendix A.

Based on this literature survey, the following is proposed as a nucleation rate expression for use in the mathematical model:

$$B_o \ (\text{meter}^{-3}\ \text{sec}^{-1}) = (nR)_{L \to o} = k_{SN}(r-1)^{i_{SN}} M_T^{j_{SN}} \qquad (4\text{-}3)$$

Here, M_T (moles/liter) is the slurry solids content and r is the relative saturation. In this simplified expression, the temperature and collision energy and crystal size effects are implicit in the rate constant k_{SN}.

Use of Equation (4-3) to describe calcium sulfite nucleation in lime/limestone scrubbing systems requires values for the exponents i_{SN} and j_{SN}, and the nucleation rate constant k_{SN}. The nucleation rate may be estimated from the crystal size distribution in an operating system, but no consistent complete data relating product size distribution to process operating conditions were available in the literature. This is primarily due to the difficulty of the size distribution measurements (see Section 5 of this report). Crystal size distribution measurements performed during the present contract show that "typical" scrubber sludge contains on the order of 10^{10} crystals per gram of calcium sulfite. This information can be used to fix an "average" nucleation rate for purposes of modeling, but examination of the individual rate parameters used in Equation (4-3) must await further experimental data.

GROWTH RATE

Several crystal growth rate correlations have been described in the literature. Furthermore, some data correlating calcium sulfite growth rates with process conditions in actual lime and limestone scrubbing systems are available. The literature referred to in Appendix A was reviewed to select the most useful correlation form for the calcium sulfite growth rate.

The growth rate R (meter/sec) appearing in the crystal population balance (Equation 4-1) is the rate of change of the characteristic dimension L. It may also be a function of crystal size. Crystals are assumed to maintain the same shape as they grow. Some data were obtained in this study and in previous related work that suggest an increasing linear growth rate with crystal size for calcium sulfite. Most available experimental data, however, are in the form of an average molar growth rate for crystals of all sizes. An "average" linear growth rate can be calculated from existing experimental data by assuming all of the crystals ultimately have the same size and shape.

For limestone systems calcium sulfite growth rate data from three widely different pilot units (TCA, marble bed, and spray tower) were in close agreement considering that no direct comparison of the size distributions in these studies was available. The data are represented by a linear growth rate expression that is a function of crystal size and relative saturation:

$$R = 3\text{x}10^{-12}(1 + 5\text{x}10^{5}L)\ (r-1)^{i_{GR}}\ \text{meter/sec} \qquad (4\text{-}4)$$

The exponent i_{GR} is expected to be one for normal operating levels of relative saturation.

For lime systems, no definite relationship between calcium sulfite growth rate and process conditions was obtained. Pilot plant and full scale data showed growth rates varying by a factor of ten at similar levels of relative saturation. This behavior may be a result of locally high supersaturations existing near dissolving lime particles.

MATERIAL BALANCES

The nucleation and growth rate expressions discussed above both include calcium sulfite relative saturation as a variable. Relative saturation is in turn a function of the liquid phase concentrations of the precipitating calcium and sulfite. As a result, the crystal population balance and the solid-liquid mass balances for a crystallizer must be solved simultaneously.

An equation relating the molar crystallization rate per volume of slurry to the linear growth rate and crystal size distribution may be written:

$$\text{Crystallization Rate (mole/meter}^3\text{ sec)} = k_v' \int_0^\infty nL^2 R\,dL \qquad (4\text{-}5)$$

Here, k_v' (mole/meter^3) is a shape factor relating the number of moles in a crystal to its characteristic length L. This relationship can be used in material balance calculations for a given process volume:

$$\Sigma Q_{in} C_{in} - \Sigma Q_{out} C_{out} = \text{Crystallization Rate} \qquad (4\text{-}6)$$

where C_{in} and C_{out} are the liquid phase concentrations of calcium or sulfite entering and leaving the volume of interest and Q_{in} and Q_{out} are the volumetric flow rates (ℓ/sec).

Equations (4-1) through (4-6) are the basis for calculating a calcium sulfite size distribution for a given set of conditions. Solution of the equations for a particular equipment configuration and various process operating conditions is addressed in Section 5 of this report.

A better physical understanding of the crystal population balance may be gained by looking at the overall steady-state balances for a system. The mass balance requires that the system SO_2 removal rate be proportional to the product of $\dot{N}(\ell^{-1}\text{sec}^{-1})$, the rate at which crystals leave the system, and $(\bar{L}_m)^3$, the mass mean crystal size to the third power:

$$\Delta SO_2 \ \frac{\text{mole}}{\text{sec}} = k_v' \dot{N} (\bar{L}_m)^3 \qquad (4\text{-}7)$$

The population balance requires that the rate of removal of crystals from the process be equal to the rate of generation (the nucleation rate) of crystals within the process:

$$\dot{N} = B_o \qquad (4\text{-}8)$$

Thus, the mass mean size of crystals leaving the system is completely dependent on the nucleation rate. Correlation of nucleation rates with process conditions will be an important aspect of the proposed test program (see Section 7).

SECTION 5

MODELING THE CALCIUM SULFITE CRYSTAL SIZE DISTRIBUTION

In the previous section, the theoretical approach and existing experimental basis for predicting calcium sulfite crystal size distribution (CSD) were examined. The particle balance Equation (3-1) and nucleation and growth rate correlations (3-2, 3-4) are the core of the resulting model. The nucleation and growth rates are coupled to the process liquor composition through their dependence on the relative saturation r. Application of these equations to lime/limestone scrubbing systems is described below. Quantitative solutions to the size distribution problem are discussed for a simplified process scheme.

THE "TYPICAL" PROCESS ARRANGEMENT

Figure 5-1 represents a typical process flowsheet for a lime or limestone scrubbing system. Flue gas (FG) enters the scrubber and is contacted with liquor (SF) recirculated from the hold tank. Spent scrubbing liquor (SB) enters the hold tank and is combined with the lime or limestone additive (LA). A slurry stream (CF) is fed from the hold tank to the clarifier. Some or all of the solids are removed from this stream and discarded with the clarifier underflow (CU) stream. The remaining liquor and some solids are returned to the hold tank with the clarifier overflow (CO) stream. Four different size distributions may be present in the system. These are indicated as n_{SB}, n_{CF}, n_{CO}, and n_{CU} on the flowsheet. Nucleation may occur in both scrubber and hold tank. Sulfite must precipitate in the hold tank but may dissolve in the scrubber.

For modeling purposes, all calcium sulfite crystals are assumed to originate through nucleation at zero size. This is equivalent to letting B(L) and D(L) be zero in the particle balance Equation (4-1). The clarifier is modeled as a solids separation unit with no significant chemical reaction.

THE SCRUBBER/HOLD TANK EQUATIONS

The essential behavior of the scrubber/hold tank loop may be examined most easily by assuming for the time being that $n_{CO} = 0$. That is, there are

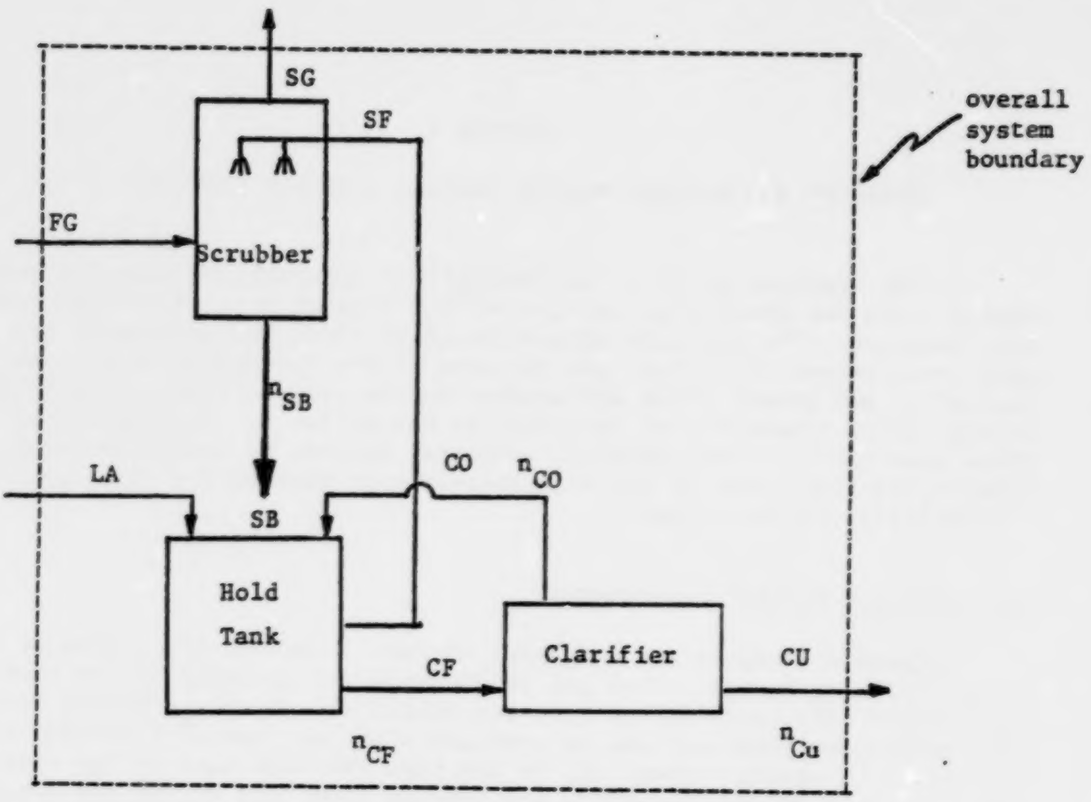
SG
SF
overall system boundary
FG
Scrubber
n_{SB}
LA
SB
CO
n_{CO}
Hold Tank
Clarifier
CF
CU
n_{CF}
n_{Cu}

Figure 5-1 . Process Flow Sheet for a Lime or Limestone Scrubbing System.

no solids in the clarifier overflow. This is a good approximation in many operating units.

A set of simultaneous particle balance equations may be written for the scrubber and hold tank:

$$V_S \frac{d(R_S n_S)}{dL} + Q_{SB} n_S = Q_{SF} n_t \tag{5-1}$$

$$V_t \frac{d(R_t n_t)}{dL} + Q_t n_t = Q_{SB} n_S \tag{5-2}$$

The boundary conditions for the size distribution equations are obtained from the nucleation rate and growth rate expressions:

$$n_s(o) = (B_o/R_o)_{\text{scrubber}} \tag{5-3}$$

$$n_t(o) = (B_o/R_o)_{\text{hold tank}} \tag{5-4}$$

B_o and R_o are evaluated at conditions in the scrubber or hold tank as indicated.

Equations (5-1) through (5-4) represent the crystal population balance for the scrubber/hold tank loop. The process material balances and chemical equilibria in the system also enter into the solution through their effects on the relative saturation, r. This quantity appears in both the nucleation and growth rate correlations (Equations 4-3 and 4-4).

An unsuccessful attempt was made to solve the entire set of population balance, material balance, and chemical equilibrium equations with a standard numerical technique. Because of the apparent complexity of the overall simulation, it was decided to solve the crystal population balance in terms of the relative saturation, r. The usefulness of the model is not seriously jeopardized since relative saturation may be measured or calculated independently for a system using an available chemical equilibrium computer routine (2).

An analytical solution to the scrubber/hold tank population balance is discussed in Appendix B. Examination of the roots of the characteristic equations shows that for the case of precipitation in both the scrubber and hold tank, the scrubber contribution is negligible. This appears to be the source of problems encountered in the numerical solution of the complete equation set. For the case of constant dissolution rate ($R < o$) in the scrubber, the integral of the resulting crystal size distribution does not converge for large values of crystal size L. More information about the dissolution rate as a function of size would be required to solve this case.

THE HOLD TANK/CLARIFIER MODEL

For cases where significant sulfite dissolution does not occur in the scrubber, the effect of the scrubber on the sulfite size distribution was found to be small. Thus, the size distribution in the system may be estimated using a simplified hold tank/clarifier model. This is shown in Figure 5-2.

Crystallization of calcium sulfite occurs in the hold tank when SO_2 from the scrubber and calcium from the additive are combined. The slurry stream leaving the hold tank has a size distribution n_t and a flow rate Q_{CF}. The clarifier splits the Q_{CF} stream into a nearly clear overflow stream, Q_{CO}, and a thickened underflow stream, Q_{CU}. The overflow has a size distribution n_{CO} and the underflow n_{CU}. Since we have assumed that the scrubber does not change the size distribution, the scrubber loop does not appear in the model.

The clarifier size distributions may be expressed in terms of the hold tank size distribution by defining a cutoff size, L_c. Crystals larger than L_c all report to the underflow. Crystals smaller than L_c are divided between the two streams according to their relative clear liquor flow rates. The resulting size distributions are:

$$n_{CO} = (1-f_{CL}) \frac{Q_{CF}}{Q_{CO}} n_t, \quad L < L_c \qquad (5\text{-}5)$$

$$n_{CO} = 0 \qquad , \quad L > L_c$$

$$n_{CU} = f_{CL} \frac{Q_{CF}}{Q_{CU}} n_t \qquad , \quad L < L_c \qquad (5\text{-}6)$$

$$n_{CU} = \frac{Q_{CF}}{Q_{CU}} n_t \qquad , \quad L > L_c$$

The quantity f_{CL} is a function which depends on the crystal density and the stream flow rates (see Appendix B for derivation).

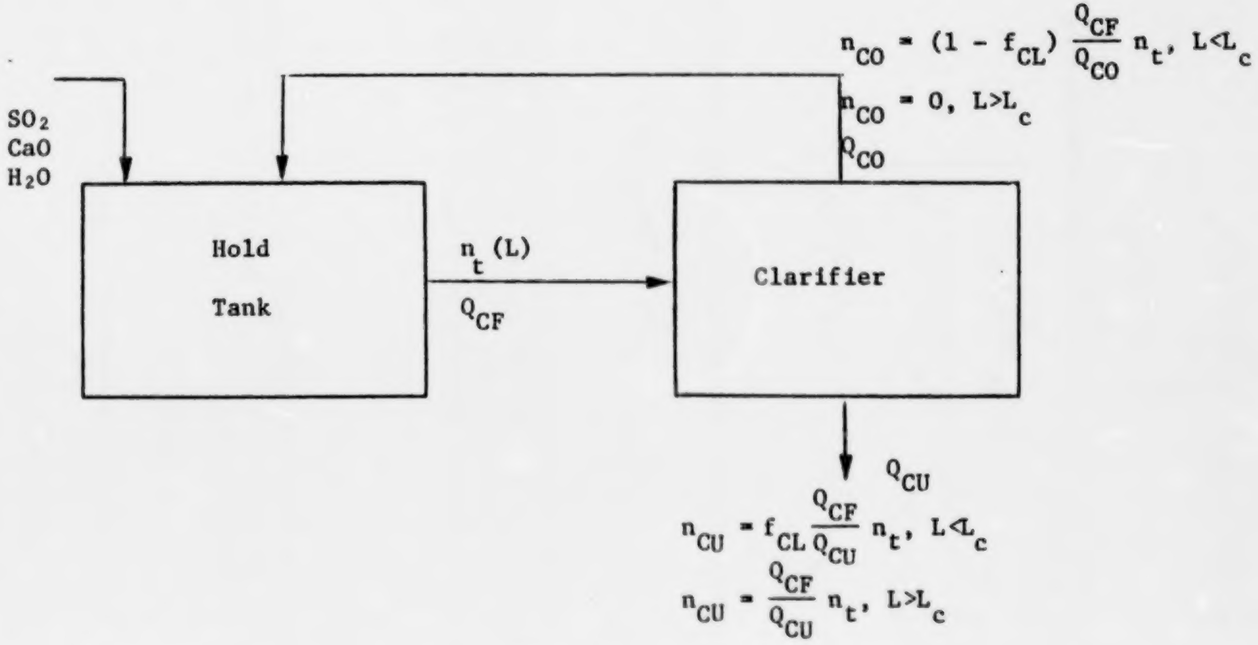

SO_2
CaO
H_2O
Hold Tank
$n_t(L)$
Q_{CF}
Clarifier
$n_{CO} = (1 - f_{CL}) \frac{Q_{CF}}{Q_{CO}} n_t, \ L<L_c$
$n_{CO} = 0, \ L>L_c$
Q_{CO}
Q_{CU}
$n_{CU} = f_{CL} \frac{Q_{CF}}{Q_{CU}} n_t, \ L<L_c$
$n_{CU} = \frac{Q_{CF}}{Q_{CU}} n_t, \ L>L_c$

Figure 5-2. Simplified Crystallization Model.

The population balance for the model shown in Figure 5-2 is:

$$\frac{d}{dL}(n_t R) + \frac{n_t}{T_{CF}} = \begin{cases} \frac{n_{CO}}{T_{CO}}, & L < L_c \\ 0, & L > L_c \end{cases} \qquad (5\text{-}7)$$

Equation (5-7) may be integrated using the growth rate expression, $R = k_{GR}(r-1)^{i_{GR}}(1+\gamma L)$. The solution is:

$$n_t = n_o \left[\frac{(1 + L_c)^{[1-f_{CL}]/\gamma R_o T_{CF}]}}{(1 + \gamma L)^{[1 + \gamma R_o T_{CF}]/\gamma R_o T_{CF}}} \right], \; L > L_c \qquad (5\text{-}8)$$

$$n_t = n_o(1 + \gamma L)^{-[f_{CL} + \gamma R_o T_{CF}]/\gamma R_o T_{CF}}, \; L < L_c$$

n_o, the zero size population density, is calculated using the nucleation and growth rate expressions:

$$n_o = \frac{B_o}{R_o} = \frac{k_{SN}}{k_{GR}} (r - 1)^{i_{SN} - i_{GR}} M_T^{j_{SN}} \qquad (5\text{-}9)$$

Given the hold tank population density quantified by Equations (5-8) and (5-9), other pertinent quantities may be calculated from the definition of the size distribution. These include the slurry solids content, M_t, (mole/liter) the total precipitation rate G (mole/liter-minute), and the mass average size, $\bar{L}_m$.

PARAMETER SENSITIVITY STUDY

A computer routine was written to implement the model described above and permit convenient parameter studies. Details of the program are given in Appendix B. The inputs to the program are:

INPUT

r = relative saturation with respect to $CaSO_3 \cdot \frac{1}{2}H_2O$

k_{GR}, i_{GR} = constants in the growth rate

k_{SN}, i_{SN}, j_{SN} = constants in the nucleation rate

γ = slope of growth rate/size function, $(\text{microns})^{-1}$

T_{CF} = V_t/Q_{CF}, minutes

T_{CU} = V_T/Q_{CU}, minutes

L_c = clarifier cut-off size, microns

The program calculates the following:

OUTPUT

n = population density, particles/ℓ/micron

$N_n, N_v(\Delta L)$ = number and volume of particles in a size range

G_{CF} = net precipitation rate, moles/ℓ/min

W_{CF}, W_{CU} = weight % solids, clarifier feed and underflow

W_{CO} = ppm solids in the clarifier overflow

$\bar{L}_{CF}$, $\bar{L}_{CU}$, $\bar{L}_{CO}$ = mass average particle sizes

B_O = nucleation rate, particles/ℓ/min

The program may be used without process material balances since the relative saturation is contained explicitly in the model. Iterative calculation may also be done to calculate the inputs for specified values of outputs.

A sample print out for the model is shown in Table 5-1. The inputs are listed first, then the various calculated quantities are printed along with the crystal size distribution. The case shown here is for operation at ten weight percent solids in the clarifier feed. The relative saturation was set at 4.0 and the solids residence time (V_{tank}/Q_{CF}) at one day (1440 minutes). For these conditions, using appropriate values for the nucleation and growth rate parameters, a size distribution is predicted which is in reasonable agreement with experimental data discussed in Section 6 of this report (see Figure 6-5).

Predicted changes in crystal size distribution with changes in process conditions are illustrated in Figures 5-3 and 5-4. The curves shown here were generated by solving the size distribution model for a range of input relative saturations and solids residence times (T_{CF} and T_{CU}). Cases having equal slurry solids content but different solids residence times were selected and plotted in Figure 5-4. The crystal size distribution is represented for convenience using the calculated mass average crystal size. Corresponding changes in relative saturation are also plotted in both figures.

Curve I in Figure 5-3 shows that the mean crystal size ($\bar{L}_{CU}$) increases with increasing solids residence time (T_{CF}) when the relative saturation exponent in the growth expression is less than that in the nucleation expression (i_{GR} = 1.0, i_{SN} = 2.0). Increasing the solids residence time increases the total crystal inventory and thus decreases the required

TABLE 5-1. SAMPLE PRINT OUT FOR SIMPLIFIED HOLD TANK/CLARIFIER MODEL

```
CRYSTALLIZATION RATES      SIMPLIFIED HOLD TANK/CLARIFIER MODEL

RELATIVE SATURATION                            4.000        GROWTH RATE CONSTANT,MICRONS/MIN               6.000-05
HOLD TANK VOL/CLARIFIER FEED RATE,MIN          1440.        REL.SAT. EXPONENT,GROWTH RATE                      1.00
HOLD TANK VOL/CLARIFIER UNDERFLOW,MIN       1.500+04        NUCLEATION RATE CONSTANT                       2.400+08
CLARIFIER CUT-OFF SIZE,MICRONS                  1.00        REL.SAT. EXPONENT,NUCLEATION RATE                  1.00
SLOPE,GROWTH RATE/SIZE RELATION,micron-1         .50        CRYSTAL CONC. EXP.,NUCLEATION RATE                  .50

                         NUCLEATION RATE,PART./L/MIN                            3.135+07
                         PPT. RATE, MOLES/L/MIN                                 1.152-06
                         WT PCT SOLIDS, CLARIFIER FEED                              .024
                                         UNDERFLOW                                  .223
                         PPM SOLIDS, OVERFLOW                                       33.8
                         MASS AVG. P. SIZE, MICRONS, CLARIFIER FEED                1.060
                                                         UNDERFLOW                 1.557
                                                          OVERFLOW                  .591


                                   CLARIFIER FEED PARTICLE SIZE DISTRIBUTION

SIZE,MICRONS        POP.DENSITY,PARTS/L/MICRON      CUMUL NO. PCT          CUMUL VOL PCT          DEL VOL PCT
     .00                    .174+12                      .00                    .00                    .00
     .10                    .162+12                    10.19                    .00                    .00
     .20                    .150+12                    19.66                    .02                    .02
     .30                    .140+12                    28.49                    .12                    .10
     .40                    .132+12                    36.75                    .37                    .25
     .50                    .124+12                    44.49                    .87                    .50
     .60                    .116+12                    51.77                   1.73                    .86
     .70                    .110+12                    58.64                   3.06                   1.33
     .80                    .104+12                    65.12                   5.00                   1.93
     .90                    .983+11                    71.26                   7.66                   2.67
    1.00                    .933+11                    77.07                  11.19                   3.53
    1.10                    .701+11                    82.04                  15.26                   4.06
    1.20                    .532+11                    85.78                  19.28                   4.03
    1.30                    .407+11                    88.63                  23.22                   3.94
    1.40                    .314+11                    90.82                  27.03                   3.81
    1.50                    .244+11                    92.51                  30.67                   3.65
    1.60                    .191+11                    93.83                  34.15                   3.47
    1.70                    .150+11                    94.86                  37.43                   3.29
    1.80                    .119+11                    95.68                  40.53                   3.10
    1.90                    .948+10                    96.32                  43.43                   2.91




    2.00                    .761+10                    96.84                  46.16                   2.72
    3.00                    .109+10                    99.48                  75.33                  29.17
    4.00                    .222+09                    99.88                  87.38                  12.06
    5.00                    .579+08                    99.96                  92.86                   5.48
    6.00                    .181+08                    99.99                  95.58                   2.72
    7.00                    .648+07                    99.99                  97.02                   1.45
    8.00                    .259+07                   100.00                  97.85                    .82
    9.00                    .113+07                   100.00                  98.34                    .49
   10.00                    .528+06                   100.00                  98.64                    .30
   15.00                    .254+05                   100.00                  99.80                   1.16
   20.00                    .268+04                   100.00                  99.96                    .16
   25.00                    .450+03                   100.00                 100.00                    .04
```

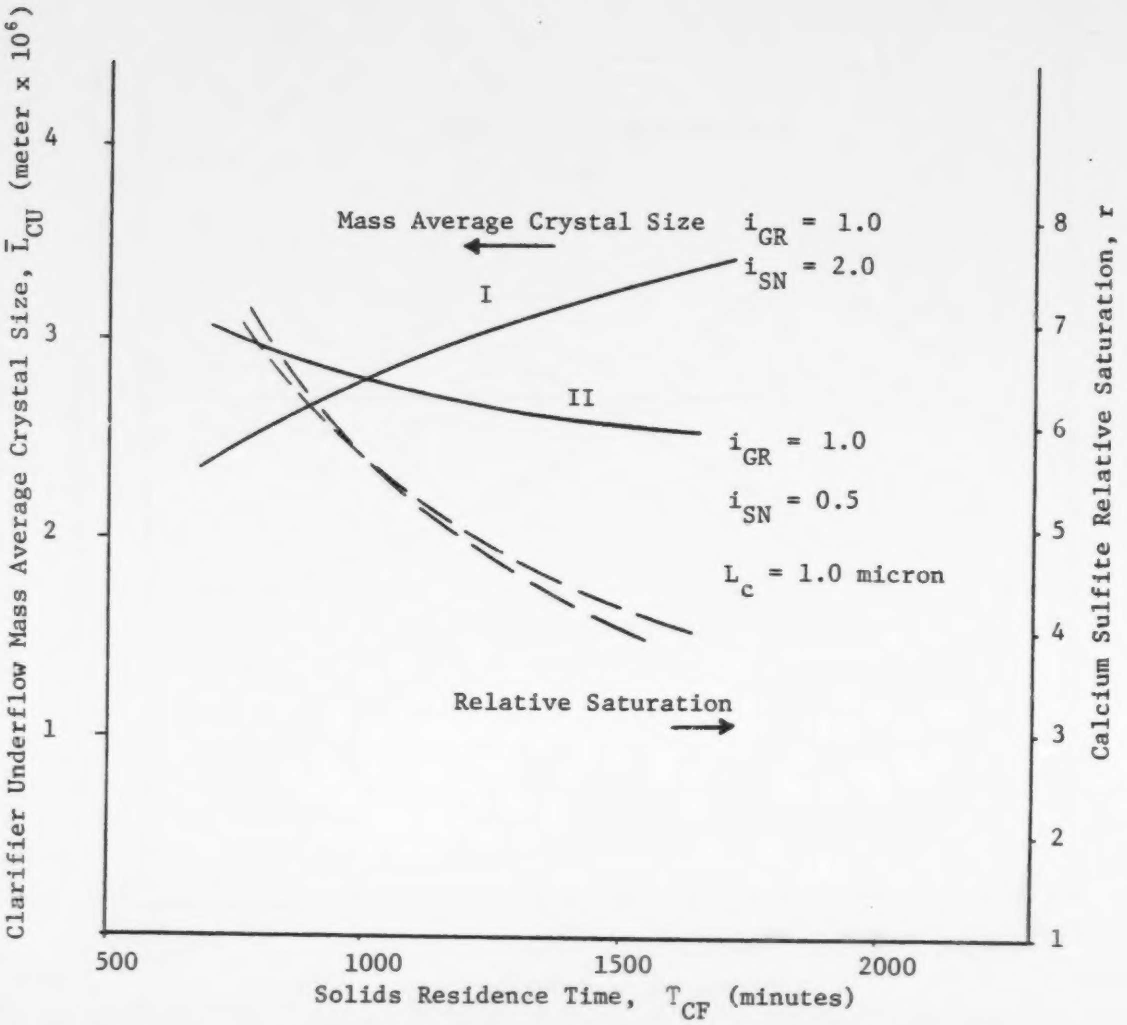

Figure 5-3. Mass Average Crystal Size and Relative Saturation Versus Solids Residence Time (Hold Tank Volume) at Constant SO_2 Removal, 10 Weight Percent Solids

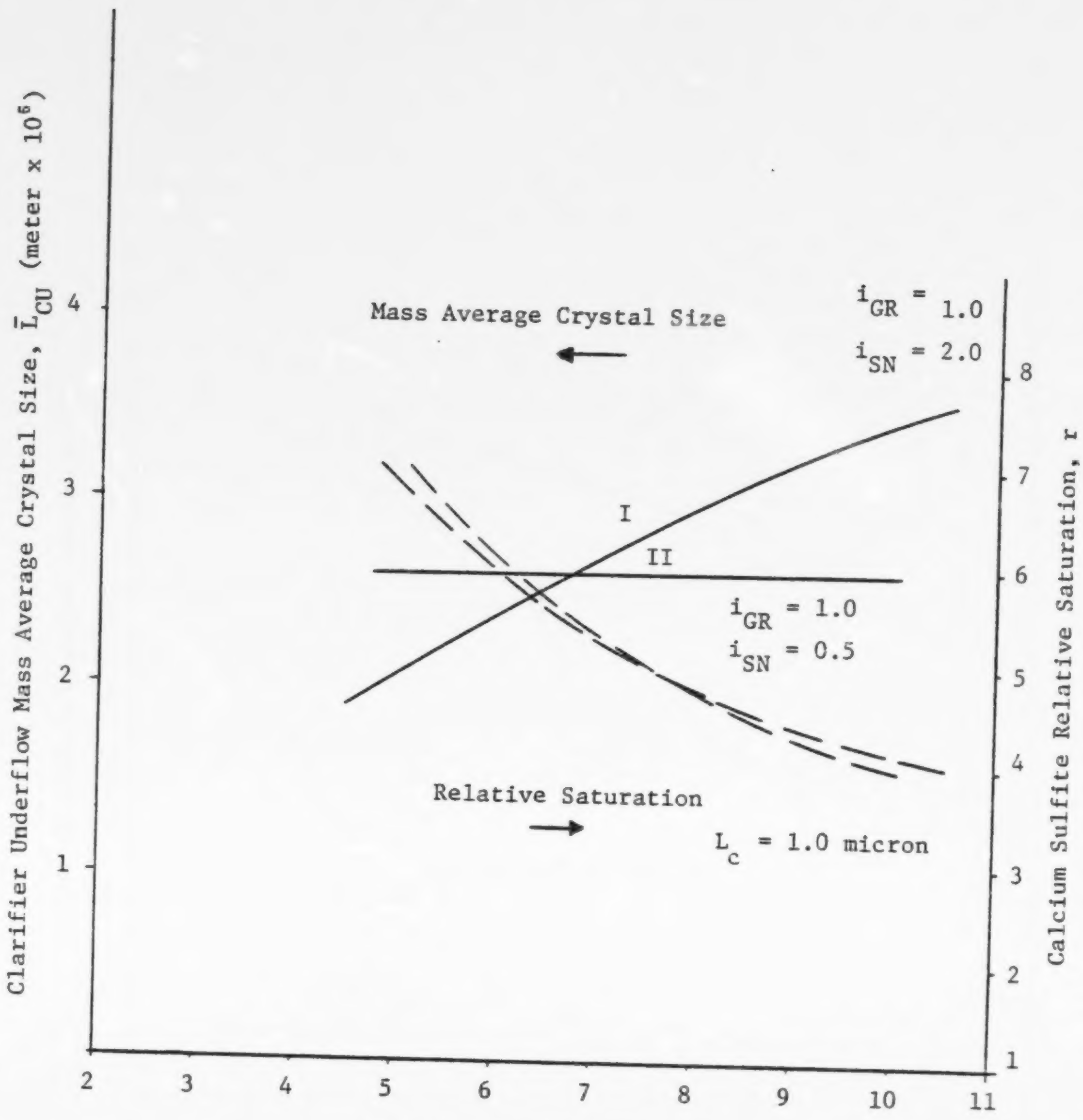

Figure 5-4. Mass Average Crystal Size and Calcium Sulfite Relative Saturation Weight Percent Versus Solids in Clarifier Feed W_{CF} at Constant SO_2 Removal and Hold Tank Volume

relative saturation at constant SO_2 removal. Since the nucleation rate decreases more sharply than the growth rate, the size distribution increases.

Curve II in Figure 5-3 shows that the size distribution decreases with increasing T_{CF} when $i_{GR} > i_{SN}$. Thus, the same process change may have the opposite effect on the crystal size distribution depending on the form of nucleation and growth rate expressions. Firm values for i_{GR} and i_{SN} will have to be obtained from a test plan such as that proposed in Section 7. If $i_{GR} = i_{SN}$, little change in the size distribution would be expected.

Curve I in Figure 5-4 shows an increase in average crystal size with increasing slurry solids content and constant hold tank size. This change is again attributed to the drop in relative saturation caused by increasing the total crystal inventory. Curve II represents an interesting case. The decrease in nucleation caused by lowering the supersaturation is counterbalanced by the increase due to increasing solids content. The net change in average particle size is negligible for this case.

The size distribution changes predicted above are related to changes in hold tank size or slurry solids content. Either of these changes amounts to a change in relative saturation at constant SO_2 removal. One can see from these figures that the size distribution may not change substantially even with large changes in operating conditions. For the cases where operation at low relative saturation is favorable (Type I behavior) limitations on tank size and slurry solids content will set a practical limit for the average crystal size. For Type II, cases where high relative saturation is favored, scaling limits will constrain the maximum attainable crystal size.

In Section 4, it was noted that the secondary nucleation rate is expected to be a function of the energy of crystal/crystal and crystal/impeller collisions in the system. These variables are not considered explicitly in the present model. From the overall material/population balances at constant SO_2 removal, we know that the mass mean particle size must be inversely proportional to the nucleation rate to the one third power:

$$\bar{L} \propto \left(\frac{1}{B_o}\right)^{1/3} \qquad (5\text{-}10)$$

Changes in the size distribution may thus be expected with changes in variables other than T_{CF} or W_{CF} if the net nucleation rate is changed. These effects can be included in the nucleation rate constant, k_{SN}, as information is developed during the test program.

SECTION 6

ANALYTICAL METHODS FOR SLUDGE QUALITY

Verification of the mathematical model requires experimental measurement of calcium sulfite size distribution. The settling rate and settled density of the sludge are also important mechanical design parameters. Potential analytical methods for particle size, settling rate, and settled density were selected for evaluation from those described in the literature. Settling rate and settled density measurements are straight forward. The particle sizing techniques agreed well for crystals larger than about 5 to 10 microns, but poor agreement was found in the submicron range. Results of the analytical methods evaluation are presented here. Details of the literature survey are included in Appendix C .

Two types of sludge were used in the evaluation; a limestone process sludge from a pilot unit operated at Pennsylvania Power and Light Company, and lime process sludge from the full-scale system at Louisville Gas and Electric. The limestone sludge contained sulfite crystals with the flat platelet habit. Calcium sulfite crystals in the lime system sludge appeared as spherical granules with a dendritic surface. Optical photomicrographs of the two sludge samples are shown in Figure 6-1 and 6-2.

SETTLING RATE AND SETTLED DENSITY

Settling tests were conducted in a series of glass graduated cylinders. The settling medium was water saturated with sludge and then filtered. Figure 6-3 shows calculated settling rate data for lime and limestone sludge at various levels of temperature and slurry solids content. Settling rate increases with temperature due to the decrease in viscosity. This is in accordance with Stokes' Law. Settling rate decreases with increasing solids content as expected for hindered settling. The effect of cylinder size (250 ml, 500 ml, 1000 ml) was not important.

Settled density for the lime sludge tests averaged 1.25 g/cm^3 (34% solids) and for the limestone sludge 1.39 g/cm^3 (48% solids). The fact that the granules settled more slowly than the platelets and attained a lower settled solids content may indicate that the effective density of the granules is less than that of the platelets. The dendritic habit of the "granules" may promote entrapment of process liquor.

FIGURE 6-1 PHOTOMICROGRAPH OF SLUDGE PLATELETS TAKEN FROM LIMESTONE SCRUBBER, 200 X

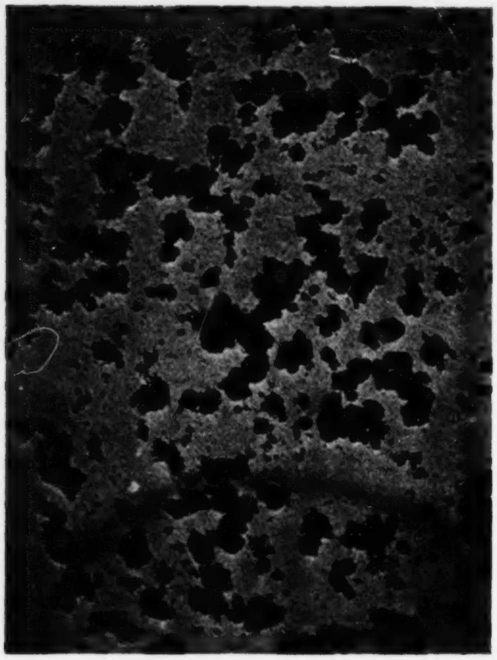

FIGURE 6-2 PHOTOMICROGRAPH OF SLUDGE GRANULES TAKEN FROM LIME SCRUBBER, 200 X

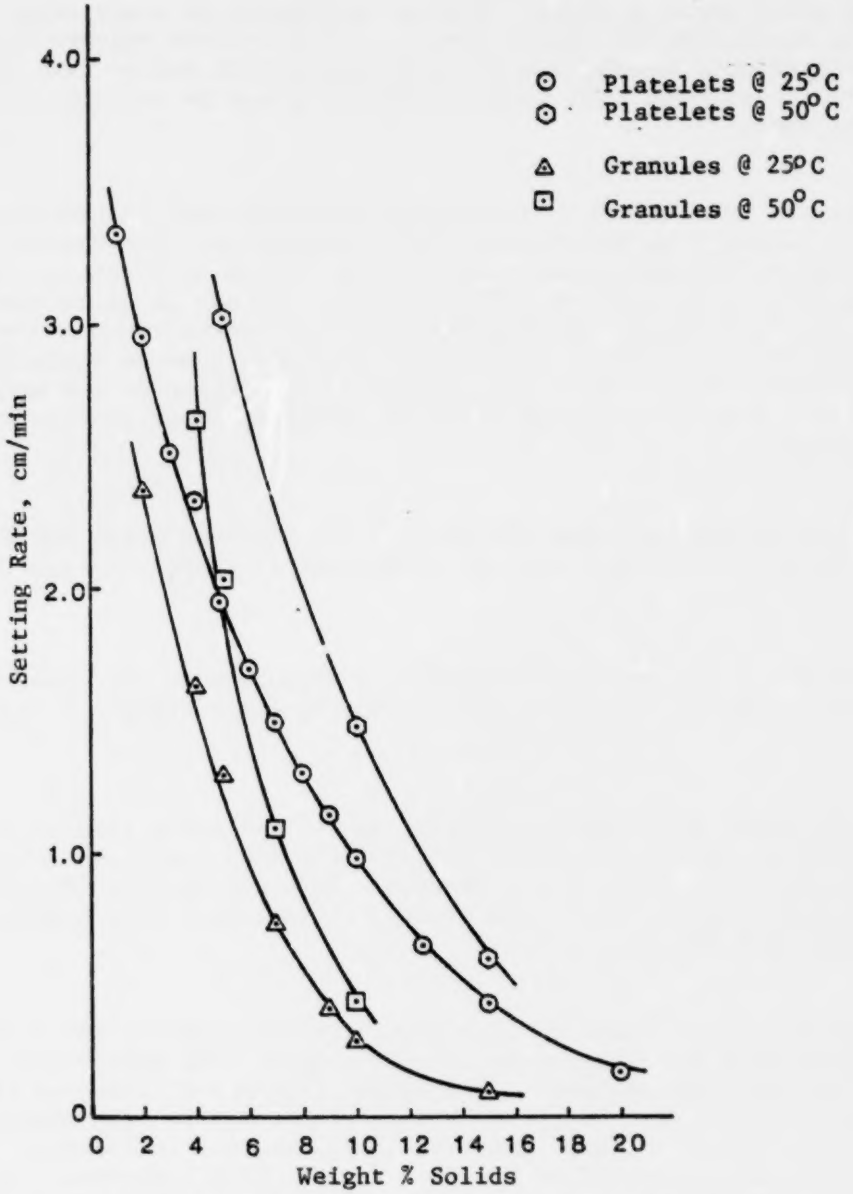

Figure 6-3. Settling Rates of Sludges Versus Weight % Solids at 25°C and 50°C

CRYSTAL SIZE DISTRIBUTION

Several methods were used to measure the size distribution of the granular (lime) and platelet (limestone) sludges. Optical microscopy is generally thought to be reliable and accurate. Microscopy also provides information about particle shape. Optical microscopy is practically limited to particles about five microns or larger. Other methods measure only a single characteristic length, but are potentially much faster than the tedious optical counting. The working size range may be extended down to about 0.3 microns.

The Coulter Counter and Micromeritics Sedigraph 5000 instrumental methods were compared to the optical size distribution. The Coulter instrument measures a signal proportional to the volume of a particle as it passes through a small aperture. The particle size may be calculated by assuming a particle shape. The Micromeritics instrument measures the settling rate of a suspension of particles and calculates an equivalent particle diameter using Stokes' Law. Since these methods do not measure particle shape, some care must be taken in comparing their results with the optical method.

Micromesh sieves were also evaluated. The smallest sieve had two micron openings. The sieve procedure was not significantly faster than the optical microscope.

Results of all of the size distribution measurements are compared for the granular sludge in Figure 6-4 and for the platelet sludge in Figure 6-5.

With the granular sludge the optical method and sieve results are in fair agreement. According to these methods, the mean particle size on a number basis is about seven to ten microns. Both the Coulter Counter and the Sedigraph data show a much smaller size distribution with a mean particle size less than one micron.

Even if the large number of fine particles indicated by the instrumental methods were not detected by the microscope, they should have posed no problem to the sieve analysis. The weight fraction of granules passing through the 5 micron sieve was less than 1% of the total. The Coulter Counter shows more than 27% of the mass was less than 5 microns in diameter. The Sedigraph indicates up to 70% of the mass is less than 5 microns. No firm explanation for this discrepancy was found. It is possible that the ultrasonic dispersion technique used in preparing samples for these instruments was sufficient to break up the spherical agglomerates present in the original sample.

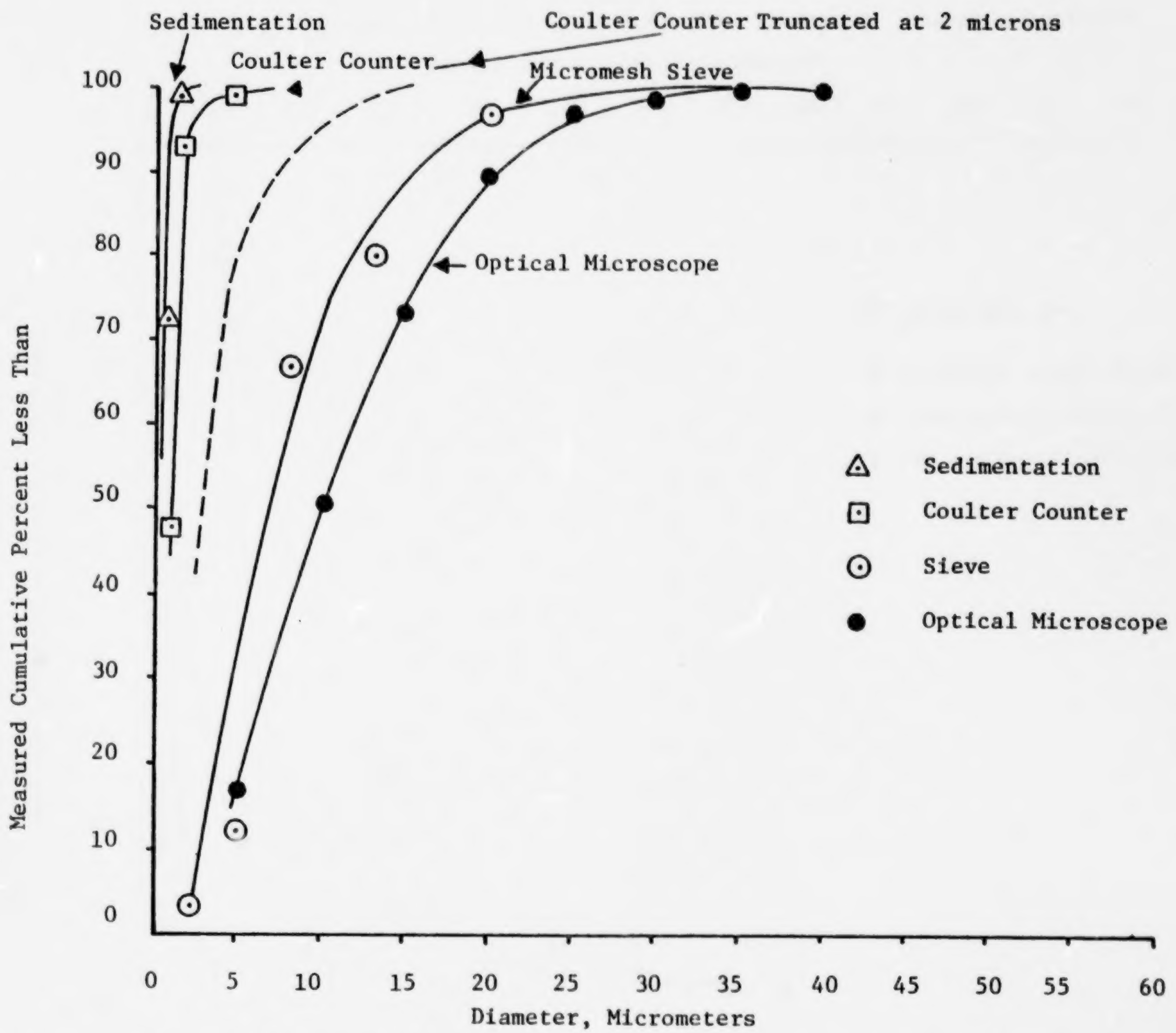

Figure 6-4. Sludge Granules from Lime Scrubber: Cumulative Percent of Particles Versus Diameter.

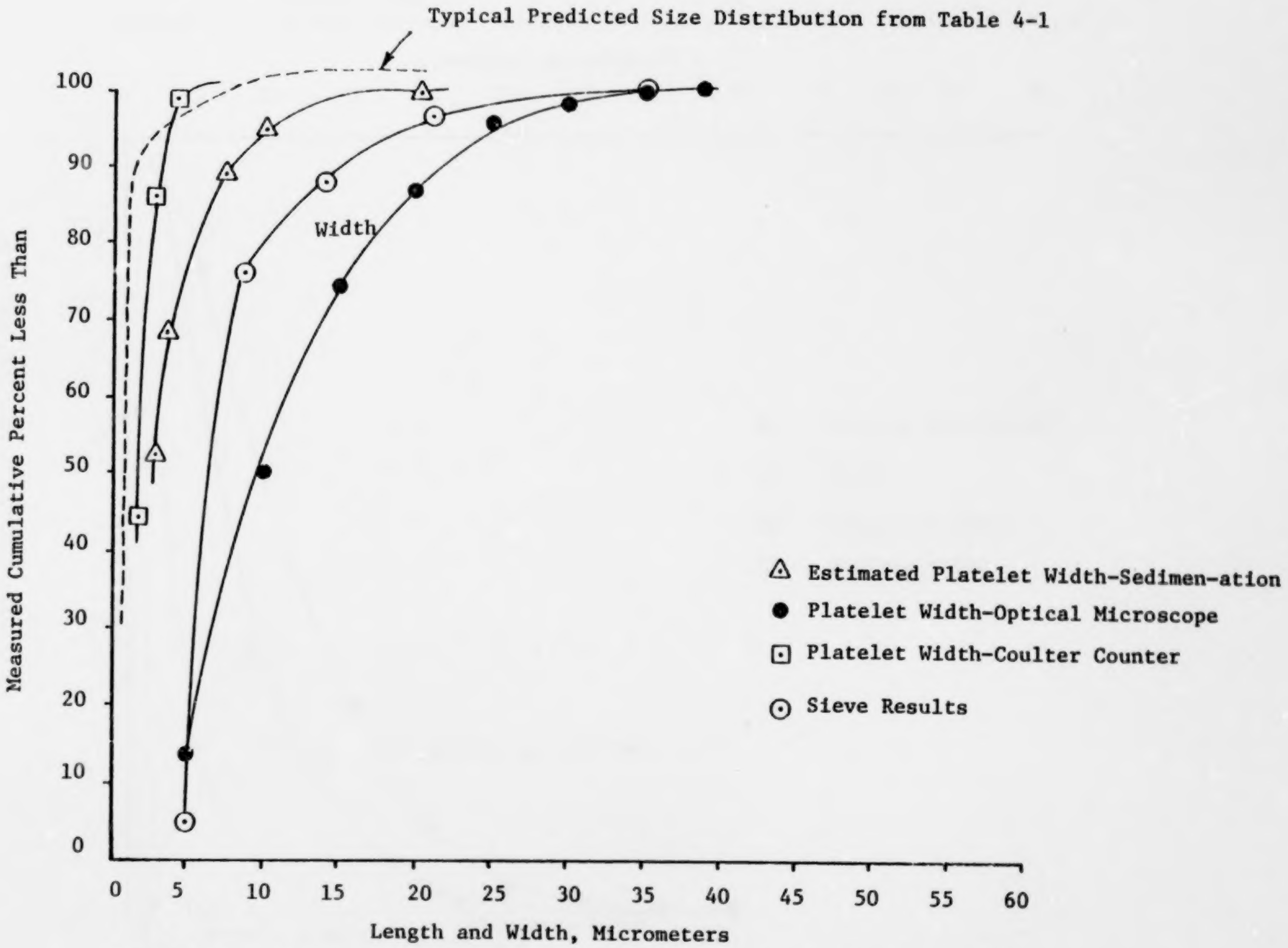

Figure 6-5. Sludge Platelets from Limestone Scrubber: Cumulative Percent of Particles Versus Width.

Figure 6-5 shows results for the platelet sludge. Since the Coulter Counter and Sedigraph both report equivalent spherical diameter, some adjustment of the raw data was required for comparison of the platelet size distributions. The Coulter Counter data were converted from equivalent spherical diameter based on a volume proportional signal to platelet width (W) by multiplying by 1.9. This is the ratio of width of a platelet with dimentions W x 1.5W x W/20 to the diameter of a sphere of equal volume.

The equivalent diameter reported by the Sedigraph is based on the terminal settling velocity of a sphere. To convert from equivalent spherical diameter to platelet width in this case, an expression for the velocity of a falling body may be used (3):

$$U_t = \sqrt{\frac{2gm_p(\rho_p - \rho_f)}{\rho_f \rho_p A_p C_d}} \text{ meter/sec} \qquad (6\text{-}1)$$

Here, U_t is the terminal velocity of a particle with mass m_p, density ρ_p, and projected area A_p, falling in a medium with density ρ_f under gravity g. C_d is a drag coefficient describing the fluid forces on the particle. Drag coefficients for a sphere and disc are nearly equal at the same Reynolds number for $N_{Re} < 0.3$ (3):

$$C_d = \frac{24}{N_{Re}} \qquad (6\text{-}2)$$

If we assume that a platelet will behave approximately the same as a disc, Equation (6-2) may be used with Equation (6-1) to estimate the size of platelet having the same settling velocity as a sphere of diameter D_s. The resulting conversion factor is:

$$D_{platelet} = 3.6\ D_{sphere} \qquad (6\text{-}3)$$

As shown in Figure (6-5), size distribution data for the platelet sludge are again strongly sensitive to the method used. The correction factors move the Coulter Counter data and Sedigraph data towards the distributions of the optical and sieve methods, but the overall agreement is still poor.

Additional work with the instrumental methods will be required to investigate the above discrepancy before selecting a method for use in the test plan. Different methods of sample preparation should be checked for their effect on measured size distribution.

SECTION 7

TEST PLAN

EPA has been operating a pilot scale SO_2 scrubbing unit at their Research Triangle Park laboratory in support of full-scale process development efforts. The test plan described here is specifically intended for this unit. The scrubber is a one to three-stage TCA type with a nominal gas flow of 500 $meter^3$/hour. The inlet SO_2 concentration can be fixed at any desired level. Several hold tank sizes and arrangements are possible. For purposes of this test program, continuous operation for a five-day period is required. The test plan objectives and test conditions described here are based on the literature survey and mathematical development presented in Sections 3 and 4 of this report.

OBJECTIVES

The major objective of the test plan will be to identify and characterize nucleation sources in lime/limestone wet scrubbing systems for the purpose of increasing the average crystal size to improve settleability of solids. The modeling effort has shown that correlations describing nucleation and growth as a function of operating conditions can be used to predict a calcium sulfite size distribution. Some data pertaining to the growth rate are available, but the nucleation phenomena in this crystal system have not yet been investigated.

Once the predominant sources of calcium sulfite nuclei have been identified, a series of tests will be conducted to define the effects of important process variables on both the nucleation rate and growth rate. The results of these tests will be used to improve the accuracy and usefulness of the size distribution model by quantifying the rate parameters used (k_{GR}, k_{SN} i_{SN}, j_{SN}).

The tests described below are intended for a limestone system. Analysis of available data indicated that this system may be more easily modeled than the lime process.

TEST SEQUENCE AND OPERATING CONDITIONS

The proposed test plan is divided into three phases. The purpose of this strategy is to make full use of experimental data as it is obtained so that subsequent experiments move operationally towards improved sludge quality. Test conditions for Phases I and II are presented in Tables 7-1 and 7-2 reproduced from Appendix E .

Phase I includes eight individual five-day tests. In each test, a single set of operating conditions is maintained for the entire period. The first test period establishes "base case" operating conditions. Then, changes are made to try to identify important nucleation sources in the system. Tests 2, 3, 6, and 7 examine the effects of changes in the mechanical energy sources in the system. In these experiments, the pump and mixer impeller materials and operating speeds are varied. Tests 4, 5, and 8 screen for chemical nucleation in the scrubber or hold tank.

The most important dependent variable in the Phase I tests will be the calcium sulfite crystal size distribution. It is expected that changes in variables affecting nucleation rate will lead to measurable changes in the steady-state size distribution. Settling properties of the crystallized product will also be measured as an indication of changes in the sludge quality.

The mechanical and process configuration of Phase II tests will be based on results of Phase I. Operating conditions producing the best sludge quality will be selected. A series of ten five-day experiments will be run to further correlate calcium sulfite nucleation and growth rates with process operating conditions.

Tests 10 and 11 involve changes in the slurry solids content. If secondary nucleation involves crystal-crystal collisions, this may lead to measureable changes in the sulfite size distribution. Tests 12 through 15 investigate the effect of scrubbing liquor composition by changing levels of soluble magnesium, chloride, and sodium. Tests 16, 17, and 18 involve changes in hold tank size and use of a slurry grinder to promote mechanical nucleation.

As the results of Phases I and II become available, the usefulness of the computer model should be increased. The constants and exponents in the nucleation and growth rate expressions can be adjusted to agree with experimental results. If the physical basis for the model is realistic, the model can then be used to look at design and operating changes to improve sludge quality. Phase III of the recommended test program includes eight five-day tests to verify the computer model and demonstrate improved sludge quality.

TABLE 7-1. PHASE I - TEST SCHEDULE

Test #	Days	Objective	Variable Changed	Reason
1	5	Obtain base case[(1)] system operation	None	Basis for further comparison
2	5	Observe effect of impeller material	Switch to steel impeller	Determine effect of pump energy on P.S.D.
3	5	Observe effect of pump speed	Reduce pump RPM's, maintain constant L/G, residence times.	
4	5	Observe higher scrubber supersaturation	Reduce scrubber feed flow, raise SO_2 inlet, (constant SO_2 pickup)	Determine effects of scrubber conditions on P.S.D.
5	5	Observe scrubber subsaturated operation	Scrubber feed pH 4.5	
6	5	Observe mechanical features of hold tank	Switch to steel agitator	Determine effect of hold tank conditions on P.S.D.
7	5	Same as #6	Lower agitator speed	
8	5	Same as #6	Mix additive, clarifier overflow and scrubber bottoms together	
	40			

(1) Base Case - Low oxygen content in flue gas (<3%), 3000 PPM SO_2, feed rate 83 ℓpm, 10% solids, 10 hour solids retention time. Valve positions and nozzles are not to be changed during the study.

TABLE 7-2. PHASE II - TEST SCHEDULE

Test #	Days	Objective	Variable Changed	Reason
9	5	Base Case(1)	'Best' configuration from Phase I	Future reference
10	5	Change number of crystals in system	5% solids, keep SO_2 pickup constant by raising inlet concentration	Determine effect of solids level on nucleation
11	5	Same as # 10	15% solids, keep SO_2 pickup constant by lowering inlet concentration	
12	5	Change scrubbing liquor quality	Low positive scrubbing liquor ($2Mg + Na - Cl$)	Determine effect of liquor quality and nucleation and growth rates
13	5	Same as # 12	High positive liquor	
14	5	Same as # 12	Low negative liquor	
15	5	Same as # 12	High negative liquor	
	3	System purge		Eliminate high soluble species concentration
16	5	Add seed crystals	Grind 1% of clarifier underflow stream	Increase number of growth sites
17	5	Increase solids retention time to 16 hours	Increase hold tank size	Lower relative saturation
18	5	16-hour S.R.T. and grinding	Same as #16 and #17	Same as #16 and #17
	53			

(1) Base Case - Configuration from Phase I yielding lowest amount of mechanical nucleation.

ANALYTICAL REQUIREMENTS

The data obtained here are to be used in modeling the calcium sulfite size distribution. The model itself depends on nucleation and growth rate parameters, thus these are quantities requiring experimental measurement.

The nucleation rate can be measured only by measuring the size distribution of the calcium sulfite crystals. The growth rate can be determined from both the size distribution data and the chemical species balances for the system. This material balance will provide an independent check on the size distribution measurement.

Figure 7-1 shows a size distribution for sludge obtained from a limestone scrubbing pilot unit. The size versus count data were obtained using a Coulter Counter. The linear growth rate, R, may be determined using the slope of the size distribution, $\frac{d(\ell nn)}{dL}$ and the solids residence time, T. If the distribution is curved, the growth rate varies with crystal size In this case, the term $\frac{dR}{dL}$ must be included in the calculation using an iterative approach to evaluate both R and $\frac{dR}{dL}$ such that:

$$R = \frac{\frac{-1}{T} + \frac{dR}{dL}}{\frac{d(\ell n\ n)}{dL}} \quad . \tag{7-1}$$

The nucleation rate, B_o, is the product of the growth rate and number density at zero size. The intercept of the distribution at zero size can be estimated by extrapolating the small size range data,

$$B_o = \lim_{L \to 0} (nR) \quad . \tag{7-2}$$

The importance of a reliable particle sizing method for the fine size range is easily seen. Available particle sizing methods were discussed in Section 6 of this report. In view of their uncertainty in the submicron range, some additional effort may need to be devoted to analytical methods development prior to or during the test program. An alternate approach to data analysis would be to use the model described in the previous section as a subroutine in a curve fitting program using the growth rate and nucleation rate parameters.

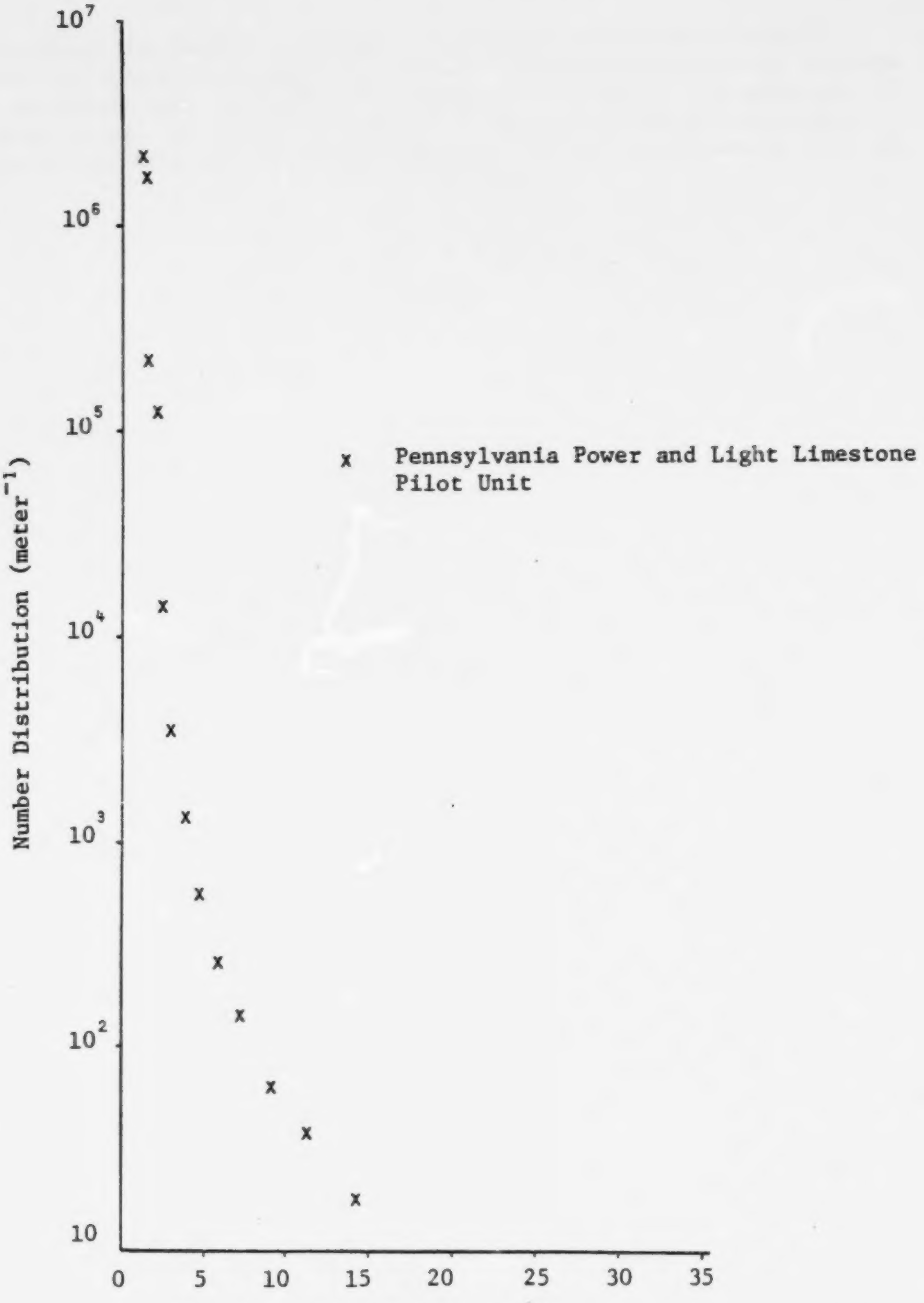

Figure 7-1. Size Distribution Data for Limestone Scrubber Slurry. (Coulter Counter) n (L) versus L

Chemical analytical methods for important liquid and solid phase species are well-established. Details of these procedures are included in Appendix E. Sufficient chemical and operating data should be obtained to complete individual calcium and sulfur balances for the process vessels as well as calculate the relative saturation of the process liquor.

NOMENCLATURE

A_p – Particle surface area (cm^2)

B – Rate of birth of particles, no/ℓ/min

C – Concentration (moles/liter)

C_d – Drag coefficient

cm – Centimeters

D – Rate of disappearance, no /ℓ/min

f_{CL} – Factor defining clarifier particle size split

G – Molar precipitation rate, moles/ℓ/min

g – Gram

i – Experimental exponent

j – Experimental exponent

k – Rate constant

$k, k_o, k_o', k_1, k_2, k_3$ – Experimental constants

k_v – Shape factor

L – Characteristic particle length (m)

L_c – Clarifier cut-off size, microns

ℓ – Liters

$\bar{L}_m$ – Mass average length (m)

m – Meters

m_p – Mass of a particle

M_T – Total slurry solids, moles/ℓ

N – Number of particles per slurry volume (ℓ^{-1})

n – Number of particles of size L volume (ℓ^{-1} m^{-1})

$\dot{N}$ – Number of particles of size L per volume leaving system (ℓ^{-1} sec^{-1})

N_{Re} – Reynolds number

Q – Volumetric flow rate (ℓ/sec)

NOMENCLATURE (continued)

R - Linear crystal growth rate (m/sec)
r - Relative saturation
ΔSO_2 - SO^2 pickup (moles/sec)
U_t - Terminal velocity of a falling particle
V - Slurry volume (ℓ)
W - Weight fraction solids
γ - slope of R vs L straight line, microns)$^{-1}$
Γ - Gamma function
ρ - Density, gm/cc
T - Characteristic time = vessel volume/ flow rate, min.

SUBSCRIPTS

CL - Clarifier
CF - Clarifier feed
CO - Clarifier overflow
CU - Clarifier underflow
GR - Growth
i - Input stream
j - Output stream
n - No (particle)
o - Zero size
p - Particle (crystal)
S - Scrubber
SB - Scrubber bottoms
SF - Scrubber feed
SN - Secondary nucleation
τ - Hold tank
T - Total
v - Volume

REFERENCES

1 Randolph, Alan D. and Maurice A. Larson, Theory of Particulate Processes. Analysis and Techniques of Continuous Crystallization. New York, Academic, 1971.

2 Ottmers, D. M., Jr., et al., A Theoretical and Experimental Study of the Lime/Limestone Wet Scrubbing Process. EPA 650/2-75-006, NTIS #PB 243-399/AS EPA Contract No. 68-02-0023. Austin, Texas, Radian Corporation, 1974.

3 Perry, John H., Chemical Engineers Handbook, 5th edition. New York, McGraw-Hill, 1973.

DCN #77-200-187-11-04

APPENDIX A

AN APPROACH TO PREDICTING CALCIUM SULFITE CRYSTAL SIZE DISTRIBUTION IN LIME/LIMESTONE WET SCRUBBING SYSTEMS

Technical Note 200-187-11-01

28 November 1977

Prepared for:
Robert H. Borgwardt
Industrial Environmental Research Laboratory/RTP (MD-61)
U. S. Environmental Protection Agency
Research Triangle Park,
North Carolina 27711

Prepared by:
James L. Phillips
Grep P. Behrens
Reviewed by:
Philip S. Lowell

TABLE OF CONTENTS

Page

1.0 INTRODUCTION.................................. A-1

2.0 THEORY OF CONTINUOUS CRYSTALLIZATION......... A-3

3.0 APPLICATION OF CRYSTALLIZATION THEORY TO LIME/LIMESTONE SCRUBBING SYSTEMS............. A-10
- 3.1 The Overall Scrubbing System............ A-11
- 3.2 Simulation of the Scrubbing System...... A-14

4.0 NUCLEATION AND GROWTH FUNCTIONS.............. A-16
- 4.1 Nucleation.............................. A-16
- 4.2 Crystal Growth.......................... A-26
- 4.3 Experimental Data for Calcium Sulfite Precipitation......................... A-31

5.0 SUMMARY AND RECOMMENDATIONS.................. A-49

NOMENCLATURE.................................. A-53

REFERENCES.................................... A-56

LIST OF FIGURES

Figure		Page
2-1	Limestone Platelets	A-4
2-2	Lime Rosettes	A-4
4-1	Comparison of Calculated Sulfite Precipitation Rates for Lime and Limestone Scrubbing Systems	A-33
4-2	Comparison of Seed Crystal Sizes for Two Laboratory Experiments Having Similar Molar Growth Rates	A-40
4-3	Size Distribution Data for Lime and Limestone Scrubber Slurries (Coulter Counter)	A-43

LIST OF TABLES

Table		Page
4-1	Results of Lime/Limestone Scrubbing Tests at Combusion Engineering Pilot Units	A-34
4-2	Results of Lime/Limestone Scrubbing Tests at EPA/RTP Pilot Unit	A-36
4-3	Results of Lime Scrubbing Tests at Louisville Gas and Electric	A-38

LIST OF TABLES (continued)

Table Page

4-4 Comparison of Liquor Compositions and Precipitation Rates for Two Lime Scrubbing Systems..A-45

1.0 INTRODUCTION

Concentration and disposal of waste slurry is an important aspect of lime/limestone wet scrubbing technology. Most research and development efforts in the past have been directed towards improving SO_2 removal and preventing scale formation in these systems. Solution of these problems is crucial to successful process application. Theoretical and experimental studies at Radian Corporation (OT-023, JO-R-214), EPA's Research Triangle Park facility (BO-144, BO-147, BO-241), and the EPA/TVA prototype scrubbing system at Shawnee have related scaling potential and SO_2 removal efficiency to important system design and operating parameters. These advances have helped make continuous operation of lime/limestone scrubbers a practical reality.

Given an operable process, the quality of waste material produced assumes greater importance. Such parameters as slurry settling rate and settled density may have a significant impact on waste disposal costs over the life of a system. The purpose of this technical note is to outline a quantitative basis for predicting the size distribution of calcium sulfite solids produced in lime/limestone scrubbers. This appears to be a logical first step in designing for optimum waste sludge quality. It is believed that sulfite crystal size distribution can ultimately be related to slurry settling and dewatering properties. In the following development, the term "calcium sulfite solids" will include any coprecipitated sulfate, but gypsum precipitation will not be considered.

Our approach will first examine the general mathematical relationships regarding conservation of particles in continuous crystallization. Section 2.0 describes this "particle balance" concept based primarily on the work of Randolph and Larson (RA-060). A general equation is derived and then simplified for the application of interest here.

In Section 3.0, the general particle balance relationships are more specifically applied to lime/limestone wet scrubbing. In addition, a qualitative discussion of the possible effects of system design and operating parameters on waste product particle size is presented.

Section 4.0 examines the physical and mathematical description of particle birth, death and growth functions necessary for solution of the particle balance equations. Correlation of nucleation and growth rates with the physical and chemical environment in various parts of the system will be central to quantitative application of the proposal model.

2.0 THEORY OF CONTINUOUS CRYSTALLIZATION

Many quantitative investigations of particle size distributions in laboratory and industrial crystallizers are described in recent chemical engineering literature. Nearly all of these have used a mathematical approach derived from the principle of particle conservation. For crystallization from solution this may be stated as follows (RA-060):

> Rate of accumulation of crystals of size L per unit volume of slurry is equal to the net input of crystals of size L via convection plus the net input via growth plus the net generation of crystals of size L via other mechanisms (e.g., breakage).

In this statement, L (meters) is a characteristic length which completely describes all three dimensions of each crystal. This is equivalent to assuming that all crystals are geometrically similar. Recent experimental work by TVA using sludge from the Shawnee test facility has shown that nucleation and/or growth mechanisms in lime and limestone scrubbing systems produce different predominant crystal shapes. Flat platelets with a length-to-width-to-thickness ratio of about 25:20:1 predominate in limestone systems while rosettes are more characteristic of lime scrubbing systems (CR-163). Figures 2-1 and 2-2 are electronmicrographs of limestone platelets and lime rosettes. The mathematical development in this technical note will be limited to a single characteristic length L. Different crystal habits may be dealt with later by specifying an applicable "shape factor" for each case. This shape factor is normally defined by the relationship between crystal volume and the characteristic length:

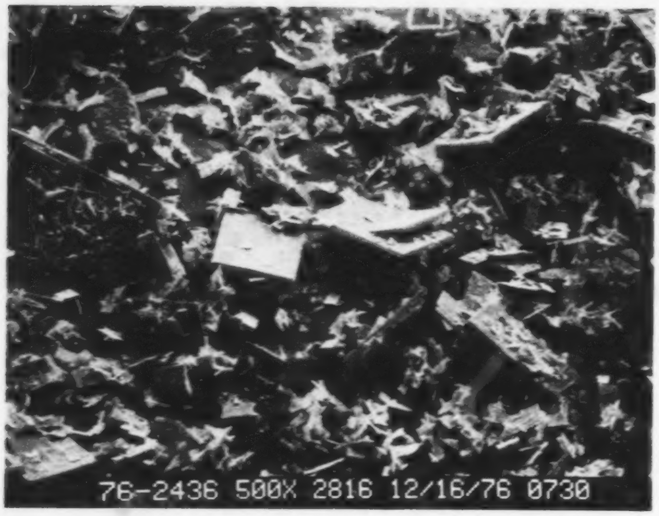
76-2436 500X 2816 12/16/76 0730

FIGURE 2-1

LIMESTONE PLATELETS (COURTESY TVA)

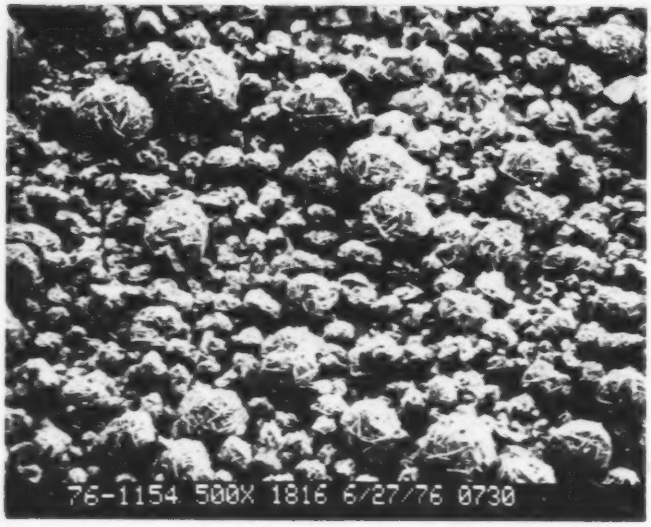
76-1154 500X 1816 6/27/76 0730

FIGURE 2-2

LIME ROSETTES (COURTESY TVA)

$$V_p = k_v L^3 \quad (m^3) \tag{2-1}$$

The possibility exists that more than one shape factor may be necessary to describe the crystals formed in a single process configuration. This can presumably be handled by calculating a separate size distribution for crystals of each shape.

A reasonably general mathematical form for the particle balance principle can be derived by considering the differential element of slurry shown in Figure 2-3.

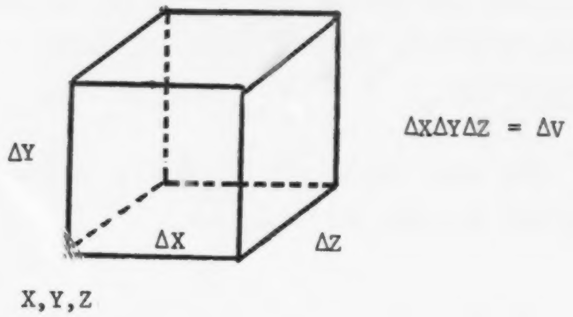

Figure 2-3.

First, define the crystal size distribution n(L,X,Y,Z) such that nΔL is equal to the number of crystals in the size range ΔL per unit volume of slurry. The dimensions of n are thus m^{-4}. The rate of accumulation of crystals in the size range ΔL in the slurry element may then be written as:

$$\text{accumulation} = \frac{\partial}{\partial t}(\bar{n}(L)\Delta L\Delta V) \quad (sec^{-1}) \tag{2-2}$$

Here $\bar{n}(L)$ is an average value of n(L,X,Y,Z) over the small volume element.

For convection in the X direction, the net input of crystals in the size range ΔL is:

$$\text{net input via X convection} = -\left[(\bar{u}_X\bar{n}(L)|_{X+\Delta X} - (\bar{u}_X\bar{n}(L)|_X\right]\Delta L\Delta Y\Delta Z \quad (\text{sec}^{-1}) \quad (2\text{-}3)$$

where $\bar{u}_X$ is the X component of slurry velocity averaged over the ΔYΔZ plane. Strictly speaking, this term should deal with convection of crystals, not slurry. The derivation is simplified by assuming that the slurry velocity and crystal velocity are identical. This appears to be a reasonable assumption for the small crystals typical of lime/limestone wet scrubbing systems. (This assumption would not apply to a clarifier, but very little change in size distribution would be expected in this vessel for any case.) Similar convection terms may be written for the Y and Z directions.

The net imput of crystals via growth to the size range ΔL in element ΔV may be written:

$$\text{net input via growth} = \left[(\bar{n}(L)\ R(L))|_L - (\bar{n}(L)\ R(L))|_{L+\Delta L}\right]\Delta V \quad (2\text{-}4)$$

where R(L) (meter/sec) is the growth rate of the L dimension for crystals of size L. This growth rate may be size dependent. The entire particle balance expression is obtained by combining Equations 2-2, 2-3, and 2-4. Thus:

$$\frac{\partial}{\partial t}\left[\bar{n}(L)\Delta L\Delta V\right] \cong -\left[(\bar{u}_X\bar{n}(L))|_{X+\Delta X} - (\bar{u}_X\bar{n}(L))|_X\right]\Delta L\Delta Y\Delta Z \qquad (2\text{-}5)$$
$$-\left[\left(\bar{u}_Y\bar{n}\ (L)\right)|_{Y+\Delta Y} - \left(\bar{u}_Y\bar{n}\ (L)\right)|_Y\right]\Delta L\Delta X\Delta Z$$
$$-\left[\left(\bar{u}_Z\bar{n}\ (L)\right)|_{Z+\Delta Z} - \left(\bar{u}_Z\bar{n}\ (L)\right)|_Z\right]\Delta L\Delta X\Delta Y$$

$$+\left[(\bar{n}(L)\ R(L))\big|_{L} - (\bar{n}(L)\ R(L)\big|_{L+\Delta L} \right] \Delta V$$

+ net generation by mechanisms other than growth

Dividing both sides of Equation 2-5 by $\Delta L \Delta X \Delta Y \Delta Z$ and taking the limit as the "Δ" values go to zero yields a partial differential equation. The "average" values $\bar{n}$ and $\bar{u}$ become point values.

$$\frac{\partial n}{\partial t} = -\frac{\partial}{\partial X}(u_X n) - \frac{\partial}{\partial Y}(u_Y n) - \frac{\partial}{\partial Z}(u_Z n) - \frac{\partial}{\partial L}\left(nR(L)\right) + G(L,X,Y,Z) \qquad (2\text{-}6)$$

The term G represents net formation of crystals of size L from mechanisms other than growth and convection. For example, a single large crystal might break to form two or more smaller crystals. Breakage has been addressed in the ball mill literature ([illegible]-272). It is itself a rather complex phenomenon. [illegible] be some function of L, X, Y, Z and must be dimensionally consistent with the remaining terms in the particle balance.

It should be noted that the G term does not include nucleation, which is defined as formation of particles of a length L near zero. Instead this is included in solutions to Equation 2-6 by specifying as a boundary condition the number concentration of nuclei, n_o, as L approaches zero. The nucleation rate, $\dot{n}_o$, is related to the nuclei concentration n_o by an expression similar to that used for the rate of appearance of crystals at larger sizes of L (see Equation 2-4):

$$\dot{n}_o = (n(L)\ R(L))\big|\text{evaluated as L becomes small} \qquad (2\text{-}7a)$$

$$\simeq \text{Lim}\left[n(L)R(L) \right]_{L \to o} \qquad (2\text{-}7b)$$

It should be realized that not all nuclei grow to mature crystals. A death rate term is implicit in an overall system nucleation rate. For example, in lime scrubbing systems, an increase in liquid phase calcium concentrations is often seen across the scrubber. This is due to the demand for extra alkalinity by the scrubbing liquor. As the calcium sulfite goes into solution, two possibilities exist. Either the fine particles dissolve first or mass is removed from each crystal in proportion to its volume. It is possible that fines dissolution is the major mechanism for extra alkalinity. This death of fine particles in the scrubber must be more than offset by the nucleation rate, in order to satisfy the overall particle balance.

Practical application of Equation 2-6 requires detailed information about the functionality of crystal nucleation rate and growth rate for a particular system. Nucleation rate is typically a function of liquid composition and may also be influenced by crystal collisions in agitated slurries. Growth rate is affected by liquid composition, crystal size, and in some cases, level of agitation. Both nucleation and growth are temperature dependent. If the other particle generation term, G, is significant, its variation with supersaturation and crystal size must also be known. Possible forms for these functions are discussed in later sections of this technical note.

Some additional simplification of the general particle balance equation is desirable before applying it to lime/limestone scrubbing systems. First of all, it seems reasonable to limit the present discussion to steady-state conditions. Mathematically, at steady state,

$$\frac{\partial n(L)}{\partial t} = 0 \text{ for all values of } L, X, Y, Z \qquad (2\text{-}8)$$

Equation 2-6 may now be written

$$-\frac{\partial}{\partial L}\left(n\,R(L)\right) + G = \frac{\partial}{\partial X}(u_X n) + \frac{\partial}{\partial Y}(u_Y n) + \frac{\partial}{\partial Z}(u_Z n) \qquad (2\text{-}9)$$

For application of Equation 2-9 to systems of fixed volume, the convection terms may be converted to entrance and exit stream flow rates and particle concentrations by integrating both sides of 2-9 over the volume of the system and applying Gauss' Theorem to the right-hand side. In vector notation, Equation 2-9 becomes:

$$\int_V \left[-\frac{\partial}{\partial L}\left(n\,R(L)\right) + G\right] dV = \int_V (\nabla \cdot \vec{u}n)\, dV \qquad (2\text{-}10)$$

In Equation 2-10, the right hand side is identically equal to $\Sigma Q_{out} n_{out} - \Sigma_{in} n_{in}$ where Q_{in} and Q_{out} are volumetric flow rates of entering and exiting slurry streams. Thus, our final form of the particle balance equation becomes

$$\Sigma Q_{out} n_{out} - \Sigma Q_{in} n_{in} = \int_V \left[-\frac{\partial}{\partial L}\left(nR(L)\right) + G\right] dv \qquad (2\text{-}11)$$

3.0 APPLICATION OF CRYSTALLIZATION THEORY TO LIME/LIMESTONE SCRUBBING SYSTEMS

In the previous section a general appraoch to predicting crystal size distribution was derived. It was pointed out that application of Equation 2-6 requires definition of suitable functions for nucleation rate (or nuclei density) and crystal growth rate. In this section, the generalized particle balance is applied to lime/limestone scrubbing systems. The qualitative effects of various process parameters on the particle balance equation will be discussed. Information required for quantitative solutions will be identified for further investigation. Mass balance equations will also be introduced so that interactions between the particle size distribution and overall material balance can be seen.

A "typical" process flow sheet for a lime or limestone scrubbing system is shown in Figure 3-1. A physical description

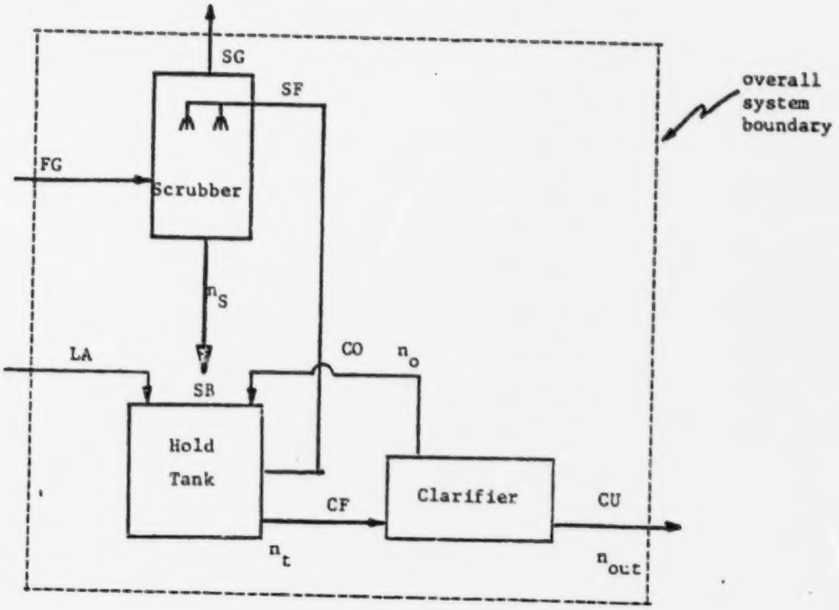

Figure 3-1.

of the process units and their possible effects on sulfite particle size distribution will aid in developing a suitable mathematical model. First, the overall system is discussed. Then the combination of individual process units on sulfite particle size distribution are considered.

3.1 The Overall Scrubbing System

Referring to Figure 3-1, SO_2 enters the system in the flue gas (FG) stream. Most of this inlet SO_2 is absorbed by the scrubber feed liquor (SF). Some of the absorbed SO_2 is oxidized in the scrubber. Depending on the specific system design, sufficient residence time and supersaturation may exist in the scrubber to form sulfite nuclei or to provide additional growth on sulfite crystals entering with the scrubber feed (OT-023). In other systems, for example the lime scrubber at Paddy's Run, sulfite crystals may dissolve in the scrubber to provide alkalinity for SO_2 absorption (HA-696). For many systems, particularly those with short slurry residence time in the scrubber, little solid-liquid mass transfer would occur until the dissolved SO_2 enters the hold tank with the scrubber bottom (SB) stream.

In the hold tank, dissolved sulfite and sulfate react with dissolved calcium from the alkaline additive to precipitate calcium sulfite and sulfate solids. Recent experimental work has shown that calcium sulfite precipitated in lime or limestone scrubbing systems may coprecipitate a limited amount of sulfate ion. A solid phase with the formula $Ca(SO_3)_{1-X}(SO_4)_X \cdot \frac{1}{2}H_2O$ has been identified (JO-R-214). Depending on system operating conditions, the value of x ranges from zero to about .2. For purposes of the present discussion, "calcium sulfite" crystals will include coprecipitated sulfate.

A waste stream is taken from the hold tank and pumped to a dewatering area (pond, filter or clarifier). The remaining slurry is recirculated to the scrubber. Nearly all of the solids are typically removed from the waste slurry stream and some or all of the clear liquor is recycled. The "dewatered solids" (actually containing up to 60 wt. % water) are contained in a suitable permanent storage area such as an ash pond or land fill. The dewatering properties of this waste slurry stream and the physical properties of the dewatered solids should be related in some way to the particle size distribution and shape of the sulfite crystals.

The overall scrubbing system may be treated as a "black box" which combines calcium from lime or limestone additive with SO_2 from the flue gas to form calcium sulfite crystals. The number and size of these crystals depends on the mechanisms and rates of nucleation and growth in the system. At steady-state or for conditions averaged over a suitable time period, the total number of moles of SO_2 removed from the gas is approximately equal to the total number of moles of sulfite + sulfate appearing in the waste slurry. This can be expressed mathematically by an overall mass balance:

$$\Delta SO_2\left(\frac{\text{mole}}{\text{sec}}\right) \cong CU\left(\frac{\ell}{\text{sec}}\right) m_s\left(\frac{g}{\ell}\right) / MW\left(\frac{g}{\text{mole}}\right) \qquad (3\text{-}1)$$

In this equation CU is the clarifier underflow rate, m_s the concentration of coprecipitate solids in the slurry, and MW the molecular weight of the sulfite/sulfate coprecipitate. The contribution of dissolved sulfur to the overall mass balance is assumed to be negligible. This relationship shows that changes in SO_2 removal rate will ultimately require a corresponding change in the slurry waste rate or slurry solids concentration.

The overall system SO_2 balance can also be related to the particle size distribution n(L) by recognizing that the sum of the individual crystals leaving the system must also account for the molar SO_2 removal rate. Thus:

$$\Delta SO_2\left(\frac{\text{mole}}{\text{sec}}\right) = \frac{k_v \rho_s CU}{MW} \int_0^\infty n(L)L^3 dL \tag{3-2}$$

The particle concentration leaving the system is:

$$N = \int_0^\infty n(L)dL \tag{3-3}$$

If we define a mass average length $\bar{L}_m$ such that

$$\bar{L}_m^3 = \int_0^\infty \bar{n}(L)L^3 dL \Big/ \int_0^\infty \bar{n}(L)dL \tag{3-4}$$

then Equation (3-2) may be written as

$$\Delta SO_2\left(\frac{\text{mole}}{\text{sec}}\right) = k_v \rho_s CU\ N\ (\bar{L}_m)^3/MW \tag{3-5a}$$

$$= k_v \rho_s\ \dot{N}(\bar{L}_m)^3/MW \tag{3-5b}$$

Where N is the total number of crystals per volume of slurry and $\dot{N}$ is the total number of crystals leaving the system per second. Equation 3-4 shows that a change in the steady-state SO_2 removal rate requires a corresponding change in the product $\dot{N}(\bar{L}_m)^3$. Either the total number of crystals leaving the system per unit time, $\dot{N}$, or the mass mean size $\bar{L}_m$ must change. The magnitude of these changes depends on the interaction of crystals growth and nucleation mechanisms with the scrubbing system design and operating variables.

3.2 Simulation of the Scrubbing System

While the system mass balance equations constrain the weighted integral of the crystal size distribution, the residence times and environments of the individual process units will control the function n(L). At this point in the program, we expect that individual models for the scrubber, hold tank, and possibly the clarifier will be combined to predict the overall particle size distribution for slurry leaving the system. This approach will be more complex than developing "average" nucleation and growth functions for an entire system, but should more closely describe reality. The flexibility of the model would be improved by considering crystallization phenomenon in each process unit. If model verification studies show that the impact of the scrubber and clarifier on particle size distribution are negligible the model can be simplified accordingly.

The solution of the particle balance around each individual process unit (scrubber, hold tank, and clarifier) involves input from the other process units. The incoming distribution must be known in order to calculate the outgoing stream. In a scrubbing system, the feed to the scrubber is the effluent of the hold tank. Conversely, the scrubber effluent enters the hold tank. The clarifier overflow, which is a fraction of the hold tank effluent, is also returned as part of the hold tank feed. An accurate model of these distributions involves the solution of several simultaneous differential equations. For a complete description of the mathematical development of these equations and the calculational scheme proposed by Radian to obtain predicted particle size distributions, the reader is referred to Radian Technical Note 200-187-11-03.

One objective of the model verification portion of this program will be to arrive at the simplest approach to the overall simulation that will still predict observed data. Hopefully, some simplifying assumptions can be applied that will reduce computational time without decreasing the utility of the simulation. These simplifying assumptions will probably center on the nucleation and growth functions appearing in the particle balance equations. In particular, the relationships between nucleation, growth, and solution composition need to be as simple as possible so that accurate simulations can be made without excessive nesting of material balance and particle balance calculations.

Another important part of the overall simulation will be arriving at a good initial guess for the calculated particle size distributions. Field data may be very important in meeting this objective.

In the following section the nucleation and growth rate functions are discussed. The impact of various forms for these on the overall simulation is also considered.

4.0 NUCLEATION AND GROWTH FUNCTIONS

In this section, some possible forms for calcium sulfite nucleation and growth functions are examined. Our objective is to select a model that adequately describes these phenomena in the scrubbing environment and can be easily related to system mass balances. A brief discussion of nucleation and growth studies appearing in the literature is followed by detailed examination of data for calcium sulfite precipitation.

4.1 Nucleation

For purposes of this study, nucleation has been defined mathematically as the rate of appearance of crystals of "zero" size. Normally, all crystals of size L greater than zero are considered to have been produced through the mechanism of growth on nuclei. Appearance of crystals of non-zero size via mechanisms other than growth (e.g. breakage) will not be considered at this point.

Nucleation phenomena are traditionally separated into three classes depending on the mechanism and circumstances of particle formation (WA-339). These are:

a. Homogeneous - spontaneous formation of solute particles from a clear supersaturated solution,

b. Heterogeneous - formation of solute particles from a supersaturated solution in the presence of a second solid phase, and

c. Secondary - formation of solute particles from a supersaturated solution in the presence of existing solute particles.

A general thermodynamic description of nucleation phenomena was developed by Gibbs and modified by Volmer (MO-311). For any phase change to occur, a net decrease in free energy is required. The total free energy change (ΔG_T) for nucleation is the sum of free energy changes associated with the volume (ΔG_V) and the surface (ΔG_S) of the solid phase:

$$\Delta G_T = \Delta G_S + \Delta G_V \tag{4-1}$$

The surface free energy change, ΔG_S, is assumed to be proportional to the surface area of the nuclei:

$$\Delta G_S = \sigma A_p \tag{4-2}$$

For one mole transferred from the liquid phase to form solid particles solid particles, the volume free energy change, ΔG_V, is equal to the difference in chemical potentials between the solid and liquid phases.

$$\Delta G_V = -(\mu_\ell - \mu_s) \tag{4-3}$$

The chemical potential of solute may be expressed as the sum of a standard state chemical potential (depending only on temperature) and a term related to the activity of the solute:

$$\mu_\ell = \mu_\ell^o + \bar{R}T\ell n\ a \tag{4-4}$$

The chemical potential of the solid phase is equal to the chemical potential of a saturated solution:

$$\mu_s = \mu_\ell^o + \bar{R}T\ell n\ a_{sat} \qquad (4\text{-}5)$$

Thus, the volume free energy change may be written in terms of solute activities by combining Equations 4-3, 4-4, and 4-5:

$$\Delta G_V = -\ (\mu_\ell - \mu_s) = -\bar{R}T\ell n\ \frac{a}{a_{sat}} \qquad (4\text{-}6)$$

At equilibrium, the total free energy change between liquid and solid phases must be zero. Thus, the equilibrium state is described thermodynamically by:

$$\bar{R}T\ell n\ \frac{a}{a_{sat}} + A_\rho \sigma = 0 \qquad (4\text{-}7)$$

The surface area formed by one mole of precipitate may be determined by the volumetric and area shape factors:

$$A_\rho = \frac{MW\ k_a a}{\rho k_v L} \qquad (4\text{-}8)$$

Combining Equations 4-7 and 4-8, we can see that the equilibrium size of a nucleus, L_{eq}, is related to the surface energy of the solid phase and the activity or supersaturation of solute:

$$L_{eq} = \frac{\sigma\ MW\ k_a}{k_v \rho_s\ \bar{R}T\ell n\ \frac{a}{a_{sat}}} \qquad (4\text{-}9)$$

According to Equation 4-9, an increase in the activity of the solute will decrease the size at which nuclei are stable. At a given level of supersaturation (a/a_{sat}), particles smaller than L_{eq} will tend to dissolve while particles larger than L_{eq} will grow to become crystals.

Equation 4-9 describes the critical size at which a nucleus begins to grow into a crystal. The rate at which nuclei of this critical size appear should be proportional to the probability of their formation. The probability of formation is related to the work of formation by an exponential function (KH-034). Thus:

$$\dot{n}_o = K \exp\left(-(\text{work})/\bar{R}T\right) \qquad (4\text{-}10)$$

The work term in Equation 4-10 can be evaluated in terms of the free energy change as the nucleus "grows" from zero size to L_{eq}:

$$\text{WORK} = \int_o^{L_{eq}} \Delta G_T (3L^2 k_v \rho_s / MW)\, dL \qquad (4\text{-}11)$$

The term in parentheses relates the change in number of moles to the change in crystal size L. If the proper relationship for ΔG_T versus L is substituted into Equation 4-11 and the integration carried out, the result is

$$\text{WORK} = \frac{4}{27} k_v \frac{\sigma^3 MW^2}{\rho_s{}^2 \bar{R}^2 T^2 \ell n^2 \frac{a}{a_{sat}}} \qquad (4\text{-}12)$$

and the nucleation rate becomes:

$$\dot{n}_o = K \exp - \left[(\tfrac{4}{27} k_v \sigma^3 MW^2) / (\rho_s^2 R^3 T^3 \ell n^2 \tfrac{a}{a_{sat}}) \right] \qquad (4\text{-}13)$$

Equation 4-12 predicts a very rapid rise in nucleation rate with supersaturation. For example, Mullin summarized Volmer's calculations for nucleation of water droplets in super cooled vapor (MU-001):

$\dot{n}_o$ (nuclei/sec liter)	$r = a/a_{sat}$
0	1
10^{-68}	2
10^{-9}	3
10	4
10^{13}	5

The functionality of Equation 4-12 is consistent with the appearance of "showers" of nuclei at certain "critical" levels of supersaturation in various systems. The region of supersaturation below the critical level for nucleation is termed the "metastable" region.

Attempts at experimental verification of Equation 4-12 for homogeneous nucleation have led to many complications. Early work by Ting and McCabe (TI-006) showed that for nucleation of magnesium chloride, the critical supersaturation for spontaneous nucleation depended on such things as the rate of stirring and the rate of increase of supersaturation. Other variable effects on "homogeneous" nucleation are summarized by Khamskii (KH-034).

Experiments showing the effect of solid impurities in a nucleating system led to the concept of "heterogeneous" nucleation. The amount of work required to form critical nuclei is apparently much less when other solid surfaces are available. If the nucleating system is seeded with crystals of the precipitating substance itself, "secondary" nucleation takes place. This can occur at levels of supersaturation approaching equilibrium. In typical industrial crsytallizers where substantial slurry densities are maintained, secondary nucleation appears to be the predominant mechanism for new particle formation. (Strickland-Constable in ES-003).

Clontz and McCabe (in LA-035) have demonstrated some important aspects of secondary nucleation in a study using single crystals of $MgSO_4 \cdot 7H_2O$. In their work, single crystals of $MgSO_4 \cdot 7H_2O$ were fixed in a flowing supersaturated solution and struck with either a rod or a second crystal. They found that the number of nuclei formed during crystal-crystal or crystal-surface collisions was a function of both supersaturation and the energy dissipated in the collisions. A correlation of the form:

$$\frac{\bar{N}}{A_c} = k_1(r-1)E \qquad (4\text{-}14)$$

was proposed where $\bar{N}$ is the number of nuclei produced by a crystal-crystal collision. A_c is the surface area involved in the collision, E is the contact energy, and r is the relative saturation (a/a_{sat}). For contact of crystals with other solid surfaces, the number of nuclei generated was less but still significant. A slightly different correlation form was found:

$$\frac{\bar{N}}{A_c} = k_2(r-1)EA_c^{-\frac{1}{2}} \qquad (4\text{-}15)$$

The actual number of nuclei produced by single collisions in Clontz and McCabe's study ranged from zero to approximately 600. The region of supersaturation studied was 0-12%, and contact energy ranged from 10 to 2600 ergs. The nucleation mechanism did not appear to require a critical level of either supersaturation or contact energy.

In an extension of this initial work on single-crystal secondary nucleation, Johnson et.al (in ES-003) demonstrated that the number of nuclei formed in crystal-surface contacts depended on the hardness of the surface used. The initial experiments had been conducted using a stainless steel rod.

Further tests with soft rubber and hard polypropylene yielded no detectable nucleation at comparable levels of supersaturation and contact energy. This observation could be of substantial importance in situations where low levels of secondary nucleation are desired.

Other investigators have studied secondary nucleation phenomena in experimental situations more closely related to continuous mixed-suspension crystallizers. Cise and Randolph (ES-003, RA-432) measured secondary nucleation in agitated suspensions of K_2SO_4 with a continuous-liquid/batch-solids reactor. An empirical correlation of their data showed that the nucleation rate was proportional to supersaturation to the .56 power, seed crystal size to the 4.1 power and stirrer speed to the 5.78 power. The strong dependence of the secondary nucleation rate on stirrer speed and crystal size is consistent with a mechanism which depends on the energy of stirrer/crystal collisions.

Rousseau, et.al. (in RO-344) studied the effects of crystal size on nucleation rate using $MgSO_4 \cdot 7H_2O$ crystals. When a single seed crystal was placed in an agitated vessel, nucleation occurred only for crystals larger than approximately 200 microns. Above this lower limit, the secondary nucleation rate increased exponentially with seed crystal size.

Ness and White (in RO-344) also studied secondary nucleation effects with $MgSO_4 \cdot 7H_2O$ crystals. They counted the number of nuclei produced in an agitated suspension of closely-sized crystals. At a given impeller speed and supersaturation, the observed nucleation rate was directly proportional to the number of seed crystals. This is consistent with a mechanism dependent on crystal-impeller contacts rather than crystal-crystal collisions. Their slurry density was very low, however; about .5 grams solids/liter. Thus the importance of crystal-crystal collisions at higher slurry densities was not ruled out.

The effects of stirrer speed and crystal size observed by Ness and White were similar to other studies. The nucleation rate was proportional to the fourth power of both stirrer speed and crystal size. The observed effect of supersaturation on nucleation rate in this study was substantially greater than seen in previous work, however. An exponent of 2.5 was used to fit their data.

When the steel impeller used for most of their experiments was replaced with polypropylene, nucleation was reduced by up to a factor of ten. Furthermore, the effect of the number of seed crystals increased over the linear relationship noted for the steel impeller. The influence of crystal-crystal collisions was thought to account for this increased dependence on slurry density.

The significance of secondary nucleation in lime/limestone wet scrubbing systems has yet to be established. Clontz and McCabe point out that in order to satisfy the particle balance constraint in a continuous crystallizer, it is only necessary for each crystal in the system to provide one nucleus before it leaves the system. Since mean solids residence times in lime/limestone scrubbing systems are typically on the order of one day, even a very low collision probability and nucleation rate would suffice.

The crystal size necessary to produce a collision energy on the order of 10 erg may be estimated for calcium sulfite. Assuming a shape factor k_v = .025 based on length, the mass of a sulfite crystal of length L will be:

$$\begin{aligned} m(\text{grams}) &= \rho_s\, .025\, L^3 \\ &= .06L^3 \end{aligned} \qquad (4\text{-}16)$$

The maximum approach velocity for a collision with an impeller will be on the order of 100 feet/sec or 3000 cm/sec. An erg is equal to one gram cm^2/sec^2. To produce a collision energy of 10 ergs:

$$10 \text{ gm } cm^2/sec^2 = \tfrac{1}{2}MV^2 = .03L^3(3000)^2 \qquad (4\text{-}17)$$

Solving Equation 4-17 for L yields $L_{min} \cong .03$ cm or 300 microns. The maximum observed size for sulfite crystals in lime/limestone wet scrubbing processes is about 100 microns. Contact energy for a 100 micron crystal would be on the order of 0.4 erg. This is substantially less than the contact energy studied by Clontz and McCabe, but secondary nucleation remains a possibility, particularly since the sulfite supersaturations in limestone scrubbing systems are up to 30 times the range considered by Clontz and McCabe and can be even higher for lime systems. In fact, the phenomena discussed above could well make production of large sulfite crystals impossible under realistic process conditions.

The discovery of the importance of secondary nucleation at moderate to low supersaturations has precluded the use of classical nucleation theories in industrial crystallization. Nearly all recent quantitative studies of nucleation kinetics in agitated suspensions have used simple "power law" correlations of the form:

$$\dot{n}_o = kr^i m_s^j \text{ (nuclei/sec liter)} \qquad (4\text{-}18)$$

In Equation 4-18, r is the relative supersaturation and m_s is the slurry solids content. This type of correlation can be used to express observed effects of slurry density and supersaturation, but must be used with care because of its obvious empirical basis. In particular, one would not expect this type of correlation to be useful over a wide range of supersaturation, since the mechanism of nucleation changes from secondary to heterogeneous to homogeneous as supersaturation increases. Also, Equation 4-18 does not explicitly include the well documented effect of crystal size on nucleation rate. The "constant" k in Equation 4-18 will also depend on other factors influencing the quality and quantity of crystal collisions, such as impeller speed.

For simulation of systems where large changes in supersaturation occur, a correlation which includes both secondary and homogeneous nucleation effects seems desirable. This will probably be the case for lime scrubbers and possibly for limestone scrubbers. An expression which sums the effects described by Equations 4-13 and 4-18 would be:

$$\dot{n}_o\text{(particles/liter-sec)} = (nR)_{L \to o} = k_1(r-1)^h m_s^i \bar{L}_n^j + k_2 \exp\left[-k_3/\ln^2 r\right] \qquad (4\text{-}19)$$

In Equation 4-19, $\bar{L}_n$, the number average crystal size has been added as an explicit parameter. The constants would be selected based on experimental data. At present, little information is known about the source of nuclei in lime/limestone scrubbing systems. Thus, explicit terms describing energy input to the nucleation source have not been included in 4-19. It should be recognized that the nucleation rate may depend on such things as agitator or pump impeller speeds and materials of construction.

Recalling Equation 3-4, the combined mass balance and particle balance for the scrubbing system is:

$$\Delta SO_2 \, \frac{\text{mole}}{\text{sec}} = k_v \rho_s \, \dot{N} (\bar{L}_m{}^3)/MW \qquad (3\text{-}4)$$

This states that the mass mean particle size for the system is completely dependent on the nucleation rate under the constraint of constant SO_2 removal. Thus, correlation of nucleation rates may be the most important aspect of the current modeling effort. It should be noted, however, that nucleation rates and growth rates are coupled for a given system by their mutual dependence on relative saturation. Thus, the form of the growth rate expression is also important.

4.2 Crystal Growth

Once nuclei larger than the initial size have been formed in a supersaturated solution, they will grow to form macroscopic crystals. The relationship between growth rate, crystal properties, and solution properties has been the subject of many studies reported in the literature. The results of these studies have not supported any one specific concept of crystal growth kinetics. Instead, a large number of difficult-to-explain variable effects have been noted. Most problems in experimental data analysis are thought to result from using macroscopic models to describe events taking place at an undefined crystal/solution interface. Some established aspects of crystal growth kinetics are outlined below.

In order for a crystal to grow, the ionic or molecular components of the precipitating substance must first diffuse from the bulk solution to the solid-liquid interface and then be incorporated into the crystal lattice. The overall rate of crystal growth may be limited by diffusion, surface reaction, or both.

The diffusion step is conventionally described by the product of a mass transfer coefficient, the crystal surface area, and a concentration driving force:

$$\bar{G}\,(\text{mole/sec}) = k_m A_p (C_b - C_i) \qquad (4\text{-}20)$$

In equation 4-20, k_m, the mass transfer coefficient is a function of the diffusivity of the species of interest and the hydrodynamic conditions that affect the fluid boundary layer near the crystal surface. A_p is the crystal surface area. The driving force term $(C_b - C_i)$ is the difference between the solute concentration in the bulk phase and at the solid-liquid interface.

Levins, et al, (LE-305) have conducted an extensive review of solid-liquid mass transfer rates in agitated vessels. Their own experimental data were used to arrive at a general correlation for predicting k_m as a function of important system variables. For small particles ($<100\mu$) with specific gravity less than three, the proposed mass transfer correlation is:

$$\frac{k_m L}{D} = 2 + .47 \left(\frac{L^{4/3}\ \bar{E}^{1/3}}{\upsilon}\right)^{.62} \left(\frac{D_s}{D_t}\right)^{.17} \left(\frac{\upsilon}{D}\right)^{.36} \qquad (4\text{-}21)$$

In equation 4-21, D is the diffusivity of the solute, $\bar{E}$ the agitation power per unit mass of slurry, υ the kinematic viscosity, and D_s/D_t is the ratio of stirrer and tank diameters. For a given solid liquid system with fixed mechanical configuration, Equation 4-21 may be simplified:

$$\frac{k_m L}{D} = 2 + aL^{.82} \qquad (4\text{-}22)$$

Equation 4-22 shows that k_m, the mass transfer coefficient increases as particle size decreases. In the limiting case of very small particles, the second term on the right hand side of 4-22 goes to zero and

$$\frac{k_m L}{D} = 2 \qquad (4\text{-}23)$$

This equation is exactly true for diffusion through a stagnant liquid surrounding the solid particle.

The mechanism and kinetics for integration of ions into the crystal lattice are less well understood than the diffusion step. As a result, there is no consistent approach in the literature for predicting the rate of surface reaction. Khamskii (KH-034) summarizes several of the more important theoretical approaches to crystal growth kinetics. Buckley (BU-090) and Nielsen (NI-001) review a wide range of experimental data for various systems in their comprehensive discussions of crystal growth. The rate of the surface reaction is generally held to be a function of temperature, solution composition, and surface characteristics of the crystals.

Many experimental investigators (CO-020, DA-006, IS-001, LU-006, MC-012, NA-015, NA-016, GA-236) have used an empirical rate expression of the form

$$G_m = k_o \alpha (C - C_s)^P = k_o \alpha (r-1)^P \text{ mole/}\ell\text{-sec} \qquad (4\text{-}24)$$

to correlate overall rates of crystal growth in supersaturated solutions. Since the rate of bulk diffusion depends on agitation parameters but the surface reaction rate does not, experiments at different levels of agitation can be used to distinguish between these two possible rate-controlling mechanisms. As would be expected, the overall rate constant k_o for a given crystallization system can exhibit variable effects typical of diffusion or surface reaction depending on the particular levels of temperature and agitation studied. The exponent, p, of the driving force term in Equation 4-24 will be 1 for the diffusion limited case but may be greater than 1 for cases where the surface reaction rate is important.

If the surface reaction rate is found to be first order with respect to supersaturation, $(p=1)$, then a combined expression may be written for the overall reaction rate using the individual rate constants for mass transfer and surface reaction:

$$G_m = k_o\alpha(C - C_s) = \frac{1}{1/k_m + 1/k_r}\alpha(C - C_s) = \frac{1}{1/k_m' + 1/k_r'}\alpha(r-1) \quad (4\text{-}25)$$

In this expression, k_m will be a function of the variables included in Equation 4-21 while k_r is normally assumed to be a function of temperature only.

The term α in Equation 4-24 is related in some manner to the surface properties of the crystal. For a diffusion-limited system, α would be equal to A_p, the crystal surface area. For the surface reaction, the situation is unclear. Many engineering studies, particularly those using the MSMPR approach of Randolph and Larson have assumed that the surface reaction rate is also proportional to crystal surface area. This is equivalent to assuming that the linear growth rate is independent of particle size; the so-called "McCabe ΔL Rule" (CA-003). On the other hand, several recent investigators have reported systems where the linear growth rate due to surface reaction is strongly size dependent (GA-234, WE-331, GA-236, PH-050). Specifically, the surface reaction rate was observed to decrease with crystal size for nickel sulfate, and potassium sulfate. A size dependent surface reaction rate could be included in Equation 4-25 by developing a suitable correlation for k_r versus crystal size. This would allow the use of $\alpha = A_p$ for both diffusion and surface reaction.

Cise and Randolph in their previously discussed study of secondary nucleation also estimated the linear growth rates of very small K_2SO_4 crystals using measured size distribution data. Growth rate was found to increase rapidly with crystal size. Crystals in the 2-3 micron range grew only one tenth as fast as those larger than 25 microns. They point out that this effect is opposite to that which might be expected from diffusion limited mechanism even if the effect of increasing solubility with decreasing crystal size is considered. An empirical correlation of their data showed that:

$$k_r = k_{r_\infty} \exp(-k/\sqrt{L}) \text{ meter/sec} \qquad (4\text{-}26)$$

In a later study, White, et.al. (in RO-344) confirmed the strong size dependence for growth rates of K_2SO_4 crystals. They suggested a growth rate expression of the form:

$$k_r/k_{r_o} = 1 + 2L^{2/3} \qquad (4\text{-}27)$$

Larson and Bendig (in RO-344) on the other hand, were unable to detect a size-dependent growth rate for $MgSO_4 \cdot 7H_2O$ crystals.

Whatever the observed form of the relationship between growth rate and crystal size, some care must be exercised in applying empirical correlation for use in particle balance calculations . Wey and Terwilliger (WE-331) have discussed application of various growth rate expressions appearing in the literature. They caution that the system mass balance requires the integral of individual particle growth rates over all particle sizes to be equal to the total precipitation rate:

$$G_{m_{total}} \text{(mole/liter sec)} = \frac{k_v \rho_s}{MW} \int_o^\infty n(L)\ L^2 R(L)\ dL \qquad (4\text{-}28)$$

If R(L) is infinite as L → o or L → ∞, then the integral in 4-28 may not converge. Also, if R(L) is zero as L → o, it is obvious that nuclei cannot grow to form macroscopic crystals.

4.3 Experimental Data for Calcium Sulfite Precipitation

Data describing the precipitation kinetics of calcium sulfite in lime/limestone wet scrubbing systems are available from several sources. These data are summarized and discussed below. Our objective is to quantify, to the extent possible, the nucleation and growth rates of calcium sulfite as a function of the variables discussed in Sections 4.1 and 4.2. Gaps in existing data will be pointed out so that they may be addressed in the test plan portion of this program.

The earliest reported data for growth of $CaSO_3 \cdot \frac{1}{2} H_2O$ crystals are those reported by Ottmers, et.al. (OT-023) under EPA contract 68-02-0023. Overall growth rates for an agitated suspension of seed crystals were measured in a continuous-liquid, batch-solids reactor. Supersaturated solutions were prepared by mixing Na_2SO_3 and $CaCl_2$ feed streams. For supersaturations below 3 x K_{sp}, the overall growth rate was correlated by:

$$\text{Rate (mole/min-gram)} = 1.2 \times 10^{10} \exp(-21{,}000/\bar{R}T)(r-1) \qquad (4\text{-}29)$$

At low supersaturations these sulfite crystals assumed the familiar flat platelet habit with a length/width/thickness rates of roughly 30:20:1. For supersaturations above 3 x K_{sp}, the growth mechanism changed to surface nucleation and the overall growth rate increased rapidly. Crystals grown at high rates showed a multi-directional dendritic habit and tended to form agglomerates.

The overall growth rate was unaffected by stirrer speed and was estimated to be less than one fourth that expected for difussion limited growth. No apparent change in overall growth rate was observed during experiments where the mass average size of the initial seed charge increased by ∿40%. Nucleation was not observed in these experiments at supersaturations below 3 x K_{sp}.

Results of a series of pilot scale lime/limestone wet scrubbing tests were also reported by Ottmers (OT-023). The tests were conducted using a pilot-scale scrubbing system built by Combustion Engineering Company. Overall growth rates for calcium sulfite* were calculated using liquid phase or solid phase material balances across the major process vessels in a more realistic scrubbing environment. The process arrangement consisted of a one or two-stage marble bed scrubber with a cross-sectional area of 25 ft^2 followed by a 6000 gallon effluent hold tank and a 20,000 gallon clarifier. Two major test series were conducted; the first using boiler calcined lime introduced with the flue gas, and the second using commercial limestone added to the effluent hold tank. Results for the lime and limestone test series are summarized in Table 4-1.

Figure 4-1 compares early laboratory results with these pilot-scale observations. On the graph, all data have been adjusted to equivalent rates at 45°C on the basis of the exponent in

---

* The actual precipitating crystals were most likely $Ca(SO_3)_{1-X} \cdot (SO_4)_X \cdot \frac{1}{2}H_2O$ in this case.

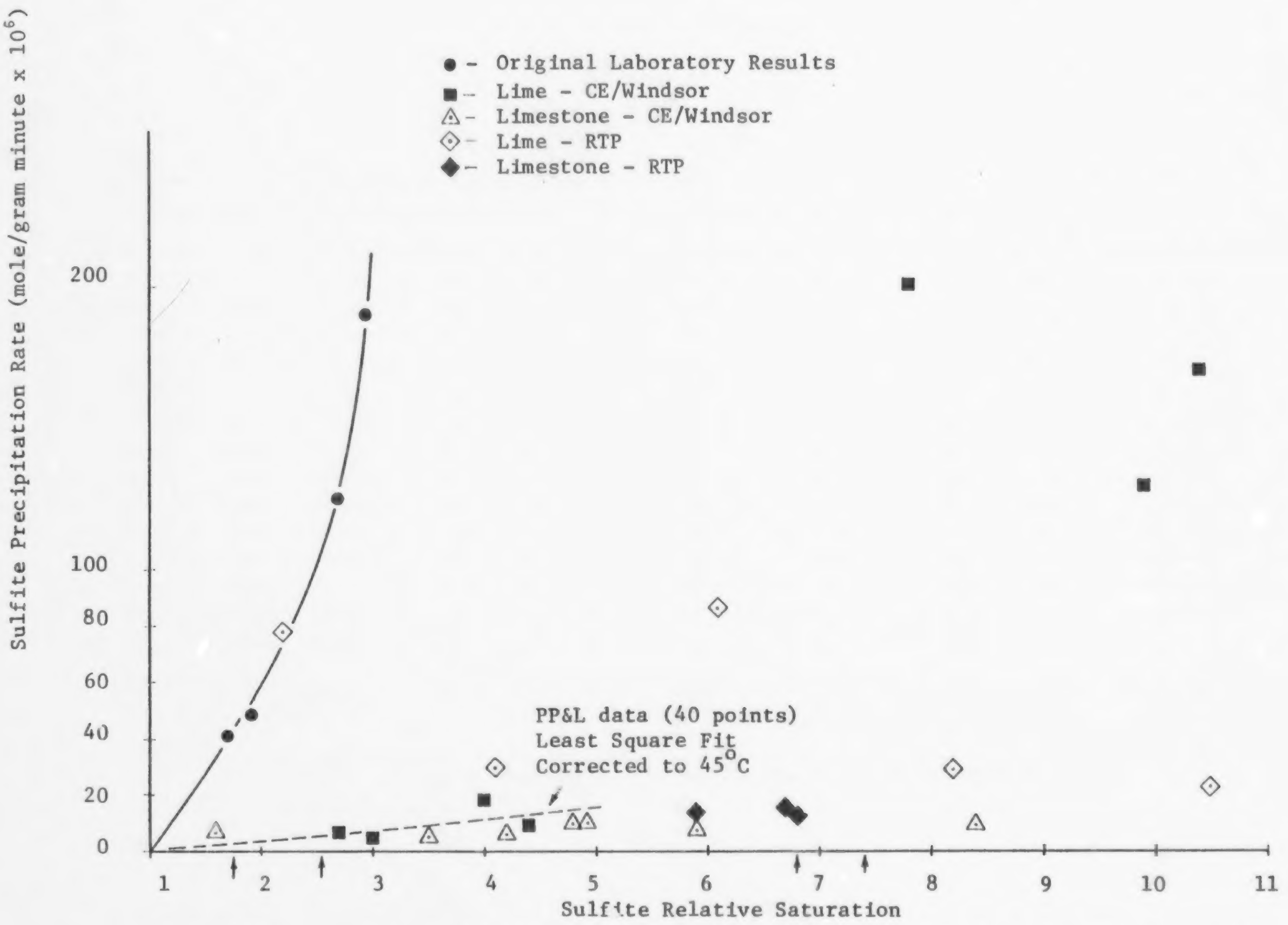

Figure 4-1. Comparison of Calculated Sulfite Precipitation Rates for Lime and Limestone Scrubbing Systems.

TABLE 4-1. RESULTS OF LIME/LIMESTONE SCRUBBING TESTS AT COMBUSTION ENGINEERING PILOT UNIT*

Test No.	Reactant	Hd.Tk.Vol. (liter)	Tot.Solids in Slurry (gm/l)	Liquor pH Scr.	Liquor pH Hd.Tk.	Liq.Temp. (°C)	Sulfite Solids in Slurry (gm/l)	Cal. Sulfite Rel.Saturations Scr.**	Cal. Sulfite Rel.Saturations Hd.Tk.	Calcium Sulfite Precipitation Rate in Hold Tank (g mole/gm-min)
18-1	Lime	22,700	46	6.0	10.7	46	14	5-8	2.7	5.7×10^{-6}
18-2	Lime	22,700	38	6.0	10.6	46	11	7-11	4.4	9.6×10^{-6}
19-1	Lime	22,700	14	4.6	5.4	39	3.1	3-5	9.9	7.8×10^{-5}
19-2	Lime	22,700	15	4.8	5.5	39	3.0	4-7	11.4	7.3×10^{-5}
20-1	Lime	22,700	7.4	4.6	5.7	40	1.5	2	7.8	1.2×10^{-4}
20-2	Lime	22,700	6.7	4.6	5.7	40	1.2	2-3	10.4	1.0×10^{-4}
21-1	Lime	11,350	84	5.6	8.5	45	25	4-6	3.0	4.6×10^{-6}
22-1	Lime	20,000	91	6.0	5.6	46	28	5	4.0	1.9×10^{-5}
1A-1	Limest.	22,700	77	5.3	6.0	48	27	11	3.5	6.5×10^{-6}
2A-2	Limest.	22,700	66	5.2	6.1	47	28	8.6	4.8	1.4×10^{-5}
3A-1	Limest.	22,700	82	5.3	6.0	49	35	9.6	8.4	1.3×10^{-5}
1B-1	Limest.	22,700	64	5.7	6.3	50	26	13	5.9	1.4×10^{-5}
2B-1	Limest.	22,700	88	5.6	6.0	51	38	6.3	4.9	9.4×10^{-6}
2B-2	Limest.	22,700	93	5.6	6.0	50	41	6.7	4.2	1.1×10^{-5}

* Boiler-calcined lime introduced via flue gas stream, Limestone introduced via hold tank.

** Range of calculated relative saturation for observed pH range.

Equation 4-29. At low supersaturations, the lime and limestone data are roughly comparable and correspond to a rate constant of $\sim 7 \times 10^8$ versus 1.2×10^{10} for the laboratory data. No good explanation for this factor of 17 difference is available. It should be noted that the results are reported on a "per gram" of seed crystal and not on a "per cm^2" of seed crystal area basis. At higher supersaturations, precipitation rates for the lime system increase rapidly. The level of supersaturation at which this occurs is much greater than the 3 x K_{sp} limit observed in the laboratory study however.

Borgwardt has reported a large number of lime and limestone scrubbing experiments in a series of EPA progress reports. (BO-146, BO-247). Several sets of results from this pilot unit have also been included on Figure 4-1 for comparison to the data discussed above. Pertinent calculated results based on reported data for this pilot unit are summarized in Table 4-2. Calculated calcium sulfite precipitation rates for the limestone system are comparable to other reported pilot unit data. Precipitation rates per unit mass of seed crystals for the lime system are more scattered and again some points lie considerably above the limestone data.

Additional pilot scale measurements of calcium sulfite precipitation rates were obtained by Phillips, et al., during Radian Corporation's large pilot-scale limestone scrubbing study at Pennsylvania Power and Light Company (internal Radian report). This unit was a high L/G spray tower operating at 80-90% SO_2 removal when treating 300 m^3/min. of gas with inlet SO_2 levels near 2,000 ppm. For most of the test program, the hold tank volume for this unit was approximately 60,000 liters and the slurry solids content was maintained at 10 weight percent. The scrubber effluent pH ranged typically from 5-5.5 while the hold tank pH was normally about 6.0. Calcium sulfite relative saturations

TABLE 4-2. RESULTS OF LIME/LIMESTONE SCRUBBING TESTS AT EPA/RTP PILOT UNIT

Test Date (1973)	Reactant	Hd.Tk.Vol. (liter)	Tot.Solids in Slurry (gm/1)	Liquor pH		Sulfite Solids in Slurry (gm/1)	Cal. Sulfite Rel.Saturations		Calcium Sulfite Precipitation Rate in Hold Tank (g mole/gm-min)
				Scr.	Hd.Tk.		Scr.	Hd.Tk.	
1/18	Limestone	300	176	5.8	6.3	50		6.7	1.6×10^{-5}
1/19	Limestone	300	176	5.6	6.2	80		6.8	1.2×10^{-5}
1/23	Limestone	300	176	5.7	6.3	65		5.9	1.7×10^{-5}
10/16-19	Lime	370	41	4.8	6.0	35		2.2	6.9×10^{-5}
10/19-23	Lime	370	41	5.0	6.7	35		6.1	8.3×10^{-5}
10/29-11/2	Lime	370	95	4.9	7.0	86		4.1	3.1×10^{-5}
11/26-30	Lime	370	106	5.0	7.1	82		8.2	2.9×10^{-5}
12/10-14	Lime	370	106	6.0	8.4	8.1		10.5	2.4×10^{-5}

ranged from 2 to 6 with most tests falling in the 3-5 region. A least squares fit of more than forty steady-state closed loop tests is shown by the dashed line on Figure 4-1. These data are in close agreement with data taken at comparable levels of supersaturation at the other pilot units.

As a final check on the magnitude of sulfite precipitation rates in a full-scale scurbbing unit, some recent test data obtained by Radian during EPA's current Louisville Gas and Electric test program were used. This unit is a full-scale Combustion Engineering design using a two-stage marble bed scrubber followed by a hold tank with a capacity of approximately 10^6 liters.

During normal operation, scrubber effluent liquor is introduced to the hold tank via a small "draft tube" section of approximately 10^4 liters capacity. The lime additive is also added to this small section of the tank and pre-mixed with the scrubber effluent before entering the main tank. During the EPA test series at this unit the piping and tank arrangement was modified so that the additive could be introduced to the main tank rather than the draft tube. Also, the main tank could be eliminated completely so that the entire precipitation reaction would be forced to occur in the small draft tube section.

Table 4-3 summarizes tests for this lime scrubbing system. Calculated precipitation rates are shown for both the draft tube and main sections of the hold tank where applicable. According to the data, nearly all of the observed sulfite precipitation occured in the draft tube portion of the hold tank even in tests where the lime additive was added to the main portion of the vessel. As a result, calculated values for calcium sulfite precipitation rate per unit mass of seed crystals are five to ten times those observed at either the CE/Windsor pilot unit of EPA/RTP unit when using lime. In the final two tests shown, the the major portion of the hold tank was physically isolated from

TABLE 4-3. RESULTS OF LIME SCRUBBING TESTS AT LOUISVILLE GAS AND ELECTRIC

Test Date	Tank Volumes (liter)		Total Solids in Slurry (gram/liter)	Liquor pH		Liquor Temp. °C	Sulfite Solids in Slurry (gram/liter)	Calcium Sulfite Relative Saturation			Calcium Sulfite Precipitation Rate (mole/gram-min$\times 10^6$)	
	Hold Tank	Draft Tube		Scrubber	Hold Tank			Scrubber	Hold Tank	Draft Tube	Hold Tank	Draft Tube
7/7/77*	9.6×10^5	1.1×10^6	43	6.1-7.1	7.9	50-53	35	2.1-2.5	2.5	3.2	∿0	980
7/8/77*	9.6×10^5	1.1×10^6	45	6.3-7.2	7.9	50-53	36	2.6-2.9	2.8	3.2	∿0	1450
7/26/77*	9.6×10^5	1.1×10^6	74	6.0-7.2	8.0	50-53	60	1.7-2.1	2.3	3.6	<0	810
8/1/77**	9.6×10^5	1.1×10^6	84	6.1-7.0	8.1	49-52	68	2.1-2.8	1.7	2.6	2.7	240
8/8/77**	9.6×10^5	1.1×10^6	58	5.1-5.6	8.5	50-53	47	1.3-3.6	3.7	--	†	†
8/22/77*	not in use	1.1×10^6	59	5.9-6.9	7.9	51-52	48	2.5-3.2	--	4.2	--	850
8/29/77*	not in use	1.1×10^6	73	5.6-6.8	7.5	50-53	59	1.4-2.9	--	3.5	--	670

† insufficient data
* Lime added to draft tube
** Lime added to hold tank

the draft tube section. In this case, the high calculated precipitation rates should be correct in spite of the difficulty of obtaining a representative sample from the draft tube effluent.

It should be emphasized at this point that the above comparison of measured calcium sulfite precipitation rates has not included information regarding the size distribution of the seed crystal mass in suspension. If the linear growth rate, R, is constant with crystal size, then the molar growth rate per unit mass of crystals should be inversely proportional to the crystal size:

$$G_g(\text{mole/gram min}) = \frac{\dfrac{k_v \rho_s}{MW} \displaystyle\int_0^\infty n(L) L^2 R\, dL \ (\text{mole/liter-min})}{k_v \rho_s \displaystyle\int_0^\infty n(L) L^3\, dL \ (\text{grams/liter})} \qquad (4\text{-}30)$$

If R increases with size as suggested by some of the previous work discussed in Section 4.2, then the molar growth rate per unit mass would be less sensitive to changes in size.

Some qualitative information on the effect of crystal size on growth rate for calcium sulfite is available as a result of work conducted at Radian Corporation under EPA contract 68-02-1883 (JO-R-214). A series of bench-scale experiments was conducted to investigate variables affecting the composition of sulfite/sulfate coprecipitate formed in lime/limestone wet scrubbing systems. The size distribution of the growing crystals was not of specific interest in this work, but photomicrographs were taken of product crystals from several kinetic experiments to document the presence or absence of gypsum. Figures 4-2a and 4-2b are photographs of product crystals from Runs K-13 and K-20. Even though there appears to be a dramatic difference in the crystal size distributions for these two experiments, the

RUN 13 10X20
4-2a

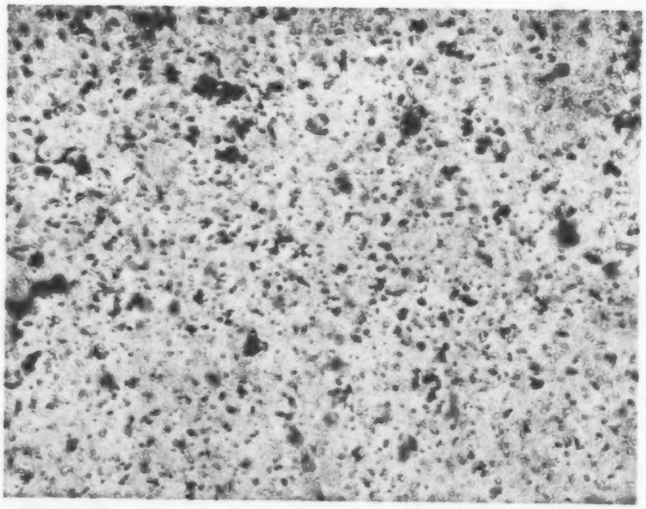

RUN 20 10X20
4-2b

FIGURE 4-2 COMPARISON OF SEED CRYSTAL SIZES FOR TWO LABORATORY EXPERIMENTS HAVING SIMILAR MOLAR GROWTH RATES.

reported molar growth rates per unit mass of solids were comparable. This observation implies that the linear growth rate of the small crystals is much less than that of larger crystals.

The effect of crystal size on the linear growth rate can also be inferred from the shape of the product crystal size distribution. If the scrubbing system approximates MSMPR crystallizer conditions, Equation 3-12, the particle balance for a well mixed vessel can be simplified to yield:

$$-\frac{d(nR)}{dL} = \frac{n}{\tau} \qquad (4\text{-}31)$$

where τ is the mean solids residence time in the system. After multiplying the right side by R/R, the variables may be separated and the equation integrated.

$$\frac{d(nR)}{nR} = \frac{-dL}{R\tau} \qquad (4\text{-}32)$$

$$n = n_c\left(\frac{R_0}{R(L)}\right) \exp\left[\frac{-1}{\tau}\int_0^L \frac{dx}{R(x)}\right] \qquad (4\text{-}33)$$

Examination of equation 4-33 shows that the number of particles of size L is directly related to the number of zero size particles. The ratio of R_0 to R(L) based on experimental observations is less than one. This is due to faster growth rates for larger crystals. Even if the growth term continues to increase with size, the exponential term will limit the number of larger particles seen in a size distribution.

Equation 4-31 can also be expanded to isolate the term $\frac{d\ln(n)}{dL}$.

$$\frac{d\ \ln(n)}{dL} = \frac{d\ \ln(R)}{dL} - \frac{1}{\tau R} \qquad (4\text{-}34)$$

If the linear growth rate is constant, $\left(\frac{d\ln(R)}{dL}\right) = 0$, then a plot of ln n(L) versus L should be a straight line with slope equal to $-\frac{1}{R\tau}$. If the growth rate increases with size, $\left(\frac{d\ln(R)}{dL}\right) > 0$ then the curve will be concave upward.

Figure 4-3 shows size distributions for product crystals from the LG&E lime and PP&L limestone scrubbing systems calculated from Coulter Counter data. Both distributions are clearly concave upward, indicating an increasing growth rate with increasing size.

Equation 4-32 can be rearranged to calculate the growth rate R using the slope of the size distribution:

$$R = -\frac{\frac{1}{\tau} + \frac{dR}{dL}}{\frac{d(\ln n)}{dL}} \tag{4-35}$$

The change in growth rates with crystal size indicated by the data in Figure 4-3 can be estimated by approximating the size distribution with the straight lines indicated on the figure. Along these lines, $dR/dL = 0$, and

$$R = -\frac{1}{\tau \frac{d\ln n}{dL}} \tag{4-36}$$

For the lime data from LG&E, τ was approximately 1300 minutes. Using this number and the slopes of the indicated lines:

$$R_{small} = 2.4 \times 10^{-10} \text{ meter/min}$$

$$R_{large} = 2.2 \times 10^{-9} \text{ meter/min}$$

Thus, the larger crystals grow about ten times faster than the smaller crystals. This is consistant with our previous observations that the molar growth rate per unit crystal mass appears to be independent of crystal size over the range of interest.

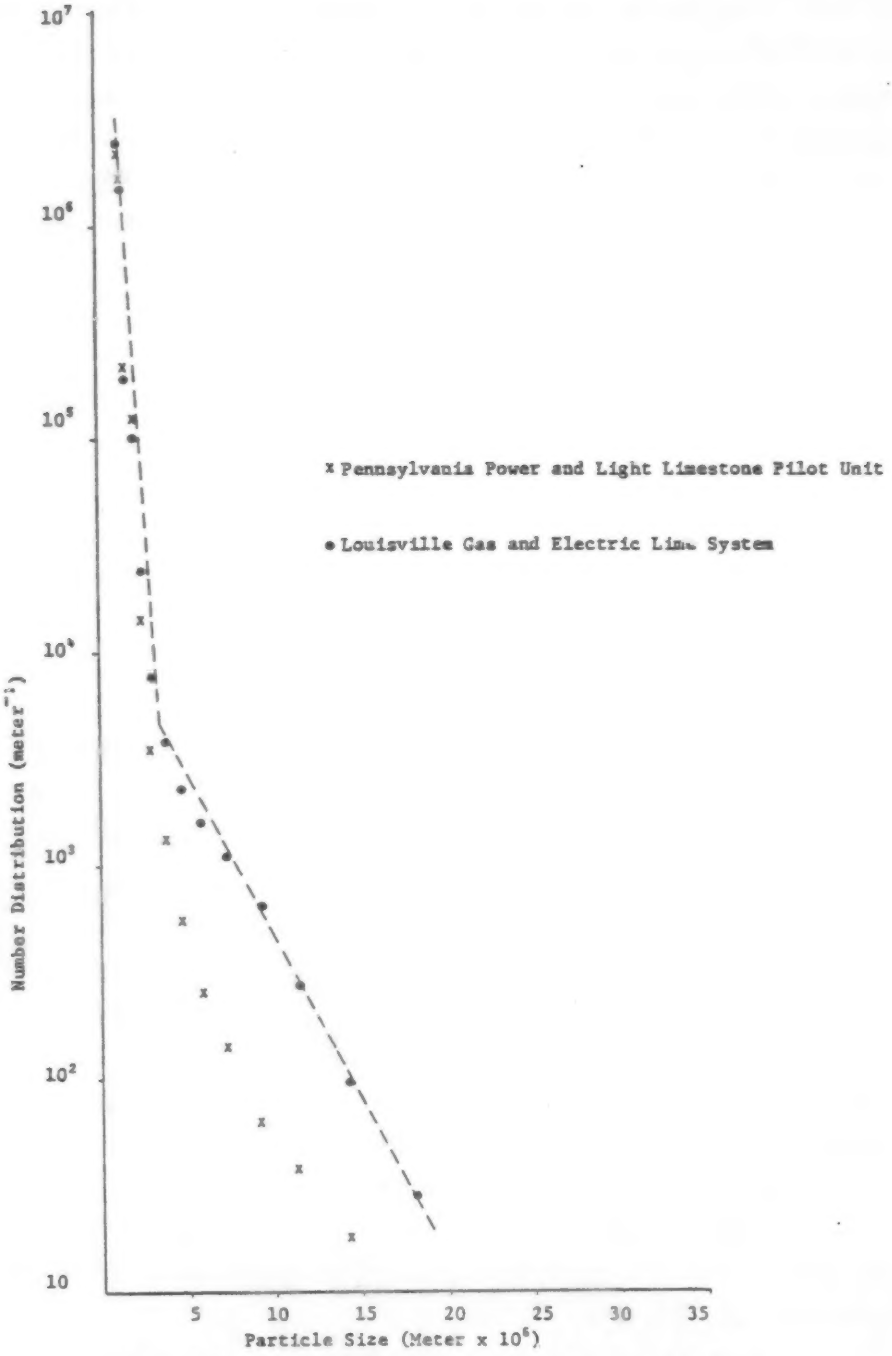

Figure 4-3. Size Distribution Data for Lime and Limestone Scrubber Slurries (Coulter Counter).

The above discussion suggests that changes in particle size distribution should not cause large changes in precipitation rate per unit mass of seed crystals. In this case, an alternate explanation for the widely different rates observed for lime systems must be found. One possible mechanism for the extremely high precipitation rates calculated for the lime system at LG&E would be the existence of locally high supersaturation in the liquid phase due to additive dissolution. The tendency for this to occur should be far greater in a lime system than a limestone system since the lime additive is much more reactive and more soluble than limestone. Thus, results from different pilot units would be similar for limestone systems, as observed, but would depend on certain aspects of the liquor composition and additive arrangement in the lime systems.

Some evidence is available to support the hypothesis that precipitation rates in lime systems are influenced more by localized conditions than by bulk liquor supersaturation. Table 4-4 summarizes reported liquor compositions and calculated precipitation rates for lime tests at EPA's RTP pilot unit and the LG&E full-scale system. As previously noted, the calculated sulfite precipitation rates for the LG&E system are ten to twenty times those observed at the RTP pilot unit at comparable levels of bulk supersaturation. A substantial difference in the liquor composition between these two sets of tests is evident, however. During this period at LG&E, the magnesium content of the liquor was maintained at a relatively high level, causing the dissolved calcium concentrations to be lowered. Under these circumstances, one would expect any effects due to localized additive dissolution to be maximized since large relative increases in calcium concentration are possible.

Equilibrium calculations have been used in a previous study (HA-696) to estimate the maximum calcium concentration and

TABLE 4-4. COMPARISON OF LIQUOR COMPOSITIONS AND PRECIPITATION RATES FOR TWO LIME SCRUBBING SYSTEMS

System	Test Date	Liquid Phase Composition(mole/liter) Ca	Mg	Cl	SO_2	Sulfite Relative Saturation	Sulfite Precipitation (Rate (mole/gram-min)
RTP	10/16/73	.016	.0054	.0076	.0017	2.2	6.9×10^{-5}
	10/19/73	.011	.024	.0096	.0040	6.1	8.3×10^{-5}
	10/29/73	.0053	.047	.013	.0057	4.1	3.1×10^{-5}
	11/26/73	.016	.034	.015	.00[illegible]	8.2	2.9×10^{-5}
	12/10/73	.017	.017	.011	.0038	10.5	2.4×10^{-5}
LG&E	7/7/77	.0013-18	.17	.006	.05	3.2	9.8×10^{-4}
	7/8/77	.0014-19	.17	.007	.05	3.2	1.4×10^{-3}
	7/26/77	.0010-16	.14	.02	.05-.07	3.6	8.1×10^{-4}
	8/22/77	.0010-15	.13	.01	.05-.06	4.2	8.5×10^{-4}
	8/29/77	.0020-30	.14	.08	.03-.05	3.5	6.7×10^{-4}

sulfite supersaturation attained by saturating a scrubbing liquor with lime. A calcium concentration of .03 mole/liter would be near the solubility limit for lime in scrubbing liquor. Thus, lime dissolution in a high magnesium liquor where the bulk concentration of dissolved calcium is only .001 mole/liter could lead to much higher localized precipitation rates than in a liquor where the bulk concentration is already .015 mole/liter. If this effect is significant, mixing differences between pilot scale and full-scale units might also be important. Explanation of these substantial differences in precipitation rates among lime systems will be one important objective of the proposed test plan.

Another, and perhaps the most important objective, will be to determine the nucleation rate function. Existing literature on this subject is sketchy at best. Some qualitative relationships have been observed, however, and the test plan will attempt to quantify these observations.

The TVA Report, Lime/Limestone Sludge Characterization -- Shawnee Test Facility (CR-163) possibly comes the closest to determining nucleation rates in a scrubbing system. No firm conclusions are offered, however, several observations are made. First, in limestone systems, the average particle size is noted to decrease with higher stoichiometry. For better filtration and clarification, the stoichiometry should approach 1. This would indicate that stoichiometry, which influences the relative saturation, also affects nucleation. The less excess calcium present, the lower the chance of nucleation occurring.

Solids surface area measurements made by TVA show an average of 5.4 square meters/gram for lime crystals and 3.3 for limestone. At this time TVA has not correlated this measurement with process variables. This could potentially provide some indication of the relationships involved.

The Aerospace Report, Disposal of By-Products from Non-Regenerable Flue Gas Desulfurization Systems: Second Progress Report (RO-362) deals mainly with the leaching of trace elements from sludges. The most important process variable for trace element leaching was determined to be scrubber pH. Physical properties of solids studied were permeability, pumpability, bulk density, compaction, and compressive strength. No data or correlation was given with these measured properties and process variables.

Some photomicrographs for nine different scrubbing systems are shown in the Appendix of the Aerospace Report. These are meant to be representative samples from typical operation, however, and cannot be used to determine a correlation between operating parameters and particle size since sufficient quantitative data are not reported.

The Final Report, Dual Alkali Test and Evaluation Program (LA-324), prepared by A. D. Little, is also primarily concerned with leaching effects. Only three solid samples were analyzed, one from a concentrated dual alkali sludge, a dilute alkali sludge and a limestone sludge. The usual bulk physical tests were made. Even if the nucleation rate had been determined with only one data point from each system no relationship could have been derived including all the process variables which influence crystal size.

These reports and other literature which has been examined have failed to yield data from which nucleation rates can be calculatd. In even fewer instances, process variables have been connected with resultant sludge properties. For this reason, the first step in optimizing sludge quality will be detailed investigation of relationships which have only previously been qualitatively observed. The first phases of the test plan are geared therefore to providing a quantitative understanding of calcium sulfite nucleation and growth.

5.0 SUMMARY AND RECOMMENDATIONS

A mathematical approach to predicting calcium sulfite crystal size distributions in lime/limestone wet scrubbing systems has been formulated. The model is based primarily on the particle balance theory of Randolph and Larson. A size distribution n(L) is defined such that the number of particles per unit volume of slurry in a small size range L is equal to the product n(L) L. The general partial differential equation for n as a function of size L and position (X,Y,Z), is:

$$-\frac{\partial}{\partial L}(nR) + G = \frac{\partial}{\partial X}(u_X n) + \frac{\partial}{\partial Y}(u_Y n) + \frac{\partial}{\partial Z}(u_Z n) \qquad (2\text{-}9)$$

where R (meter/sec) is the linear crystal growth rate. G is a function describing the appearance of crystals of finite size through mechanisms other than growth on smaller crystals. G is commonly taken to be zero in analyses of continuous crystallization appearing in the literature. This assumption will have to be checked using particle size distribution data from operating scrubbing systems.

For process vessels such as a typical hold tank and some scrubbers (e.g., TCA) where the liquid phase is approximately back-mixed, Equation 2-9 may be simplified since n is no longer a function of position. In this case:

$$\Sigma Q_{out} n_{out} - \Sigma Q_{in} n_{in} = V\left[-\frac{d}{dL}(nR) + G\right] \qquad (5\text{-}1)$$

where V is the vessel volume and Q is the flow rate of streams entering and leaving the vessel.

Equations 2-9 or 5-1 may be applied to a given process configuration by relating the growth rate, R, and the nucleation rate, $(nR)_{L\to o}$, to the composition of the circulating liquor. The liquor composition in a vessel where precipitation takes place may be related to the inlet liquor compositions by a mass balance for the components of interest:

$$\text{Precipitation Rate } \frac{\text{mole}}{\text{sec}} = \Sigma Q_{in}\, C_{in} - \Sigma Q_{out} C_{out} = \frac{k_a \rho_s}{MW} \int_0^\infty n L^2 R\, dL \qquad (5\text{-}2)$$

In Equation 5-2, C is the liquid phase concentration of the precipitating species and k_a is a constant relating crystal surface area to the square of the linear dimension L.

The overall modeling problem requires simultaneous solution of the mass balance and particle balance for each process vessel where precipitation (or dissolution) takes place. To perform this computation, a relationship between growth rate, nucleation rate, and conditions in the vessel are required.

A literature survey was conducted to determine the expected form of the nucleation and growth functions. Process variables expected to influence nucleation include relative saturation, slurry solids content, crystal size, and energy dissipation rates in pumps or mixers. An empirical correlation of the form:

$$\dot{n}_o(\text{particles/liter-sec}) = (nR)_{L \to O} = k_1 (r-1)^h m_s^{\,i} \bar{L}_n^{\,j} + k_2 \exp\left[-k_3/\ln^2 r\right] \qquad (4\text{-}19)$$

is suggested for the nucleation rate. In this equation, r is the relative saturation, m_s the slurry solids content, and $\bar{L}_n$ the number average crystal size. No experimental data are available at this time to determine the values of the exponents h, i, and j, or the constants k_1, k_2, and k_3.

Some data describing the total average nucleation rate in lime and limestone systems were expected to be derived from particle size distribution analysis of slurry samples from operating units. Optical size distribution data suggest that lime and limestone scrubbing solids contain on the order of 10^9 particles per gram. Coulter Counter data for the same samples show particle counts in the range of 10^{11} particles per gram (see Radian Technical Note # 200-187-11-2 for further discussion of these results). Until the discrepancy between these two methods is resolved, an average nucleation rate of 10^{10} particles per gram of sludge produced can be used in the modeling effort.

For crystal growth a general rate equation of the form:

$$R(\text{meter/sec}) = \frac{1}{1/k_m + 1/k_r} (r-1)^p \qquad (5\text{-}3)$$

is suggested by the literature. Experimental data from laboratory and pilot scale scrubbings systems show that k_m, the bulk mass transfer rate constant, is much larger than k_r, the surface reaction rate constant. Also, k_r appears to be a function of particle size. For modeling purposes the following growth rate expression will be used:

$$R(\text{meter/sec}) = k_r(1 + \delta L)\ (r - 1)^p \qquad (5\text{-}4)$$

For limestone systems, sufficient experimental data were available to estimate values for the constants in Equation 5-4. k_r is approximately equal to $3\text{x}10^{-12}$ meter/sec with δ equal to $5\text{x}10^5$ meter $^{-1}$. At normal levels of supersaturation the exponent p is expected to be one.

For lime systems, Equation 5-4 does not adequately describe crystal growth. Additional data will be required to examine effects of liquor composition on growth rate of particles in lime systems.

After reviewing both theoretical and experimental aspects of calcium sulfite particle size distribution in lime/limestone wet scrubbing systems, we have found that sufficient information is not presently available to predict what process variables can be used to improve sludge quality. Specifically, the mechanism of particle generation must be identified before any rational approach to controlling particle size distribution can be devised. Thus, we recommend that the test plan document produced during this program be directed towards correlating nucleation rate as a function of important process variables identified in the present literature survey.

NOMENCLATURE

a - Chemical Activity

a_{sat} - Chemical Activity at Saturation

$\bar{a}$ - Interfacial Area (m^2/m^3)

A_c - Crystal-Crystal Contact Area (cm^2)

A_p - Particle Surface Area (cm^2)

C - Concentration (moles/liter)

C_b - Concentration in Bulk Phase (moles/liter)

CF - Clarifier Feed (liters/sec)

C_i - Concentration at Solid-Liquid Interface (moles/liter)

cm - Centimeters

CO - Clarifier Overflow (liters/sec)

C_s - Saturation Concentration (moles/ℓ)

CU - Clarifier Underflow (liters/sec)

D - Diffusivity (m^2/sec)

D_s - Stirrer Diameter (m)

D_t - Hold Tank Diameter (m)

E - Collision Contact Energy (ergs)

$\bar{E}$ - Agitation Power per Unit Mass of Slurry (ergs/gram)

FG - Flue Gas Rate (m^3/hr)

G - Particle Generation Term other than growth and convection (ℓ^{-1} sec^{-1})

g - gram

$\bar{G}$ - Molar Diffusion Rate (moles/sec)

G_g - Molar Growth Rate per Unit mass (moles/g sec)

G_m - Molar Growth Rate (moles/ℓ sec)

ΔG_S - Surface Free Energy Change (ergs)

ΔG_T - Total Free Energy Change (ergs)

ΔG_v - Volume Free Energy Change (ergs)

h - Experimental Exponent

NOMENCLATURE (continued)

i - Experimental Exponent

j - Experimental Exponent

K - Pre-exponential Constant (ℓ^{-1} sec^{-1})

$k, k_o, k'_o, k_1, k_2, k_3$ - Experimental Constants

k_a - Constant Relating Surface Area to the Square of the Characteristic Length, L^2

kg - Kilogram

k_m - Diffusion Rate Constant (m^2/sec)

k_r - Surface Reaction Rate Constant (m^2/sec)

K_{sp} - Solubility Product

k_v - Shape Factor

L - Characteristic Particle Length (m)

ℓ - Liters

LA - Limestone Additive Rate (ℓ/sec)

L_{eq} - Equilibrium Particle Length (m)

$\bar{L}_m$ - Mass Average Length (m)

$\bar{L}_n$ - Number Average Length (m)

m - Meters

m_s - Calcium Sulfite Coprecipitate Solids Concentration (g/ℓ)

MW - Molecular Weight (g/mole)

N - Number of Particles Per Slurry Volume (ℓ^{-1})

n - Number of Particles of Size L Volume (ℓ^{-1} m^{-1})

$\dot{N}$ - Number of Particles of Size L per Volume Leaving System (ℓ^{-1} sec^{-1})

$\bar{N}$ - Number of Nuclei Produced by Crystal-Crystal Collisions (collision^{-1})

n_o - Nuclei Concentration (ℓ^{-1})

$\dot{n}_o$ - Nucleation Rate (ℓ^{-1}sec^{-1})

Δn - Change in Number of Moles

p - Experimental Exponent

NOMENCLATURE (continued)

Q - Volumetric Flow Rate (ℓ/sec)
R - Linear Crystal Growth Rate (m/sec)
r - Relative Saturation
$\bar{R}$ - Gas Constant (atm ℓ/mole K^o)
SB - Scrubber Bottoms Flow Rate (ℓ/sec)
SF - Scrubber Feed Flow Rate (ℓ/sec)
SG - Stack Gas Flow Rate (m^3/hr)
ΔSO_2 - SO_2 Pickup (moles/sec)
T - Temperature (K^o)
$\bar{u}_i$ - Slurry Velocity in the ith direction (m/sec)
V - Slurry Volume (ℓ)
V_p - Particle Volume (m)
X - Length Dimension (m)
Y - Length Dimension (m)
Z - Length Dimension (m)

α - Experimental Constant
δ - Growth Constant (m^{-1})
σ - Surface Energy (ergs/m^2)
ρ_s - Slurry Density (g/ℓ)
μ_ℓ - Liquid Phase Chemical Potential
μ_ℓ^o - Standard State LIquid Phase Chemical Potential
μ_s - Solid Phase Chemical Potential
ν - Kingmatic Viscosity (m^2/sec)
τ - Mean Solids Residence Time (sec)

REFERENCES

AU-013 Austin, L. G., "Understanding Ball Mill Sizing", *Ind. Eng. Chem., Process Des. Develop. 12*(2), 121 (1973).

BO-144 Borgwardt, Robert H., *Sulfate Scale Control in Lime/Limestone Scrubbers by Unsaturated Operation*, Draft Report. Research Triangle Park, N. C., EPA, May 1974.

BO-146 Borgwardt, Robert H., *Limestone Scrubbing of SO_2 at EPA Pilot Scrubber*. Progress Report 15. Research Triangle Park, N.C., EPA, Feb. 1974.

BO-147 Borgwardt, Robert H., "EPA Pilot Plant Support at Research Triangle Park, N.C. Summary of research related to process improvement", Presented at the Industry Briefing on Progress at Shawnee Lime/Limestone Wet Scrubbing Prototype Facility, NERC, Research Triangle Park, N.C., Dec. 1973.

BO-272 Bond, Fred C., "Crushing and Grinding Calculations", 2 parts. Milwaukee, WS, Allis-Chalmers Manufacturing Company, Jan. 1961.

BO-241 Borgwardt, Robert H., "EPA/RTP Pilot Studies Related to Unsaturated Operation of Lime and Limestone Scrubbers", *Combustion 47*(4), 37-42 (1975).

BO-247 Borgwardt, Robert H., *Limestone Scrubbing of SO_2 at EPA Pilot Plant*. Progress Report 9. St. Louis, Mo., Monsanto Research Corp., April 1973.

BU-090 Buckley, H. E., *Crystal Growth*. Chapman and Hall, 1958.

CA-003 Canning, T. F. and A. D. Randolph, "Some Aspects of Crystallization Theory: Systems that Violate McCabe's Delta L Law", *AIChEJ 13* (1), 5-10 (1967).

CO-020 Collins, F. C. and J. P. Leineweber "The Kinetics of the Homogeneous Precipitation of Barium Sulfate", *J. Phys Chem. 60*, 389-94 (1956).

CR-163 Crowe, J. L. and S. K. Seale, *Processing Sludge: Lime/Limestone Sludge Characterization -- Shawnee Test Facility*, draft report. Chattanooga, TN and Muscle Shoals, AL, TVA, June 1977.

DA-006 Davies and Nancollas, "The Precipitation of Silver Chloride from Aqueous Solutions. Part 3. Temperature Coefficients of Growth and Solution", *Trans. Faraday Soc. 51,* 818-23 (1955).

ES-003 Estrin, Joseph, ed., *Crystallization From Solution*: *Nucleation Phenomena in Growing Crystal Systems*. AIChE Symposium Series 68(121). N.Y., AIChE, 1972.

GA-234 Garside, John, et al., "On Size-Dependent Crystal Growth", *I&EC Fund*. 15(3), 230-33 (1976).

GA-236 Garside, John, John W. Mullin, and Sibendu N. Das, "Growth and Dissolution Kinetics of Potassium Sulfate Crystals in an Agitated Vessel", *I&EC Fund. 13*(4), 299 (1974).

HA-696 Hargrove, O. W. and D. M. Ottmers, Review and Analysis of Louisville Gas and Electric Scrubbing System Data, final report. EPA Contract No. 68-02-1319, Task 30, Radian Project No. 200-045-30, Reviewed by W. E. Corbett and J. L. Phillips. Austin, Tx., Radian Corporation, December 1975.

IS-001 Ishii, T. and S. Fugita, Chem. Engr. (Japan 3(2), 236-81 (1965).

JO-R-214 Jones, Benjamin F., Philip S. Lowell, and Frank B. Meserole, Experimental and Theoretical Studies of Solid Solution Formation in Lime and Limestone SO_2 Scrubbers, final report. EPA 600/2-76-273a, EPA Contract No. 68-02-1883, Radian Project No. 200-144. Austin, Tx., Radian Corp., Oct. 1976.

KH-034 Khamskii, Eugenu V., Crystallization from Solutions. New York, Consultants Bureau, 1969. Translated by Alvin Tybulewicz.

LA-035 Larson, M. A., ed. Crystallization from Solution: Factors Influencing Size Distribution, CEP Symp. 67 (110), (1971)

LA-324 LaMantia, C. R., et al., Dual Alkali Test and Evaluation Program Vol. II, Laboratory and Pilot Plant Programs, final report. EPA Contract No. 68-02-1071, EPA 600/7-77-050b. Cambridge, MA, Arthur D. Little, Inc., May 1977.

LE-305 Levins, D. M. and J. R. Glastonbury, "Particle-Liquid Hydrodynamics and Mass Transfer in a Stirred Vessel", 2 pts. *Trans. Inst. Chem. Engrs. 50*, 32 (1972), pt. 1; *Trans. Inst. Chem. Engrs. 50*, 132 (1972), pt. 2.

LU-006 Lucchesi, Peter S., "Oscillometric Investigation of Precipitation and Dissolution Rates of Sparingly Soluble Sulfates", *J. Colloid Sci 11*; 113-123 (1956).

MC-012 McCabe, W. L., and R. P. Stevens, "Rate of Grwoth of Crystals in Aqueous Solutions", *CEP 47* (4), 168-74 (1951)

MO-311 Moore, Walter J., *Physical Chemistry*, 4th edition. Englewood Cliffs, NJ, Prentice-Hall, 1972.

MU-001 Mullin, J. W., *Crystallization*, Butterworths, London, 1961.

NA-015 Nancollas and Purdie, "Crystallization of Barium Sulfate in Aqueous Solution", *Trans. Farad. Soc. 59*, 735 (1963).

NA-016 Nancollas and Purdie, *Trans. Farad. Soc. 57*, 2272 (1961).

NI-001 Nielsen, A. E., *Kinetics of Precipitation*. Pergamon Press, Oxford, 1964.

OT-R-023 Ottmers, D. M., Jr., et al., *A Theoretical and Experimental Study of the Lime/Limestone Wet Scrubbing Process*. PB 243-399/AS, EPA 650/2-75-006, EPA Contract No. 68-02-0023. Austin, Tx., Radian Corp., 1974

PH-050 Phillips, V. Roger and Norman Epstein, "Growth of Nickel Sulfate in a Laboratory-Scale Fluidized-Bed Crystallizer", *AIChE 20*(4), 678 (1974).

RA-060 Randolph, Alan D. and Maurice A. Larson, *Theory of Particulate Processes. Analysis and Techniques of Continuous Crystallization*. New York, Academic, 1971.

RA-432 Randolph, Alan D. and Michael D. Cise, "Nucleation Kinetics of the Potassium Sulfate-Water System", *AIChE J. 18*(4), 798 (1972).

RO-344 Rousseau, R. W. and M. A. Larson, eds., *Analysis and Design of Crystallization Processes*. AIChE Symposium Series 72(153). NY, AIChE, 1976.

RO-362 Rossoff, J., et al., *Disposal of By-Products From Nonregenerable Flue Gas Desulfurization Systems*, second progress report. EPA Contract No. 68-02-1010, EPA-600/7-77-052. Los Angeles, CA, Aerospace Corporation, Environment and Energy Conservation Division, May 1977.

TI-006 Ting, H. H., and W. L. McCabe "Supersaturation and Crystal Formation in Seeded Solutions", *I&EC 26*, 1201-07 (1934).

WA-339 Walton, A. G., "Principles of Precipitation of Fine Particles", in *Dispersion Powders and Liquids*, 2nd ed., G. D. Parfitt, ed. New York, Halsted Press, 1973, pp. 175-220

WE-331 Wey, J. S. and J. P. Terwilliger, "On Size-Dependent Crystal Growth Rates", AIChE J. 20(6), 1219 (1974).

DCN #78-200-187-11-12

APPENDIX B

AN ANALYSIS OF CRYSTALLIZATION DYNAMICS AND PARAMETER SENSITIVITY IN LIME/LIMESTONE WET SCRUBBING SYSTEMS

Technical Note 200-187-11-03

17 February 1978

Prepared for:

Robert H. Borgwardt
Industrial Environmental Research Laboratory RTP (MD-61)
U. S. Environmental Protection Agency
Research Triangle Park,
North Carolina 27711

Prepared by:

Kenneth A. Wilde

Reviewed by:

Philip S. Lowell
D. M. Ottmers, Jr.

TABLE OF CONTENTS

Page

1.0 SUMMARY B-1

2.0 RECOMMENDATIONS B-7

3.0 DISCUSSION OF MODELS B-8
- 3.1 Scrubber/Hold Tank/Clarifier Model B-8
- 3.2 Simplified Hold Tank/Clarifier Model B-17

4.0 MODEL PARAMETER SENSITIVITY STUDIES B-31
- 4.1 Computer Program B-31
- 4.2 Discussion of Input Parameters B-32
- 4.3 Parameter Variation Studies B-35

5.0 REFERENCES B-50

6.0 NOMENCLATURE B-51

APPENDIX A - PROGRAM DESCRIPTION B-53

LIST OF FIGURES

Figure		Page
3-1	Process Flow Sheet for a Lime or Limestone Scrubbing System	B-9
3-2	Simplified Cyrstallization Model	B-18
4-1	Population Density vs Particle Size	B-38
4-2	Average Particle Size vs Growth Rate Parameter, p_{CF}	B-39
4-3	Average Particle Size vs Clarifier Cut-off Size	B-40
4-4	Relative Saturation, Particle Size and Precipitation Rate vs Solids Residence Time	B-42
4-5	Mass Average Crystal Size and Relative Saturation vs Solids Residence Time (Hold Tank Volume) at Constant SO_2 Removal, 10 Weight Percent Solids	B-43
4-6	Mass Average Crystal Size and Calcium Sulfite Relative Saturation Weight Percent vs Solids in Clarifier Feed W_{CF} at Constant SO_2 Removal and Hold Tank Volume	B-44
4-7	Particle Size and Precipitation Rate vs Growth Rate-Size Slope	B-46
4-8	Precipitation Rate vs Growth Rate Constant	B-47

LIST OF FIGURES (continued)

Figure   Page

4-9 Particle Size and Precipitation Rate *vs* Nucleation Rate Constant.................... B-48

LIST OF TABLES

Table   Page

4-1 Sample Computer Program Output, Typical Particle Size.............................. B-36

4-2 Sample Computer Program Output, Small Particle Size.............................. B-37

1.0 SUMMARY

This technical note presents a study of models for calculating calcium sulfite particle size distribution in lime/limestone SO_2 scrubbing systems. Particle size plays a key role in determining sludge handling and disposal characteristics. The objective of this study was to explore the feasibility of predicting the effects of system parameters on sludge properties. Equations were developed for the particle size distributions in a coupled scrubber/hold tank/clarifier. For the case of precipitation in the scrubber, the general model could be simplified. In this case just the hold tank and clarifier were considered since precipitation was negligible in the scrubber. Closed analytical solutions were possible.

A computer program was written to implement the simplified model equations. A limited parameter study of the model characteristics was made. The lack of applicable rate data prevented definitive evaluation of the model. The rate parameters in the model must be determined to assess its ultimate utility and indicate possible refinements.

The basic particle balance equations which determine particle size distribution were discussed in Technical Note (#200-187-11-01). Nucleation and growth rate phenomena were also discussed. This current note is a continuation and implementation of those ideas. The basic model structure involves equations for all process units considered together. Critical unit interactions can then be studied. Closed analytical solutions of the equations are thus more likely than in a separate unit approach.

The system equations have markedly different behavior depending on whether there is precipitation or dissolution of calcium sulfite in the scrubber. These two cases occur when the scrubber is supersaturated or subsaturated with respect to calcium sulfite. Other general model features include a clarifier which separates particles at a given size, without precipitation or reaction. Particle growth rate is considered to be either constant or a linear function of particle size.

The case of supersaturation with precipitation of calcium sulfite in the scrubber was considered for a well-mixed scrubber. It was found that precipitation in the scrubber was negligible compared to that in the hold tank. The well-mixed approximation is best for longer residence time scrubbers such as the marble bed or turbulent contacting type. Thus, precipitation for shorter residence time scrubbers should also be negligible. The added complexity of another variable to describe precipitation and SO_2 pick-up along the scrubber is avoided.

The case of subsaturation with dissolution of calcium sulfite in the scrubber presents some special problems. There is an almost total lack of data on particle dissolution rates. The nature of the solutions of the particle balance equations for dissolution in the scrubber also presents some mathematical problems. In particular, more must be known of the particle size dependence of dissolution rate to resolve the problems with the theory. The possibility of smaller particles dissolving faster than larger ones in the scrubber is suggested. Larger particle sizes in the clarifier underflow sludge could result from dissolution of small particles in the scrubber. It was not possible to pursue the dissolution case any further, due to limitations in the data and scope of effort.

The model which has been developed and tested is a simplified one for just the hold tank and clarifier. It is applicable to the case of negligible precipitation in the scrubber.

It is not applicable to subsaturation and dissolution of calcium sulfite in the scrubber. The model is defined by the following features and assumptions:

- there is negligible change in solids in the scrubber,
- the clarifier divides particles at a given size, with no precipitation,
- growth rate is either a linear function of particle size or is constant,
- zero-size growth rate is a power function of relative saturation, and
- nucleation rate is a power function of relative saturation and molar solids concentration.

It was possible to derive closed analytical solutions for all quantities of interest. The case of constant growth rate could not be derived by specialization of the results for the linear case. Separation equations were necessary. Equations were derived for the clarifier feed particle size distribution, average particle size, total solid concentration, and total precipitation rate.

The equations for the general case of non-clear clarifier overflow are algebraically cumbersome. To illustrate the properties of the model, some simplified equations for the case of clear clarifier overflow will be given. A basic result is the relationship for the number of particles of a given size, the particle size distribution. For particle growth rate as a linear function of size, the result is

$$n/n_o = \frac{1}{(1 + \gamma L)^{1+\frac{1}{\gamma R_o T_{CF}}}} \qquad (1\text{-}1)$$

where:

n = number of particles per unit volume of a given size, L, no./ℓ/micron,
n_o = particles of zero size, no./ℓ/micron,
L = particle size, microns,
γ = slope of the growth rate - particle size relation,
R_o = growth rate at zero size, and
T_{CF} = solids residence time.

The number of particles, n, decreases monotonically with increasing particle size, L, starting at essentially zero size. These zero size particles come from nucleation. The rapidity of this decrease is greater for smaller values of γ, R_o, and T_{CF}. The average particle size would be correspondingly smaller.

An expression for the mass average particle size of the clarifier feed, $\bar{L}_{CF}$, is:

$$\bar{L}_{CF} = \frac{6^{1/3} R_o T_{CF}}{\left[(1-\gamma R_o T_{CF})(1-2\gamma R_o T_{CF})(1-3\gamma R_o T_{CF})\right]^{1/3}} \qquad (1\text{-}2)$$

If the growth rate R is independent of particle size, γ=0, and Equation (1-2) reduces to

$$\bar{L}cf = 6^{1/3}\ R_o T_{CF} \qquad (1\text{-}3)$$

Thus, larger particle sizes are favored by longer solids residence times and higher particle growth rates. The same result is true for $\gamma \neq o$, except dependence is stronger for larger positive values for γ.

Another significant result is a relation between the total precipitation rate, G, moles/ℓ/min, and the total solids concentration, M_T, moles/ℓ:

$$G/M_T = 1/T_{CF} \tag{1-4}$$

The relation of G/M_T to the growth rate can be shown by substituting for T_{CF} from Equation (1-3):

$$G/M_T = 6^{1/3}R_o/\bar{L} \tag{1-5}$$

Most of the data on calcium sulfite precipitation is reported as correlations of G/M versus relative saturation. The present results indicate that meaningful rate parameters cannot be found unless particle sizes are measured.

The simplified hold tank/clarifier model has been programmed, including non-clear clarifier overflow and both constant and linear growth rate laws. The program is a relatively simple one since analytical solutions are possible. The input parameters include relative saturation, solids residence time, and nucleation and growth rate parameters. Outputs include average particle size, molar precipitation rate, and particle size distribution. The program can be used along with data-fitting programs to deduce crystallization rate parameters. Given the rate parameters, it can be used in an iterative fashion to find inputs such as relative saturation and solids residence time for required outputs such as net precipitation rate (SO_2 pick-up). The program can also be used as a subroutine of a complete SO_2 scrubbing system simulation.

Almost no rate data were available either for nucleation or growth. Physically reasonable results for particle sizes were obtained with typical system parameters and order of magnitude rate parameters. Additional data are required to verify the model further.

Parameter studies were made to illustrate the use of the model and the interrelations of the rate and system parameters. An example is given of determination of hold tank size for a given maximum relative saturation and total SO_2 pick-up rate.

2.0 RECOMMENDATIONS

More bench and pilot scale work is needed to define both nucleation and growth rate parameters. Particle size distributions must be measured to have useful data.

The bench and pilot unit data should be correlated with the model. The computer program should be used as a subroutine of widely available non-linear curve-fitting programs. Then rate parameters can be deduced from particle size distributions and total solids concentrations.

The model should be extended to include growth rate-size relations intermediate between constant and linear in particle size. Incorporation of the model into complete SO_2 scrubbing system simulations should be explored.

Scrubber dissolution of fines could be examined as a possibility of increased sludge particle size. Further definition of this aspect will require considerably more work, both experimental and modeling. Since dissolution is much faster than precipitation, its study on a pilot scale may not be feasible. The best approach may be bench scale dissolution rate studies to provide data for resolution of the present model's problems with the dissolution case.

The basis of hold tank sizing should be reexamined. The present model provides a better basis for system design than conventional methods. Although rate parameters in the model are not yet known, a better use of available information should be possible.

3.0 DISCUSSION OF MODELS

The coupled scrubber/hold tank/clarifier system forms the basis of the first model. Two sub-cases for this model will be discussed: precipitation or dissolution of calcium sulfite in the scrubber. The system equations for these two possibilities have a different nature. Examination of the case of precipitation in the scrubber indicates that precipitation of $CaSO_3$ in the scrubber is negligible compared to precipitation in the hold tank. The case of negligible precipitation in the scrubber leads to a simplified model for just the hold tank and clarifier. Equations for the quantities of interest for this simplified model will be derived. Implementation of the simplified model is discussed in Section 4.

3.1 Scrubber/Hold Tank/Clarifier Model

The "typical" lime or limestone scrubbing system discussed in Technical Note #200-187-11-01 will be the basis for this section. A schematic flow sheet is shown in Figure 3-1. Both the scrubber and hold tank will be modeled as "perfectly stirred tanks". That is, the mixing will be rapid enough compared to reaction and crystallization so that an essentially uniform composition prevails. This idealization will usually be reasonable for hold tanks. It is also reasonable for certain types of scrubbers such as the turbulent contacting adsorbers (TCA).

Residence times for TCA scrubbers are considerably longer than for Venturi scrubbers, for example. The result found for negligible precipitation in a well-mixed scrubber would certainly hold true for those which are not well-mixed but have lesser residence times. Thus, the problem is avoided of modeling scrubbers with an added variable for precipitation along the length of the scrubber. The model in that case would be much more difficult to solve computationally.

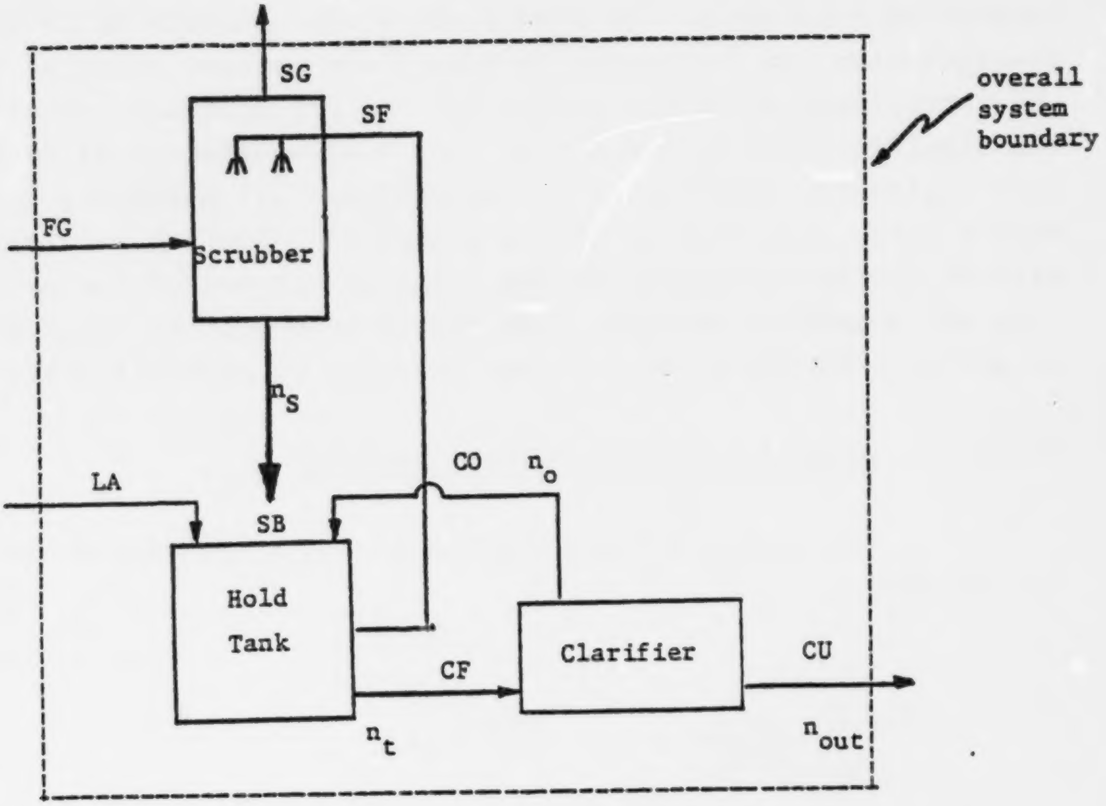
SG
SF
overall system boundary
FG
Scrubber
n_S
LA
SB
CO
n_o
Hold Tank
Clarifier
CU
CF
n_t
n_{out}

Figure 3-1. Process Flow Sheet for a Lime or Limestone Scrubbing System.

The basic particle balance equations have been discussed in the Technical Note # 200-187-11-01. Oxidation will not be considered explicitly. An amount of calcium sulfate up to the co-precipitation limit of about 15 mole % can be considered by using the appropriate molecular weight for the precipitated crystals. The clarifier will be treated as just a size separations device with negligible reaction or precipitation. All particles greater than a given size will go in the underflow. Smaller particles will be divided according to the relative volumes of the overflow and underflow streams. The growth rate will be considered as either constant or as a linear function of particle size.

3.1.1 General Particle Balance Equation

The particle balance equation for a well-mixed vessel is (RA-060):

$$\frac{d(Rn)}{dL} + \sum \frac{n_j}{T_j} + D(L) = \sum \frac{n_i}{T_i} + B(L) \qquad (3\text{-}1)$$

where:

R = linear growth rate, microns/min
n = particle population density, no./liter/micron
L = length (size) characterizing particle growth, microns
T_j = characteristic time for output stream j, minutes
T_i = time for input stream i, minutes
B = rate of birth of particles, no./liter/micron/min
D = rate of disappearance of particles, no./liter/micron/min

The formation of crystals of size L by other than growth and convection has been divided into birth and death functions, B and D. The lefthand terms are the output from the slurry volume of particles of a size L by crystal growth, bulk convection and particle death. The righthand side has terms for inputs by convection and birth.

The characteristic times, T, are defined as V/Q, the vessel volume divided by the volumetric flow rate of the particular stream. They are not necessarily residence times. Equation (3-1) is a steady-state balance in the (single) dimension of particle size. The vessel is also assumed to be at steady-state with respect to the conventional material balances, including numbers of particles. However, in this Note the term particle balance will refer to relations such as Equation (3-1).

The birth and death functions represent the effects of crystal breakage and attrition. They are even less well characterized than other aspects of crystallization. Randolph and Larson (RA-060, p. 121) considered in a general approximate way the case of breakage into equal pieces. This produces the maximum effect on the form of the crystal size distribution. The relative number of smaller particles remained about the same, while larger particle numbers were appreciably reduced. The limit of smaller and smaller fragments breaking off represents crystal attrition. The net effects of attrition were an apparent increase in nucleation, decrease in growth rate, possible rounding of crystals, and no major change in the form of the crystal size distribution.

The birth and death functions, B and D, will be taken as zero. The particle size change effects considered will be net effects including such terms. Separate consideration is not feasible within the scope of this work.

3.1.2 Scrubber/Hold Tank Equations

It is essential in modeling the scrubber/hold tank combination to recognize that the output of one is the input of the other. The conventional approach is to consider separate models and equations for each process unit. Here the close interaction of the equations for scrubber and hold tank would cause vital model details to be lost in the separate unit approach. Also, the opportunity for closed analytical solutions without iteration would be lost.

In order to demonstrate the nature of the model including the scrubber, two further simplifications will be made: growth rate independent of particle size and no particles in the clarifier overflow, i.e., perfect clarification. Implications of these approximations will be noted. There is an equation of the form of (3-1) for both the scrubber and hold tank:

$$V_S \frac{d(R_S n_S)}{dL} + Q_{SB} n_S = Q_{SF} n_\tau \qquad (3\text{-}2)$$

$$V_\tau \frac{d(R_\tau n_\tau)}{dL} + Q_\tau n_\tau = Q_{SB} n_S \qquad (3\text{-}3)$$

where the subscripts s and τ are for scrubber and hold tank. SB and SF represent scrubber bottoms and feed. If the clarifier overflow were not clear, a term $Q_{CO} n_{CO}$ would be added to the right hand side of (3-3). The overflow particle size distribution would be some fraction of the clarifier feed n_{CF} (or n_τ). For constant growth rates R, Equations (3-2) and (3-3) can be written as:

$$\frac{dn_S}{dL} + an_s - a'n_\tau = 0 \qquad (3\text{-}4)$$

$$\frac{dn_{\tau}}{dL} + bn_{\tau} - cn_{S} = 0 \qquad (3\text{-}5)$$

where:

$$a = Q_{SB}/R_{S}V_{S} = 1/R_{S}T_{SB}$$
$$a' = Q_{SF}/R_{S}V_{S} = 1/R_{S}T_{SF}$$
$$b = Q_{\tau}/R_{\tau}V_{\tau} = 1/R_{\tau}T_{\tau}$$
$$c = Q_{SB}/R_{\tau}V_{\tau} = 1/R_{\tau}T_{s\tau}$$

We thus have two first-order ordinary differential equations in the two particle size distributions n_S and n_{τ}, for the scrubber and hold tank. The boundary conditions $n_S(o)$ and $n_{\tau}(o)$ are found from the nucleation rate B_o and the zero size growth rate R_o (RA-060, p. 70):

$$n(0) = B_o/R_o \qquad (3\text{-}6)$$

For R independent of L, the coefficients a, a', b and c are constants. Then the equations have a relatively simple analytical solution. If R is a function of the particle size, L, the coefficients are functions of the dependent variable, L. Then they have no general analytical solution.

3.1.3 Nature of the Solutions and Characteristic Roots

The solution of a set of simultaneous linear first-order differential equations can be found by several standard methods (PE-030, p. 38, MA-766). It involves a sum of exponential terms:

$$n_S = C_1 e^{m_1 L} + C_2 e^{m_2 L} \qquad (3\text{-}7)$$

$$n_\tau = \frac{C_1 e^{m_1 L}}{a'} (m_1 + a + \frac{C_2 e^{m_2 L}}{a'} (m_2 + a) \qquad (3\text{-}8)$$

where C_1 and C_2 are constants to be determined from the boundary conditions $n_S(0)$ and $n_\tau(0)$:

$$n_S^o = n_S(0) = C_1 + C_2 \qquad (3\text{-}9)$$

$$n_\tau^o = n_\tau(0) = \frac{1}{a'} \left[C_1(m_1 + a) + C_2(m_2 + a) \right] \qquad (3\text{-}10)$$

Solving Equations (3-9) and (3-10) for C_1 and C_2,

$$C_1 = \frac{(m_2 + a)\, n_S^o - a' n_\tau^o}{m_2 - m_1} \qquad (3\text{-}11)$$

$$C_2 = \frac{a' n_\tau^o - C_1(m_1 + a)}{m_2 + a} \qquad (3\text{-}12)$$

m_1 and m_2 are the roots of a quadratic involving the coefficients of the original differential Equations (3-4) and (3-5):

$$m = \frac{-(a + b) \pm \sqrt{(a + b)^2 - 4(ab - a'c)}}{2} \qquad (3\text{-}13)$$

Thus, the complete solution for the particle size distributions is contained in Equations (3-7, 8, 11, 12, 13). Neither of the exponential terms or roots m_1 and m_2 can be identified with the scrubber or hold tank. Both are necessary for both process units. The nature of the solutions is profoundly affected by the signs of the roots m_1 and m_2 in the exponents. From the general expression for the product of the roots of any quadratic,

$$m_1 m_2 = ab - a'c = \frac{Q_{SB}(Q_\tau - Q_{SF})}{R_S V_S R_\tau V_\tau} \qquad (3\text{-}14)$$

Since Q_τ is the total hold tank outflow and Q_{SF} is that part going to the scrubber, $Q_\tau - Q_{SF}$ must always be positive. Thus, the sign of the proudct $m_1 m_2$ depends on the particle size change rates R_τ and R_S. Precipitation must occur in the hold tank for the system to work at all, i.e., R_τ must be positive. The root product $m_1 m_2$ must then have the same sign as R_S, the scrubber growth (R_s is +) or dissolution (R_s is -) rate.

It can also be shown that the roots m_1 and m_2 cannot be imaginary. The quantity under the radical in Equation (3-13) can be written as:

$$(a - b)^2 + 4\, a'c, \qquad (3\text{-}15)$$

which cannot be negative for $R_S>0$, since a' and c are positive. If $R_S<0$, a and a' will be negative. The sum in Equation (3-15) will still be positive, since the square of sum of a and b will be greater than $4a'c$. We are thus assured that the exponent terms will not be complex. The solutions in that case would contain sine/cosine terms according to DeMoivre's Theorem:

$$e^{i\theta} = \cos\theta + i \sin\theta \qquad (3\text{-}16)$$

The solutions with all real roots will be stable with no "wiggles" in the particle size distributions.

The consequences of the above will be considered first for precipitation, then for dissolution in the scrubber.

3.1.4 Precipitation in the Scrubber

Here the roots m_1 and m_2, of the same sign, must both be negative. The radical in Equation (3-13) must be less than

$(a + b)^2$, since $ab - a'c$ is positive. Therefore, the root for the plus radical sign must also be negative, as well as the other one for the negative sign. We are thus assured that the particle size distributions will decrease monotonically with increasing particle size, L, and approach zero as L approaches infinity. This aspect is important in integration of particle size distributions to obtain other quantities.

The foregoing equations can be used to relate crystallization to process conditions. Overall material balances provide other relations. The relation between solution supersaturation is provided by an aqueous ionic equilibrium computer program, such as those developed by Radian (LO-007). The complete scrubbing system can then be simulated, at least insofar as the crystallization is concerned.

A computer program was written to solve the resulting set of non-linear algebraic equations. The equations for constant R were used for varying R by dividing the size range into a number of parts, each with a different constant R. A pair of constants C_1 and C_2 results for each size division. The resulting additional computation is still much less than a numerical solution. Details will not be given here as complete solutions were not obtained. It was discovered that the precipitation in the scrubber is small enough compared to the hold tank to prevent numerical solution of the complete problem. In any case, the problem can be simplified by considering only the hold tank and clarifier, as shown in Section 3.2.

3.1.5 Dissolution in the Scrubber

It has been recognized in practice that sometimes the scrubber may be subsaturated with respect to $CaSO_3$. Dissolution would then take place in the scrubber with precipitation in the supersaturated hold tank still occurring. Returning to the product of roots, Equation (3-14), m_1 and m_2 must be of opposite sign if R_S is negative for dissolution in the scrubber. This means that one of the exponential terms will increase with increasing L. There would be no bounds on integrals over the particle size distribution as L goes to infinity. Unfortunately very little is known about dissolution rates except that they are presumably much faster than precipitation. Thus there could be appreciable dissolution in the short residence times in scrubbers. Also, it appears that dissolution cannot continue to larger sizes for finite particle size distributions. An intriguing possibility is that smaller sizes may dissolve more rapidly than large ones. Operation of the scrubber subsaturated would then be a means to increase particle size and sludge qualities. More definitive data on dissolution rates are needed to investigate this possibility. It could not be pursued further in this program.

3.2 Simplified Hold Tank/Clarifier Model

The model in this section is depicted in Figure 3-2. It has the following characteristics:

- negligible solids change in the scrubber,
- clarifier divides particles at given size,
- growth rate a linear function of L (or constant), and
- relative saturation a given input quantity.

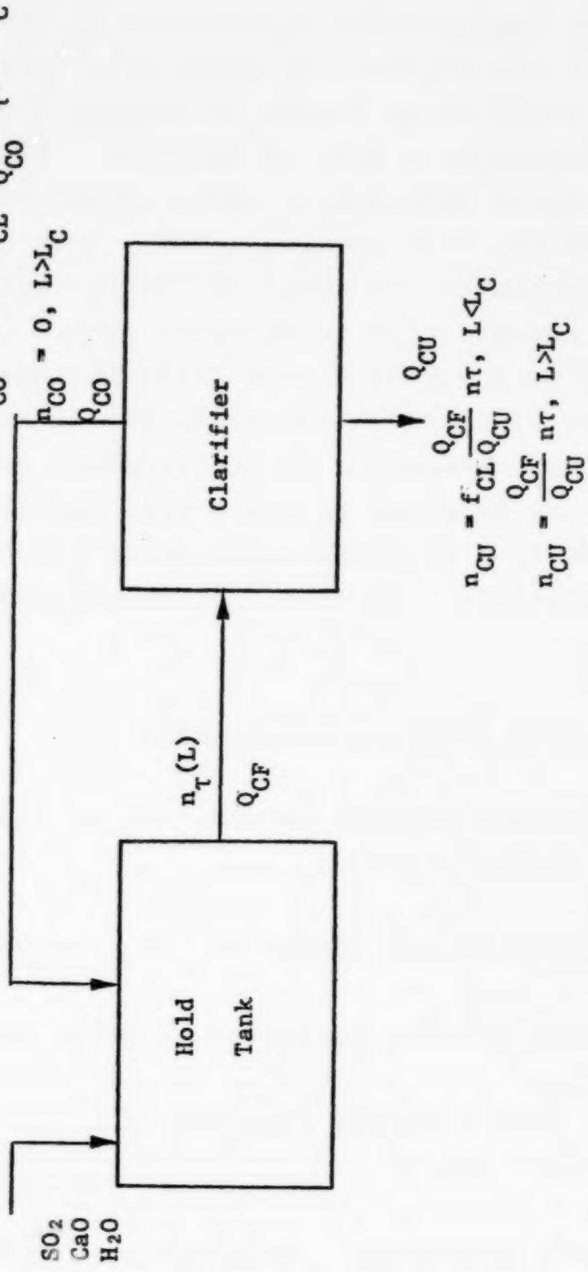
SO_2
CaO
H_2O
Hold
Tank
$n_\tau(L)$
Q_{CF}
Clarifier
$n_{CO} = (1 - f_{CL}) \frac{Q_{CF}}{Q_{CO}} n_\tau, L<L_C$
$n_{CO} = 0, L>L_C$
Q_{CO}
Q_{CU}
$n_{CU} = f_{CL} \frac{Q_{CF}}{Q_{CU}} n\tau, L<L_C$
$n_{CU} = \frac{Q_{CF}}{Q_{CU}} n\tau, L>L_C$

Figure 3-2. Simplified Crystallization Model.

The hold tank has two feeds: (1) a sulfite stream from the SO_2 picked up in the scrubber and (2) calcium from the lime or limestone addition. Thus, the key species in the feed streams are total sulfite (SO_2), total calcium (CaO), and water (H_2O). Precipitation takes place to form calcium sulfite hemihydrate, $CaSO_3 \cdot \frac{1}{2}H_2O$.

The circulating loop between the scrubber and hold tank is ignored. No material balances are used. The model is intended to display the interrelationships of the parameters. If enough of the parameters can be defined by future experimental programs, the present model can be used with other relations to simulate hold tank precipitation and clarifier underflow sludge qualities. From Equation (3-1), the hold tank particle balance is

$$\frac{d(nR)}{dL} + \frac{n}{T_{CF}} = \begin{cases} \frac{n_{CO}}{T_{CO}}, & L < L_C \\ 0, & L > L_C \end{cases} \qquad (3\text{-}17)$$

$$T_{CF} = V_\tau / Q_{CF}, \; T_{CO} = V_\tau / Q_{CO}$$

The subscript τ on n and R is dropped in this section.

3.2.1 Clarifier Model

The clarifier particle size distribution for particles less than L_C is found by dividing them according to the ratio of clear overflow and underflow volumes. Particles greater than L_C

all go to the underflow. Since n is a concentration, the particle distribution greater than L_C in the underflow is described by:

$$n_{CU} = \frac{Q_{CF}}{Q_{CU}} n_\tau, \; L>L_C \tag{3-18}$$

The n_{CU} less than L_C is less than that in Equation (3-18) by the ratio of the clear liquid volumes, approximately:

$$n_{CU} = \frac{(Q_{CU})\text{ clear}}{(Q_{CF})\text{ clear}} \cdot \frac{Q_{CF}}{Q_{CU}} \cdot n_\tau, \; L<L_C \tag{3-19}$$

The ratio of clear volumes is found from the clear volume fraction in the clarifier underflow, Y_{CU}:

$$Y_{CU} = \frac{\left(\frac{1 - W_{CU}}{W_{CU}}\right)\rho_P}{1 + \left(\frac{1 - W_{CU}}{W_{CU}}\right)\rho_P} \tag{3-20a}$$

$$\frac{(Q_{CU})\text{ clear}}{(Q_{CF})\text{ clear}} = \frac{Q_{CU}\,Y_{CU}}{(Q_{CF} - Q_{CU}) + Q_{CU}\,Y_{CU}} \tag{3-20b}$$

It is assumed in Equation (3-20b) that the volume of solids in the clarifier overflow is negligible. W_{CU} is the overall weight fraction solids in the clarifier underflow. ρ_P is the particle (crystal) density. If the complete Equation (3-20) were used, the model would have to be solved iteratively. W_{CU} is an output and would require an initial estimate to be corrected and converged on. Since the clarifier separation is arbitrary anyway, it was decided to simplify Equation (3-20) to eliminate

W_{CU} by using a typical value of 0.5. The split of the small particles is not sensitive to the value of W_{CU} and a reasonable approximation will result:

$$n_{CU} \cong \left[\frac{\frac{\rho_p}{1 + \rho_p}}{\frac{Q_{CF}}{Q_{CU}} - 1 + \frac{\rho_p}{1 + \rho_p}} \right] \frac{Q_{CF}}{Q_{CU}} n_\tau \qquad (3\text{-}21)$$

The quantity in brackets is subsequently defined as f_{CL}. The particle distribution in the overflow is then:

$$n_{CO} = (1 - f_{CL}) \frac{Q_{CF}}{Q_{CO}} n_\tau \qquad (3\text{-}22)$$

3.2.2 Solution for Particle Size Distribution

For the linear growth rate law,

$$R = R_o(1 + \gamma L) \qquad (3\text{-}23)$$

the particle balance, Equation (3-17) becomes:

$$\frac{dn}{dL} + \frac{n}{1 + \gamma L} \left[\gamma + \frac{f_{CL}}{T_{CF} R_o} \right] = 0 \qquad (3\text{-}24)$$

where γ is the slope of the R vs. L relation, in (microns)$^{-1}$, and $f_{CL} = 1$ for $L > L_C$. The time T_{CF} is the ratio of hold tank volume and clarifier feed rate. It is often referred to as the solids residence time. It is the important time parameter, rather than the residence time as determined by the total circulating liquor volume.

Equation (3-24) is readily integrated to give the particle size distribution of the clarifier feed.

$$n = n_o\left[\frac{(1 + \gamma L_C)^{p_{CF} - p_{CU}}}{(1 + \gamma L)^{p_{CF} + 1}}\right], \; L > L_C \tag{3-25a}$$

$$n = n_o(1 + \gamma L)^{-p_{CU}-1}, \; L < L_C \tag{3-25b}$$

$$p_{CF} = \frac{1}{\gamma R_o T_{CF}}, \; p_{CU} = f_{CL} p_{CF} \tag{3-25c}$$

Equation (3-25) is a power law relationship rather than the usual exponential one for constant R. This is a consequence of the linear growth rate, Equation (3-23). The n - L relation is monotonically decreasing but not a straight line on a semi-log plot. The zero size growth rate is taken as an empirical function of relative saturation, r, of $CaSO_3 \cdot \frac{1}{2}H_2O$:

$$R_o = k_{GR}(r - 1)^{i_{GR}}, \tag{3-26}$$

where k_{GR} and i_{GR} are growth rate constants. A similar function is used for the nucleation rate, B_o, with an added term for the total $CaSO_3$ crystal density, M_T, in moles/liter:

$$B_o = k_{SN}(r - 1)^{i_{SN}} M_T^{j_{SN}} \tag{3-27}$$

where SN represents secondary nucleation, the presumably predominant nuclei formation mode. The zero-size population density is given by Equation (3-6), B_o/R_o:

$$n_o = \frac{k_{SN}}{k_{GR}}(r - 1)^{i_{SN} - i_{GR}} M_T^{j_{SN}} \tag{3-28}$$

Other quantities of interest derived from the particle size distribution include M_T, total crystal concentration in moles/liter, precipitation rate, G, in moles/ℓ/min, and mass average particle size, $\bar{L}$, in microns. Expressions for these quantities will be derived for the particle size distribution, n(L), given by Equations (3-25).

3.2.3 Total Crystal Concentration

M_T is found by integrating n(L) times the mass of an individual particle:

$$M_T = \frac{\rho_p k_v}{MW} \int_o^\infty L^3 n(L)\,dL \tag{3-29}$$

where k_v is the factor converting L^3 to particle volume. k_v is $\pi/6$ for a sphere. The integration is carried out from zero to L_C using Equation (3-25a) and from L_C to infinity using Equation (3-25b).

$$M_T = f_\rho n_o \left[\int_o^{L_C} \frac{L^3 dL}{(1 + \gamma L)^{1 + p_{CU}}} + (1 + \gamma L_C)^{p_{CF} - p_{CU}} \int_{L_C}^\infty \frac{L^3 dL}{(1 + \gamma L)^{1 + p_{CF}}} \right] \tag{3-30}$$

where f_ρ is a factor lumping together $\rho_p kv/MW$. The result is:

$$M_T = \frac{f_\rho n_o}{\gamma^4}\left\{\left[\frac{(X_c^{3-p_{CU}} - 1)}{(3 - p_{CU})} - \frac{3(X_c^{2-p_{CU}} - 1)}{(2 - p_{CU})} + \frac{3(X_c^{1-p_{CU}} - 1)}{(1 - p_{CU})} + \frac{(X_c^{-p_{CU}} - 1)}{p_{CU}}\right]\right.$$

$$\left. - \frac{1}{X_c^{p_{CU}}}\left[\frac{X_c^3}{(3 - p_{CF})} - \frac{3X_c^2}{(2 - p_{CF})} + \frac{3X_c}{(1 - p_{CF})} + \frac{1}{p_{CF}}\right]\right\} \qquad (3\text{-}31)$$

where $X_c = 1 + \gamma L_c$. If $L_c = 0$ (clear clarifier overflow), a simpler equation for M_T can be found:

$$M_T = f_\rho n_o \int_o^\infty \frac{L^3 dL}{(1 + \gamma L)^{1 + p_{CF}}} \qquad (3\text{-}32)$$

The integral in Equation (3-32) can be written in terms of the Gamma and Beta functions (MA-766, DW-006):

$$\int_o^\infty \frac{u^{m-1} du}{(1 + u)^{m+n}} = B(m,n) = \frac{\Gamma(m)\cdot\Gamma(n)}{\Gamma(m + n)} \qquad (3\text{-}33)$$

where the Beta function B is defined in Equation (3-33) in terms of the Gamma function, Γ, which is defined as

$$\Gamma(p) = \int_o^\infty u^{p-1} e^{-u} du \qquad (3\text{-}34)$$

$$= (p-1)!, \text{ if } p \text{ is an integer.}$$

The parameters in Equation (3-32) can be identified with those in the integral in (3-33):

$$m = 4, \; p = p_{CF} - 3, \; u = \gamma L.$$

The results for M_T is

$$M_T = \frac{6f_\rho n_o}{\gamma^4 p_{CF}(p_{CF}-1)(p_{CF}-2)(p_{CF}-3)} \qquad (3\text{-}35)$$

The dependence of (secondary) nucleation on crystal density, M_T, means that M_T occurs in both input and output. However, it can be isolated to avoid iterations. From Equation (3-32) for M_T we have:

$$M_T = \frac{f_p B_o I(\gamma,\ p_{CF})}{R_o} \qquad (3\text{-}36)$$

where I is the integral over $\frac{n}{n}L^3 dL$, and n_o is replaced by B_o/R_o. Substituting Equation (3-27), the power law, for B_o and solving for M_T,

$$M_T = \left[\frac{f_\rho k_{SN}(r-1)^{i_{SN}}\ I\ (\gamma,\ p_{CF})}{k_{GR}(r-1)^{i_{GR}}}\right]^{\frac{1}{1-j_{SN}}} \qquad (3\text{-}37)$$

3.2.4 Average Particle Size

The mass average particle size, $\bar{L}$ is defined through M_T and N, the total number of particle/liter:

$$M_T = f_\rho N\bar{L}^3 \qquad (3\text{-}38a)$$

$$N = \int_o^\infty n\,dL \qquad (3\text{-}38b)$$

The particle concentration in the clarifier feed is found using $n_{CF} = n_\tau$ from Equation (3-25) in (3-36b):

$$\frac{N_{CF}}{T_{CF}} = n_o R_o \left[f_{CL}^{-1} - x_c^{-p_{CU}} (f_{CL}^{-1} - 1) \right] \tag{3-39}$$

$$\bar{L}_{CF} = \left(\frac{M_T}{f_\rho N_{CF}} \right)^{1/3} \tag{3-40}$$

$$= \left(\frac{M_T}{f_\rho n_o R_o T_{CF}} \right)^{1/3}, \quad L_c = 0 \tag{3-41}$$

The average sizes in the overflow and underflow are similarly found.

A check on the internal consistency of the model can be made by expressing the net nucleation rate as the particle concentration in the clarifier underflow times the underflow volumetric flow rate, divided by the hold tank volume:

$$B_o = \frac{N_{CU} Q_{CU}}{V_t} \tag{3-42}$$

If the expression in Equation (3-40) is evaluated for any L_c, we find

$$B_o = n_o R_o, \tag{3-43}$$

as expected.

3.2.5 Total Precipitation Rate

The total precipitation rate, G, moles/ℓ/ min, is found by integrating the particle size distribution times the particle area times the growth rate. The volume of a particle, v_p, is

$$v_p = k_v L^3 \qquad (3\text{-}44)$$

The single particle volumetric growth rate, dv_p/dt, is found as:

$$\frac{dv_p}{dt} = \frac{d(k_v L^3)}{dt} = 3k_v L^2 \frac{dL}{dt} \qquad (3\text{-}45)$$

The characteristic dimension L is usually taken as the particle diameter. The growth rate, dL/dt, is twice that needed to multiply the surface area to get the volume change. This is because the crystal diameter is growing twice as fast as the radius. We can define a factor k_a for area analogous to k_v:

$$a_p = k_a L^2 \qquad (3\text{-}46)$$

For spheres and other regular shapes, $k_a = 6k_v$, if L is the diameter. The volume change rate is then given by

$$\frac{dv_p}{dt} = \frac{k_a}{2} L^2 R = \frac{Ra_p}{2} \qquad (3\text{-}47)$$

dL/dt has been replaced by R. The factor of two appears because the growth rate defined in terms of particle diameter is twice that needed to go with particle surface area. Thus G can be written as

$$G = \frac{k_a \rho_p}{2(MW)} \int_o^\infty n(L)\ L^2 R(L) dL \qquad (3\text{-}48)$$

For the linear growth rate and clear clarifier overflow, an expression similar to that for M_T can be derived:

$$G = \frac{k_a \rho_p n_o R_o}{(MW)\gamma^3 (p_{CF}-1)(p_{CF}-2)(p_{CF}-3)} \qquad (3\text{-}49)$$

Since $k_a = 6k_v$, the ratio of G to M_T from Equations (3-47) and (3-35) is

$$G/M_T = 1/T_{CF} \qquad (3\text{-}50)$$

The same result is obtained for constant growth rate. A different result is found for the case of $L_c \neq 0$. However, the same considerations would apply to the net particle production, and are used in the equations for the parameter study in Section 3.

Equation (3-48) states that the total precipitation rate divided by the total crystal concentration is a function only of the solids residence time T_{CF}. This is unfortunate, since much of the crystallization rates reported for $CaSO_3$ are as the rate per unit mass of crystals, moles/gm/min. This quantity has ostensibly been correlated with relative saturation. The rate per unit mass would be different only by dividing the right-hand side of Equation (3-48) by the molecular weight. If the particles did not follow the relation $k_a = 6\,k_v$, we would have

$$G/M_m = \frac{k_a/6k_v}{(MW)\ T_{CF}} \qquad (3\text{-}51)$$

where the subscript m on M is for mass concentration. The reported quantity, G/M_m, is not expressable only in terms of either growth or nucleation rate. The relationship to growth rate can be shown by substituting a relation between average particle size and growth rate, such as Equation (3-39). For simplicity using a constant growth rate,

$$G/M_T = \frac{6^{1/3}R}{\bar{L}}, \; [R \neq f(L)] \tag{3-52}$$

One conclusion from the above results is that particle sizes must be determined in precipitation kinetics studies to deduce useful parameters. Another is that apparent correlations of G/M with relative saturations that do not have specific surface included are in fact reflections of residence time, variation of $k_a/6k_v$, or other factors not considered in the basic models.

3.2.6 Growth Rate Independent of Particle Size

The constant rate case cannot be deduced by specializing the linear one, but similar integrations are involved. The resulting equations are given below. Computations and parameter studies with both cases are given in Section 4.

$$n = n_o e^{-p_{CU}L}, \; L < L_c \tag{3-53}$$

$$n = n_o e^{(p_{CF}-p_{CU})L_c} \cdot e^{-p_{CF}L}, \; L > L_c \tag{3-54}$$

$$M_T = f_\rho n_o \left[\frac{6}{p_{CU}^4} - e^{-p_{CU}L_c}\left(\frac{L_c^3}{p_{CU}} + \frac{3L_c^2}{p_{CU}^2} + \frac{6L_c}{p_{CU}^3} + \frac{6}{p_{CU}^4} - \frac{L_c^3}{p_{CF}} - \frac{3L_c^2}{p_{CF}^2} - \frac{6L_c}{p_{CF}^3} - \frac{6}{p_{CF}^4}\right)\right] \tag{3-55}$$

$$M_T = 6 f_\rho n_o R^4 T_{CF}^{\,4} , \; L_c = 0 \tag{3-56}$$

$$G = \frac{k_a \rho_p}{MW} n_o R^4 T_{CF}^{\,3} , \; L_c = 0 \tag{3-57}$$

$$G/M_T = 1/T_{CF} , \; L_c = 0 \tag{3-58}$$

4.0 MODEL PARAMETER SENSITIVITY STUDIES

The equations derived in the previous section comprise closed analytical solutions to the particle balance equations. A computer program was written based upon these analytical solutions to specialized cases of the particle balance equation. This section discusses the model input and output quantities. Examples of use of the model are also discussed. The sensitivity of the model to both system and rate parameters is illustrated. Possible refinements to the model are indicated.

4.1 Computer Program

A computer program has been written in FORTRAN language for the equations of the hold tank/clarifier model of Section 3.2. The inputs and outputs are defined as follows:

INPUT

r = relative saturation with respect to $CaSO_3 \cdot \frac{1}{2}H_2O$
k_{GR}, i_{GR} = constants in the growth rate
k_{SN}, i_{SN}, j_{SN} = constants in the nucleation rate
γ = slope of growth rate/size function, $(\text{microns})^{-1}$
τ_{CF} = $V\tau/Q_{CF}$, minutes
τ_{CU} = V_τ/Q_{CU}, minutes
L_C = clarifier cut-off size, microns

OUTPUT

$n(L)$ = population density, particles/ℓ/ micron
$N_n(\Delta L)$ = number of particles per liter in a size range ΔL
$N_v(\Delta L)$ = volume of particles per liter in a size range ΔL

G_{CF} = net precipitation rate, moles/ℓ/min
W_{CF}, W_{CU} = weight % solids, clarifier feed and underflow
W_{CO} = ppm solids in the clarifier overflow
$\bar{L}_{CF}$, $\bar{L}_{CU}$, $\bar{L}_{CO}$ = mass average particle sizes, microns
B_o = nucleation rate, particles/ℓ/min

The above choice of dependent and independent variables was made to obtain a straight-forward, noniterative calculation. Thus, the program and equations can serve both to indicate relative parameter sensitivity and as a building block for further work. If some of the output variables were measured in a bench or pilot scale, the unknown nucleation and growth constants could be found. The present program would then be used as a subroutine in a nonlinear curve fitting program.

Another application would be the determination of required residence times and relative saturations for given values of precipitation rate (SO_2 pick-up) and circulating solids concentration. This would be an iterative calculation It would require knowledge of the input rate constants. Scrubber system behavior would be more closely simulated. A discussion of the input parameters will be followed by the results of the parameter variation runs. Further details of the program and a FORTRAN listing are given in the Appendix.

4.2 Discussion of Input Parameters

The equations for the model are set up without reference to any particular scrubbing system. The input parameters can be divided into two classes: operational and rate. The operational ones are relative saturation, r, solids residence time, T_{CF}; underflow residence time, T_{CU}; and clarifier overflow maximum size, L_C. The relative saturation will be treated as a free parameter here. In applications of the model, it would come from experimental data, material balances or other auxiliary conditions. A typical T_{CF} of one day was used in most of the present results. The T_{CU} value in practice might be determined by that necessary to give the desired solids content in the clarifier underflow. It affects the model only through the clarifier split factor, f_{CL}. A typical range value of 7-10 times T_{CF} was mainly used. The clarifier size L_C will, of course, be a function of the flows and times in the clarifier. Perhaps typical values of one-half to one micron were used, along with consideration of values down to zero.

The only direct information available on the rate parameters is that given in Technical Note #200-187-11-01 on the linear growth rate law. R_o and γ in Equation (3-23),

$$R = R_o(1 + \gamma L) \tag{3-23}$$

were deduced from experimental sludge particle size distributions. However, the approximate nature of both the data and the deduction of rate parameters from the data makes the result of only order-of-magnitude significance. It is encouraging that these rough values, along with typical other parameters, do give reasonable results for particle sizes. The value of gamma of 0.5 is similar to values in the literature for other crystals (RA-543).

The relative saturation dependence of both the growth and nucleation rates is not well-defined. As discussed in

Section 3.2, the reported linear correlations of precipitation rates with relative saturation are not meaningful. The dependence may be more or less linear, as indicated by some literature data on other crystals.

Also, the $CaSO_3$ relative saturation values are actually maximum ones based on limiting cases of aqueous ionic equilibrium programs. The linearity of the relationship between theoretical maximum relative saturations and actual values is a question which has not as yet been addressed. The relative saturation exponents for growth, i_{GR}, and nucleation, i_{SN}, were taken to be unity for most cases. The exponent on M_T, j_{SN} (as defined in Equation 3-28), is an important parameter, especially if it approaches one. The exponent of the RHS of Equation (3-37) is $1/(1 - j_{SN})$ which approaches infinity as j_{SN} approaches 1. In fact, it cannot approach one unless there are compensating changes in the other parameters, so that Equation (3-37) is not the only one involving those variables to be satisfied.

One recent study reported a value of j_{SN} about 0.5 (RA-543). Others have suggested a value of unity (HE-287, RA-060). The full implications of a value of or near unity have not been addressed in $CaSO_3$ crystallization kinetics and modeling. A "standard" value of $j_{SN} = 0.5$ has been used here.

The dependence of nucleation rate on hold tank momentum transfer was not included in this study. It has been reported for a laboratory study that the nucleation rate is a function of the 2.5 power of the stirrer RPM (RA-543). This aspect should be considered in any treatment of data or scale-up considerations.

4.3 Parameter Variation Studies

Program outputs for two typical cases are shown in Tables 4-1 and 4-2. The semi-log plots of n versus particle size in Figure 4-1 are concave upward at larger particle sizes, as with the experimental data in Figure 4-3 of Technical Note #200-187-11-01. Calculated numbers for n cannot be compared to experimental as the experimental slurry particle concentrations are unknown. There is an abrupt change of slope in the curves at the particle size of one micron. This is due to the sharp cut-off of one micron for the clarifier overflow.

The mass average particle size, $\bar{L}_{CF}$ is plotted vs $1/p_{CF}$ in Figure 4-2. The constant growth rate case does not include γ in p_{CF}, of course. The constant R used was taken to be the value of R for the linear case at five microns. The sharp upswing in $\bar{L}$ as $1/p$ approaches the limiting value of 1/3 is an artifact of the simple linear growth law. The rate R probably does not continue to increase linearly to very large particle sizes. Values of $1/p$ greater than 1/3 have no physical significance.

The foregoing results illustrated the use of the program in a noniterative fashion. Some parameter studies were also made with some of the outputs held constant and inputs varied. The desired values of the outputs were found by interpolation and cross-plotting of a series of noniterative runs.

In order to find the effect of varying clarifier cut-off size, L_C, the total precipitation rate G (SO_2 pick-up) was held constant by varying the relative saturation. The

TABLE 4-1. SAMPLE COMPUTER PROGRAM OUTPUT, TYPICAL PARTICLE SIZE

```
 CRYSTALLIZATION RATES      SIMPLIFIED HOLD TANK/CLARIFIER MODEL

RELATIVE SATURATION                          7.000       GROWTH RATE CONSTANT,MICRONS/MIN          5.000-05
HOLD TANK VOL/CLARIFIER FEED RATE,MIN        1440.       REL.SAT. EXPONENT,GROWTH RATE                 1.00
HOLD TANK VOL/CLARIFIER UNDERFLOW,MIN    2.400+04       NUCLEATION RATE CONSTANT                  2.400+08
CLARIFIER CUT-OFF SIZE,MICRONS               1.00       REL.SAT. EXPONENT,NUCLEATION RATE             1.00
SLOPE,GROWTH RATE/SIZE RELATION               .50       CRYSTAL CONC. EXP.,NUCLEATION RATE             .50

                        NUCLEATION RATE,PART./L/MIN                              1.366+09
                        PPT. RATE, MOLES/L/MIN                                   6.284-04
                        WT PCT SOLIDS, CLARIFIER FEED                            10.866
                                           UNDERFLOW                             98.500
                        PPM SOLIDS, OVERFLOW                                     823.1
                        MASS AVG. P. SIZE, MICRONS, CLARIFIER FEED               2.677
                                                     UNDERFLOW                   3.599
                                                      OVERFLOW                    .600


                               CLARIFIER FEED PARTICLE SIZE DISTRIBUTION

SIZE,MICRONS        POP.DENSITY,PARTS/L/MICRON     CUMUL NO. PCT        CUMUL VOL PCT         DEL VOL PCT
        .00                 .379+13                     .00                  .00                  .00
        .10                 .358+13                    7.57                  .00                  .00
        .20                 .339+13                   14.72                  .00                  .00
        .30                 .322+13                   21.51                  .01                  .00
        .40                 .307+13                   27.96                  .02                  .01
        .50                 .292+13                   34.10                  .04                  .02
        .60                 .279+13                   39.96                  .08                  .04
        .70                 .267+13                   45.57                  .14                  .06
        .80                 .256+13                   50.94                  .23                  .09
        .90                 .246+13                   56.09                  .36                  .13
       1.00                 .236+13                   61.03                  .53                  .17
       1.10                 .202+13                   65.53                  .74                  .21
       1.20                 .173+13                   69.37                  .97                  .23
       1.30                 .149+13                   72.66                 1.23                  .26
       1.40                 .129+13                   75.51                 1.51                  .28
       1.50                 .112+13                   77.97                 1.81                  .30
       1.60                 .975+12                   80.12                 2.13                  .32
       1.70                 .853+12                   82.00                 2.47                  .34
       1.80                 .750+12                   83.64                 2.82                  .35
       1.90                 .661+12                   85.09                 3.19                  .37
       2.00                 .584+12                   86.36                 3.57                  .38
       3.00                 .190+12                   94.38                 8.60                 5.03
       4.00                 .815+11                   97.25                13.53                 4.93
       5.00                 .385+11                   98.46                18.03                 4.50
       6.00                 .201+11                   99.08                22.05                 4.02
       7.00                 .114+11                   99.40                25.62                 3.56
       8.00                 .682+10                   99.59                28.77                 3.16
       9.00                 .429+10                   99.72                31.58                 2.81
      10.00                 .281+10                   99.78                34.09                 2.51
      15.00                 .510+09                   99.95                47.47                13.38
      20.00                 .148+09                   99.98                54.81                 7.34
      25.00                 .547+08                   99.99                59.56                 4.75
      30.00                 .240+08                  100.00                62.92                 3.37
      35.00                 .110+08                  100.00                65.45                 2.53
      40.00                 .639+07                  100.00                67.43                 1.98
      45.00                 .370+07                  100.00                69.03                 1.60
      50.00                 .227+07                  100.00                70.34                 1.32
     100.00                 .858+05                  100.00                92.76                22.42
     150.00                 .124+05                  100.00                94.71                 1.95
     200.00                 .310+04                  100.00                96.41                 1.71
     250.00                 .106+04                  100.00                97.39                  .98
     300.00                 .440+03                  100.00                98.03                  .64
     350.00                 .209+03                  100.00                98.49                  .45
     400.00                 .110+03                  100.00                98.84                  .35
     450.00                 .621+02                  100.00                99.11                  .27
     500.00                 .373+02                  100.00                99.33                  .22
     550.00                 .235+02                  100.00                99.51                  .18
     600.00                 .154+02                  100.00                99.66                  .15
     650.00                 .105+02                  100.00                99.79                  .13
     700.00                 .731+01                  100.00                99.90                  .11
     750.00                 .523+01                  100.00               100.00                  .10
```

TABLE 4-2. SAMPLE COMPUTER PROGRAM OUTPUT, SMALL PARTICLE SIZE

```
CRYSTALLIZATION RATES      SIMPLIFIED HOLD TANK/CLARIFIER MODEL

RELATIVE SATURATION                          4.000        GROWTH RATE CONSTANT,MICRONS/MIN            6.000-05
HOLD TANK VOL/CLARIFIER FEED RATE,MIN        1440.        REL.SAT. EXPONENT,GROWTH RATE                   1.00
HOLD TANK VOL/CLARIFIER UNDERFLOW,MIN     1.500+04        NUCLEATION RATE CONSTANT                    2.400+08
CLARIFIER CUT-OFF SIZE,MICRONS                1.00        REL.SAT. EXPONENT,NUCLEATION RATE               1.00
SLOPE,GROWTH RATE/SIZE RELATION                .50        CRYSTAL CONC. EXP.,NUCLEATION RATE               .50

                    NUCLEATION RATE,PART./L/MIN                         3.135+07
                    PPT. RATE, MOLES/L/MIN                              1.152-06
                    WT PCT SOLIDS, CLARIFIER FEED                           .024
                                     UNDERFLOW                              .223
                    PPM SOLIDS, OVERFLOW                                    33.8
                    MASS AVG. P. SIZE, MICRONS, CLARIFIER FEED             1.060
                                                UNDERFLOW                  1.557
                                                 OVERFLOW                   .591


                              CLARIFIER FEED PARTICLE SIZE DISTRIBUTION

SIZE,MICRONS        POP.DENSITY,PARTS/L/MICRON     CUMUL NO. PCT        CUMUL VOL PCT        DEL VOL PCT
     .00                     .174+12                       .00                  .00                .00
     .10                     .162+12                     10.19                  .00                .00
     .20                     .150+12                     19.66                  .02                .02
     .30                     .140+12                     28.49                  .12                .10
     .40                     .132+12                     36.75                  .37                .25
     .50                     .124+12                     44.49                  .87                .50
     .60                     .116+12                     51.77                 1.73                .86
     .70                     .110+12                     58.64                 3.06               1.33
     .80                     .104+12                     65.12                 5.00               1.93
     .90                     .983+11                     71.26                 7.66               2.67
    1.00                     .933+11                     77.07                11.19               3.53
    1.10                     .701+11                     82.04                15.26               4.06
    1.20                     .532+11                     85.78                19.28               4.03
    1.30                     .407+11                     88.63                23.22               3.94
    1.40                     .314+11                     90.82                27.03               3.81
    1.50                     .244+11                     92.51                30.67               3.65
    1.60                     .191+11                     93.83                34.15               3.47
    1.70                     .150+11                     94.86                37.43               3.29
    1.80                     .119+11                     95.68                40.53               3.10
    1.90                     .948+10                     96.32                43.43               2.91
    2.00                     .761+10                     96.84                46.16               2.72
    3.00                     .109+10                     99.48                75.33              29.17
    4.00                     .222+09                     99.88                87.38              12.06
    5.00                     .579+08                     99.96                92.86               5.48
    6.00                     .181+08                     99.99                95.58               2.72
    7.00                     .648+07                     99.99                97.02               1.45
    8.00                     .259+07                    100.00                97.85                .82
    9.00                     .113+07                    100.00                98.34                .49
   10.00                     .528+06                    100.00                98.64                .30
   15.00                     .254+05                    100.00                99.80               1.16
   20.00                     .268+04                    100.00                99.96                .16
   25.00                     .450+03                    100.00               100.00                .04
```

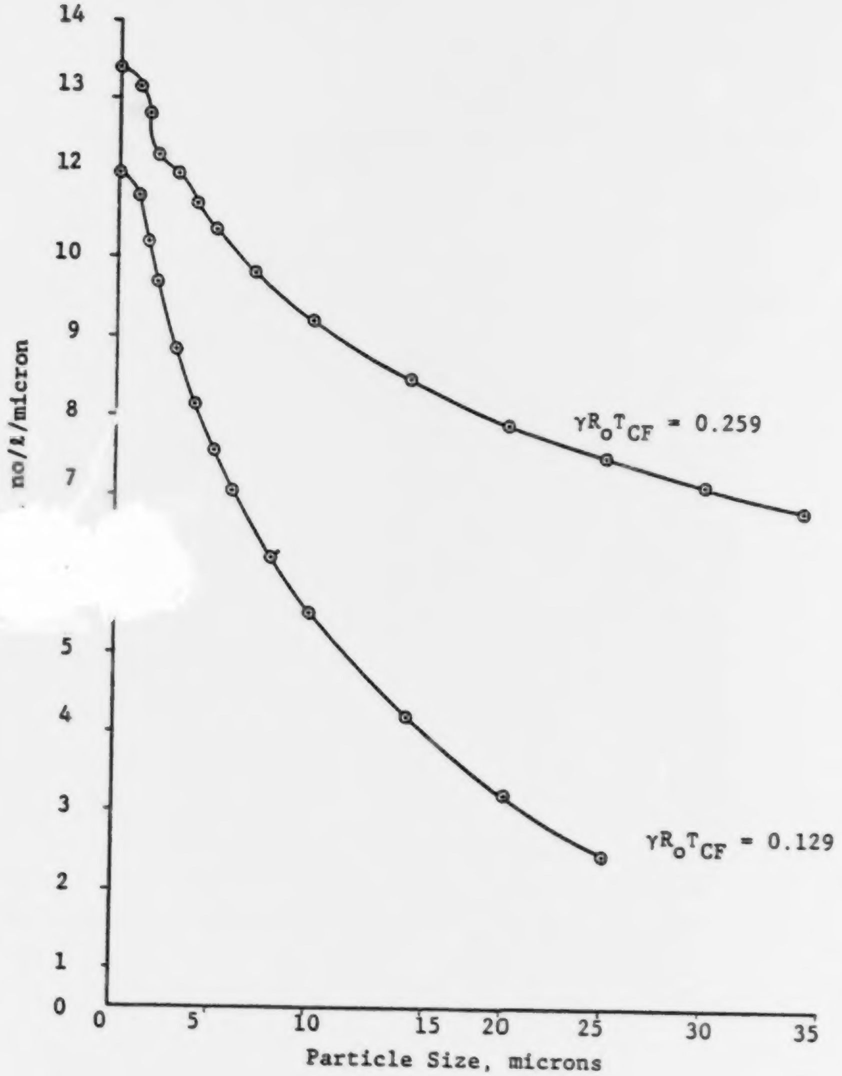

Figure 4-1. Population Density *vs* Particle Size.

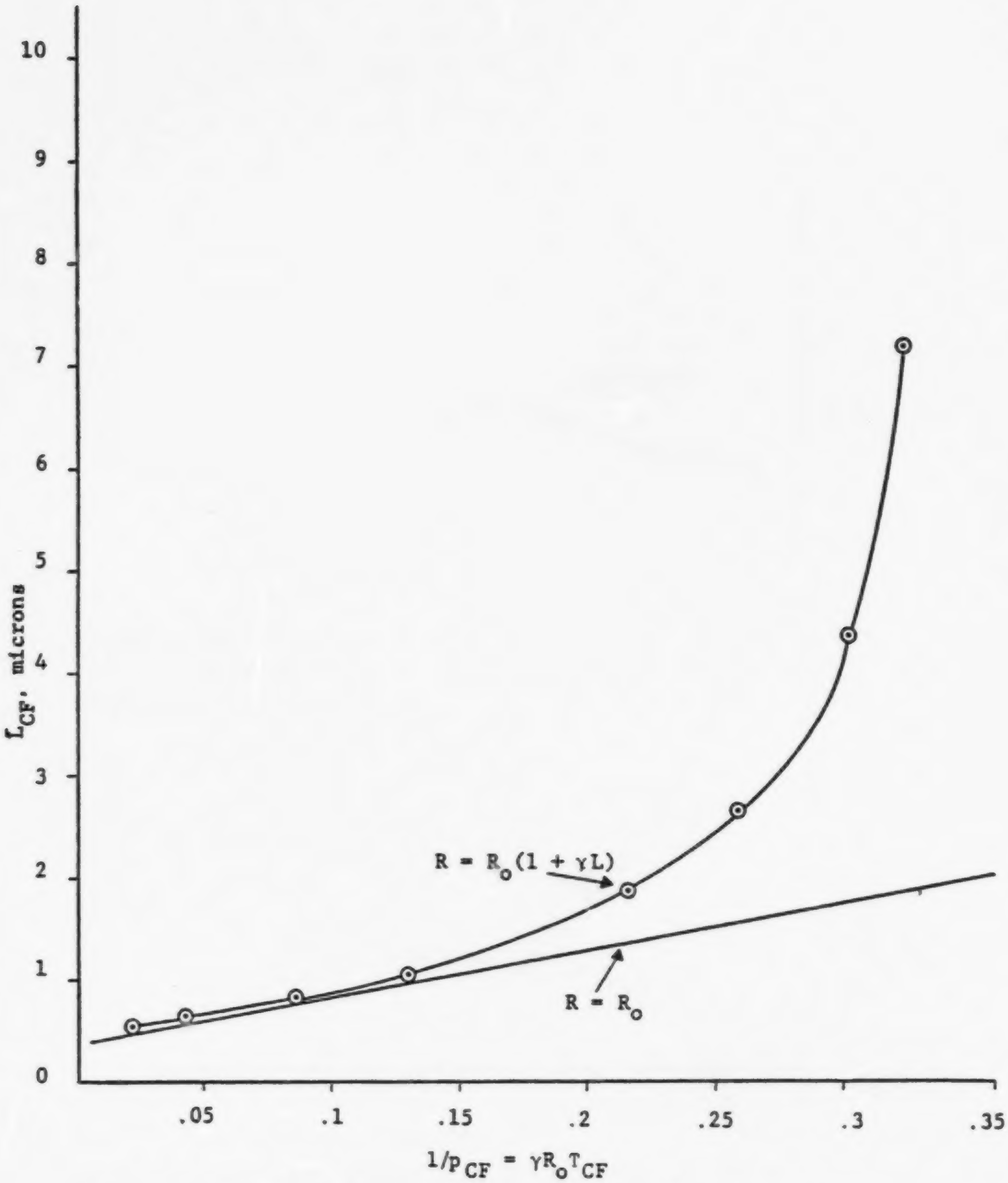

Figure 4-2. Average Particle Size vs Growth Rate Parameter, p_{CF}

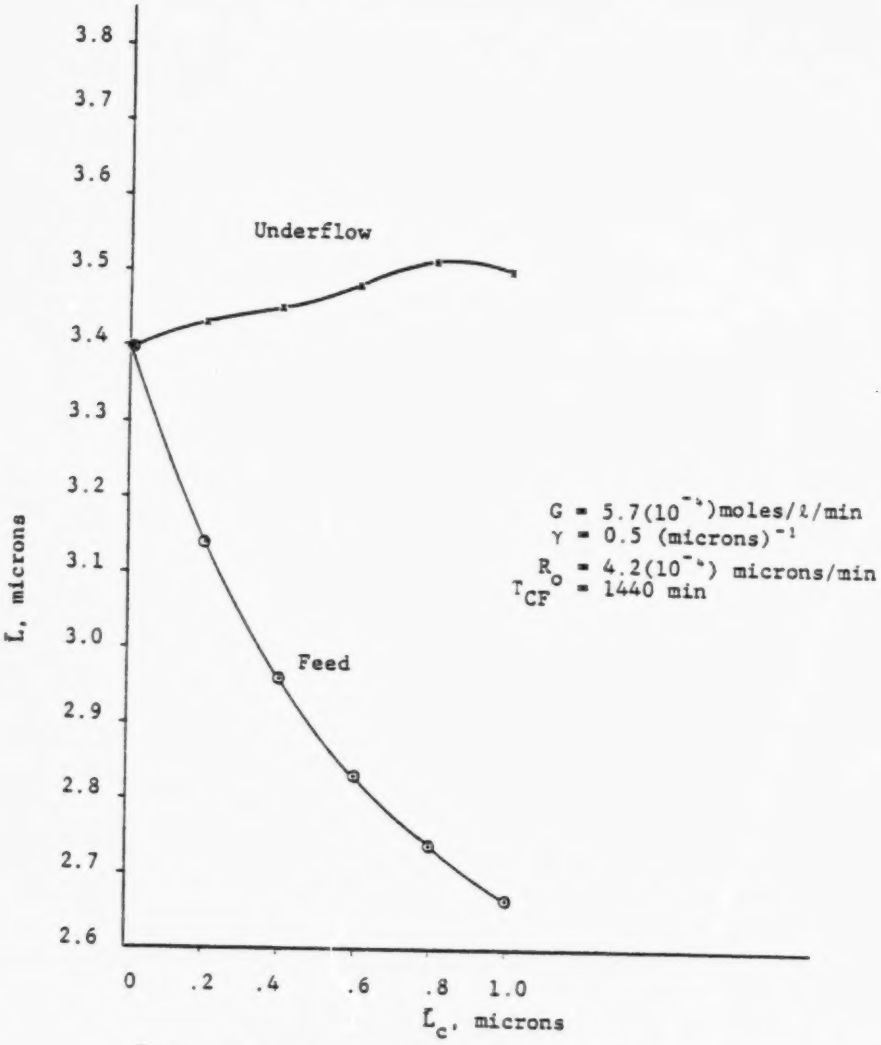

Figure 4-3. Average Particle Size vs Clarifier Cut-off Size.

results are shown in Figure 4-3. Improving clarifier performance by decreasing L_C increases the feed particle size. The underflow (sludge) particle size does not change as much. It goes through a slight maximum with decreasing L_C and then decreases.

The effect of solids residence time, τ_{CF} is shown in Figure 4-4. Here the clarifier feed solids content was held constant while relative saturation was varied. Particle sizes remain constant since the group P_{CF} determining particle size remains constant, and the exponents i_{GR} and i_{SN} are equal. From Equation (3-37) for M_T it is seen that the relative saturation cancels out of the nucleation and growth rate terms in brackets if these two exponents are equal (one in this case). Then relative saturation appears only in the parameter p_{CF} in the integral. When solids residence time τ_{CF} is varied to keep M_T and W_{CU} constant, relative saturation varies inversely with τ_{CF} and p_{CF} is constant. Thus, particle size remains constant. This will not be true for unequal values of i_{GR} and i_{SN}. This possibility is illustrated in Figures (4-5) and (4-6) for $i_{GR} = 1$ and $i_{SN} = 2$ and 0.5. It is seen that for $i_{SN} = 2$ ($i_{SN} > i_{GR}$) particle size increases with increasing solids residence time. The opposite is true for $i_{SN} = 0.5$ ($i_{SN} < i_{GR}$).

Plots such as Figures 4-4 can be used to illustrate the possible use of the model in a design problem. Suppose one had a given SO_2 removal rate in moles/min and wished to find the required hold tank size. A maximum relative saturation of six might be determined from other system considerations. From Figure 4-4 at this relative saturation we find a solids residence τ_{CF} of 1750 minutes and precipitation rate G of 4.7×10^{-4} moles/ℓ/min. The hold tank size, V_τ, is then found from the ratio of the required total SO_2 removal rate and the precipitation rate. The clarifier feed rate can then be found from the hold tank volume and solids residence time.

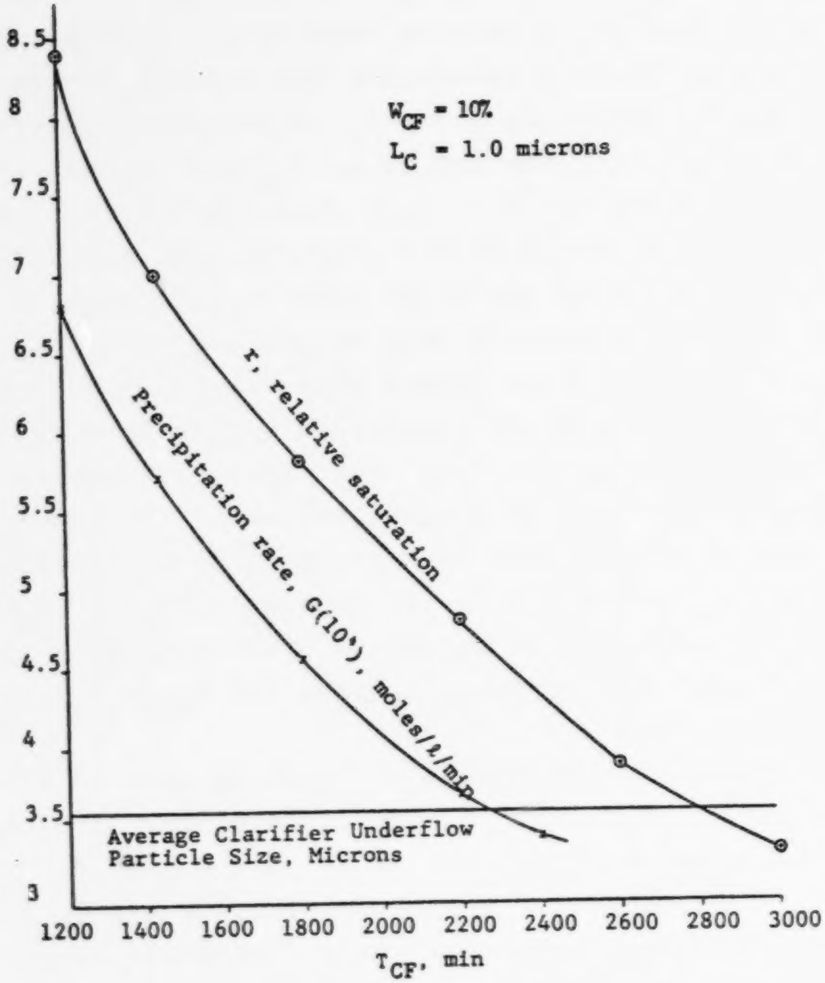

Figure 4-4. Relative Saturation, Particle Size and Precipitation Rate vs Solids Residence Time.

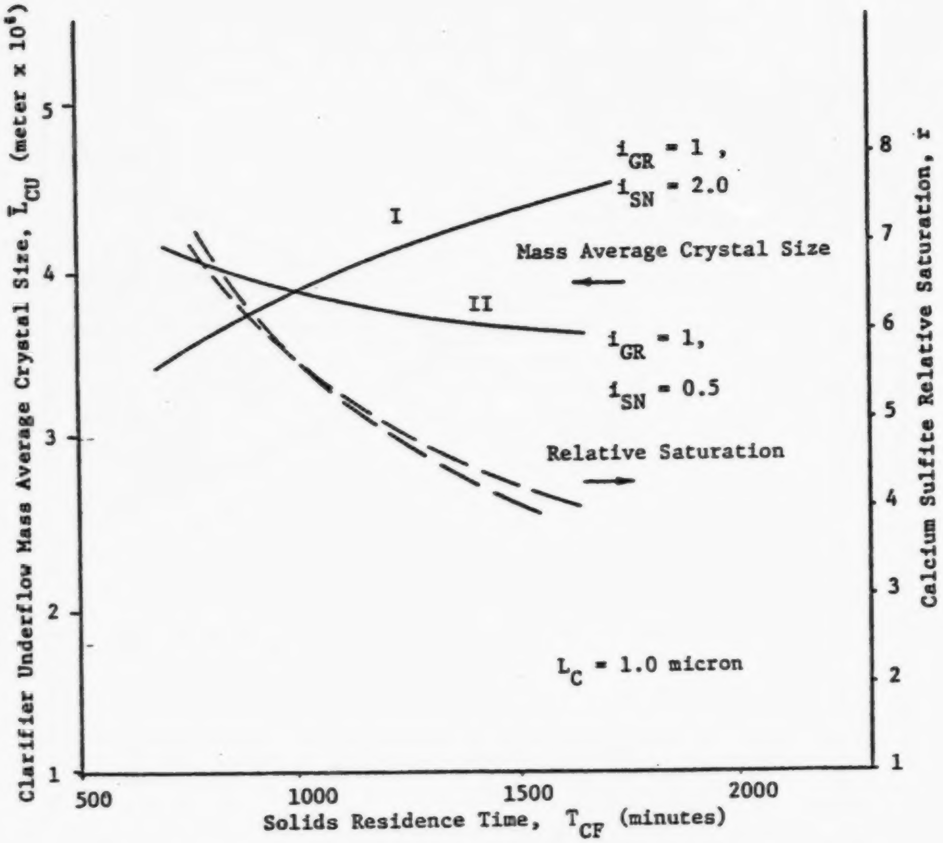

Figure 4-5. Mass Average Crystal Size and Relative Saturation Versus Solids Residence Time (Hold Tank Volume) at Constant SO_2 Removal, 10 Weight Percent Solids

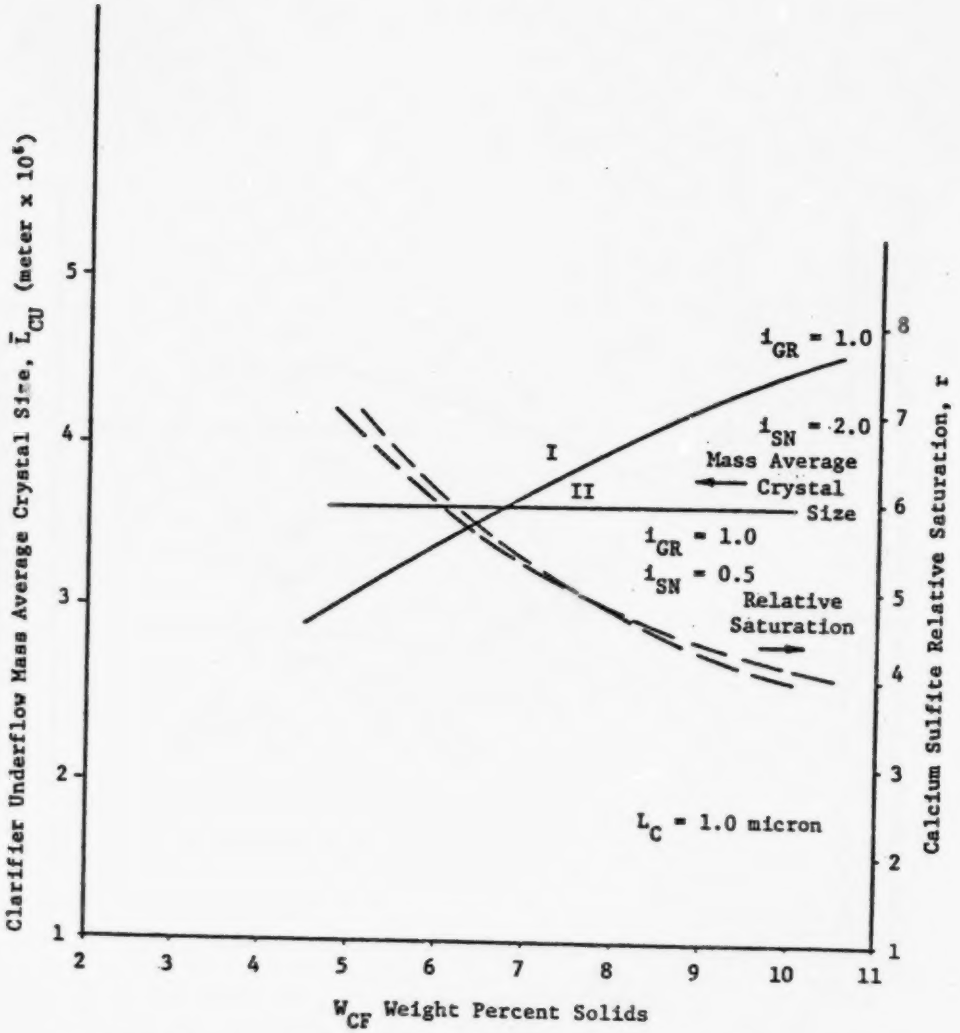

Figure 4-6. Mass Average Crystal Size and Calcium Sulfite Relative Saturation Weight Percent Versus Solids in Clarifier Feed W_{CF} at Constant SO_2 Removal and Hold Tank Volume

The next three figures, Figures 4-7 through 4-9 display sensitivity of outputs to some of the rate parameters in the model. Weight percent solids in the clarifier feed was held constant at 10 per cent by varying solids residence time, τ_{CF}.

The values of the rate parameters used were chosen to give physically reasonable model output values. The use of the model to predict the effect of system parameters on particle size distributions must be based on experimentally determined rate parameters. The exponents i_{GR}, i_{SN}, and j_{SN} are unknown but critical to model behavior. There are six rate parameters in the model which must be determined from experimental data: k_{GR}, i_{GR}, k_{SN}, i_{SN}, j_{SN} and r. The amount and quality of data necessary to determine these parameters cannot be judged at this time.

Another rate parameter which should be added to the present model is one involving the stirring and mass transfer characteristics of the hold tank, as they affect the nucleation rate. This dependence will be necessary if it is desired to transfer information from one size of equipment or type of stirring to another.

A desirable extension to the model would be growth rate laws intermediate between the linear and constant cases considered here. These represent two limiting cases. The particle size dependence probably falls in between. One possibility is to have an exponent less than one in the growth rate equation:

$$R = R_o(1 + \gamma L)^{\beta} \qquad (4\text{-}1)$$

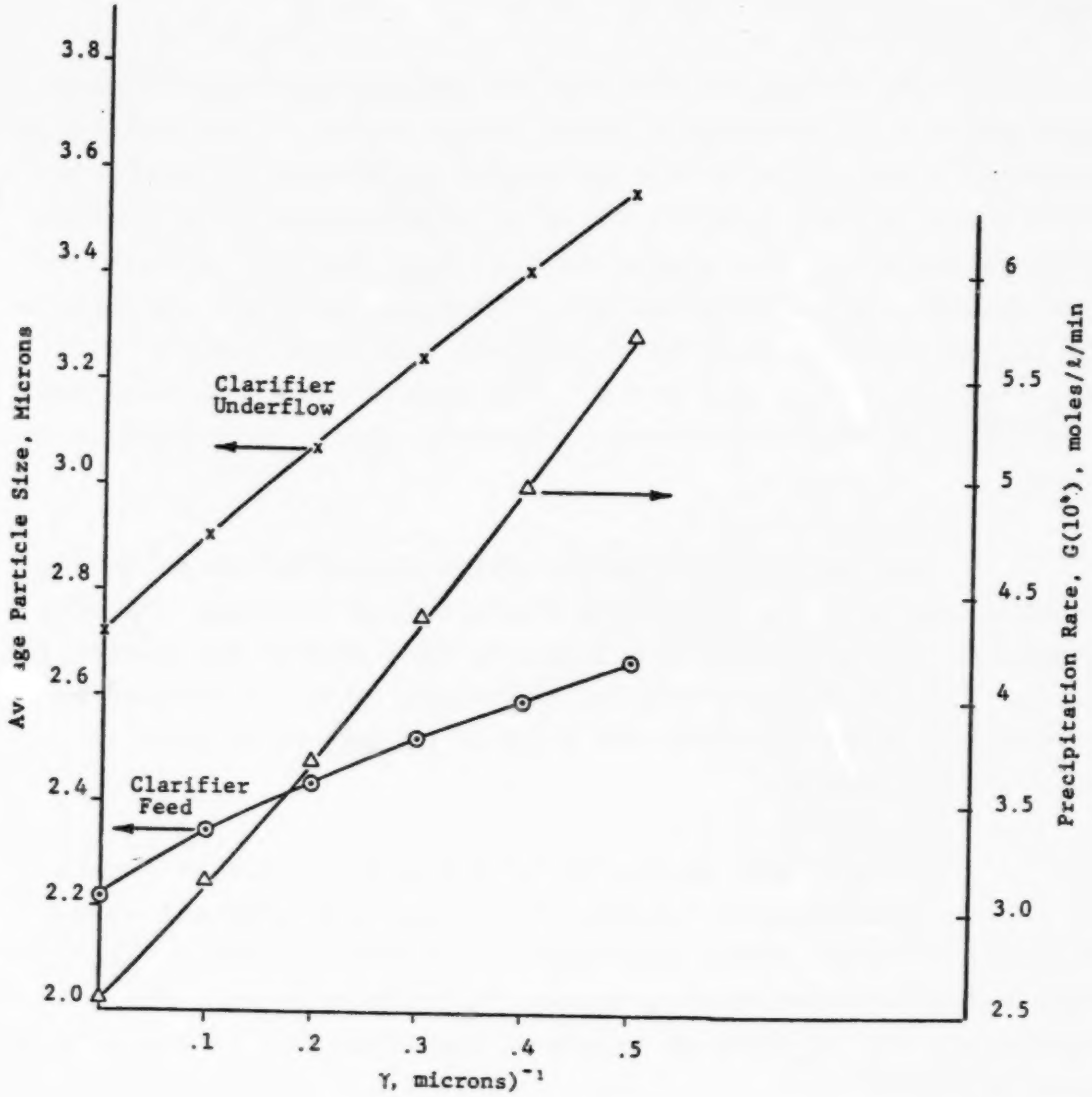

Figure 4-7. Particle Size and Precipitation Rate vs Growth Rate-Size Slope.

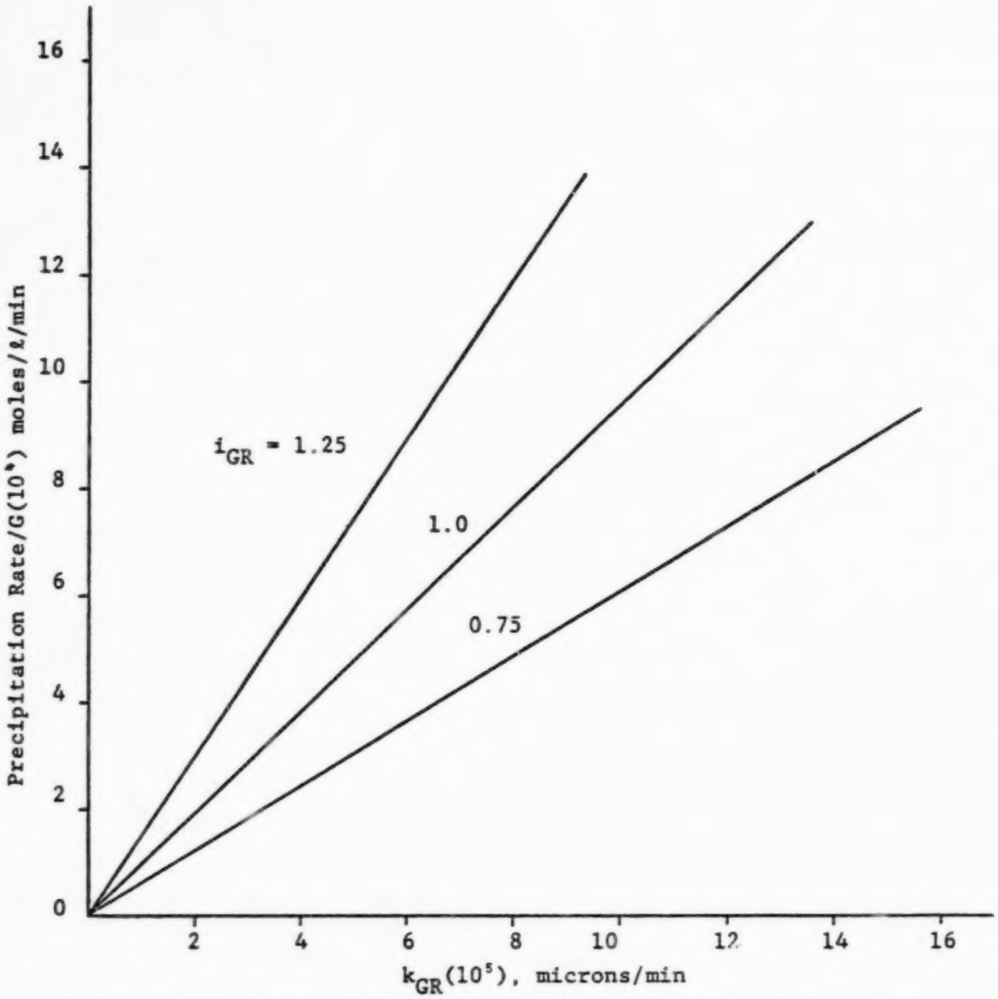

Figure 4-8. Precipitation Rate vs Growth Rate Constant.

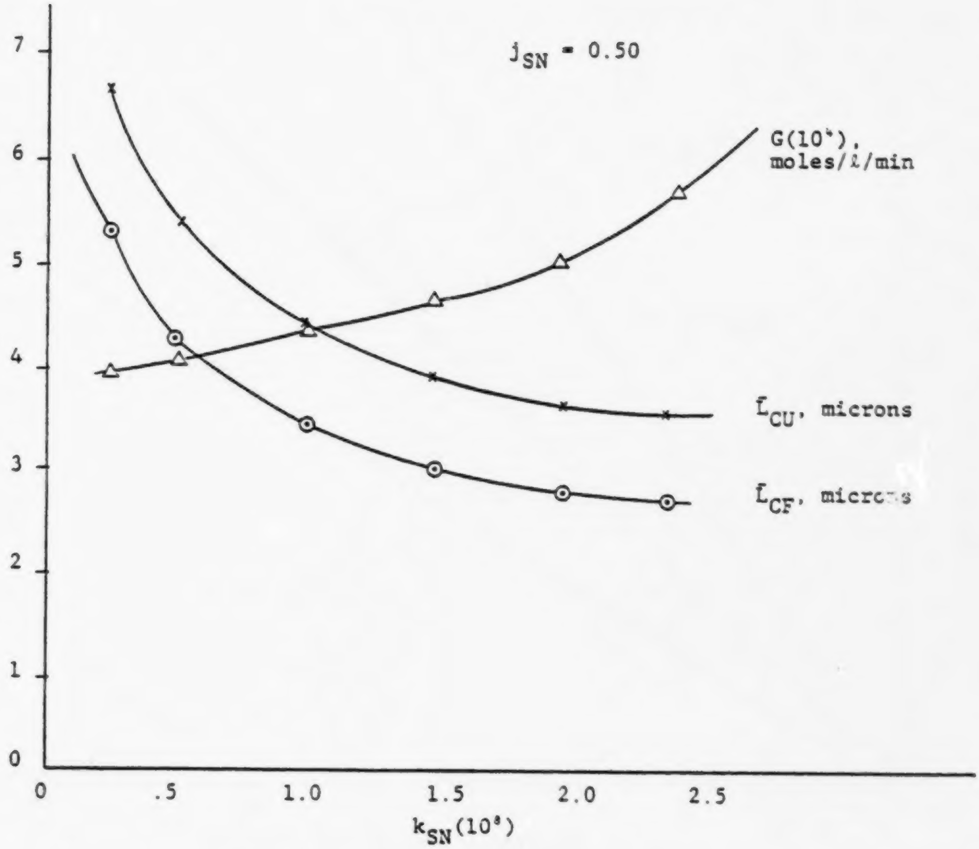

Figure 4-9. Particle Size and Precipitation Rate vs Nucleation Rate Constant.

where β is still another parameter to be determined. Its value would be between zero (constant case) and one (linear case). With Equation (4-1) an analytical solution for the particle size distribution would still be possible. But numerical integration would be necessary for the total solids concentration, M_T.

Another possible rate law would be to stop the increase in R at some size L_{max}, beyond which the growth rate would be constant:

$$\begin{aligned} R &= R_o\,(1 + \gamma L),\ L < L_{max} \\ R &= R(L_{max})\ ,\ L > L_{max} \end{aligned} \qquad (4\text{-}2)$$

This rate law would allow all analytical solutions as with the present model. The solutions would be algebraically more complex.

Either of the above rate laws would give finite particle sizes over the whole range of parameters. The present linear growth rate cannot be used beyond a maximum value of p_{CF} of 1/3.

5.0 REFERENCES

DW-006 Dwight, H. Bristol, *Tables of Integrals and Other Mathematical Data*, revised. New York, MacMillian, 1947

HE-287 Helt, James E. and Maurice A. Larson, "Effects of Temperature on the Crystallization of Potassium Nitrate by Direct Measurement of Supersaturation", *AIChE J. 23*(6), 822 (1977).

LO-R-007 Lowell, P. S., et al., *A Theoretical Description of the Limestone Injection Wet Scrubbing Process*, final report, 2 vols. PB 193-029, PB 193-030, Contract No. CPA-22-69-138. Radian Project No. 200-002. Austin, Texas, Radian Corporation, June 1970.

MA-766 Margenau, Henry and George M. Murphy, *The Mathematics of Physics in Chemistry*, New York, Van Nostrand, 1943

OT-A-56 Ottens, Erroll P. K. and Esso J. deJong, "A Model for Secondary Nucleation in a Stirred Vessel Cooling Crystallizer", *I&EC, Fund. 12*(2), 179 (1973).

PE-030 Perry, John H., *Chemical Engineers Handbook*, 4th ed. New York, McGraw-Hill, 1963.

RA-060 Randolph, Alan D. and Maurice A. Larson, *Theory of Particulate Processes. Analysis and Techniques of Continuous Crystallization*. New York, Academic, 1971.

RA-543 Randolph, Alan D. and Subhas K. Sikdar, "Creation and Survival of Secondary Crystal Nuclei. The Potassium Sulfate-Water System", *I&EC, Fund. 15*(1), 64 (1976).

6.0 NOMENCLATURE

$a = Q_{SB}/R_S V_S$ = $1/R_S T_{SB}$, also particle area (a_p)
$a^1 = Q_{SF}/R_S V_S$ = $1/R_S T_{SF}$
B = rate of birth of particles, no/ℓ/min
$b = Q_\tau/R_\tau V_\tau$ = $1/R_\tau V_\tau$
$c = Q_{SB}/R_\tau V_\tau$ = $1/R_\tau T_{S\tau}$
C = Arbitrary constant of Equation (2-7)
D = Rate of disappearance, no/ℓ/min
f_ρ = Define as $\rho p k \gamma / MW$
f_{CL} = Factor defining clarifier particle size split, Equation (2-21)
G = Molar precipitation rate, moles/ℓ/min
i = Exponent on relative saturation
I = Integral defined in Equation (3-1)
j = Exponent on M_T, nucleation rate
k_a = Factor converting L^2 to area
k_v = Factor converting L^3 to particle volume
k = Rate constant
L = Particle size, microns
m = Characteristic root, Equation (2-13)
M = Crystal concentration moles/liter slurry
MW = Molecular weight of crystals
N = Particle concentration, no/liter
n = Particle population density, no/ℓ/micron
p = Parameter in growth rate, Equation (2-25)
Q = Volumetric total slurry flow rate, liters/min
r = Relative saturation
R = One-dimensional particle growth rate, microns/min
v = Particle volume
V = Vessel volume, liters
W = Weight fraction solids
X_c = $1 + \gamma L_c$
Y = Volume fraction clear liquor

β = Exponent in general growth rate, Equation (4-1)
γ = Slope of R *vs* L straight line, (microns)$^{-1}$
Γ = Gamma function, Equation (2-34)
ρ = Density, gm/cc
T = characteristic time = vessel volume/flow rate, min.

SUBSCRIPTS

C = Clarifier
CF = Clarifier feed
CO = Clarifier overflow
CU = Clarifier underflow
GR = Growth
i = Input stream
j = Output stream
n = No (particle)
o = Zero size
p = Particle (crystal)
S = Scrubber
SB = Scrubber bottoms
SF = Scrubber feed
SN = Secondary nucleation
τ = Hold tank
T = Total
v - Volume

SUPERSCRIPTS

- = Average

APPENDIX A
PROGRAM DESCRIPTION

The program was written in FORTRAN V for a Univac 1108. However, no sophisticated hardware or compiler features were used. The program should be essentially machine independent and transferable to any computer system with FORTRAN capability.

For maximum flexibility and ease of use, NAME LIST input is used, except for an initial alphanumeric identification card. NAME LIST input is of the form

```
VRBNAM = xx.xx ,
```

The variables can be in any order. The beginning and end of data sets are indicated by the master NAME LIST name (here INPUT) and END cards. Any or all parameters can be changed in serial runs. The user is referred to the FORTRAN manual for implementation details for the computer used. The variable names in the input are shown below with their standard or default values. These numbers are stored internally in the program and are used unless other values are assigned in the input data.

Variable	NAME LIST Name	Default Value
k_v	KV	$\pi/6$
ρ_p	RHŌP	2.4
MW	WTMŌL	129.
r	RELSAT	
k_{GR}	GRK	
i_{GR}	GRI	1.0
k_{SN}	SNK	
i_{SN}	SNI	1.0
j_{SN}	SNJ	0.5
γ	GAMMA	

(continued)

Variable	NAME LIST Name	Default Value
T_{CF}	TAUCF	
T_{CU}	TAUCU	
L_c	LC	
	CALCN	

The last name, CALCN, is an array of up to ten numbers controlling the particle sizes computed and printed out in the output. The odd values are size intervals in microns. The even values are sizes to stop the preceding interval and switch to the next. Thus the combination:

.1, 2., 1., 10., 5., 50.,

would give results every 0.1 microns up to 2 microns, then 1 micron intervals to 10, then 5. to 50., and so on up to 5 changes.

The program names for the output parameters are as follows:

Program Name		Definition
N	-	Population density
PCN	-	Percent particles less than a given size
PCV	-	Volume (mass) percent less than a given size
DELV	-	Volume (mass) percent in a given size range
CUM	-	Net precipitation rate
WCF	-	Weight percent solids in the clarifier feed
WCU	-	Weight percent solids in the clarifier underflow

Program Name		Definition
CFL	-	Average particle sizes
CUL	-	in the clarifier feed,
COL	-	underflow and overflow

The particle size distribution will be computed until the increment in the volume, N_v, is less than 10^{-3} of the total. Or to a maximum of 200 increments, where a warning message to that effect is printed. The results are printed anyway, as they may be useful.

An error message is printed if the value of p_{CF} is less than 3.0, the minimum value for the linear growth rate law.

The FORTRAN listing is given on the next pages.

```
00100   C     CRYSTALLIZATION RATE , HOLD TANK/CLARIFIER ONLY
00100   C     GROWTH RATE LINEAR IN PARTICLE SIZE
00101         REAL NPZ,NZ,N(200),KV,LC,MT,L(200) ,MTEJ
00103         DIMENSION CALCN(10),CUMN(200),VOL(200),PCN(200),PCV(200),DELV(200)
00104         DATA RHOP/2.40/,KV/.5236/,WTMOL/129./,GRI/1./,SNI/1./,SNJ/.5/
00113         NAME LIST/INPUT/ KV,RHOP,WTMOL,RELSAT,GRK,GRI,SNK,SNI,SNJ,GAMMA,
00113        1 TAUCF,TAUCU,LC,CALCN ,DELTA
00114       1 READ(5,2)
00116       2 FORMAT('
00116        1                         ')
00117       5 READ(5,INPUT,END=60)
00122     501 WRITE(6,2)
00124         WRITE(6,6) RELSAT,GRK,TAUCF,GRI,TAUCU,SNK,LC,SNI,GAMMA,SNJ
00140       6 FORMAT('0RELATIVE SATURATION',T40,F10.3,
00140        1T60,'GROWTH RATE CONSTANT,MICRONS/MIN',T100,1PE10.3/
00140        2' HOLD TANK VOL/CLARIFIER FEED RATE,MIN',T40,0PF10.0,
00140        3T60,'REL.SAT. EXPONENT,GROWTH RATE',T100,F10.2/
00140        4' HOLD TANK VOL/CLARIFIER UNDERFLOW,MIN'T40,1PE10.3,
00140        5T60,'NUCLEATION RATE CONSTANT',T100,E10.3/
00140        6' CLARIFIER CUT-OFF SIZE,MICRONS',T40,0PF10.2,
00140        7T60,'REL.SAT. EXPONENT,NUCLEATION RATE',T100,F10.2/
00140        8' SLOPE,GROWTH RATE/SIZE RELATION',T40,F10.2,
00140        9T60,'CRYSTAL CONC. EXP.,NUCLEATION RATE',T100,F10.2)
00141         FRHO = RHOP*KV/WTMOL*1.E-12
00142         RRP = RHOP/(1. + RHOP)
00143         FCL = RRP/(TAUCU/TAUCF - 1. + RRP)
00144         RZ = GRK*(RELSAT - 1.)**GRI
00145         NPZ = SNK*(RELSAT - 1.)**SNI/RZ
00146         IF(GAMMA .GT. 1.E-5) GO TO 8
00150         PCF = 1./RZ/TAUCF
00151         PCU = PCF*FCL
00152         FM = FRHO*NPZ
00153         COMP = FM*(6./PCU**4 - EXP(-PCU*LC)*(LC**3/PCU + 3.*LC**2/PCU**2
00153        1 + 6.*LC/PCU**3 + 6./PCU**4))
00154         CUMP = FM*EXP(-PCU*LC)*(LC**3/PCF + 3.*LC**2/PCF**2 + 6.*LC/PCF**3
00154        1 + 6./PCF**4)
00155         GO TO 25
00156       8 PCF = 1./GAMMA/RZ/TAUCF
00157         IF(PCF .GT. 3.) GO TO 20
```

```
00161          WRITE(6,15) PCF
00164       15 FORMAT('0PCF LESS THAN MIN OF 3.,  ',F10.3)
00165          GO TO 5
00166       20 PCU = PCF*FCL
00167          XC = 1. + GAMMA*LC
00170          FM = FRHO*NPZ/GAMMA**4
00171          XEPCU = XC**(-PCU)
00172          COMP = FM*((XC**3*XEPCU - 1.)/(3.-PCU) - 3.*(XC**2*XEPCU - 1.)/
00172         1 (2.-PCU) + 3.*(XC*XEPCU - 1.)/(1.-PCU) + (XEPCU - 1.)/PCU)
00173          CUMP = FM*XEPCU*(XC**3/(PCF-3.) + 3.*XC**2/(2.-PCF) - 3.*XC/
00173         1 (1. - PCF) - 1./PCF)
00174       25 MT = (CUMP + COMP)**(1./(1.-SNJ))
00175          WCF = MT/(MT*(1. - 1./RHOP) + 1000./WTMOL)*100.
00176          MTEJ = MT**SNJ
00177          NZ = NPZ*MTEJ
00200          BZ = NZ*RZ
00201          CFN = BZ*TAUCF*(1./FCL - XEPCU*(1./FCL - 1.))
00202          CON = (CFN/TAUCF - BZ)
00202    C*********       CON = NCO/TAUCO,   CUN/TAUCU = BZ
00203          CFL = (MT/FRHO/CFN)**.33333333
00204          COM = COMP*MTEJ*(1. - FCL)/TAUCF
00205          COL = (COM/FRHO/CON)**.33333333
00206          N(1) = NZ
00207          FNLC = XC**(PCF - PCU)
00210          IF(GAMMA .LT. 1.E-5) FNLC = EXP((PCF - PCU)*LC)
00212          ZN = NZ
00213          P = PCU
00214          K = 2
00215          I = 1
00216          KLC = 0
00217          L(1) = .0
00220          CUMN(1) = .0
00221          VOL(1) = .0
00222       29 L(K) = L(K-1) + CALCN(2*I-1)
00223          IF(L(K) .LE. LC .OR. KLC .GT. 0) GO TO 30
00225          KLC = 1
00226          ZN = ZN*FNLC
00227          P = PCF
00230       30 IF(GAMMA .GT. 1.E-5) GO TO 31
00232          N(K) = ZN*EXP(-P*L(K))
00233          GO TO 32
00234       31 N(K) = ZN/(1. + GAMMA*L(K))**(1. + P)
00235       32 DELN = (N(K) + N(K-1))*CALCN(2*I-1)/2.
```

```
00236            IF (L(K) .GE. CALCN(2*I)) I = I + 1
00240            CUMN(K) = CUMN(K-1) + DELN
00241            DELV(K) =            DELN*((L(K) + L(K-1))/2.)**3
00242            VOL(K) = VOL(K-1) + DELV(K)
00243            IF(DELV(K) .LT. 1.E-3*VOL(K)) GO TO 40
00245            IF (K .LT. 200) GO TO 35
00247            WRITE(6,34)
00251         34 FORMAT('0NO CONVERGENCE OF MASS/VOL IN 200 INCREMENTS')
00252            GO TO 40
00253         35 K = K + 1
00254            GO TO 29
00255         40 DO  45  J = 1,K
00260            PCN(J) = CUMN(J)/CUMN(K)*100.
00261            DELV(J) = DELV(J)/VOL(K)*100.
00262         45 PCV(J) = VOL(J)/VOL(K)*100.
00264            CUM = MI/TAUCF - CUM
00265            CUL = (CUM/FRHO/BZ)**.33333333
00266            WCU = CUM*TAUCU/(CUM*TAUCU*(1. - 1./RHOP) + 1000./WTMOL)*100.
00267            WCO = COM*1000.*WTMOL/(1. /TAUCF - 1./TAUCU)
00270            WRITE(6,50) BZ,CUM,WCF,WCU,WCO,CFL,CUL,COL
00302         50 FORMAT('0',T28,'NUCLEATION RATE,PART./L/MIN',T77,1PE10.3/T27,
00302           1' PPT. RATE, MOLES/L/MIN',T77,E10.3/T27,
00302           2' WT PCT SOLIDS, CLARIFIER FEED',T77,0PF10.3/
00302           3 T48,'UNDERFLOW',T77,F10.3/T27,
00302           X ' PPM SOLIDS, OVERFLOW', T77,F10.1/T27,
00302           4' MASS AVG. P. SIZE, MICRONS, CLARIFIER FEED',T77,F10.3/
00302           5 T61,'UNDERFLOW',T77,F10.3/
00302           6 T62,'OVERFLOW',T77,F10.3)
00303            IF(WCF .GT. 10.) GO TO 5
00305            TAUCF = TAUCF + DELTA
00306            TAUCU = TAUCU + DELTA*10.2
00307          . GO TO 501
00310         60 CALL EXIT
00311            END

   END OF UNIVAC 1108 FORTRAN V COMPILATION.     0 *DIAGNOSTIC* MESSAGE(S)
```

DCN #77-200-187-11-07

APPENDIX C

STANDARD METHODS DEVELOPMENT FOR THE DETERMINATION OF SLUDGE QUALITY

Technical Note #200-187-11-02

1 December 1977

Prepared for:

Robert H. Borgwardt
Industrial Environmental Research Laboratory/RTP (MD-61)
U. S. Environmental Protection Agency
Research Triangle Park,
North Carolina 27711

Prepared by:

K. W. Luke
J. L. Skloss

TABLE OF CONTENTS

Page

1.0 INTRODUCTION.................................. C-1

2.0 SUMMARY OF RESULTS........................... C-2

3.0 RECOMMENDATIONS.............................. C-4

4.0 EXPERIMENTAL PROCEDURES AND RESULTS.......... C-6
  4.1 Particle Size Distribution by Visual Microscopy........................ C-6
  4.2 Particle Size Distribution by Wet Sieving............................ C-11
  4.3 PSD by Coulter Counter.................. C-25
  4.4 Standardization of Settling Rate and Settled Density Tests............... C-27

5.0 RESULTS OF THE LITERATURE SURVEY............. C-35
  5.1 Methods for Particle Size Determination............................ C-35
  5.2 Methods for Settling Rate and Density Measurements.................... C-50

REFERENCES....................................... C-51

LIST OF FIGURES

Figure Page

4-1 Photomicrograph of Sludge Granules Taken from Lime Scrubber, 200 X.............. C-12

4-2 Photomicrograph of Sludge Platelets Taken from Limestone Scrubber, 200 X......... C-13

4-3 Sludge Granules from Lime Scrubber: Cumulative Percent of Particles Versus Diameter...................................... C-15

4-4 Sludge Platelets from Limestone Scrubber: Cumulative Percent of Particles Versus Length and Width............................. C-16

4-5 Sieved Sludge Granules: Average Cumulative Percent of Particles Versus Diameter......... C-23

4-6 Sieved Sludge Platelets: Average Cumulative Percent of Particles Versus Width............ C-24

4-7 Sieved Sludge Platelets: Corrected Cumulative Percent of Particles Versus Width.. C-26

4-8 Settling Rates of Sludges Versus Weight % Solids at 25°C and 20°C.................... C-34

LIST OF TABLES

Table Page

4-1 Particle Size Distribution by Microscopic Method.......................... C-14

4-2 Particle Size Determination by Wet Sieving of Granules...................... C-21

4-3 Particle Size Distribution by Wet Sieving of Platelets..................... C-22

4-4 Coulter Counter Data for the Sludge Granules............................... C-28

4-5 Coulter Counter Data for the Sludge Platelets.............................. C-29

4-6 Settling Rate of Sludges Versus Weight % Solids at 25°C and 50°C.................... C-33

5-1 Particle Size Determination.................. C-36

5-2 Bulk Density and Settling Rate Measurements................................ C-47

1.0 INTRODUCTION

The flue gas desulfurization (FGD) sludges produced in lime, limestone, and double alkali systems generally are difficult to settle. Radian Corporation was contracted by the EPA to investigate the prospects for improving the quality of FGD scrubber sludges. This technical note reports the work performed to develop standard analytical techniques for measuring particle size distribution (PSD), settling rate, and settled density. A literature survey is also presented.

Particle size distribution of the precipitated solids is an important factor in the settling and dewatering characteristics of FGD sludges. Numerous methods for measuring PSD are available. However, most of these are time consuming, require expensive equipment, or give only approximations of the PSD.

A survey of the literature showed that optical microscopic methods have been used to size FGD sludges. Two additional sizing methods were selected for this study. These methods are wet micromesh sieving and Coulter Counter analysis. The results of both of these techniques were compared to the PSD determined by microscopic measurements. The literature was also surveyed for methods to measure settling rate and settled density of sludges. Specific results of the literature survey are given in Section 5.

The methods development and standardization studies were carried out using two types of sludges: granular particles from a lime scrubber and platelet particles from a limestone scrubber. Tests were also performed to determine the effect of several variables on settling rates of these sludges. These included temperature, cylinder size, and weight percent solids in the slurry.

2.0 SUMMARY OF RESULTS

The optical microscopic method for the measurement of PSD worked well for both the granular and platelet sludges. A representative distribution of particles on a slide was obtained by filtering a dilute suspension of the particles onto a Millipore (cellulose acetate) filter membrane and rendering the membrane transparent with acetone. Other methods such as dry or wet mounting of the particles directly on the slide were also satisfactory, although these methods do not give as consistently reliable particle distributions.

The photomicrographs were taken at 200X magnification. This offered a compromise between having large, easily measured particles, and having a sufficient number of particles in each photograph available for sizing. At this magnification the smallest particles visible were about 1 micron in size.

The micromesh sieves gave results comparable to those obtained by the microscopic method when granular particles were tested. The number of particles retained on each sieve was calculated from the weight of sludge on each sieve by assuming an average particle size, shape, and density. The micromesh sieve and optical microscope results were then compared on the basis of a population distribution as a function of average particle diameter. The sieves worked equally well for the platelets. Comparison of the sieve data for platelets with the microscopic results was possible by making some assumptions about the relative dimensions of the particles and their orientation as they passed through the sieves. Specifically, it was assumed that the platelets passed through the square holes of the sieves in a lengthwise fashion such that the diagonal width of the square opening was equal to the width of the thin platelet particle. With the above assumption the optical and sieve results agreed fairly well for particles in the range of 10-40 microns.

The Coulter Counter method generally observed and measured particles much smaller in size than the other two methods for both types of sludges. Reasonable agreement between results for all three methods was obtained, however, when comparing PSD's for particles greater than 2μ diameter only.

Settling rates were found to be dependent on the weight percent of solids in the slurry, the temperature, and the type of particles. The settling rate is independent of cylinder size in the range tested. An increase in weight percent solids resulted in a significant decrease in the settling rate. A 50 to 60 percent increase in the settling rate was observed when the temperature was increased from 25° to 50°C. This increase was attributed to a decrease in the viscosity of the liquid. The granular particles settled slower than the platelets, indicating that the granules had an effectively smaller particle size.

The settled density was found to be dependent on particles type with the granules having the lower settled density.

3.0 RECOMMENDATIONS

The microscopic method for determining particle size distribution is recommended based on the results of this work. The method has the following advantages:

- The individual particles are visible.
- Using good mounting techniques, the accuracy of PSD is dependent only on the visual measuring technique.
- A permanent record is obtained in the form of a photograph.
- The morphology of the particles can be seen.
- Results are on a population basis.

The main problem encountered in the microscopic method was obtaining a representative distribution of particles on the microscope slide. This was overcome by slurrying the solids in an alcohol-water solution and filtering the slurry on a thin membrane. After mounting, the membrane was rendered transparent with acetone vapors making the sludge particles clearly visible.

Best results were obtained at 200X magnification. The images were sufficiently magnified to see the 1μ particles, and a total of 250 particles could easily be included in the photomicrograph field. In this work the particle size was measured with a transparent ruler. However, another good and perhaps faster method would be to use a template with circles or holes of a known size. The circles or holes could be placed over the particles on the photomicrograph until a proper match was located. This method would be most applicable to spherical or granular-shaped particles.

The micromesh sieves gave satisfactory particle size distributions on a weight basis. No significant saving of time compared to optical microscopic methods was noticed, however, because of time required for the weighing, drying, and sieving procedural steps. Because of their small size and weight, the sieves may be useful in the field where an expensive microscope is not available.

The Coulter Counter method for sizing FGD sludges may have great potential. It is faster than the other methods, and a large number of samples may be run to determine relative PSD. More work needs to be done to obtain proper calibration and optimization of the method, particularly for particles less than 1-2μ.

The settling rates for slurries should all be measured at constant weight percent solids and constant temperature if meaningful comparisons are to be made. Any selected constant concentration between 3 and 10 percent solids should be satisfactory. The recommended liquor temperature is any specific value between 25 and 50°C which simulates the FGD scrubber operational mode for settling solids. After the solids have settled overnight the settled density may be calculated.

4.0 EXPERIMENTAL PROCEDURES AND RESULTS

As a result of the literature survey, several methods of solids characterization were chosen for further investigation. These included particle size distribution by visual microscopy, wet sieving, and Coulter Counter (Sections 4.1, 4.2, and 4.3), and the standardization of settling rate and settled density measurements (Section 4.4).

The standard method for particle size determination is currently visual microscopy. The purpose of this study was to compare the results obtained by wet micromesh sieving and Coulter Counter to the results obtained by optical microscopy. Also, the effects of cylinder size, temperature, and weight percent solids on settling rate was determined and a standard procedure recommended.

There are two main types of sludge to be considered: 1) those produced from limestone scrubbing processes, which consist of thin plates of approximate dimensions 30:20:1, and 2) those produced from lime scrubbers which are granular and approximate a spherical shape. Because of this great difference in shape, tests were performed on both types of sludge.

4.1 Particle Size Distribution by Visual Microscopy

Visual microscopy is the standard to which the other methods will be compared. A description of the method development and results follows.

4.1.1 Microscopic Method Development

The ASTM E-20 Method was used as a reference in this study to determine particle size distribution. This method consists of mounting the sludge solids on a glass microscope slide and taking photomicrographs to include a total of 250 particles. Measurement of the particle sizes is made on the photomicrographs with a finely divided transparent ruler. The microscopic method allows direct viewing of the individual particles. The photomicrograph provides a record of the sludge solids, and further qualitative observations of the crystal form, size, and texture of the solids may be made.

Most attention in this study was directed to finding a suitable method to mount the sludge solids on a microscope slide such that a representative distribution of the particles was obtained and sharply contrasted photomicrographs could be taken. The various mounting techniques tried were:

- spreading dried solids over a microscope slide,
- pressing slurried solids between two microscope slides, and
- filtering slurried solids on a filter membrane and clearing the membrane while on the microscope slide.

Spreading Dried Solids Over Microslide

The dried solids when spread over a microscope slide with a spatula or pointer provided excellent visibility and contrast for taking photomicrographs. However, the distribution of particles was not sufficiently uniform to determine particle size distribution. Better results were obtained when the solids were smeared over the microscope slide with a smooth fabric. Also, uniform distribution of particles was accomplished by mixing the solids in methanol-water solution and filtering on Nuclepore polycarbonate filter membrane. After drying, the membrane containing the solids was inverted on a dry microscope slide and gently smeared. This procedure gave acceptable results.

Pressing Slurried Solids Between Two Microscope Slides

Various materials were mixed with the dried sludge to make slurries which were smeared on microscope slides. These were:

- water,
- water plus surfactants,
- water plus glycerol,
- glycerol,
- mineral oil,
- silicone grease, and
- silicone glue.

Each slurry was smeared on a microscope slide, and another microscope slide was placed on top. When the two slides were pressed together, a thin film of the slurry spread between the slides.

Best results were obtained with the silicone grease and silicone glue. These materials afforded good mounting characteristics, and sufficient contrast was present in the photomicrograph to allow particle measurement. The other materials listed above for making slurries are not recommended, because the smaller particles tended to move about on the slide when handled. Even while being viewed the slurries were set in motion by the heat from the microscope objective light which shined through the microscope slide. Also, contrast was poor between the crystals and the background in most cases.

Filtering Slurried Solids on a Membrane

The sludge sample was slurried in methanol-water solution and was filtered and dried on filter membranes. Two types of membranes were tried - Nuclepore and Millipore. The filter membranes used were 47 mm diameter and 0.8μ pore size. It was assumed that the majority of particles exceeded 1μ.

The Nuclepore polycarbonate membrane was thin, smooth, and transparent to the light. However, when viewed at 200X magnification, the pores in the filter membrane cast an etched background which blended with some of the sludge particles. Repeated attempts to render the membrane transparent without losing particles from the smooth surface were not successful.

The Millipore membrane made of cellulose acetate was preferred in these tests for their handling ease. The cellulose acetate membranes were thicker and provide a coarser surface for holding the particles. After the solids were filtered and dried on the membrane, the membrane was placed on the microscope slide and rendered transparent with acetone vapors. Reliable particle size distributions were obtained by this recommended procedure.

4.1.2 Recommended Millipore Membrane-Acetone Vapor Method for Mounting Solids on Microslides

A 2-8 mg sample of dried sludge solids is placed on a piece of smooth, water resistant paper. Two-three drops of

50% methanol-water solution are added to the solids, and the slurry is gently mixed with a spatula or pointer to separate any clumps into individual particles. The slurry is quantitatively transferred using a wash bottle to a 125 ml flask containing 50 ml of 50% by volume methanol-water solution. (If the original FGD sludge slurry is available, it is necessary only to transfer an aliquot containing 2-8 mg of solids to the methanol-water solution.)

The flask is swirled to insure uniform mixing, and the slurry is filtered on a 47 mm Millipore membrane using a suction filtering assembly. The membrane is the plain white cellulose acetate, 0.8µ pore size variety (Millipore Catalog No. AAWP-04700). After filtering, the membrane is placed in a petridish to dry for 15-30 minutes in an oven set at 50°C.

The dried membrane containing the solids is removed from the petridish, and a 1 cm strip is cut with scissors and placed on a microscope slide (1 x 3 inch). Warm acetone vapor is directed over the membrane until it turns clear. Acetone vapor is supplied from a heated side arm flask containing acetone.

Another microscope slide is placed over the first slide and membrane, and the two microscope slides are taped together and labeled. The slides are ready for microscopic examination and taking photomicrographs. 200X magnification works well for including 250 particles in a single photomicrograph field.

4.1.3 Equipment and Materials for the Millipore-Acetone Method

Microscope and camera attachment
Glass microscope slides, 1 x 3 inch , 1 mm thick

Oven set at 50°C
Hot plate
Suction flask assembly, 47 mm filter
Millipore filter membranes, white plain, 47 mm diameter, 0.8 pore size
50-50% by volume methanol-water solution
125 ml erlenmeyer flask
Wash bottle
Spatula
Smooth, water-resistant paper
Petridishes, 50 mm
Side arm flask and stopper
Acetone
Scissors and transparent tape

4.1.4 Optical Microscope PSD Results

The two types of sludge solids were mounted on microscope slides using the filter membrane-acetone method described in Section 4.1.3. Several photomicrographs were taken at 200X magnification of each sample. Figure 4-1 is an example of the sludge granules from a lime scrubber; Figure 4-2 is an example of the sludge platelets from a limestone scrubber. Ruler measurements were made on sufficient photos to include at least 250 particles of each sample. The results are shown in Table 4-1. Diameters are reported for the granules, and both the length and width are reported for the platelets. The cumulative percent of particles less than the largest size in each range is plotted in Figure 4-3 and 4-4 on a number basis.

4.2 Particle Size Distribution by Wet Sieving

A set of six micromesh sieves was obtained from the Buckbee Mears Company of St. Paul Minnesota. The sieves measured

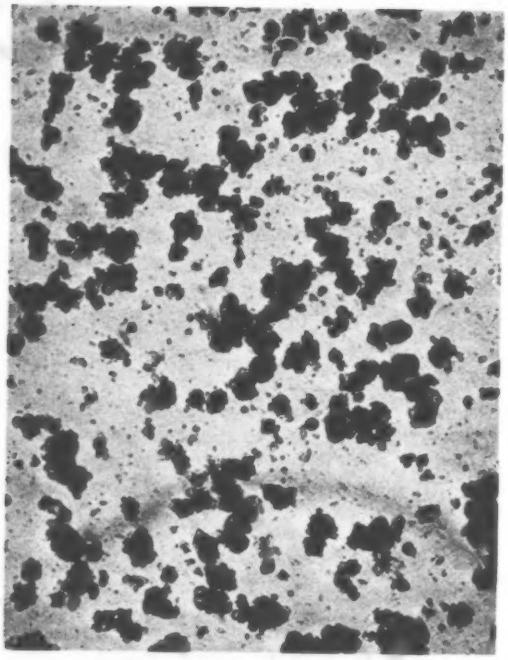

FIGURE 4-1 PHOTOMICROGRAPH OF SLUDGE GRANULES TAKEN FROM LIME SCRUBBER, 200 X

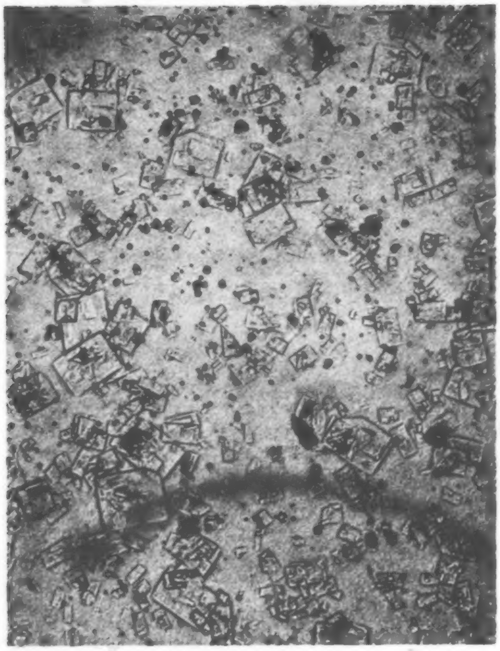

FIGURE 4-2 PHOTOMICROGRAPH OF SLUDGE PLATELETS TAKEN FROM LIMESTONE SCRUBBER, 200 X

TABLE 4-1. PARTICLE SIZE DISTRIBUTION BY MICROSCOPIC METHOD

Size Range(μ)	Granules		Platelets			
	# Of Particles	Cumulative % Less Than	Length # Of Particles	Cumulative % Less Than	Width # Of Particles	Cumulative % Less Than
1 - 5	56	16.2	5	1.6	45	13.9
5 - 10	121	51.3	35	12.5	117	50.3
10 - 15	77	73.6	79	37.2	72	72.7
15 - 20	56	89.8	78	61.6	48	87.6
20 - 25	26	97.4	54	78.4	27	95.9
25 - 30	6	99.1	36	89.7	8	98.4
30 - 35	3	99.9	18	95.3	3	99.4
35 - 40	0	∿100	9	98.1	2	∿99.9
40 - 45	--	--	2	98.7	--	
45 - 50	--	--	4	∿99.9	--	

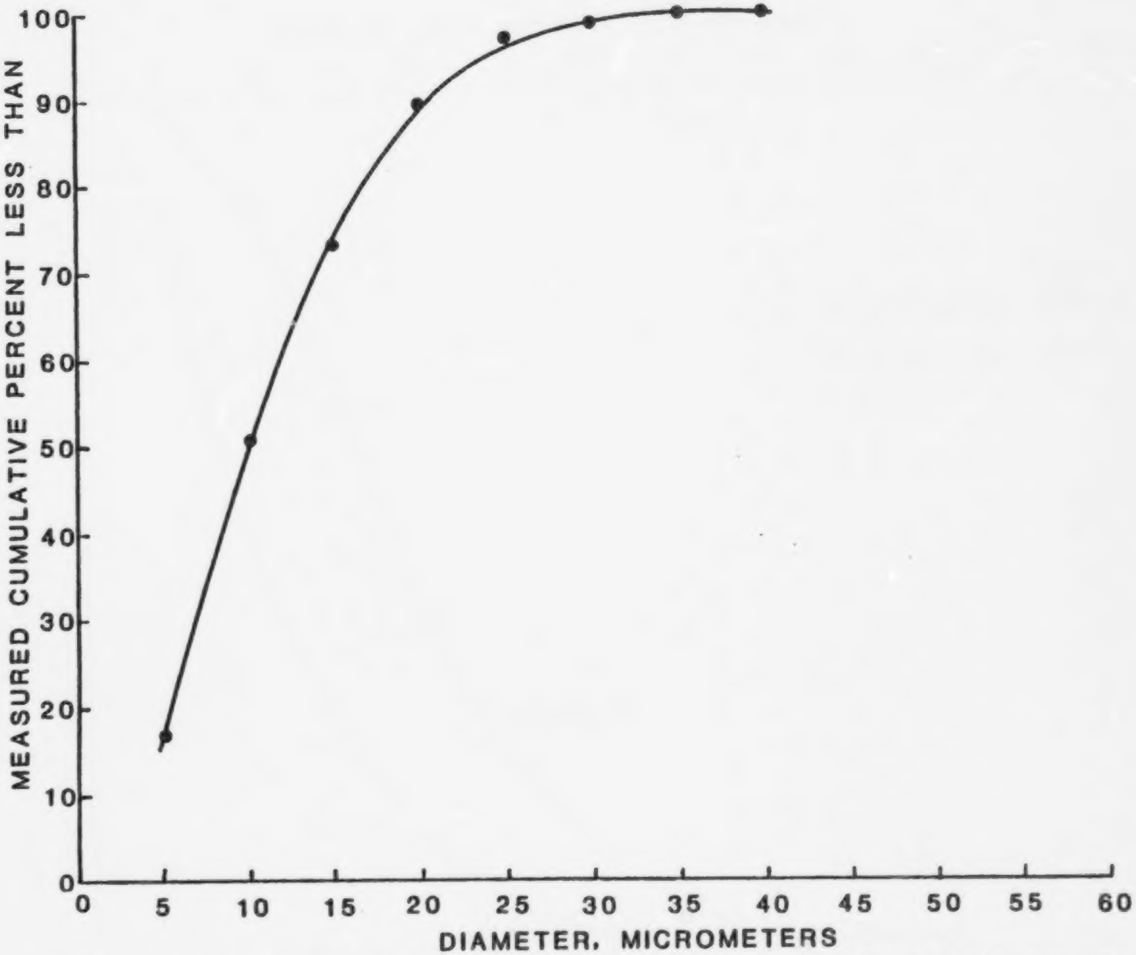

Figure 4-3. Sludge Granules from Lime Scrubber: Cumulative Percent of Particles Versus Diameter.

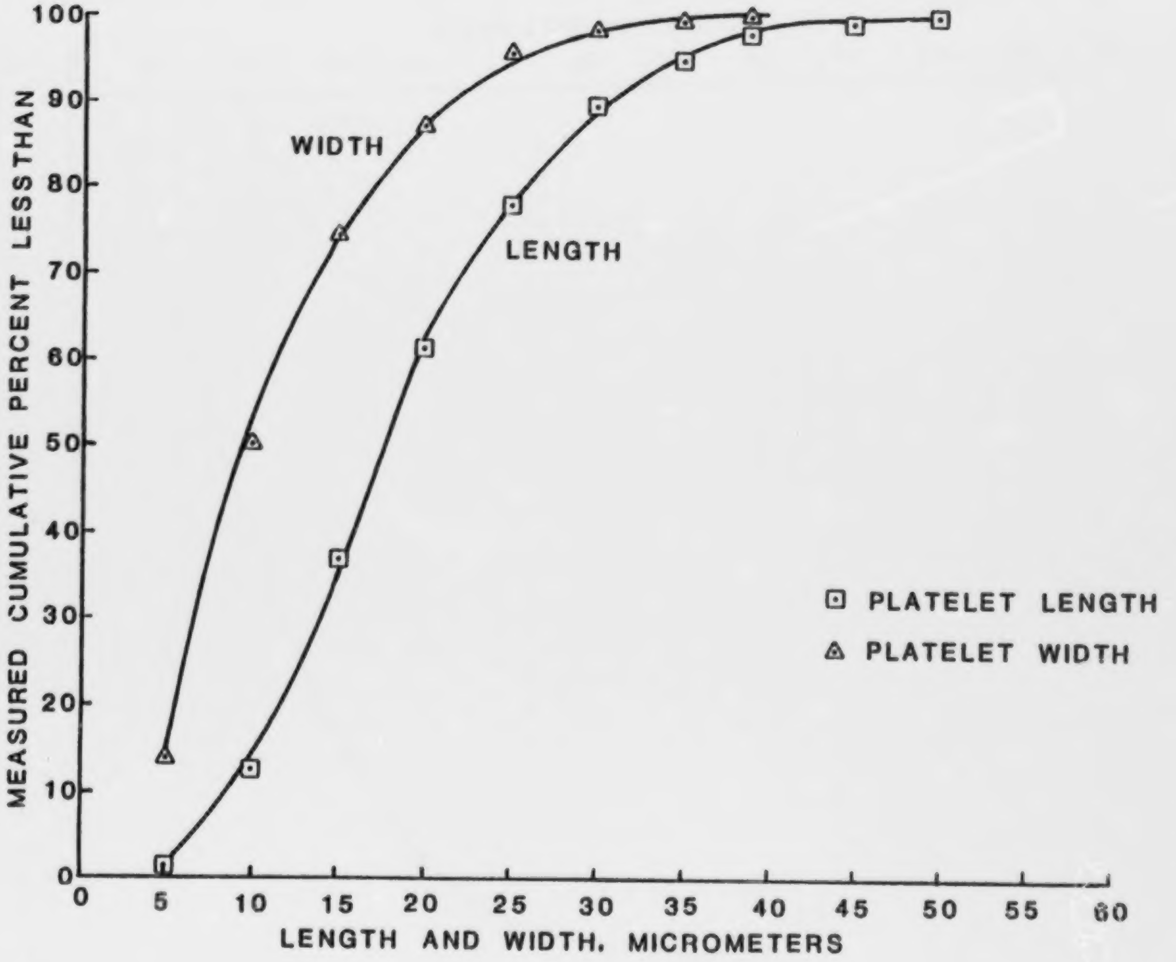

Figure 4-4. Sludge Platelets from Limestone Scrubber: Cumulative Percent of Particles Versus Length and Width.

3 inches in diameter and about 1 inch in depth. The mesh had precision electro-formed square openings with sides of 2, 5, 8, 13, 20 and 35 microns in length. The tolerance for each opening was ±2 microns which limited the accuracy of the smaller sieves relative to the larger ones.

4.2.1 Wet Sieving Method Development

There are several steps in the sieving procedure which deserve special attention. These are sample preparation, sieve preparation, the actual sieving, and calculations of results and are described in the following sections.

Sample Preparation

A dried representative sludge sample is required. The slurry cannot be filtered directly because the aqueous slurry liquor is too viscous to permit rapid filtration through the micromesh sieve. If the sample is taken as a slurry it is filtered and then dried at 40-50^{o}C. The sample is allowed to equilibrate with the atmosphere at room temperature before weighing because the sludge solids tends to absorb some moisture from the atmosphere. The dry sludge should be free of clumps and have a consistency similar to that of flour. A sample size of 500 to 700 mg is used. If the sample is unusually fine-grained a smaller sample may be more desirable.

Sieve Preparation

The sieves are thoroughly cleaned before use. The best method for cleaning them is by ultrasonic cleaning, since compressed air jets and brushes may damage the mesh. A mixture of methanol and water is used in the cleaner with the solution completely covering the sieves. The small size of the sieves usually allows several of them to be cleaned at the same time. The time required to clean the sieves varies according to the efficiency of the cleaner. When clean, the sieves are removed, rinsed on both sides with methanol, and dried at 40-50°C. They are then weighed on an analytical balance capable of an accuracy of at least 1 milligram. The sieves weigh about eighty grams each.

Sieving Procedure

Because of the small size of the particles, dry sieving is impractical. The smallest particles become airborne when the sample is shaken. Therefore, the particles are washed through the screens with methanol delivered in a jet from a polyethylene wash bottle. Other liquids may be used if they have a low viscosity and surface tension and do not dissolve calcium sulfite.

The sieves were stacked with the largest screen openings (35μ) placed on top. The sludge sample may be added directly to the top sieve from a piece of weighing paper. The particles are washed through until the effluent from the first sieve is clear, which may be observed by lifting and tilting the sieve slightly. Then it is washed once more to make sure all of the undersize particles reach the next sieve. The top sieve is removed and the process is repeated for the next one, and so on.

A tapping up and down motion of the sieve while rotating it will help to prevent blinding of the holes and will speed up the particle sizing separation. The liquid drains through the smaller sized sieves very slowly, so they should be checked often to avoid over filling and thus spillage and sample loss. The drainage through the smaller sieves was increased by the application of a light vacuum from a water aspirator. The filtrate was collected in a filter flask and saved to pour through the next smaller sized sieve.

The entire sieving procedure uses about 500 ml of methanol and takes about two hours, not including weighing, cleaning or sample preparation. After all of the particles were sized, the sieves were dried and weighed in the same manner as before. They are then ready to be cleaned for sieving the next sample.

Calculations

After the weight of particles on each sieve has been determined, the data may be compiled in several ways: cumulative percent greater than or less than each sieve size, or percent between sievessizes. Data is usually plotted on probability graph paper as cumulative percent less than or greater than a size.

When attempting to compare sieving results to those of photomicrographs, problems were encountered because sieve results are based on the weight of particles in a size range and photomicrographs give the number of particles in a size range. In order to compare these two methods, the weights of particles retained on each of the sieves were converted to the number of particles contained in that mass. This was done as follows:

$$\#\text{ of particles} = \text{weight (g)}/[\text{density (g/cm}^3) \cdot \text{volume (cm}^3)]$$

Clearly, to compute the volume of a particle, its shape must be known. The granular particles are assumed to be spheres and platelets are given dimensions of 30:20:1. For example, if 0.2 grams of sludge are retained on the 13μ sieve, following a 20μ sieve, the average diameter of a spherical particle is calculated to be 16.5 microns. This would give an average volume of 2.35×10^{-9} cm^3. If the sludge density is assumed to be 2.5 g/cm , then the number of particles is

$$0.200/(2.35 \times 10^{-9} \times 2.5) = 3.4 \times 10^7$$

particles between 20 and 13 microns. The data is then graphed in the usual manner.

It was found that the best agreement between micromesh sieve and optical microscope PSD's for platelets was obtained when the platelets were assumed to pass through the sieve holes lengthwise. In this case the PSD is more a measure of the platelet width than of the length or thickness. Also, assuming that the platelets pass through the square sieve holes according to the diagonal width of the hole further improves the agreement between sieve and optical data.

For the example given above the average width of a platelet would be $16.5 \times \sqrt{2}$ microns; the length and height are calculated using the ratios of length 30:width 20:height 1.

4.2.2 Results of Sieving Tests

Duplicate sieving tests were performed on each type of sludge, granules and platelets. The weights of particles retained on each screen were converted to the number of particles. The percent of particles smaller than each sieve size was calculated and the average values were used for plotting the data. The data are shown in Table 4-2 for granules and Table 4-3 for platelets. The graphs are shown in Figure 4-5 and 4-6 on a number basis.

TABLE 4-2. PARTICLE SIZE DETERMINATION BY WET SIEVING OF GRANULES

	Test #1			Test #2			Average
Sieve Size μ	Weight of Particles g	Est. # of Particles	Cumulative* % Less Than	Weight of Particles g	Est. # of Particles	Cumulative* % Less Than	Cumulative* % Less Than
2	0.00293	5.24×10^7	∿3	0.00216	3.86×10^7	2	2.5
5	0.07999	2.23×10^8	13.0	0.06991	1.95×10^8	11.0	12.0
8	0.06963	4.59×10^7	67.9	0.07933	5.23×10^7	66.4	67.2
13	0.39921	6.79×10^7	79.3	0.33543	5.71×10^7	81.2	80.2
20	0.39908	1.47×10^7	96.1	0.22033	8.10×10^6	97.4	96.8
35	0.05850	6.99×10^5	99.7	0.03839	4.58×10^5	99.7	99.7

* On a number basis

TABLE 4-3. PARTICLE SIZE DISTRIBUTION BY WET SIEVING OF PLATELETS

	Test #1			Test #2			Average
Sieve Size μ	Weight of Particles g	Est. # of Particles	Cumulative* % Less Than	Weight of Particles g	Est. # of Particles	Cumulative* % Less Than	Cumulative* % Less Than
2	0.00036	4.49×10^7	0	0.00128	1.60×10^8	2	1
5	0.06670	1.29×10^9	2.5	0.08436	1.64×10^9	7.1	4.8
8	0.05789	2.67×10^8	72.5	0.04723	2.18×10^8	79.6	76.1
13	0.14245	1.69×10^8	87.1	0.15773	1.87×10^8	89.3	88.2
20	0.17920	4.59×10^7	96.2	0.16790	4.31×10^7	97.6	96.9
35	0.22119	1.84×10^7	98.7	0.20637	1.72×10^7	99.5	99.1

* On a number basis.

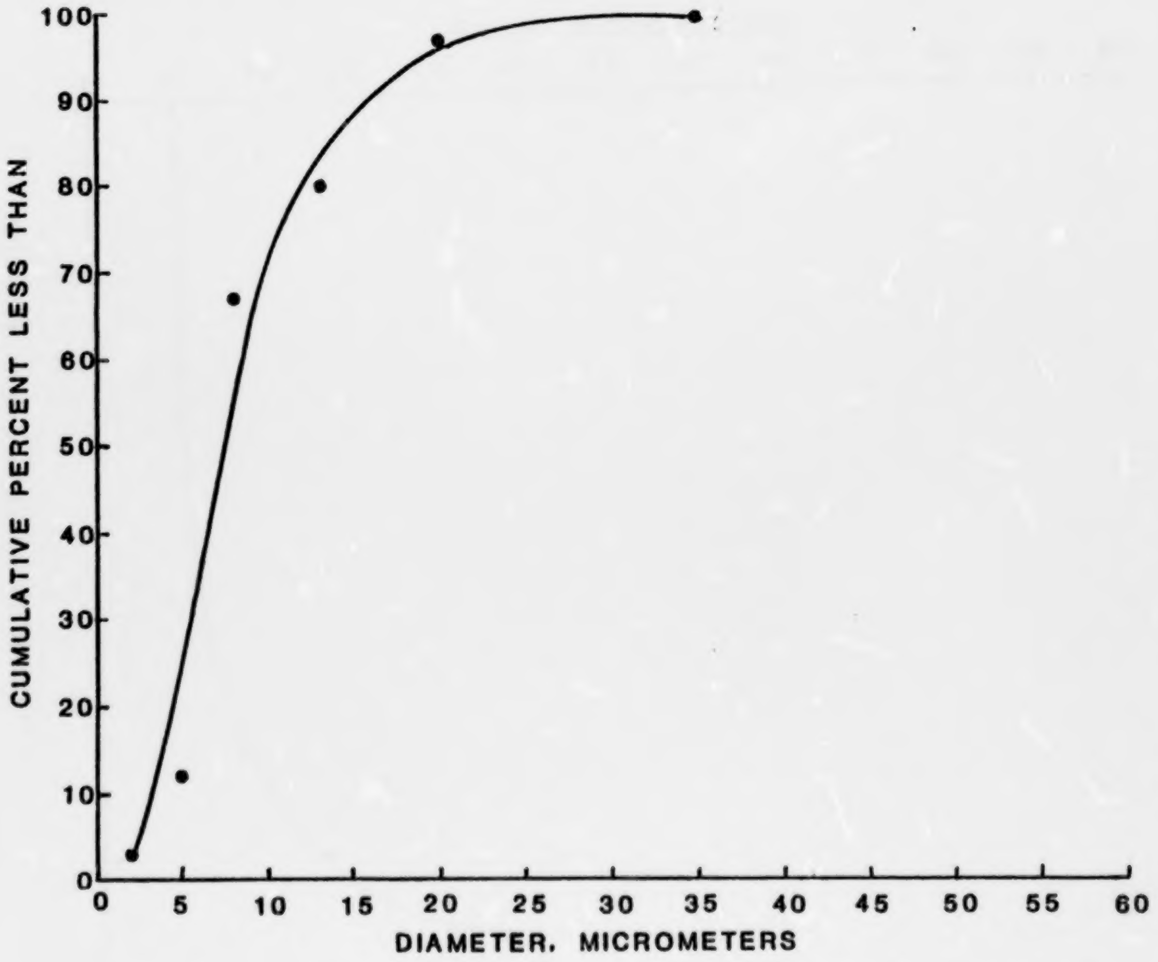

Figure 4-5. Sieved Sludge Granules: Average Cumulative Percent of Particles Versus Diameter.

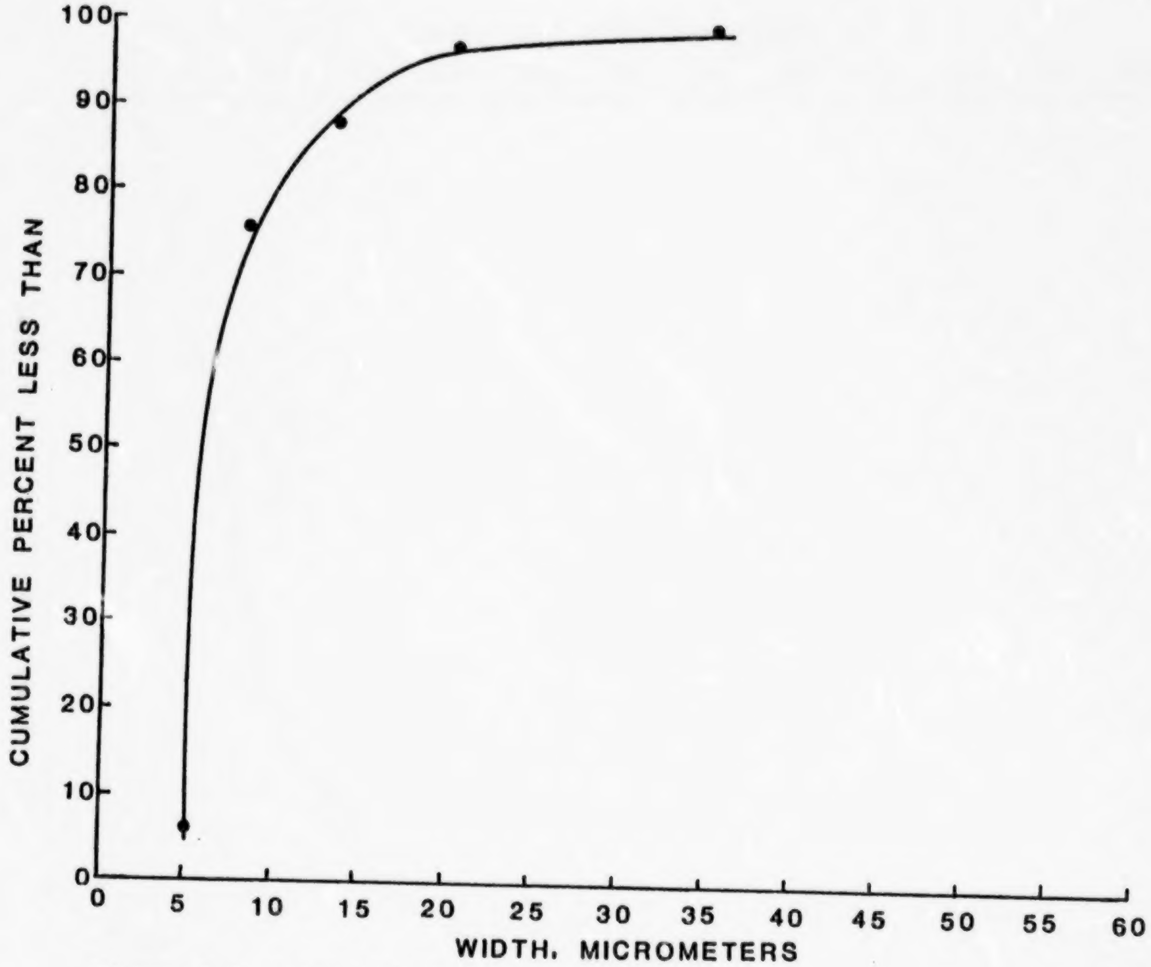

Figure 4-6. Sieved Sludge Platelets: Average Cumulative Percent of Particles Versus Width.

If it is assumed that the plates pass through the sieve holes diagonally then the apparent size of the openings is increased by a factor of 1.414 ($\sqrt{2}$). This made the particle size distribution larger and the data agree better with the photomicrographs. A plot of this data may be found in Figure 4-7.

4.3 PSD by Coulter Counter

Two samples were sent to an independent laboratory for particle size distribution analysis by Coulter Counter.

This instrument measures the number and diameter of particles in an electrically conductive fluid. As a suspension of the particles is drawn through a small aperture the resistance across it is measured by electrodes on both sides. The resistance change across the aperture is proportioned to the size of the particle passing through it.

4.3.1 Procedure

A small amount of the sample was dispersed in Coulter isoton solution with Triton X-100 added as a surfactant to reduce particles agglomeration. Dispersion of particles was completed by ultrasonic vibration. After 1:10 dilution the samples were then analyzed in a Coulter Counter Model TA with aperture setting at 70μ. The PSD data was recorded as the number of particles in each size range. The particle sizes are expressed as diameters in microns.

Because the particle sizes are reported as diameters, the data may be sized as is for granular or spherical-shaped particles. The platelets sample cannot be treated this way. Assuming dimensions of 30:20:1, the diameter was converted to the width of the particle as follows:

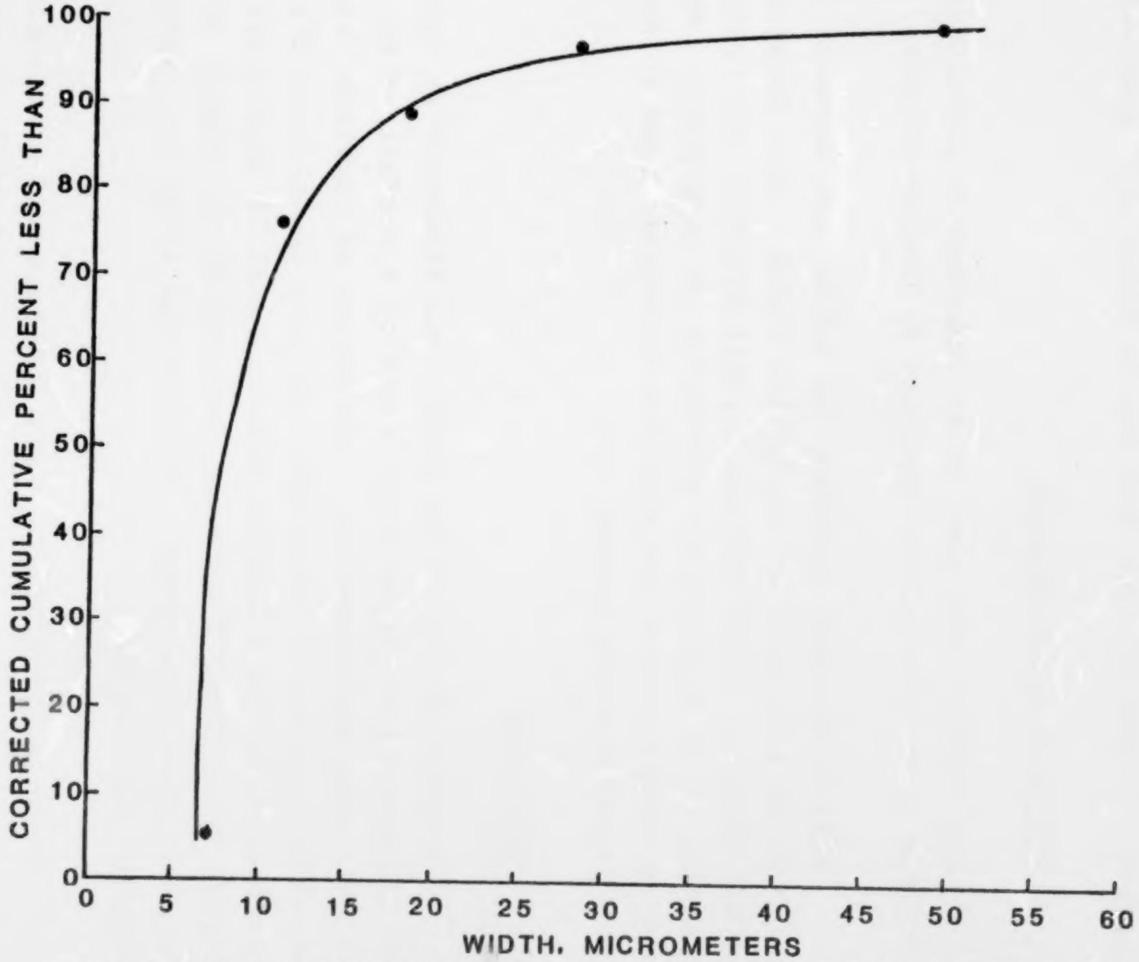

Figure 4-7. Sieved Sludge Platelets: Corrected Cumulative Percent of Particles Versus Width.

$$20 \times \sqrt[3]{\text{volume of particle}/600} = \text{width of a particle.}$$

The width dimension was chosen to allow comparison with the sieve and optical microscope data.

4.3.2 Results

The results of the Coulter Counter sizing are found in Table 4-4 and 4-5. The size distributions obtained by this method were lower than those obtained by the other two methods. Best comparisons were obtained by considering only the Coulter Counter data above 2μ for the granules diameters and above 3μ for the platelets widths. Below these limits a large number of particles were reported by the Coulter Counter method that were not observed in either the photomicrographs or the scanning electron micrographs of the same sludge samples. The ultrasonic dispersion step may have broken the sludge crystals, however, there is no evidence that this occurred.

4.4 Standardization of Settling Rate and Settled Density Tests

The purpose of this work was to determine the effect of cylinder size, weight percent solids, temperature, and particle size on settling rates and settled bulk density of FGD sludges.

4.4.1 Procedure

Settling Rate

A sample of dry sludge was added to a weighed graduated cylinder and sufficient water was added to bring the slurry to

TABLE 4-4. COULTER COUNTER DATA FOR THE SLUDGE GRANULES

Diameter μ	% Volume	Number	% Number	Cumulative* % Less Than
2.00-2.52	2.5	12467	42.4	42.4
2.52-3.17	2.0	4987	17.0	59.4
3.17-4.00	2.5	3116	10.6	70.0
4.00-5.04	3.9	2415	8.2	78.2
5.04-6.35	6.7	2103	7.1	85.3
6.35-8.00	11.9	1805	6.3	91.6
8.00-10.1	16.7	1305	4.4	96.0
10.1-12.7	18.1	706	2.4	98.4
12.7-16.0	16.2	316	1.1	99.5
16.0-20.2	12.4	120	0.41	99.9
20.2-25.4	4.9	23	0.08	100
25.4-32.0	2.2	5	0.02	100

* On a number basis.

TABLE 4-5. COULTER COUNTER DATA FOR THE SLUDGE PLATELETS

Diameter μ	% Volume	Number	% Number	Cumulative % Less Than
3.8-4.8	8.0	8134	61.2	61.2
4.8-6.1	4.7	2392	18.0	79.2
6.1-7.6	4.7	1196	9.0	88.2
7.6-9.6	4.7	598	4.5	92.7
9.6-12.1	5.6	358	2.7	95.4
12.1-15.3	8.0	254	1.9	97.3
15.3-19.3	8.7	138	1.0	98.3
19.3-24.3	13.1	104	0.78	99.1
24.3-30.6	15.9	63	0.47	99.4
30.6-38.6	18.7	37	0.28	99.4
38.6-48.5	5.6	5	0.04	99.4
48.5-61.2	2.3	1	0.01	99.4

* On a number basis.

the desired weight percent solids. The water used to make the slurry was previously equilibrated with similar scrubber solids and filtered. This helped prevent any of the crystals from dissolving. The slurry was mixed thoroughly by repeated inversion of the cylinder. A ruler graduated in centimeters was attached to the cylinder. A timer was then started and the height of the liquid solids interface was measured at one minute intervals for 10 to 15 minutes.

If the settling tests are to be performed in the field, a more convenient way to prepare the sample might be to determine the weight percent solids of the slurry, and then dilute it to the desired value obviating the need for slurry filtration.

The data is plotted on regular graph paper. The settling rate is determined from the slope of the line for the first 5 or 6 minutes of settling. This region of the settling rate curve is for the hindered settling mode.

Settled Density

After the slurry has settled for at least six hours, but preferably overnight, the density of the settled fraction is calculated from the following equation:

$$\text{Settled density} = \frac{Wt_T - \rho_\ell (V_T - V_s)}{V_s}$$

where,

Wt_T = total slurry weight (grams)
V_T = total slurry volume (mls)
V_s = volume of settled solids (mls)
ρ_ℓ = supernatant density (g/ml)

The measurement of ρ_ℓ was made with a hydrometer calibrated over the range of 1.000 to 1.200 g/mℓ.

By knowing or assuming a solids density, ρ_s, the weight percent solid in the settled fraction can also be calculated using the the following equation:

$$\text{Weight \% Solids in Settled Fraction} = \left(\frac{\rho_s}{\rho_s - \rho_\ell}\right)\left(\frac{Wt_T - \rho_\ell V_T}{Wt_T - \rho_\ell V_T + \rho_\ell V_s}\right)$$

4.4.2 Results

Effect of Cylinder Size

Tests were performed to determine the effect of container diameter on settling rates. Settling data were recorded as a function of time in three containers of different diameters. The cylinders used were 250 ml, 500 ml and 1000 ml capacity each. Although the initial height of the slurry in each cylinder was different for a constant slurry volume, the observed settling rates were constant, indicating that settling rate is not a function of container size within the size range tested.

Effect of Percent Solids

The weight percent solids was varied over the range of 1% to 20% and was found to have a large effect on settling rates. For the platelet sludge sample the settling rate at 25°C ranged from 3.4 cm/min at 1% solids to 0.18 cm/min at 20% solids. The granular sludge sample which consisted of smaller particles showed a range of 2.45 cm/min at 2% solids to 0.10 cm/min at 15% solids at 25°C. By extrapolating these results it is estimated that the two sludges will have approximately equal settling rates at about 25% solids. The results of these tests are shown in Table 4-6 and in Figure 4-8.

Effect of Temperature

It was found that upon increasing the slurry temperature from 25°C to 50°C the solids settling rate increased by 50-60% for both types of samples over the entire range of weight % solids investigated (Table 4-6 and Figure 4-8). The difference in settling rate was attributed to changes in the viscosity of the water and agrees with rate changes predicted from Stoke's Law calculations.

Effect of Particle Size

The smaller granular particles settled slower than the platelet particles at all the weight % solids concentrations that were compared.

Results of Settled Density Tests

The settled density was calculated for each type of sample. The settled density for the platelet-type particles was 1.39 g/cm^3 and for the granules the settled density was 1.25 g/cm^3.

TABLE 4-6. SETTLING RATE OF SLUDGES VERSUS WEIGHT % SOLIDS AT 25°C AND 50°C

Weight % Solids	Granules Settling Rate (cm/hr)		Platelets Settling Rate (cm/hr)	
	25°C	50°C	25°C	50°C
1	--	--	3.35	--
2	2.38	--	2.95	--
3	--	--	2.51	--
4	1.64	2.64	2.34	--
5	1.30	2.04	1.95	3.03
6	--	--	1.70	--
7	0.74	1.10	1.50	--
8	--	--	1.30	--
9	0.42	--	1.15	--
10	0.30	0.45	0.98	1.48
12.5	--	--	0.65	--
15	0.10	--	0.44	0.60
20	--	--	0.18	--

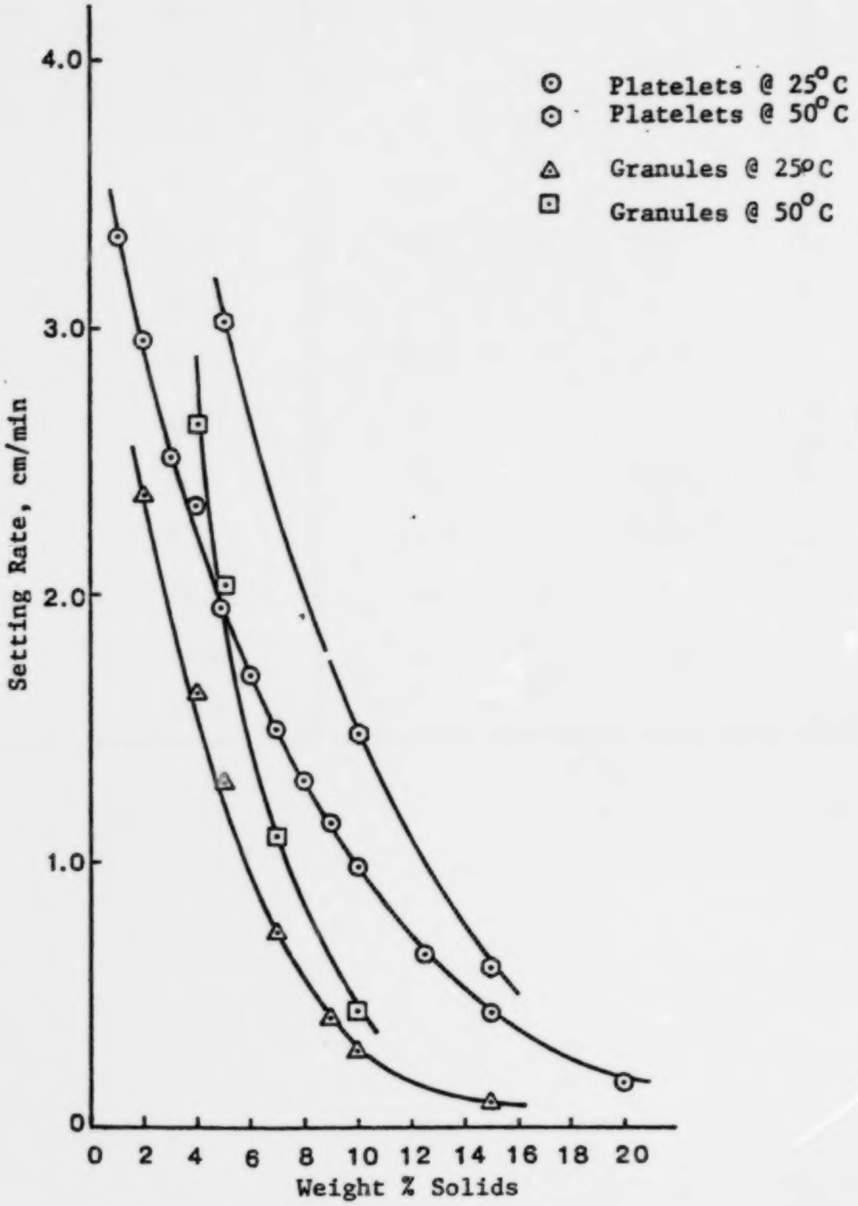

Figure 4-8. Settling Rates of Sludges Versus Weight % Solids at 25°C and 50°C

5.0 RESULTS OF THE LITERATURE SURVEY

The literature was searched for methods to determine particle size distribution, settling rate, and settled density of fine powders. The results are given in Tables 5-1 and 5-2.

5.1 Methods for Particle Size Determination

There are a large number of methods which have been used for particle size determination. These methods fall into the following broad categories:

- direct measurement with the aid of a visual or electron microscope (or a hologram),
- sieving,
- sedimentation in a fluid,
- measurements based upon particle trajectories,
- measurements based upon radiation scattering, and
- electrical measurements.

More detailed descriptions of the principles involved, the apparatus required and the applicability of these methods are given in Table 5-1.

Optical methods (visible light microscopy, electron microscopy, and holography) provide a direct measure of the

TABLE 5-1. PARTICLE SIZE DETERMINATION

Method	Principle	Apparatus	Applicability and Constraints	Accuracy and Precision	Reference
1.0 Microscopic					
1.1 Visible Light Manual Scan	A prepared sample is observed visually under a microscope. Particles are counted and sized individually usually by comparison with circles of a known size on a transparent plate, or by measurement of a horizontal or verticle linear dimension combined with statistical data treatment. ASTM E20-68 calls for measurement of at least 250 particles in each of three randomly selected fields to insure calculation of a statistically reliable size distribution. Counting and sizing may also be done using a photomicrograph projected on a grided screen.	A good quality microscope is required. The instrument characteristics, primarily aperture and magnification, must be sufficient to resolve the edges of the smallest particle class size of interest.	Microscopy is generally considered as a standard method for absolute particle size measurement. Unfortunately, manual microscopy is tedious and time consuming, about 3-4 hours are usually required for one sample. An operator must be skilled in sample preparation as well as counting and size determination. This method is applicable to nearly any particulate matter ranging in size from .2μ to ~ 74μ. The measurement of only two dimensions (those in the plane of the field) may lead to serious errors in case of disc-like particles. Normally, the assumption is made that a randomly sampled field will contain particles with no preferred orientation.	The accuracy and precision of microscopic sizing (assuming an adequate instrument) are dependent primarily on three factors: 1) the skill and experience of the operator, 2) the representative character of the prepared sample, and 3) the number of particles counted. The statistical reliability of the results increases as $(n)^{\frac{1}{2}}$ where n is the number of particles counted. To obtain the number of particles of a given size in a sample within ± 2%, ~ 10,000 particles would have to be counted. ASTM E20-68 recommends a count of at least 250 particles in each of three randomly sampled fields.	AM-011 CA-040 HA-044 KI-014 LA-022 SI-010 ST-040 SU-011 MO-016 OR-006 SC-R-141 IR-016
1.2 Visible Light Automatic Scan	In this method, the human observer is replaced by an automatic counting and sizing system. These systems scan the sample slide or photograph using a narrow slit or dot of light. Interception of this light by a particle is detected photometrically. The problem of meaningful interpretation of scanning results is not simple. The information derived is dependent on the number and shapes of the scanning beams. Also, the concentration of the sample being scanned affects errors caused by overlapping or coincident particles. Sophisticated electronics are required to provide particle size readout.	Commercial instruments such as the Quantimet are available. These consist of scanning and photometric equipment along with a minicomputer for interpretation of raw output.	Primary constraints on the use of automatic scanning are the effects of particle size, shape, and concentration on results. Irregularly shaped particles or particles too close together in the field may lead to counting and sizing errors. The lower particle size limit for automatic scanning is generally higher than for manual scanning, about .8μ. Proper form is essential as in manual scanning. As many as 100 fields may be counted in 2 minutes with one commercial instrument (Quantimet).		CA-040 HA-044 KA-021 MO-016 OR-006 SM-007 WA-022 IR-016

(continued)

TABLE 5-1. (Cont'd.)

Method	Principle	Apparatus	Applicability and Constraints	Accuracy and Precision	Reference
1.3 Electron Microscope	The electron microscope extends the range of microscopic size determination to as low as .001 μ by using electrons instead of visible light as the image producing beam. A sample of particles is usually fixed in a very thin membrane by methods similar to those used in visible microscopy. The image may be viewed directly on a cathode ray tube, or photographed for measurement and sizing.	The electron microscope is a sophisticated instrument requiring skilled operators. It is also a relatively expensive particle sizing technique ($50,000 +).	Particles as small as .001 μ may be sized via electron microscopy. The upper limit of the sizing range is approximately 10 μ since particles larger than this will block the field. A distribution requiring both electron and visible microscopy, presents some problem since the greater resolution of the former in the 1-10 μ range results in a curve which does not "mesh" with the visibly determined distribution for the upper range. Time required for image analysis is similar to visible microscopy (manual or automatic image analysis is available).	The precision of this method is similar to that of visible microscopy.	CA-040 JO-019 OR-006 ST-039 IR-016
1.4 Holography	Holography is a means of imaging an object by photographing interference patterns formed when a volume of small particles is illuminated with laser light. An image of the sample is reconstructed when the resulting hologram is illuminated by a second laser. The reconstructed volume is a perfect model of the original volume with uniform magnification throughout and all objects located at coordinates corresponding to their original position. Particles may then be counted and sized as in standard microscopy. In theory, the particles must be stationary, but in practice a rapid pulsed laser can be used to "stop" a dynamic situation.	A pulsed ruby laser with a collimator and a camera with a common longitudinal axis are required to record the hologram. The image is reconstructed using a second laser.	The equipment required for this method is obviously not justified except where "stop action" in-situ imaging of fast moving particles is required. Determination of particle size distribution from a hologram is as time consuming as from a photomicrograph. The system discribed by Zinley records particle sizes in the range 3.5-100 μ mean diameter.		ZI-003
2.0 Sieving					
2.1 Sieving	This method is conceptually one of the simplest particle sizing techniques. A sample of particulate is passed through a series of sieves of decreasing grid size so that particle size fractions are separated. These fractions are collected and weighed to calculate a size distribution. Actually, size separation by sieving is a probabilistic process depending on both (cont.)	Standard sieves are employed usually having grid sizes with a lower limit of 37 μ and ascending in the ratio $(2)^{1/2}$:1 [or $(2)^{1/4}$:1]. A mechanical shaker is preferred for (cont.)	Sieving is normally used for particles greater than 50 μ in size. Electroformed "micromesh" sieves are available in sizes as fine as 5 μ, however. Probably the greatest single drawback in sieve analysis is the dependence of results on shape and sieving time. In general, sieve analyses do not agree well with microscopic or sedimentation techniques. (cont.)	When a mechanical shaker is used with a specified sieving time, reproducibility between runs should be within 2% for standard sieves. Standard deviations from 3% to 25% have been reported using electroformed micromesh sieves in the 30 to 5 μ range.	BR-023 CA-040 DA-019 GR-016 HU-012 LA-022 LU-012 OR-006 RO-014 SC-027 SU-005 AM-275 PR-091 DA-264

TABLE 5-1. (Cont'd.)

Method	Principle	Apparatus	Applicability and Constraints	Accuracy and Precision	Reference
2.1 Sieving (cont.)	size and shape. A particle shaped like a square flat plate, for example, has only a small probability of passing through a square grid of the same or nearly the same width. This means that the end point for a sieve test must be an arbitrary time limit, usually 7-9 minutes.	improved accuracy. Equipment for normal sieve sizes is inexpensive, about $1000 including a mechanical shaker. Equipment for micromesh sieving would cost an additional $1000 ("sonic sifter" + sieves).	On the other hand, this method is fast (½ hour) and inexpensive. A relatively large sample is required compared to the other methods (50-100 gms).		IR-016 LA-159 LO-089 AM-269 AM-270
3.0 **Methods Based on Particle Settling Velocity**					
3.1 Gravity Sedimentation in Liquid	In general, these methods measure an "equivalent" diameter by observing the settling rate of the sample in a viscous fluid. Stoke's law for viscous flow around a spherical body is used as a basis for calculation of particle size distribution. This is given by: $U_t = D_p^2 g(\rho_p - \rho_f)/18\mu$ Where U_t is the terminal settling velocity, D_p the Stoke's particle diameter, ρ_f and ρ_p the fluid and partical densities respectively, and μ the fluid viscosity. The relationship between actual particle shape and dimensions and Stoke's diameter is not known in general. Different methods use different means of measuring settling rates and extracting particle size data from these measurements. It should be noted that the particles must be of uniform density in order for accurate particle size data to result.		Accumulative or fixed level sensing methods require up to 24 hours for small (< 1 μ) particles to settle. More sophisticated scanning instruments reduce this to as little as one hour.	The accuracy and reproducibility of all sedimentation devices depends strongly on the care with which the sample is dispersed before settling.	CA-040 HE-010 HI-020 — OR-006 PH-002 SM-006 SO-010 IR-016

TABLE 5-1 (Cont'd.)

Method	Principle	Apparatus	Applicability and Constraints	Accuracy and Precision	Reference
3.1.1 Pipette Method	A sample of particulate is dispersed and suspended in a graduated cylinder in which a pipette is mounted at a fixed level. After uniform suspension is achieved by shaking, the particles are allowed to settle. Samples are withdrawn using the pipette at various times over the test period. These samples are dried and weighed, providing a measure of concentration vs. time at the pipette level in the cylinder. These data are easily converted to a cumulative weight-undersize plot via the Stoke's equation and a knowledge of the distance from the top of the suspension cylinder to the pipette mouth.	The apparatus for this method is quite simple. It consists of a sedimentation vessel graduated from 0-20 cm. in height and holding approximately 500 ml of sample suspension. A 10 ml. pipette is fitted to the top with a ground glass joint so that the tip extends down to a fixed level in the vessel. For precise work, a constant temperature bath is desirable. A drying oven and precision balance are also required. Multiple pipettes fixed at different levels have been used to shorten overall time required for a given size distribution. A fluid must be selected that will have no effect on the size and density of the settling particles.	As with other gravity settling methods, the particle size range for which this method is convenient is determined by the settling velocities of the largest and smallest particles. For example, a one u sphere with a specific gravity of two would settle at a $\sim 5.4\text{x}10^{-5}$ cm/sec. in water requiring over 100 hours to settle 20 cm A 100 μ particle on the other hand would settle this far in only 37 seconds, giving rise to great variation in a method using a 10-20 second pipette sample time (large particles also may settle outside the Stoke's law range of velocity). The sample must be well dispersed usually with an agent added to reduce agglomeration tendencies. Sample concentration must be low to avoid particle interaction (hindered settling).	If performed carefully, the method is quite reproducible. Crindrod (GR-016) reports a standard deviation of 1-2% on repetitive tests with portland cement particles. Results are similar to other sedimentation methods. In the very fine particle (< 5 μ) range, however, standard deviations up to 10-20% have been noted. In this range, turbulence caused by sampling or convection can effect results. Error is also introduced by non-instantaneous sampling and variation in operator technique.	CA-040 GR-016 HU-012 OR-006 SI-010 IR-016
3.1.2 Balance Method	The settling rate of a sample is measured by cumulative collection and in situ "weighing" of the settled particles. This is accomplished by placing a balance pan or other force transducer at the bottom of a settling tube. Two methods of introducing the sample have been used. In one, the sample is dispersed throughout the tube by shaking. In the other, the sample is introduced at the top of the tube at time zero. The former method requires graphical differentiation of the weight settled vs. time plot to extract a particle size distribution. The latter does not (cont.)	Apparatus consists of a settling tube (in a constant temperature bath for precise work with small particles) with a sensitive force transducing apparatus at the bottom. An amplifier/meter recorder combination may be used to provide direct readout of data, after calibration. Commercial apparatus (Cahn) is available for about $3,000.	Problems are similar to other sedimentation methods. In addition, sample size must be selected with the sensitivity of the balance in mind.	Accuracy and precision compare to those of the pipette method	CA-040 BO-016 FE-009 JA-011 OR-006 RA-025 SI-010 SM-005 SU-011

TABLE 5-1. (Cont'd.)

Method	Principle	Apparatus	Applicability and Constraints	Accuracy and Precision	Reference
3.1.2 Balance Method (cont.)	and is more amenable to inexpensive direct reading and recording devices.				
3.1.3 Hydrometer Method	A sample is mixed with an appropriate fluid and dispersant in a settling tube as in other gravity settling methods. In this case, the concentration of suspension at a given level and time is determined by insertion of a calibrated hydrometer into the fluid. Once the concentration at a level is known, particle size distribution data are obtained in the same manner as the pipette method using Stoke's law. The results are obtained in the form of a weight fraction-oversize vs. size plot.	The apparatus consists of a calibrated hydrometer, a settling tube, and a constant temperature bath.	The minimum particle size class measurable by this technique is on the order of one micron. This lower limit is fixed by error in hydrometer readings arising from convection, vibration, and Brownian movement. The maximum size is limited by rapid settling of large particles as in the other settling methods. A rather concentrated suspension is required, making deviation from free settling likely. The particle size distribution must be fairly uniform since the hydrometer covers a finite level in the settling tube.	This method generally agrees with other sedimentation methods. Some error arises from disturbances caused by manipulating the hydrometer. Additional error is introduced in reading it and estimating an equivalent level to which the reading corresponds.	CA-040 LE-013 MA-057 MC-019 OR-006 LA-159 IR-016 AM-275
3.1.4 Diver Method	This technique is similar in principle to the hydrometer method except that the density of the suspension at different times and levels is determined by carefully inserting "divers" of known density into the suspension. The diver will sink to a level at which the suspension density is equal to its own. This level is measured. Computation of particle size distribution from density data is straightforward.	Apparatus is similar to other settling methods with the hydrometer or pipette exchanged for calibrated glass spheres of known density.	Similar to hydrometer method.	Similar to hydrometer method.	CA-040 OR-006 IR-016
3.2 Gravity Sedimentation in Air	These methods are similar to sedimentation techniques using liquids. Cumulative determination of settled weight by balance pan is the most practical route to data reduction.	Air settling tubes are usually quite long compared to their liquid counterparts. One commercial apparatus employs a tube about 90 inches long. A means of dispersing a sample in air is not straightforward. One instrument uses a blast of compressed air. A precision recording balance is required.	This technique is capable of measuring small particles (< 5 μ) in much less time than that required for liquid settling. It is also useful for very light materials which settle very slowly in liquid media. Large particles (> 50 μ) settling in air deviate significantly from Stoke's law, making some correction necessary.	A commercial instrument, the Sharples Micromerograph claims an accuracy of ± 3%. It is doubtful whether this can be achieved for particles smaller than 5 μ or larger than 50 μ. Wall losses with small particles may be significant.	CA-040 OR-006 SO-010

TABLE 5-1. (Cont'd.)

Method	Principle	Apparatus	Applicability and Constraints	Accuracy and Precision	Reference
3.3 Centrifugal Sedimentation	The limitations imposed by slow settling of very fine particles may be overcome by use of a centrifuge. The "g" in Stoke's equation is replaced by $R\omega^2$ where R is the radius of rotation and ω the angular velocity of the centrifuge. The variation in R as the particle settles leads to $D = \frac{1}{\omega}\left[\frac{18\mu \, \ell n(X_2/X_1)}{(\rho_p - \rho_f)t}\right]^{\frac{1}{2}}$ as a modified version of Stoke's law. Here, ω is the angular velocity, X_1 is the distance from the center of rotation to the liquid surface, and X_2 the distance from the center to the point to which the particle settles.	For small particles (< 1 μ), a high speed centrifuge is required.	Centrifugation to determine particle size distribution can extend the range of sedimentation methods to particles as small as .05 μ.		LE-013 MU-010 OR-006 SO-010 IR-016
4.0 Particle Trajectories					
4.1 Elutriation	Instead of allowing particles to settle in a fluid, particles of a given diameter are removed from a sample by a flowing fluid with its velocity equivalent to the Stoke's velocity of a particular size particle. All particles smaller than this size will be carried away. Repeated fraction at ions at different velocities followed by collection and weighing of the fractions yields a size distribution.	An elutriator consists, in general, of a tube, a means of controlling fluid flow through this tube, and a means of introducing a sample and collecting elutriated fractions. This equipment can range considerably in complexity and cost.	Separation of a number of particle size fractions by elutriation is time consuming. Also, the existence of a parbolic velocity profile in the tube tends to make the distribution within fractions relatively broad. Additional errors arise from selection of an arbitrary end point (as in sieving) and deposition of material on the elutriator walls. About 30 minutes are required to separate one fraction.		CA-040 HU-012 OR-006 IR-016
4.2 Combined Centrifugation/ Elutriation (Bahco Classifier)	This method combines air elutriation with centrifugal sedimentation in a manner which both decreases classification time and improves the separation between successive size fractions. The resulting size fractions are weighed to yield a weight-undersize plot.	A relatively inexpensive commercial instrument ($3300) is available.	Elutriation combined with centrifugal separation of fractions enables a single size cut to be made in 15 minutes.	In tests with fly ash reproducability is reported to be better than 1%. For a given material, accuracy is improved by calibration of each size fraction against a slower sedimentation method.	CR-012 DI-021 GR-032 SI-010 TO-008 IR-016

Table 5-1. (Cont'd.)

Method	Principle	Apparatus	Applicability and Constraints	Accuracy and Precision	Reference
4.3 Inertial Impaction	Particles suspended in air are drawn through a series of jets or slots of decreasing size, each of which is followed by a flat plate. As the high velocity air stream flows around a plate, particles larger than a given size will be separated from the gas stream since their inertia prevents them from following the air stream. The collected particles may be sized independently or the instrument may be calibrated so that after weighing the fractions, a mass-undersize plot is obtained directly. The minimum size particle removed by a given stage (jet/plate combination) is given by: $d_{min} = \left(\frac{36\ \omega' u}{\pi \rho u}\right)^{\frac{1}{2}}$ when ω' is the half width of the jet vena contracta, μ is the fluid viscosity, ρ the particle density, and u the particle velocity.	A basic cascade impactor is quite simple in construction, consisting of an airtight container with jets and impaction plates mounted within. Associated equipment includes a pump, valve, and flow meter arrangement to reproduce sampling conditions. Prices range from $100-$2000).	This method is normally used in situ to size particles suspended in air. The possibility exists of redispersing a bulk solids sample so that it can be sized by impaction. Impaction may be used to classify particles from .1 to 100 μ in diameter. Operating time is dependent on concentration of particles in the sample stream. Sufficient sample must be collected for accurate weighing.	Accuracy varies with instruments. Some sources of error include secondary deposition and wall deposition. These can be minimized by proper design and operation.	CA-040 OR-006
5.0 Methods Based on Radiation Transmission or Scattering					
5.1 Radiation Scattering (Visible Light Range)	These methods use the principles of radiation scattering as a means of counting and sizing particles. When a narrow beam of incident radiation is intercepted by a particle, a portion of the energy is absorbed and a portion scattered. The remainder is transmitted. The intensity of scattered energy is a function of scattering angle, particle shape, size, and optical properties, and the wavelength of incident radiation. For particle size determinations it is desirable that the particles not absorb light at the wavelength of the incident radiation. Complex indices of refraction also cause errors in interpretation of data.	This type of instrument requires complex and precise means of transmitting and detecting narrow beams or slits of the detecting radiation. If direct readout is desired, considerable electronic sophistication results.	The primary constraint associated with scattering methods is the difficulty in relating measured intensity to particle size and concentration. Theory is well developed only for monodispersed spherical particles of uniform optical properties. A second consideration is sample concentration. Too many particles per unit volume cause interactions that are not easily interpreted. Particle size may range from .2 to 100 μ, although background noise may cause significant deviations in the lower range. The real-time, on-line capability of this method is attractive.	For most applications this method measures a rather qualitative "equivalent" diameter which may differ widely from that determined by other methods. Counts for particles less than 1 μ in diameter may be seriously in error (on the low side) in some circumstances.	AP-004 AU-003 CA-026 DI-012 LI-019 MA-059 MU-013 MU-014 OR-006 RI-007 WE-022 ZI-003

TABLE 5-1. (Cont'd.)

Method	Principle	Apparatus	Applicability and Constraints	Accuracy and Precision	Reference
5.2 Turbidimetric Methods	These methods measure photometrically extinction of light by a settling suspension to determine particle size distribution. The intensity of transmitted light, I, is given for monodispersed spherical particles by: $I/I_0 = \exp[-K\pi r^2 n\ell]$ where I_0 in the incident intensity, K is a scattering coefficient, r the particle radius, n the number of particles per unit volume, and ℓ the path length. For nonspherical particles having a wide range of sizes, this equation is not useful in practice, thus the turbidimetric method requires calibration with a known distribution of the particular material of interest. Beginning with a uniform suspension and a transverse light beam at a fixed depth below the surface, no change in absorbance of the suspension will occur until the largest particles in the suspension have fallen from the surface to the level of the measuring beam. At this time the absorbance will decrease by an amount proportional to the concentration of the largest particles. Any point on the absorbance vs. time curve then represents the concentration of particles smaller than a size of particle which would fall the distance "h" from the surface to the measuring beam in a time "t". Thus a size-distribution curve is obtained with the "y" or absorbance ordinate representing concentration of particles less than stated size and the "x" or time ordinate representing particle size in terms of Stoke's diameter. This method has the capability of rapid measurement at several levels in a settling tube, thus shortening the time required for a wide size distribution.	The apparatus is not very complex. It consists of a settling cell surrounded by a barrier through which a narrow collimated beam of light may pass. The extinction is measured photometrically and can be recorded. A vertical adjustment for the cell platform permits rapid measurements at different levels. An elegant variation in approach using the principles of the blocking of radiation by solid particles is described by Ricci and Cooper (RI-009). A scanning laser beam is directed at a flowing slurry under conditions such that settling will not occur. Sophisticated electronic circuitry converts the output of a photodetector to particle size distribution information.	The requirement that this method be calibrated with a known sample of the same material may be a serious handicap when particle size analyses of nonuniform materials is necessary, since results can be affected by color and shape and even initial suspension concentration as well as size. The total analysis time of approximately one hour is attractive. Also very small samples are needed as compared to gravimetric techniques. A .01% suspension is used vs. 1-2% for other settling methods. The photometric output is amenable to automatic readout. The apparatus described by Ricci and Cooper (see Apparatus column) must still be calibrated for each particulate system. It is designed to monitor particle size distribution in the range 5 μ to 2000 u on an on-stream, real-time basis.	Reproducibility is reported to be in the range of ± 2%. In view of questionable theoretical basis for this method, there is some question as to what "size" is actually measured. This method does not in general give similar results to most other particle sizing methods, especially for smaller particles.	AM-006 CA-040 BE-035 BR-023 LA-021 OR-006 RI-009 TA-012

Table 5-1. (Cont'd.)

Method	Principle	Apparatus	Applicability and Constraints	Accuracy and Precision	Reference
5.3 X-Ray Absorption Detection	Similar in principle to turbidimetry, small angle X-ray scattering can be used to determine the concentration of a settling suspension at a given level and time. A particle size distribution can easily be extracted from these data. Ebel, et al., (EB-001) discuss the theory involved.	The X-ray scattering apparatus is more complex than the visible light extinction method. A very finely collimated X-ray beam is directed through the sample cell and small angle scattering intensity is detected by a Geiger counter. Electronic conversion of raw data directly to particle size distribution is possible. A commercial instrument (Micromeritics) is available for $14,000.	Small angle X-ray scattering is more accurate than light extinction since the optical properties of the sample do not affect results. Also, the capability of a multilevel scan as in turbidimetry reduces the time required and extends the particle size range to ~ .5-100 μ.	Precision of a commercial instrument by Micromeritics is reported to be ± 1%.	EB-001 KA-026 MI-024 OR-006 BU-259
5.4 X-Ray Fluorescence	The intensity of fluorescent X-rays from an element in a particle is dependent on particle size. The effect can be expressed by the intensity ratio R, the ratio of the intensity from a sample containing particles of size S to the intensity from a sample containing particles of zero size, both samples having the same concentration of the fluorescing elements.	X-ray fluorescence spectrometer.	The following requirements must be met in order for this method to be applicable. 1. The concentration of the element for which the fluorescent radiation is being measured must be known. 2. The X-ray properties of the unknown sample must be close to those of the comparison sample. 3. The desired information is average particle size. 4. The matrix cannot contain the same element as the particle element whose fluorescence is being measured. 5. The particles must contain an element above atomic number 11. 6. The particles must be distributed randomly in the sample. The particle size - intensity effect is greatest for particles in the 1-200 μ size range.		HO-024 IR-016

TABLE 5-1. (Cont'd.)

Method	Principle	Apparatus	Applicability and Constraints	Accuracy and Precision	Reference
5.5 X-Ray Scattering	X-ray scattering at very small angles, i.e., scattering in the forward direction of propagation of the radiation is employed for particle size measurement. If a single small spherical particle is irradiated by a narrow monochromatic beam of X-rays, the radiation will be scattered when normalized (intensity is unity for r=0) in accordance with the relation: $I = C\Phi^2 k\rho$ where I is the scattered intensity; C a constant depending on electron charge, density, number of electrons in the particle, etc.; ρ the radius of gyration of the particle; $k = 4\pi \sin(\gamma/2)/\lambda$; γ the scattering angle; λ the wavelength of the radiation; and Φ the scattering function of spherical particles.	X-ray source and detector system.	This method gives average particle size in the range 0.005 to 0.05 μ. If X-rays in the wavelengths requiring evacuated systems are used larger particles may be examined.		BR-027 OR-006
6.0 Electrical					
6.1 Coulter Counter	This instrumental method measures the number and "diameter" of particles in an electrically conductive system. A suspension of the material to be measured is drawn through a small aperture having an immersed electrode on each side. As each particle passes through the aperture it displaces a volume of solution proportional to its own volume. This displacement momentarily produces a change in resistance between the electrodes creating a voltage pulse the magnitude of which is related to the volume of the passing particle. The pulses are electronically counted and scaled. A direct fraction undersize distribution may be obtained by setting different "threshold" limits for the largest or smallest particle size to be counted.	The apparatus consists of a sample cell and aperture with arrangements for drawing the sample through it, an amplifier and pulse height analyzer, and an oscilloscope display and or x-y plotter. The basic unit costs ~ $5000. An automatic plotter is an additional $2000.	A primary source of error in this method is coincidental passage of more than one particle through the aperture. Additional error results from electrical noise and some variation of response with particle shape. Aperture blockage may occur when large particles are present. On the other hand, use of a larger aperture leads to errors in the small particle size range. Applicable size range is .5-100 μ.	Since response is nearly linear with particle volume, particle size is inferred only by assuming a shape. The instrument must be calibrated with a known particle size sample. Standard deviation of repetative counts is reported to be 1-5% depending upon particle size, shape, and concentration. In general, smaller particles are subject to larger variation in count.	BR-023 DI-012 EC-002 ED-004 GR-014 GR-015 HU-010 HU-012 KE-025 RO-014 SC-018 IR-016

TABLE 5-1. (Cont'd.)

Method	Principle	Apparatus	Applicability and Constraints	Accuracy and Precision	Reference
6.2 Electrostatic	Particles are charged according to their size in a corona discharge and then precipitated by an electric field.	The device described basically consists of a chamber in which the particles acquire charges upon traversing a corona discharge from a length of wire. The aerosol then goes into a cylindrical condensor with the inner rod maintained on a fixed potential and the outer cylinder grounded. The electric field causes the charged particles to follow different trajectories and be precipitated on the cylinder wall.	Applicable to aerosols in the 1-20 micron size range.		YO-004

TABLE 5-2. BULK DENSITY AND SETTLING RATE MEASUREMENTS

Method	Principle	Apparatus	Applicability and Constraints	Accuracy and Precision	References
1. Slurry Bulk Density	A representative sample of the slurry is added to a preweighed volumetric flask. Small deviations from the full mark can be made up with water. The flask and contents are then reweighed. The bulk density is calculated from the following equation: $D = (W_s - W_f)/V_f$ where: W_s = Weight of sample and flask (g) W_f = Weight of the empty flask (g) V_f = Volume of the sample (ml)	Volumetric flasks, analytic balance, constant temperature bath	The slurry sample to be analyzed must be thoroughly mixed before addition to the volumetric flask. This will avoid forming any density gradients in the sample which could seriously affect the density measurements when only a portion of the original sample is used. A constant temperature (which is specified on the flask) should be maintained since density is a function of temperature.		RO-133 AU-063
2. Settled Bulk Density	A slurry is added to a preweighed graduated cylinder, and the total weight and volume are measured. The settled bulk density is calculated from the following equation: $\rho_{sb} = \frac{(B-A)-D(C-E)}{E}$ where: A = wt. of empty cylinder (g) B = wt. of cylinder + slurry (g) C = initial volume of slurry (ml) D = density of resultant supernatant fluid after settling (g/ml) E = volume of settled solids (ml) The settled bulk density of FGD sludges varies as a function of	The density measurement, D, is made with a hydrometer calibrated over the range of 1.00 to 1.200 g/cm^3. Accurate graduated cylinders and a constant temperature bath are also required.	The apparatus is inexpensive and the method may be applied to any type of slurry stream. The time requirement for each analysis is dependent on the settling rate of the solids, however many samples can be run at the same time.	The accuracy of the method is limited primarily by the accuracy of the cylinder which is used to make the volume measurements.	TE-304 RO-133 JO-083 PR-091 EN-269

TABLE 5-2. (Cont'd.) - BULK DENSITY AND SETTLING RATE MEASUREMENTS

Method	Principle	Apparatus	Applicability and Constraints	Accuracy and Precision	References
	water content. Peak bulk densities are usually found at between 20% and 40% water content.				
3. Solids Content, "Quick Method"	If the specific gravity of the scrubber solids ($CaSO_4 \cdot 2H_2O$, $CaSO_3 \cdot \frac{1}{2}H_2O$, and fly ash) is assumed to be 2.47, then the solids content of the slurry in grams per liter of slurry is calculated as: $1680\left(\frac{W_s - W_f - V_f}{V_f}\right)$ where: W_s = Weight of Sample + flask (g) W_f = Weight of empty flash (g) V_f = Volume of Slurry (ml)	Analytical balance and volumetric flasks.	This method is quick in that it does not require filtering or drying the solids.	This method is convenient when the solids content of the slurry need only be determined within a ±10% accuracy.	AU-063
4. Solids Content, "Standard Method"	A known weight and volume of the slurry is drawn through a weighed filter by application of a vacuum. The filter and solids are dried in an oven at 40-50°C and then reweighed. The solids content can then be calculated as the percent solids or in grams of solids/liter of slurry.	Drying oven, vacuum filtration apparatus, analytical balance, volumetric flasks.	When drying the solids, the oven temperature should not exceed 50°C which will drive off the water of hydration of the sulfite crystals.	This is a very accurate method when sufficient care is taken during the filtration not to lose any of the solids.	AU-063, MI-262, PR-091 SC-R-141
5. Settling Rate, Visual	Settling rates are determined by visual observation of the liquid-solids interface during settling in a 1000 ml graduated cylinder. The height of the interface (cm) is plotted versus time (min.). The settling rate is determined from the slope of the graph.	1000 ml Graduated Cylinder, timer	The settling rate is a function of weight percent solids, temperature, and particle morphology. For a valid comparison of sludges, the temperature and weight percent solids should be held constant. Settling rates for sludges of less than 2% solids by weight are difficult to measure because of the indistinctness of the interface.	Dependent on the care with which the sample is dispersed before settling.	TE-304, MI-262, PR-091

size and shape of the particles present. Many indirect methods require calibration and occasional checking by microscopic measurements.

Separation of particle fractions by sieving is an inexpensive and fast method for measuring size distribution for relatively large particles. Sieves are available for small particles but the separations are not as satisfactory as for large particles.

The various sedimentation procedures are very popular for routine work and give satisfactory particle size distributions on many samples when properly calibrated. In order to obtain satisfactory results the sample should be fairly homogeneous.

Elutriation is a very valuable tool for particle size determination. In combination with other techniques (e.g., screening, centrifugation) phase separation of particles with differing densities may also be effected. Inertial impaction requires that the particles be suspended in air. It is not useful for particles larger than 100μ in diameter.

Scattered light measurements can be useful for determinating an "average diameter" for small particles. Transmission or "turbidity" measurements are ususally used when the particles are considerably larger than the wavelength of the incident radiation. Very small angle X-ray scattering can be applied to the estimation of average particle size in the range 0.005 to 0.05μ.

The Coulter counter electrically measures the volume of individual particles as they displace a conducting medium in an aperture. Some disagreement exists in the literature as to the speed and reliability of this method. Electrostatic charging of small particles may be used to determine particle sizes in some cases.

5.2 Methods for Settling Rate and Density Measurements

The settling rate and settled density are both affected by the particle size and morphology. If the settling rate and settled density are known, then estimates of the relative particle sizes of different sludges can be made. The methods for measuring these quantites are presented in Table 5-2 along with several other related measurements.

REFERENCES

AM-006 American Society for Testing and Materials, *1970 Annual Book of ASTM Standards, Part 9, Cement, Lime, Gypsum*, Philadelphia, 1970.

AM-011 American Society for Testing and Materials, "Recommended Practice for Analysis by Microscopic Methods for Particle Size Distribution of Particulate Substances of Subsieve Sizes", #20-68. in *1968 ASTM Standards, General Test Methods, Part 30*. Philadelphia, 1968, pp. 117-29.

AM-269 American Society for Testing and Materials, "Standard Specification for Precision Electroformed Sieves", E 161-70. in *1976 Annual Book of Standards, Pt. 41, General Test Methods, Non-metal; Statistical Methods; Space Simulation; Particle Size Measurement; General Laboratory Apparatus; Deterioration of Nonmetallic Materials; Metric Practice*. Philadelphia, ASTM, 1976, pp. 157ff.

AM-270 American Society for Testing and Materials, Committee E-1, *Manual on Test Sieving Methods*. STP 447, Philadelphia, PA, 1969

AM-275 American Society for Testing and Materials, "Standard Method for Particle-Size Analysis of Soils", D422-63 (Reapproved 1972). in *1976 Annual Book of ASTM Standards, Part 19-Soil and Rock. Building Stones; Peats.* Philadelphia, 1976, p. 69ff.

AP-004 Appino, James B., and Ross U. Robinson, "Instrumental Approaches to Particle-Counting in Pharmaceutical Liquids", *Ann. N.Y. Acad. Sci. 158*, 80-88 (1969).

REFERENCES (Cont'd.)

AU-003 Aughey, W. Henry, and F. J. Baum, "Angular-Dependence Light Scattering -- A High Resolution Recording Instrument for the Angular Range 0.05-140", J. Opt. Sci. 44, 833-37 (1954).

AU-063 Aul, E. F., Jr., et al., Chemical Process Control Procedures for the Sunbury Limestone Scrubbing Pilot Unit. Technical Note 200-031-25. Austin, TX, Radian Corporation, May 1974.

BE-035 Bergin, M. J., and K. H. Butler, "Measurement of Particle Size Distribution of Phosphors", J. Electrochem. Soc. 101, 149-54 (1954).

BO-016 Bostock. W., "A Sedimentation Balance for Particle Size Analysis in the Sub-Sieve Range", J. Sci. Instr. 29, 209-11 (1952).

BR-023 Brown, O. E., G. S. Bobrowski, and G. E. Kovall, "Use of the Counter Counter and Alpine Sieve for Particle Size Analysis of Cement", in Fineness of Cement. STP 473. Philadelphia, ASTM, 1970, pp 82-97.

BR-027 Brusset, H. and J. R. Donati, "Un Nouvel Aspect du Calcul des Distributions de Tailles de Particules en Diffusion Centrale Des Rayons X", J. Appl. Chryst. 2, 55-64, (1969).

BU-259 Burek, R., "Particle Size Effects in X-Ray Absorption Analysis: Formulae for Size Distributions", J. Radioanal. Chem 33, 263-72 (1976).

REFERENCES (Cont'd.)

CA-026 Carman, P. C., "The Surface Area Measurement of Paint Pigments", J. Oil and Colour Chem. Assoc. 37 (406), 165-73 (1954).

CA-040 Cadle, Richard D., Particle Size; Theory and Industrial Application. New York, Reinhold, 1965.

CR-012 Crandall, Willard A., "Development of Standards for Determining Properties of Fine Particulate Matter", Paper No. 64-WA/PTC-3. New York, ASME, 1964.

DA-019 Daeschner H. W., "Wet Sieving with Precision Electro-Formed Sieves", Powder Tech. 2, 349-55 (1969).

DA-264 Daeschner, H. W., E. E. Siebert, and E. D. Peters, "Application of Electroformed Precision Micromesh Sieves to the Determination of Particle Size Distribution", Reprint. Symposium on Particle Size Measurement. STP 234. Philadelphia, ASTM, 1958.

DI-012 DiGrado, C. Joseph, "Panel Discussion: Liquid-Borne Particle Counting in the Pharamceutical Industry. III. Method Examination", Bull. Parenteral Drug Assoc., 24 (2), 62-67 (1970).

DI-021 Dietert, Harry W. Company, "Micro Particles Classified Centrifugally", Company Brochure SL-52.

EB-001 Ebel, Horst, et al., "Die Pulverkorngrossenbestimmung mit Hilfe der Rontgenabsorptionmetrie", Acta Physica Austriaca 30, 242-59, (1969).

REFERENCES (Cont'd.)

EC-002 Eckhoff, R. K., "Experimental Indication of the Volume Proportional Response of the Coulter Counter for Irregularly Shaped Particles", J. Sci. Instrum 44, 648-49 (1967).

ED-004 Edward, Victor H. and Charles R. Wilke, "Electronic Sizing and Counting of Bacteria", Biotechn. Bioeng. 9, 559-74 (1967).

EN-269 Environmental Protection Agency, (Office of Research and Development), Symposium on Flue Gas Desulfurization, Atlanta, Nov. 1974, Proceedings, 2 vols. EPA 650/2-74-126 a,b. Research Triangle Park, N. C., Dec. 1974.

GR-014 Grover, N. B. et al., "Electrical Sizing of Particles in Suspension. I. Theory." Biophysical J. 9, 1398-414 (1969).

GR-015 Grover, N. B., et al., "Electrical Sizing of Particles in Suspensions. II. Experiments with Rigid Spheres," Biophysical J. 9, 1415-25 (1969).

GR-032 Graham, A. L. and T. H. Hanna, "The Micro-Particle Classifier", Reprint. Ceramic Age, 1962 (Sept.)

HA-044 Hawksley, P. G. W. and J. H. Blackett, "The Design and Construction of a Photoelectronic Scanning Machine for Sizing Microscopic Particles", Brit. J. Appl. Phys. Supp. 3, 165-73 (1954).

REFERENCES (Cont'd.)

HE-010 Heiss, John F. and James Coull, "The Effect of Orientation and Shape on the Settling Velocity of Non-Isometric Particles in a Viscous Medium", CEP 48 (3), 133-40 (1952).

HI-020 Hime, W. G., "ASTM Method for the Surface Area Analysis of Portland Cement", in Fineness of Cement. STP 473. Philadelphia, ASTM, 1970, pp. 3-19.

HO-024 Hockings, W. A., "Particle- and Grain-Size Measurement by X-Ray Fluorescence", Powder Tech. 3, 29-40 (1969).

HU-012 Hunt, C. M., and A. R. Woolf, "Comparison of Some Different Methods for Measuring Particle Size Using Microscopically Calibrated Glass Beads", Powder Tech. 3, 9-23 (1969).

IR-016 Irani, Riyad R. and Clayton F. Callis, Particle Size: Measurement, Interpretation, and Application. New York, Wiley, 1963.

JA-011 Jacobsen, A. E. and W. F. Sullivan, "Method for Particle Size Distribution for the Entire Subsieve Range", Anal. Chem. 19 (11), 855-60 (1947).

JO-019 Johari, O., and S. Bhattacharyya, "The Application of Scanning Electron Microscopy for the Characterization of Powders", Powder. Tech. 2, 225-48 (1969).

REFERENCES (Cont'd.)

JO-083 Jones, Julian W. and Richard D. Stern, "Waste Products from Throwaway Flue Gas Cleaning Processes - Ecologically Sound Treatment and Disposal", Presented at the Flue Gas Desulfurization Symp., New Orleans, May 1973.

KA-021 Kaye, B. H., "Automatic Microscopes for the Paint Technologist, Part II. Particle System Evaluation Using the Quantimer.", Paint, Oil Colour J., 1968 (Aug. 30), 372-75 (1968).

KA-026 Karansek, F. W., "Micromeritics" R/D, 59-62 (1970). (Sept.)

KE-025 Kendall, C. E., "Comparative Data and Requirements for Determination of Particle Size Distribution in Australian Pharmaceuticals", Ann. N. Y. Acad. Sci. 158, 640-50 (1969).

KI-014 Kirnbauer, Erwin, Panel Discussion: Liquid-Borne Particle Counting in the Pharmaceutical Industry. I Microscopic Counting.", Bull. Parenteral Drug Assoc., 24 (2), 53-58 (1970).

LA-021 Lamar, Richard S., "Particle-Size Distribution Analysis by a Modification of the Turbidimetric Procedure of Musgrave and Horner", J. Am. Cer. Soc. 37, 386-90 (1954).

LA-022 Lapple, C. E., "Particle-Size Analysis and Analyzers", Chem. Eng. 1968 (May 20), 149-56 (1968).

REFERENCES (Contd'.)

LA-159 Lambe, T. William, *Soil Testing for Engineers*. N.Y., Wiley, 1951.

LE-013 Lester, R. H., "Subsieve Particle Size Measurements on Porcelain Materials", *Am. Cer. Soc. Bull. 37*, 129-34 (1958).

LI-019 Livesy, P. J. and F. W. Billmeyer, Jr., "Particle Size Determination by Low-Angle Light Scattering: New Instrumentation and Rapid Method of Interpreting Data", *J. Colloid Interface Sci. 30* (4), 447-72 (1969).

LO-089 Lord, William H., "FGD Sludge Fixation and Disposal", Presented at the Flue Gas Desulfurization Symposium, Atlanta, Ga., Nov. 1974.

LU-012 Ludwick, John C. and Patricia L. Henderson "Particle Shape and Inference of Size from Sieving", *Sedimentology 11*, 197-235 (1968).

MA-057 Maguire, S. G., Jr. and G. W. Phelps, "Practical Particle-Size Analysis of Clays: II, a Simplified Procedure", *J. Am. Cer. Soc. 40*, 403-49 (1957).

MA-059 Martens, Alexander H., "Measurement of Small Particles Using Light-Scattering: A Survey of the Current State of the Art", *Ann. N. Y. Acad. Sci. 158*, 690-702

MC-019 McCann, C., "The Measurement of the Sizes of Nonspherical Particles by the Hydrometer Method," *Sedimentology 13*, 307-9 (1969).

REFERENCES (Cont'd.)

MI-024 Micromeritics Instrument Corp., "Sedigraph 5000 Particle Size Analyzer", Company brochure.

MI-262 Mijares-Lopez, C., *Dynamics of the Continuous Settling of Discrete-Particle Slurries*. Doctoral Thesis, University of Colorado, 1976.

MO-016 Morgan, B. B., "Automatic Particle Counting and Sizing", *Research 10*, 271-79.

MU-010 Murley, R. D., "An Improved Method of Calculating Particle Size Distribution from Centrifugal Sedimentation Experiments", *Nature 207* (5001), 1089-90 (1965).

MU-013 Mullaney, P. F. and P. N. Dean, "Cell Sizing: A Small-Angle Light-Scattering Method for Sizing Particles at Low Relative Refractive Index", *Appl. Opt. 8*, 2361-62 (1969).

MU-014 Muslin, Lawrence, "Panel Discussion: Liquid-Borne Particle Counting in the Pharmacuetical Industry. II. Light-Scattering Instruments", *Bull. Parenteral Drug Assoc. 249*(2), 59-63 (1970).

OR-006 Orr, Clyde, *Fine Particle Measurement: Size, Surface, and Pore Volume*. New York, Macmillan, 1959.

PH-002 Phelps, G. W. and S. G. Maguire, Jr., "Practical Particle-Size Analysis of Clay, I, Sample Preparation", *J. Am. Cer. Soc. 40*, 399-402 (1957).

REFERENCES (Cont'd.)

PR-091 Princiotta, Frank T., *Sulfur Oxide Throwaway Sludge Evaluation Panel (SOTSEP)*, 2 vols. EPA 650/2-75-010 a, b. Research Triangle Park, N.C., Control Systems Lab., NERC, 1975.

RA-025 Rabatin, J. G. and R. H. Gale, "Determination of Particle Size with a Simple Recording Sedimentation Balance", *Anal. Chem. 28* (8), 1314-16 (1956).

RI-007 Rimburg, D. and D. Keafer, "Accuracy of Measuring Aerosol Concentration with Particle Counters", *J. Colloid Interface Sci. 33* (4), 628 (1970).

RI-009 Ricci, R. J., and H. R. Cooper, "A Method for Monitoring Particle Size Distribution in Process Slurries", *ISA Trans. 9*, 28-36 (1970).

RO-014 Rosen, Howard N. and Hugh M. Hulburt, "Size Analysis of Irregular Shaped Particles in Sieving. Comparison with the Coulter Counter". *I&EC Fundam. 9* (4), 658-61 (1970).

RO-133 Rossoff, J. and R. C. Rossi, *Disposal of By-Products From Nonregenerable Flue Gas Desulfurization Systems:* Initial Report. EPA-650/2-74-037-a. El Sugundo, Ca., Aerospace Corp., 1974.

SC-018 Scrag, K. R., and M. Corn., "Comparison of Particle Size Determined with the Coulter Counter and by Optical Microscopy", *Amer. Ind. Hyg. Assoc. J. 31* (4), 446-53 1970.

REFERENCES (Cont'd.)

SC-027 "Screening and Size Analysis", *Ceramic Age, 1969* (July), 66-70 (1969).

SC-R-141 Schwitzgebel, Klaus and F. B. Meserole, *Determination of the Molecular Parameters Important to the Performance of Scaling Inhibitors*, Final Report. Contract No. 14-30-2914. Radian Project No. 400-012, Austin, Tx., Radian Corp., 1973.

SI-010 Simecek, Jaroslav, "Vergleichende Untersuchung Von Methoden Zur Korngrossenbestimmung", *Staub-Reinhalt. Luft 26* (9), 372-79 (1966).

SM-005 Smith, George B. and G. V. Downing Jr., "Objective Method of Data Reduction for Particle Size Analysis by Cumulative Sedimentation Method.", *Anal. Chem. 42* (1), 136-38 (1970).

SM-006 Smith, T. N., "The Differential Sedimentation of Particles of Two Different Species", *Trans. Instn. Chem. Engrs. 43*, T69-73(1965).

SM-007 Smith, M. J., "A Quantitative Evaluation of Pigment Dispersions", *Microscope 16*, 123-35 (1968).

SI-010 Society for Analytical Chemistry, Particle Size Analysis Sub-Committee. *The Determination of Particle Size. I. A Critical Review of Sedimentation Methods.* London, 1968.

REFERENCES (Cont'd.)

ST-039 Strang, A., "Direct Image Analysis in the Electron Microscope", J. Sci. Instr. 2, 45-47 (1969).

ST-040 Stein, Felix, "Particle Size Measurements With Phase-Contrast Microscopy", Powder Tech. 2, 327-34 (1969).

SU-005 Suhm, H. O., "Oscillating Air Column Method for the Dry Separation of Fine and Subsieve Particle Sizes", Powder Tech. 2, 356-62 (1969).

SU-011 Suito, H. et al., "The Effect of Particle Shape on the Measurement of Particle-Size Distribution", Int'l. Chem.Eng. 11 (1), 134-9 (1971).

TA-012 Talvite, N. A. and H. J. Paulus, "Recording, Photometric Particle-Size Analyzer", Rev. Sci. Instr. 27 (9), 763-7 (1956).

TE-304 Tennessee Valley Authority, Division of Chemical Development,"Processing Sludge: Sludge Characterization Studies May to June 1975," Quarterly Report for the Period April 1 to June 20, 1975. EPA Contract No. EPA-IAG D5-0721, IAP No. 77 BBA. Muscle Shoals, Alabama, July 1975.

TO-008 Todd, W. F., J. E. Hagan, and P. W. Spaite, Test Dust Preparation and Evaluation. Cincinnati, Ohio, Public Health Service, Div. of Air Pollution, undated.

REFERENCES (Cont'd.)

WA-022 Walton, W. H., "Session F. Automatized Counting and Sizing Theory", Brit. J. Appl. Physics. Supp. 3, 121-5 (1954).

WE-022 Weersing, James R., "Light-Scatter Measurements for Counting and Sizing Particles", Ann. N. Y. Acad. Sci. 158, 722-30 (1969).

YO-004 Yoshikawa, Herbert H. et al., "Electrostatic Particle Size Analysis", Rev. Sci. Instruments 27 (6), 359-62 (1956).

ZI-003 Zinky, William R., "Hologram Techniques for Particle-Size Analysis", Ann. N. Y. Acad. Sci. 158, 741-52 (1969).

DCN #78-200-187-11-14

APPENDIX D
COMPARISON OF METHODS FOR MEASURING THE PARTICLE SIZE DISTRIBUTION OF SMALL PARTICLES

Technical Note #200-187-11-05

1 February 1978

Prepared for:

Mr. Robert H. Borgwardt, Task Officer
Industrial Environmental Research Laboratory/RTP
U. S. Environmental Protection Agency
Research Triangle Park, North Carolina 27711

Prepared by:

J. C. Terry

TABLE OF CONTENTS

Page

1.0 INTRODUCTION.................................. D-1

2.0 SUMMARY OF RESULTS AND CONCLUSIONS............ D-3

3.0 RECOMMENDATIONS............................... D-5

4.0 EXPERIMENTAL PROCEDURES AND RESULTS........... D-6
- 4.1 Particle Size Distribution by Coulter Counter................................ D-6
- 4.2 Particle Size Distribution by Sedimentation.................................. D-17
- 4.3 Comparison of Results.................... D-20

LIST OF FIGURES

Figure — Page

4-1 Sludge Granules: Cumulative Number Percent of Particles Versus Equivalent Spherical Diameter Measured by Coulter Counter Single Tube Method. D-11

4-2 Sludge Granules: Cumulative Volume Percent of Particles Versus Equivalent Spherical Diameter Measured by Coulter Counter Single Tube Method.................................... D-12

4-3 Sludge Platelets: Cumulative Number Percent of Particles Versus Equivalent Spherical Diameter Measured by Coulter Counter Single Tube Method.................................... D-13

4-4 Sludge Platelets: Cumulative Volume Percent of Particles Versus Equivalent Spherical Diameter Measured by Coulter Counter Single Tube Method.................................... D-14

4-5 Sludge Platelets: Cumulative Number Percent of Particles Versus Equivalent Spherical Diameter Measured by Coulter Counter Multiple Tube Method.................................... D-15

4-6 Sludge Platelets: Cumulative Volume Percent of Particles Versus Equivalent Spherical Diameter Measured by Coulter Counter Multiple Tube Method.................................... D-16

LIST OF FIGURES (continued)

Figure Page

4-7 Sludge Granules: Cumulative Number Percent of Particles Versus Equivalent Spherical Diameter Measured by Sedimentation Method................ D-21

4-8 Sludge Granules: Cumulative Volume Percent of Particles Versus Equivalent Spherical Diameter Measured by Sedimentation Method................ D-22

4-9 Sludge Platelets: Cumulative Number Percent of Particles Versus Equivalent Spherical Diameter Measured by Sedimentation Method................ D-23

4-10 Sludge Platelets: Cumulative Volume Percent of Particles Versus Equivalent Spherical Diameter Measured by Sedimentation Method................ D-24

4-11 Sludge Granules: Number Percent of Particles Versus Equivalent Spherical Diameter Measured by Optical Microscopy and Wet Micromesh Sieve Methods.................................... D-29

4-12 Sludge Granules: Number Percent of Particles Versus Equivalent Spherical Diameter Measured by Single Tube Coulter Counter and Sedimentation Methods....................................... D-30

4-13 Sludge Platelets: Number Percent of Particles Versus Equivalent Spherical Diameter Measured by Optical Microscopy and Wet Micromesh Sieve Methods....................................... D-31

LIST OF FIGURES (continued)

Figure Page

4-14 Sludge Platelets: Number Percent of Particle Versus Equivalent Spherical Diameter Measured by Single Tube Coulter Counter and Sedimentation Methods.................................... D-32

LIST OF TABLES

Table Page

4-1 Particle Size Distribution of the Sludge Granules by the Coulter Counter Single Tube Method........ D-8

4-2 Particle Size Distribution of the Sludge Platelets by the Coulter Counter Single Tube Method........ D-9

4-3 Particle Size Distribution of the Sludge Platelets by the Coulter Counter Multiple Tube Method...... D-10

4-4 Particle Size Distribution of the Sludge Granules by the Sedimentation Method..................... D-18

4-5 Particle Size Distribution of the Sludge Platelets by the Sedimentation Method..................... D-19

4-6 Mean Particle Diameter on Volume Basis........... D-25

4-7 Mean Particle Diameter on Number Basis........... D-25

4-8 Particle Size Distribution of Sludge Granules on a Number Percent Basis...................... D-27

4-9 Particle Size Distribution of Sludge Platelets on a Number Percent Basis...................... D-28

1.0 INTRODUCTION

The flue gas desulfurization (FGD) sludges produced in lime, limestone and double alkali systems generally are difficult to settle and dewater. Sludge disposal therefore is a problem and represents a significant operating cost in scrubbing processes. Radian Corporation was contracted by the EPA to investigate the prospects for improving the quality of FGD scrubber sludges. Briefly, the approach taken was to develop a mathematical basis for relating sludge quality to scrubber operating conditions. Scrubber sludge quality was defined as the particle size distribution (PSD) of calcium sulfite hemihdyrate.

One phase of the project was the development of standard analytical techniques for measuring sludge properties. It was found that optical microscopy and wet micromesh sieve methods for measuring the particle size distribution of sludge resulted in PSD data which was not in agreement with Coulter Counter results. Specifically, it was found that the optical and sieve PSD curves showed maxima in the range of about 5 to 10 microns whereas the Coulter Counter PSD curve continued to increase smoothly with decreasing particle size. This difference suggested two possible mechanisms for new particle generation, attrition and nucleation. The Coulter Counter results showed a large number of small and submicron size particles which were not observed by the optical and sieve methods.

These differences in the FGD scrubber sludge PSD's are important in the formulation, verification, and refinement of the scrubber model. In order to understand the origin of the differences in the PSD data and to provide a basis for selecting an accurate particle sizing method, it was felt that additional study was needed.

The methods selected for additional study of small and submicron size particles were Coulter Counter and sedimentation. This report presents the results of PSD studies on FGD sludge granules and platelets down to 0.3 microns in size. A comparison of optical, sieve, Coulter Counter, and sedimentation results are given.

2.0 SUMMARY OF RESULTS AND CONCLUSIONS

The FGD sludge granule and platelet samples were analyzed by Coulter Counter and sedimentation methods down to a lower particle cut off size of about 0.3 microns. These results were compared to those previously obtained by optical microscopy and wet micromesh sieves.

On a mass or volume basis the mean particle size of the granule and platelet samples varied widely as measured by Coulter Counter, sedimentation, optical microscopy, and sieve techniques. Generally, the optical and sieve methods tended to give larger PSD's than did the Coulter Counter and sedimentation methods. The optical and sieve methods used a lower cut-off limit which was larger but this should not have significantly effected the PSD on a volume or mass basis since the bulk of the particle mass and volume are represented by the larger particles. The mean equivalent spherical diameter for the granular sample varied between 1.7 and 18.5 microns and the platelet sample varied between 1.8 and 10.2 microns on a volume or mass basis.

The Coulter Counter and sedimentation results on a number basis agreed reasonably well. Likewise, the optical and sieve results were in good mutual agreement. The equivalent spherical diameters measured by the optical and sieve methods, however, were much larger than those measured by sedimentation and Coulter Counter. This is a result of using a 1-2 micron lower cut off size for the optical and sieve methods whereas the sedimentation and Coulter Counter methods had cut-off sizes down to 0.3 microns. The mean equivalent spherical diameters for the granular sample varied between 0.4 and 7.5 microns and the platelet sample varied between 0.4 and 4.0 microns on a number basis.

Graphs of the optical and sieve number percent of particles versus size data for both granule and platelet samples show a maximum in the PSD curve. This suggests that particle breakage or attrition is a major or at least a significant mechanism for new particle generation. The PSD curves for the Coulter Counter and sedimentation data decrease monotonically with increasing particle size and do not show any maxima. The range of particle sizes covered by the two groups of methods do not overlap well and provides for the possibility of both sets of data being correct. That is, there could be two mechanisms for new particle generation, nucleation and attrition. The proponderance of the data does not support this two mechanism theory, however, and the maxima in the optical and sieve data curves are probably due to limitations in the methods to measure small particles. The maxima in the PSD curves occurred at 6 to 8 microns. This further suggests that optical and sieve [illegible] w 5 to 10 microns are questionable. Measurements [illegible] of 1 to 2 microns are probably highly inaccurate and measure far too few particles in the smaller size ranges.

Based on these results, it is not possible to select any one of the analytical methods as correct. It is clear that some of the methods have inherent limitations which necessarily prevent them from giving accurate data on small or submicron size particles. These are optical microscopy and microsieves. The necessity of using the same particle size cut off limits is obvious and is clearly illustrated by comparing the various particle size data on a number basis. It is also clear that comparing PSD data between different analytical techniques is highly questionable. Even comparison of PSD data on different FGD sludges would be suspect if the particle shape was different such as granules versus platelets.

3.0 RECOMMENDATIONS

When comparing particle size distribution data, it is very important to know the analytical method used and also the details of how that method was applied. As has been shown, even particle sizing methods that are generally accepted as accurate and suitable for small particles can give widely varying results. Certainly when measuring particle size distribution on a number basis the cut off sizes should be held constant for data comparisons. Also there would be considerable uncertainty in comparing the results of different analytical PSD methods.

Although the results of this project have provided standard analytical methods for determining FGD scrubber sludge quality, these methods are directed at the bulk mass of sludge. The data collected have not clearly established a method for measuring the PSD of submicron size particles. The sedimentation and Coulter Counter results presented in this technical note are based on only one or two tests per method and thus cannot be regarded as definitive indications of the ultimate abilities of these methods. Additional tests are needed on a wider variety of scrubber sludges and under highly controlled conditions in order to more clearly establish the accuracy and limitations of the methods. Also, PSD measurements using scanning electron micrographs should be studied as this method could prove to be an accurate and highly accepted technique for submicron particles.

4.0 EXPERIMENTAL PROCEDURES AND RESULTS

The standard method for measuring particle size distribution is optical microscopy. A problem with this method, however, is its inability to measure particles less than about 5 microns. Based on the literature survey presented in Technical Note #200-187-11-02, there are a number of other methods which appear to be suitable for accurately sizing submicron particles. The two methods selected for study were sedimentation and Coulter Counter. Another method which should also be applicable is electron microscopy. This method was not specifically studied in this work.

The sludge samples used to test the analytical methods were the same as those used for the standard analytical methods development. Specifically, a platelet sample from a limestone scrubber and a granular sample from a lime scrubber were utilized.

4.1 Particle Size Distribution by Coulter Counter

The two sludge samples were sent to an independent laboratory for particle size distribution analysis by Coulter Counter. In addition, the platelet sample was sent to a second independent laboratory to obtain comparison results.

The Coulter Counter measures the number and equivalent spherical diameter of particles in a electrically conductive fluid. As a suspension of the particles is drawn through a small aperture the resistance across it is measured by electrodes on both sides. The resistance change across the aperture is proportional to the volume of the particle passing through it. The equivalent spherical diameter is calculated from the measured particle volume assuming spherical particle shape.

4.1.1 Procedure

The laboratory analyzing both the platelet and granular sludge samples prepared the samples for analyses by dispersing a small amount of sludge in Coulter isoton solution with Triton X-100 added as a surfactant to reduce particle agglomeration. Dispersion of particles was completed by ultrasonic vibration. After 1:10 dilution the samples were analyzed on a Coulter Counter Model TA with aperture setting at 70 microns. The PSD data was recorded as the number and volume percents finer than each size range.

The platelet sample analyzed at the second independent laboratory was prepared by dispersion into 30% glycerine/70% isoton for the 560μ aperture and saturated 4% $NaCl/H_2O$ electrolyte for the 200, 70, and 16μ apertures, with 30 second ultrasonic agitation and Type I-A dispersant. The analysis was conducted on a Coulter Counter Model TA II using a multiple tube overlap technique. The data was processed on a Coulter M3 data processor/calculator system. The PSD was recorded as the number and volume percents finer than each size range.

4.1.2 Results

The results of the Coulter Counter single tube method analyses for the granular and platelet sludge samples are in Tables 4-1 and 4-2. The results of the Coulter Counter multiple tube analyses for the platelet sample are in Table 4-3. Figures 4-1 through 4-6 are plots of the Coulter Counter data as cumulative number and cumulative volume percent of particles versus equivalent spherical diameter.

TABLE 4-1. PARTICLE SIZE DISTRIBUTION OF THE SLUDGE GRANULES BY THE COULTER COUNTER SINGLE TUBE METHOD

Size Range E.S.D.*, μ	Volume %	Cum Vol % Finer	Number %	Cum Number % Finer
0.80-1.00	4.9	4.9	47.8	47.8
1.00-1.26	8.0	12.9	39.0	86.8
1.26-1.59	2.5	15.4	6.1	92.9
1.59-2.00	3.4	18.8	4.2	97.1
2.00-2.52	2.0	20.8	1.2	98.3
2.52-3.17	1.6	22.4	0.5	98.8
3.17-4.00	2.0	24.4	0.3	99.1
4.00-5.04	3.1	27.5	0.2	99.3
5.04-6.35	5.4	32.9	0.2	99.5
6.35-8.0	9.5	42.4	0.2	99.7
8.0-10.1	13.4	55.8	0.1	99.8
10.1-12.7	14.5	70.3	0.1	99.9
12.7-16.0	13.0	83.3	--	--
16.0-20.2	9.9	93.2	--	--
20.2-25.4	3.9	97.1	--	--
25.4-32.0	1.8	98.9	--	--

* Equivalent spherical diameter

TABLE 4-2. PARTICLE SIZE DISTRIBUTION OF THE SLUDGE PLATELETS BY THE COULTER COUNTER SINGLE TUBE METHOD

Size Range E.S.D.*, μ	Volume %	Cum Vol % Finer	Number %	Cum Number % Finer
0.80-1.00	12.6	12.6	44.2	44.2
1.00-1.26	24.3	36.9	42.6	86.8
1.26-1.59	7.9	44.8	6.9	93.7
1.59-2.00	11.7	56.5	5.1	98.8
2.00-2.52	3.4	59.9	0.7	99.5
2.52-3.17	2.0	61.9	0.2	99.7
3.17-4.00	2.0	63.9	0.1	99.8
4.00-5.04	2.0	65.9	0.1	99.9
5.04-6.35	2.4	68.3	--	--
6.35-8.0	3.4	71.7	--	--
8.0-10.1	3.7	75.4	--	--
10.1-12.7	5.6	81.0	--	--
12.7-16.0	6.8	87.8	--	--
16.0-20.2	8.0	95.8	--	--
20.2-25.4	2.4	98.2	--	--
25.4-32.0	1.0	99.2	--	--

* Equivalent spherical diameter

TABLE 4-3. PARTICLE SIZE DISTRIBUTION OF THE SLUDGE PLATELETS BY THE COULTER COUNTER MULTIPLE TUBE METHOD

Size Range E.S.D.*, μ	Volume %	Cum Vol % Finer	Number %	Cum Number % Finer
0.32-0.40	8.3	8.3	40.8	40.8
0.40-0.50	11.9	20.2	32.7	73.5
0.50-0.63	11.8	32.0	18.3	91.8
0.63-0.80	7.7	39.7	6.6	98.4
0.80-1.00	2.7	42.4	1.0	99.4
1.00-1.26	1.6	44.0	0.3	99.7
1.26-1.59	1.5	45.5	0.1	99.8
1.59-2.00	1.4	46.9	0.1	99.9
2.00-2.52	1.7	48.6	--	--
2.52-3.17	2.0	50.6	--	--
3.17-4.00	2.0	52.6	--	--
4.00-5.04	2.1	54.7	--	--
5.04-6.35	1.9	56.6	--	--
6.35-8.0	1.8	58.4	--	--
8.0-10.1	2.1	60.5	--	--
10.1-12.7	2.6	63.1	--	--
12.7-16.0	3.3	66.4	--	--
16.0-20.2	3.9	70.3	--	--
20.2-25.4	4.7	75.0	--	--
25.4-32.0	5.6	80.6	--	--
32.0-40.3	6.4	87.0	--	--
40.3-50.8	3.9	90.9	--	--
50.8-65.0	2.6	93.5	--	--
64.0-80.6	1.4	94.9	--	--
80.6-102	1.1	96.0	--	--
102-128	0.9	96.9	--	--
128-161	1.2	98.1	--	--
161-203	1.0	99.1	--	--
203-256	0.4	99.5	--	--
256-	0.4	99.9	--	--

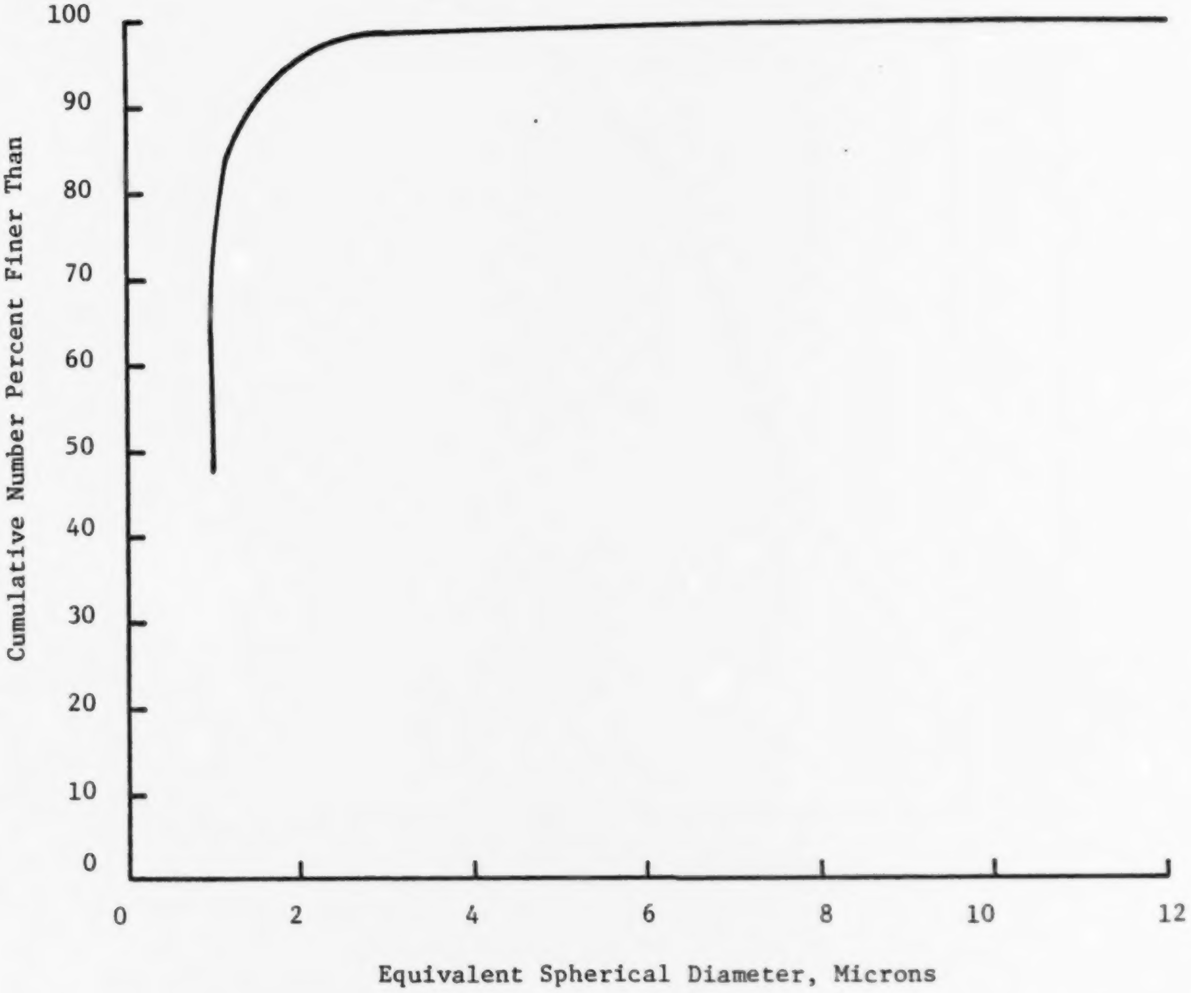

Figure 4-1. Sludge Granules: Cumulative Number Percent of Particles Versus Equivalent Spherical Diameter Measured by Coulter Counter Single Tube Method.

02 2552-1

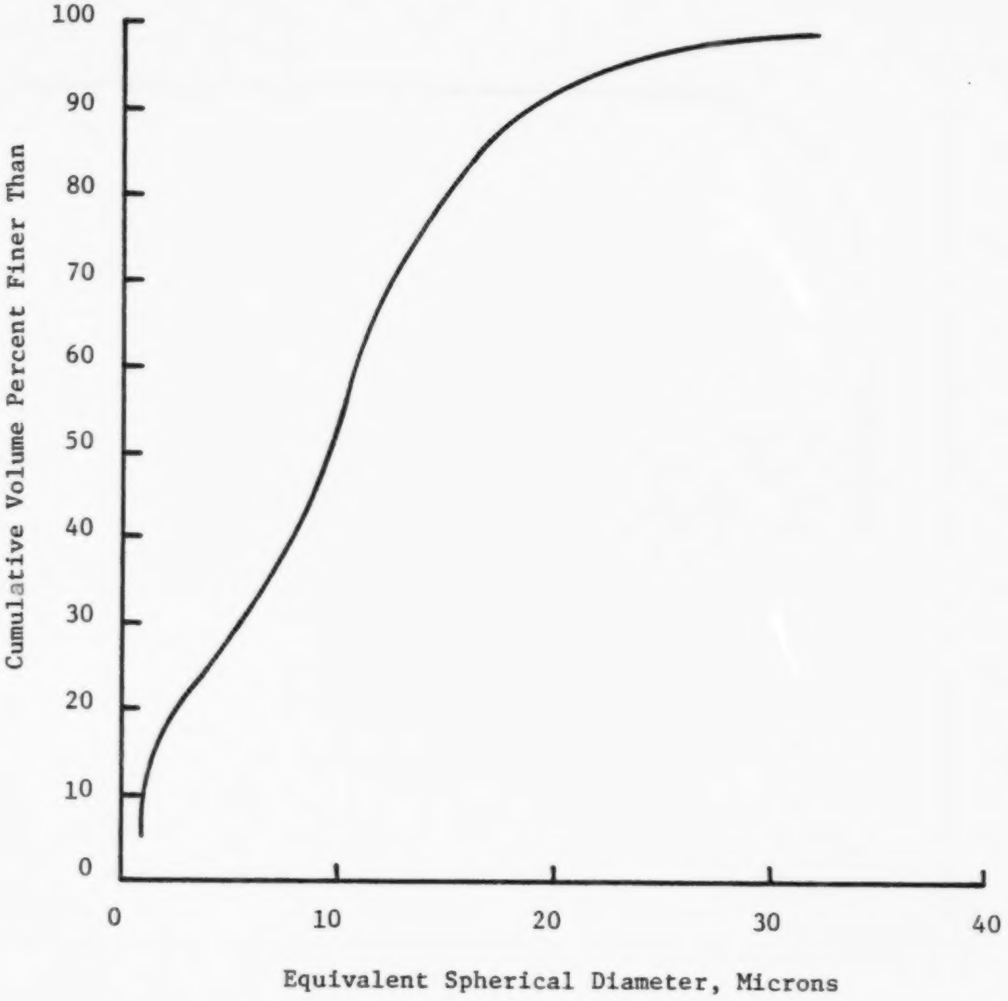

Figure 4-2. Sludge Granules: Cumulative Volume Percent of Particles Versus Equivalent Spherical Diameter Measured by Coulter Counter Single Tube Method.

02 2551-1

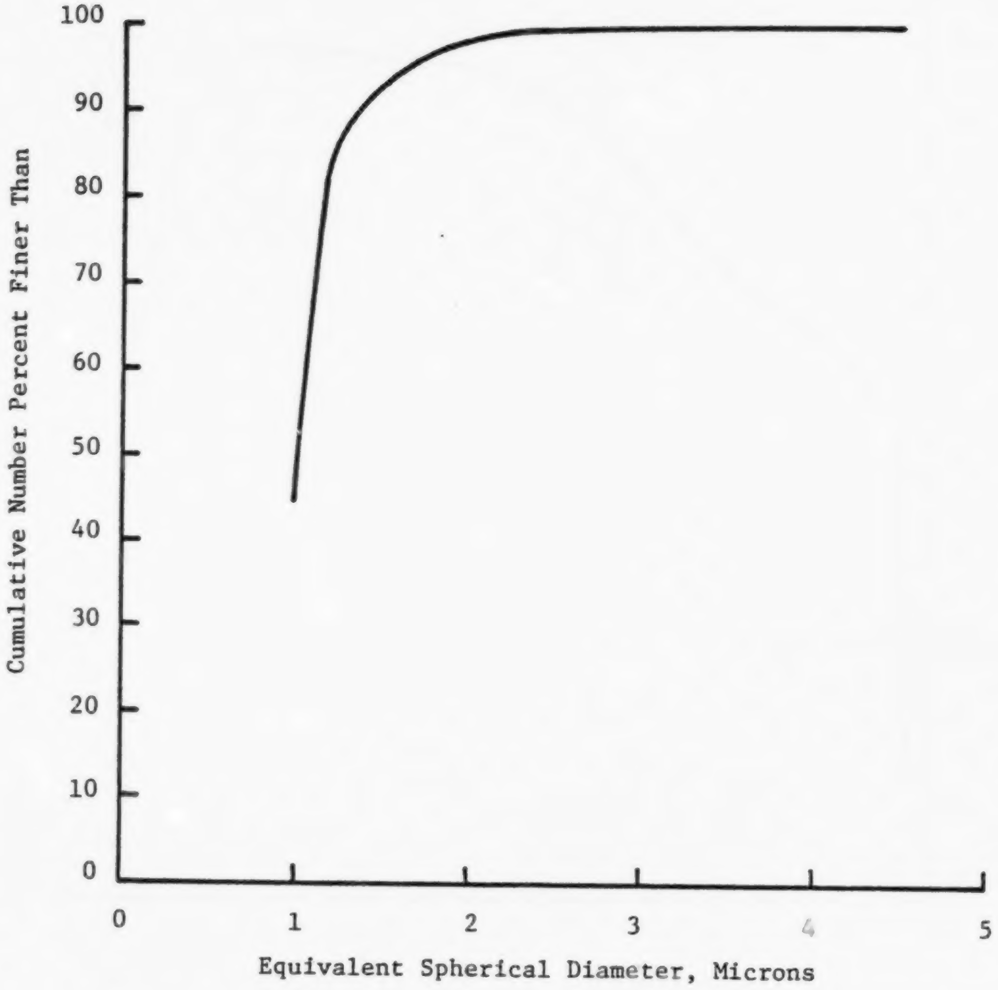

Figure 4-3. Sludge Platelets: Cumulative Number Percent of Particles Versus Equivalent Spherical Diameter Measured by Coulter Counter Single Tube Method.

02 2554-1

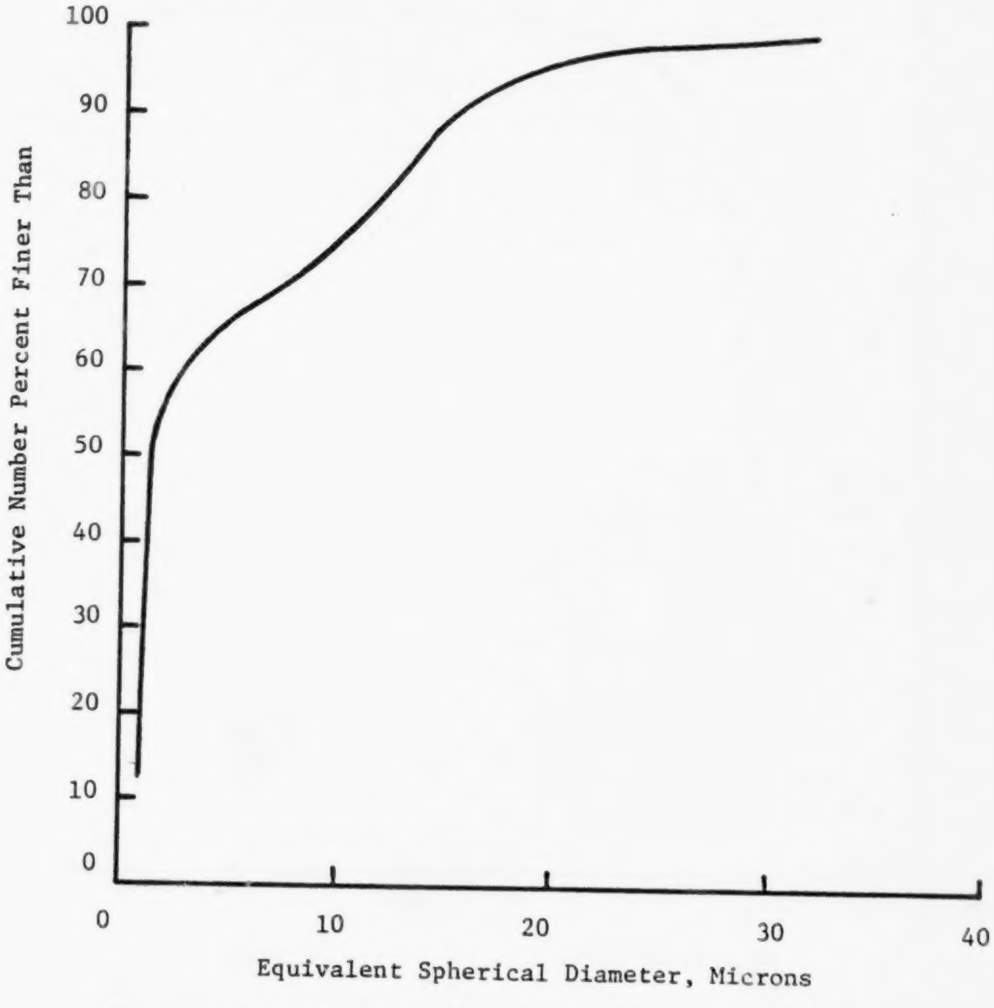

Figure 4-4. Sludge Platelets: Cumulative Volume Percent of Particles Versus Equivalent Spherical Diameter Measured by Coulter Counter Single Tube Method.

02 2553-1

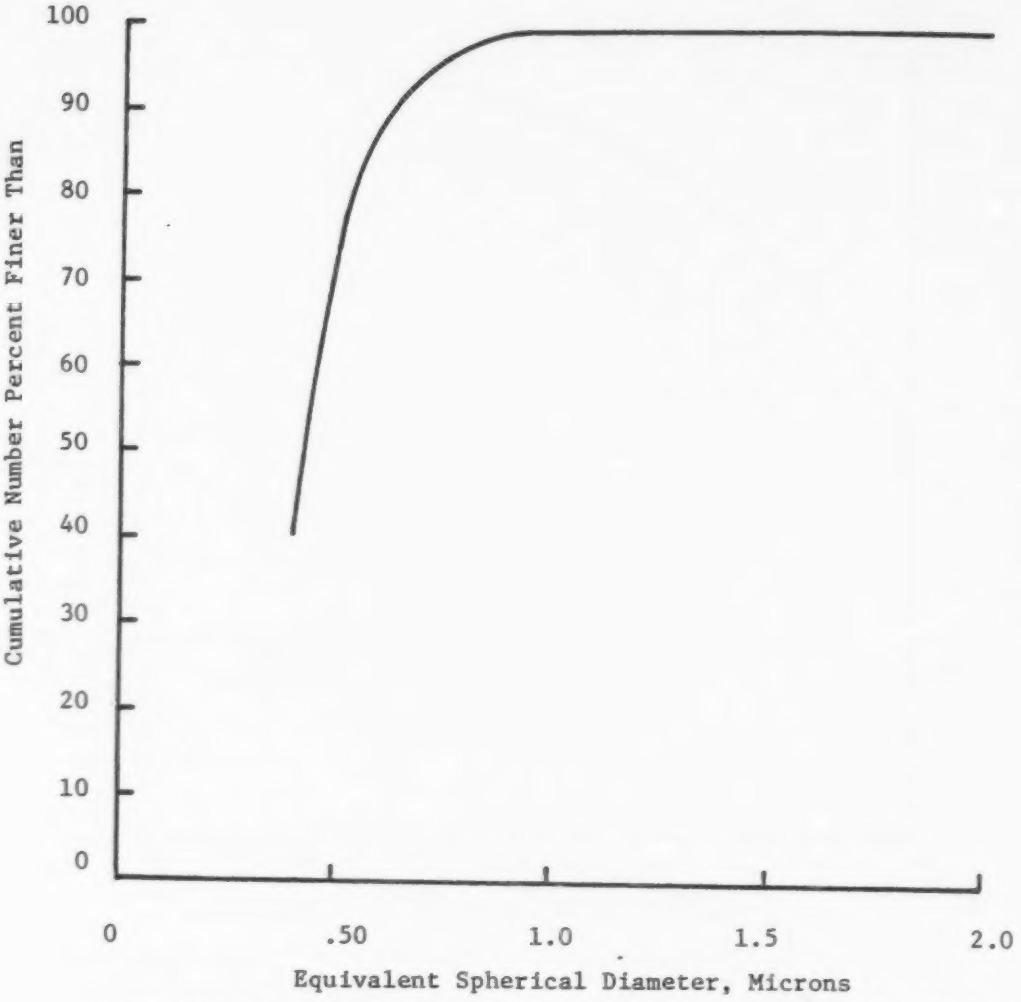

Figure 4-5. Sludge Platelets: Cumulative Number Percent of Particles Versus Equivalent Spherical Diameter Measured by Coulter Counter Multiple Tube Method.

02 2555-1

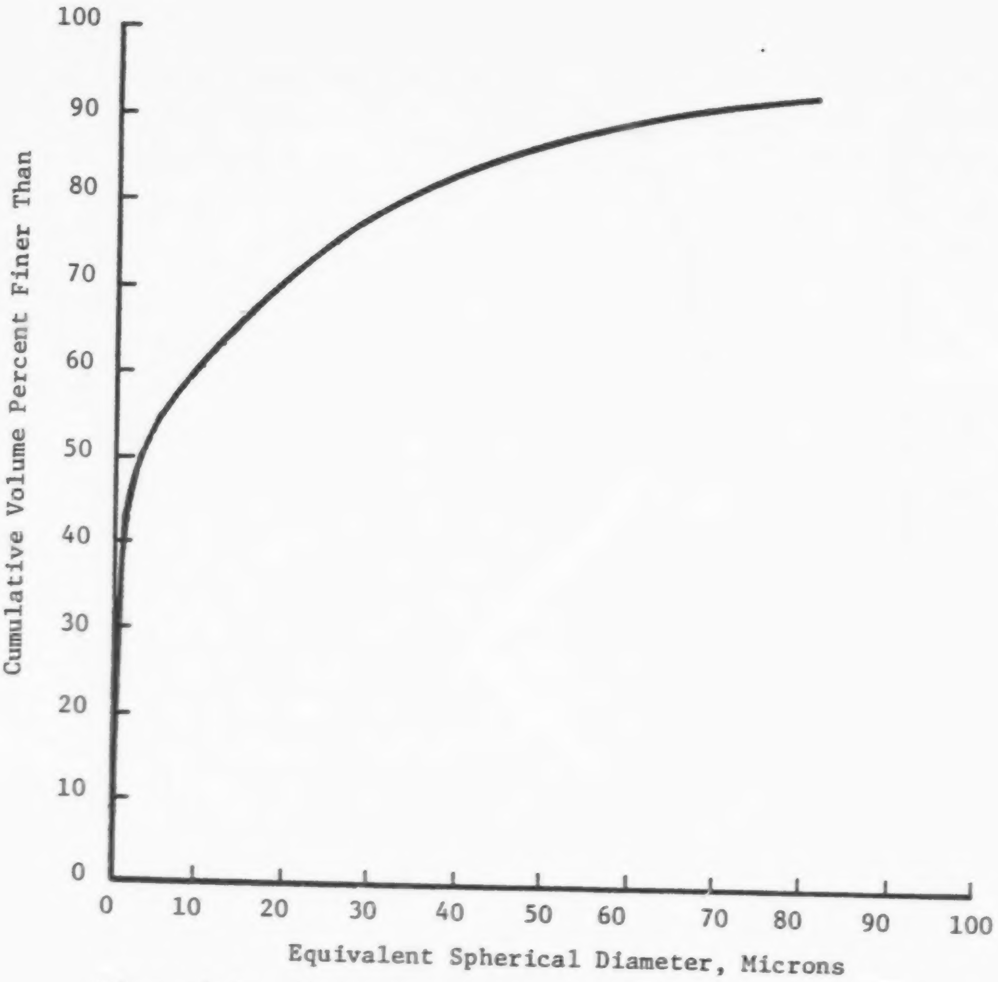

Figure 4-6. Sludge Platelets: Cumulative Volume Percent of Particles Versus Equivalent Spherical Diameter Measured by Coulter Counter Multiple Tube Method.

C2 2556-1

4.2 Particle Size Distribution by Sedimentation

The granular and platelet samples were sent to an independent laboratory for particle size distribution analysis by sedimentation.

In general, sedimentation methods measure an equivalent particle diameter by observing the settling rate of the sample in a viscous fluid. Stoke's law for viscous flow around a spherical body is used as the basis for calculation of particle size distribution. The relationship between actual particle shape and dimensions and Stoke's diameter is not known in general. Different methods use different means of measuring settling rates and extracting particle size data from these measurements. The particles must be of uniform density in order to obtain accurate particle size data.

4.2.1 Procedure

The sludge samples were analyzed on a Micromeritics Sedigraph 5000 by adding 1.0 gram of sample to 25 ml Sedispore "W-11", an aqueous medium containing 0.05% surfactant. Dispersion was accomplished by placing the slurry in an ultrasonic bath for two minutes. The running time for the samples was about 50 minutes each with a cell temperature of 32-33°C. The particle size range cut off levels were 80 to 0.29µ for granules and 70 to 0.25µ for the platelets. The PSD data was recorded as cumulative mass percent finer than each size range where the particle sizes are calculated as equivalent spherical diameters.

4.2.2 Results

The results of the sedimentation analyses are given in Tables 4-4 and 4-5. The cumulative number percent finer than each size range was calculated for the sedimentation analyses

TABLE 4-4. PARTICLE SIZE DISTRIBUTION OF THE SLUDGE GRANULES BY THE SEDIMENTATION METHOD

Size Range E.S.D.*, μ	Mass** %	Cum Mass % Finer	Number %	Cum Number % Finer
<0.3	11.5	11.5	—	--
0.3-0.4	5.0	16.5	47.9	47.9
0.4-0.5	5.5	22.0	24.8	72.7
0.5-0.6	5.0	27.0	12.4	85.1
0.6-0.8	7.5	34.5	9.0	94.1
0.8-1.0	5.5	40.0	3.1	97.2
1.0-1.2	5.0	45.0	1.6	98.8
1.2-1.5	3.5	48.5	0.6	99.4
1.5-2.0	4.5	53.0	0.3	99.7
2.0-2.5	3.5	56.5	0.1	99.8
2.5-3.0	3.0	59.5	0.1	99.9
3-4	5.0	65.5	--	--
4-5	6.5	71.0	--	--
5-6	6.5	77.5	--	--
6-8	14.5	92.0	--	--
8-10	5.0	97.0	--	--
10-13	2.0	99.0	--	--
13-16	0.5	99.5	--	--
16-20	0.4	99.9	--	--

* Equivalent spherical diameter

** Mass % ≡ Volume %

TABLE 4-5. PARTICLE SIZE DISTRIBUTION OF THE SLUDGE PLATELETS BY THE SEDIMENTATION METHOD

Size Range E.S.D.*, μ	Mass** %	Cum Mass % Finer	Number %	Cum Number % Finer
0.25-0.8	0.5	0.5	53.3	53.3
0.8-1.0	0.7	1.2	14.8	68.1
1.0-1.2	0.8	2.0	9.3	77.4
1.2-1.5	1.0	3.0	6.3	83.7
1.5-2.0	2.0	5.0	5.8	89.5
2.0-2.5	2.5	7.5	3.4	92.9
2.5-3.0	3.5	11.0	2.6	95.5
3-4	5.0	16.0	1.8	97.3
4-5	7.0	23.0	1.2	98.5
5-6	6.0	29.0	0.6	99.1
6-8	14.5	43.5	0.6	99.7
8-10	11.0	54.5	0.2	99.9
10-13	14.0	68.5	0.1	--
13-16	12.5	81.0	--	--
16-20	9.0	90.0	--	--
20-30	7.5	97.5	--	--
30-40	1.0	98.5	--	--
40-50	1.0	99.5	--	--
50-60	0.4	99.9	--	--

* Equivalent spherical diameter

** Mass % ≡ Volume %

and is also given. Figures 4-7 through 4-10 are plots of cumulative number and volume percent of particles versus equivalent spherical diameter.

4.3 Comparison of Sedimentation and Coulter Counter Results

From plots of the data given in Figures 4-1 through 4-10 the mean particle size for the sludge granules and platelets was determined for each analysis method. The mean particle size on a volume or mass basis is given in Table 4-6 and on a number basis in Table 4-7.

Comparison of the mean particle sizes given in Table 4-6 shows a reasonably good agreement between Coulter Counter results on platelets but a very poor agreement between Coulter Counter and sedimentation results. Specifically, the granular sludge sample had a mean equivalent spherical diameter of 9.3 microns by Coulter Counter and 1.7 micron by sedimentation. The platelet sample had 1.8 and 2.9 micron diameter by Coulter Counter measurements and 9.2 microns by sedimentation. Based on these results it would appear that the samples were accidentally reversed during analysis. This possibility was carefully checked and was found not to be the case.

The mass mean particle size of the granular sludge particles measured by micromesh sieves (Technical Note #200-187-11-02) is about 12.5 microns. This is larger than the 9.3 microns measured by Coulter Counter but is at least directionally more in agreement than the sedimentation results. The mass mean diameter of the granular sample calculated from the optical PSD data is 18.5 microns.

The platelet particles had a mass mean equivalent spherical diameter of 5.2 microns by sieve measurement and 10.2

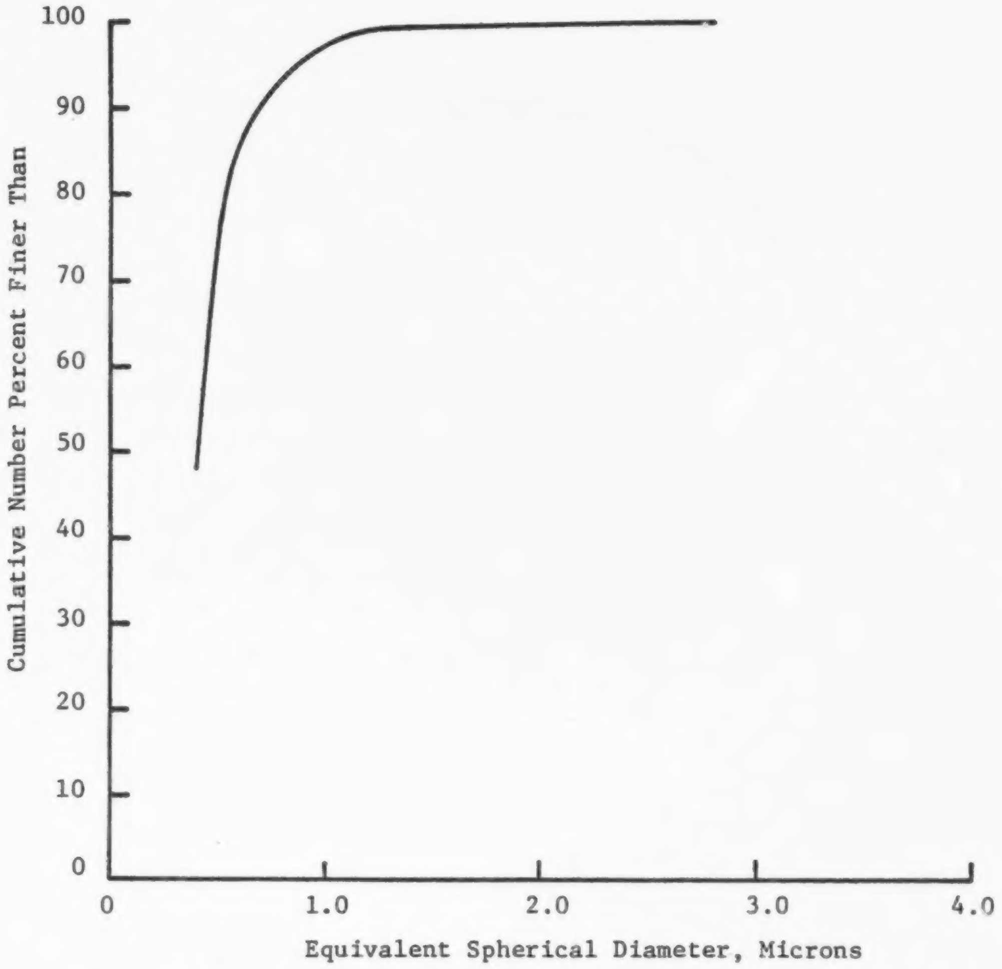

Figure 4-7. Sludge Granules: Cumulative Number Percent of Particles Versus Equivalent Spherical Diameter Measured by Sedimentation Method.

02 2557-1

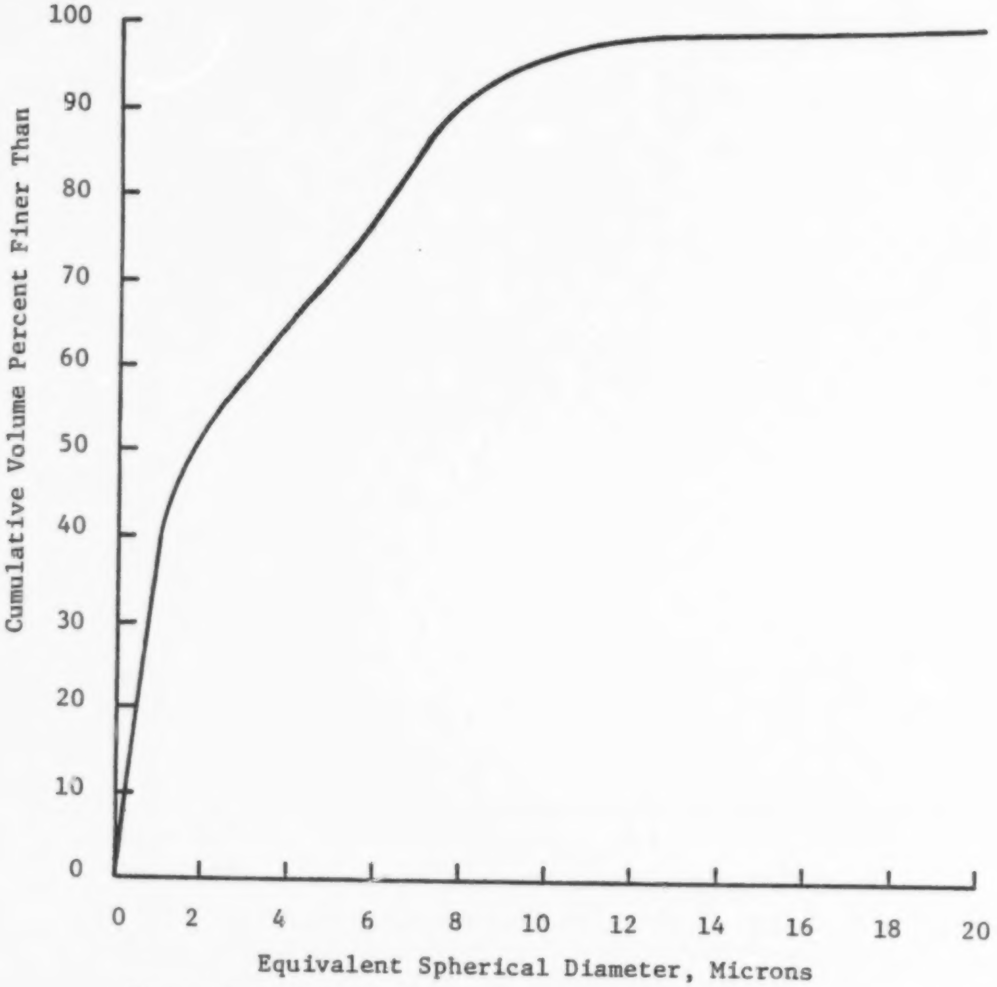

Figure 4-8. Sludge Granules: Cumulative Volume Percent of Particles Versus Equivalent Spherical Diameter Measured by Sedimentation Method.

02 2558-1

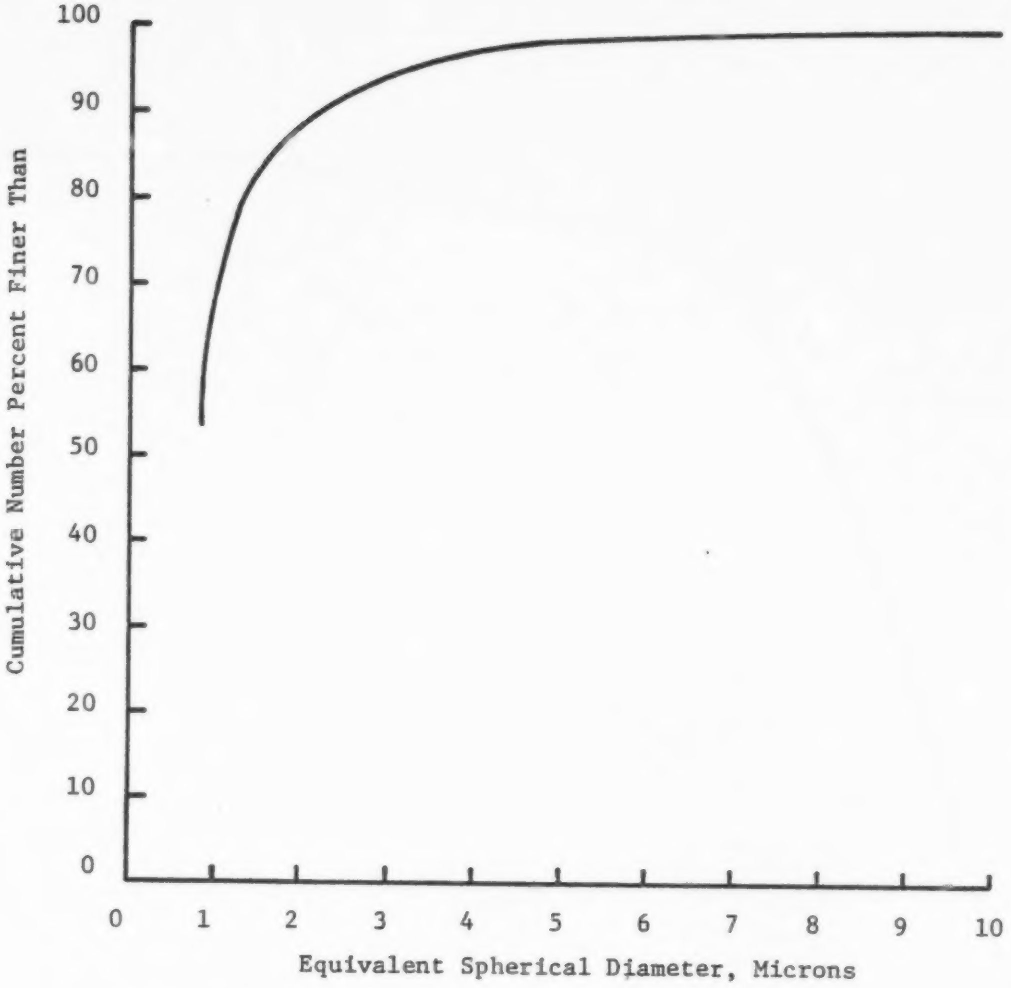

Figure 4-9. Sludge Platelets: Cumulative Number Percent of Particles Versus Equivalent Spherical Diameter Measured by Sedimentation Method

02 2559-1

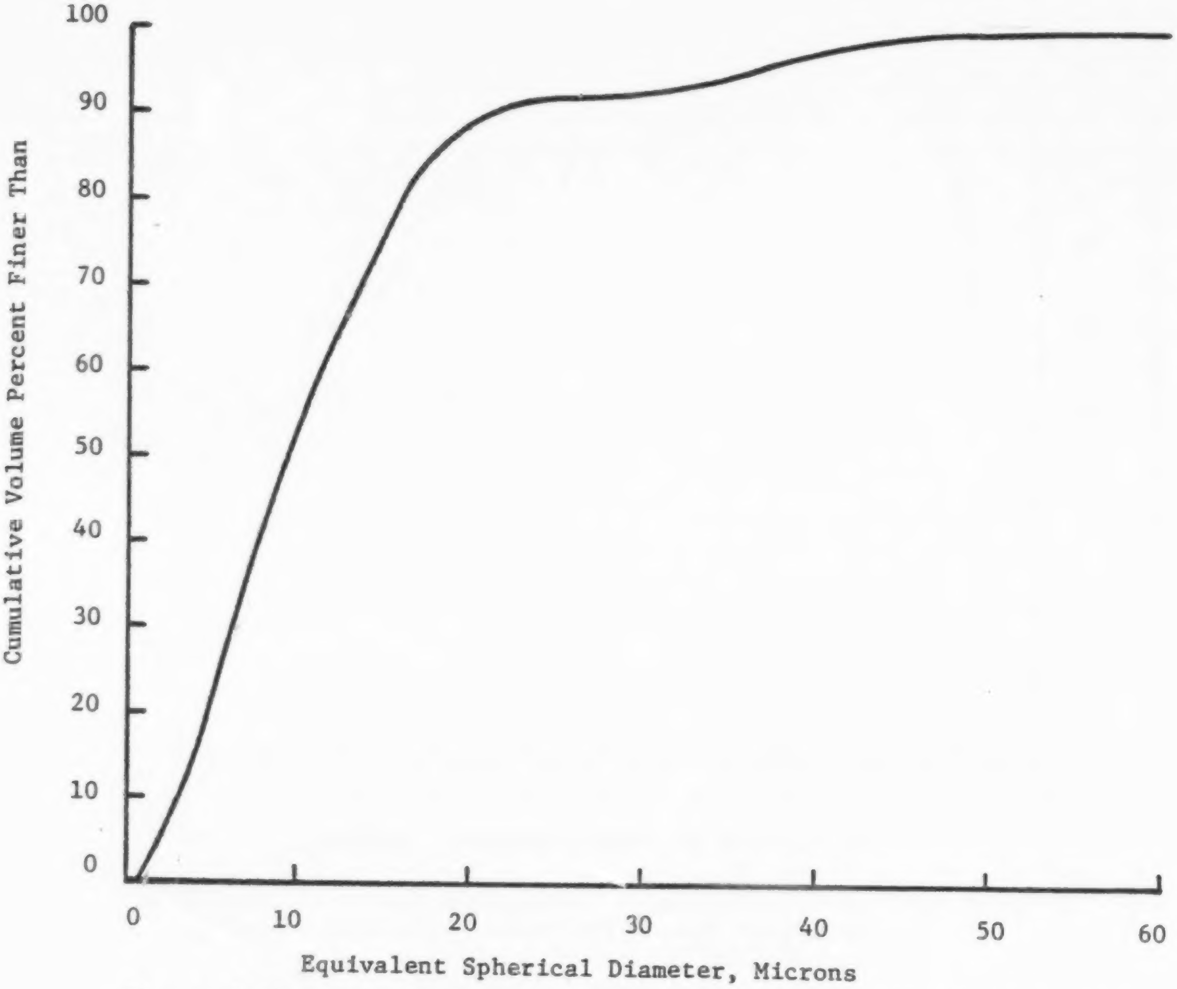

Figure 4-10. Sludge Platelets: Cumulative Volume Percent of Particles Versus Equivalent Spherical Diameter Measured by Sedimentation Method.

TABLE 4-6. MEAN PARTICLE DIAMETER ON VOLUME BASIS*

Method of Analysis	Sludge Type Granule (μ)	Sludge Type Platelet (μ)
Coulter Singletube	9.3	1.8
Coulter Multitube	--	2.9
Sedimentation	1.7	9.2
Optical Microscopy	18.5	10.2
Micromesh Sieve	12.5	5.2

TABLE 4-7. MEAN PARTICLE DIAMETER ON NUMBER BASIS*

Method of Analysis	Sludge Type Granule (μ)	Sludge Type Platelet (μ)
Coulter Singletube	1.0	1.0
Coulter Multitube	--	0.4
Sedimentation	0.4	0.7
Optical Microscopy	7.5	4.0
Micromesh Sieve	7.0	3.5

* Equivalent spherical diameter

microns calculated from optical measurements. As was the case with the sludge granules, the optical and sieve results are higher than the Coulter Counter results. The sedimentation data is high in the case of the platelets, however, and does not follow the same trend as with the granules.

Comparing the results given in Table 4-7 for the mean equivalent spherical diameter on a number basis, the Coulter Counter and sedimentation results agree much more closely than did the data on a volume basis. The granules had a mean diameter of 1.0 and 0.4 microns by the Counter Counter and sedimentation methods, respectively. The platelets measured 1.0 and 0.4 microns by Coulter Counter and 0.7 microns by sedimentation. The Coulter Counter and sedimentation results on a number basis do not compare well to the optical and wet micromesh sieve results since the latter did not measure any particles less than about 1-2 microns. Since a large number of particles if not the vast majority of particles are less than one micron, the optical and sieve methods necessarily give much larger mean particle sizes. Similarly, the use of a larger or smaller lower cut off size for Coulter Counter and sedimentation would give a correspondingly larger or smaller mean particle size on a number basis for any given sample.

There is another very significant difference between the various particle size distributions which is not obvious from plots of cumulative percent of particles versus size data. Namely, the optical and sieve data on a number basis show maxima in their PSD curves but the Coulter Counter and sedimentation data do not. This is illustrated by the data in Tables 4-8 and 4-9 which are the particle size distributions of sludge granule and platelet samples on a noncumulative number percent basis. Plots of these data are given in Figures 4-11 through 4-14. A comparison of Figures 4-11 and 4-12 for granular sludge

TABLE 4-8. PARTICLE SIZE DISTRIBUTION OF SLUDGE GRANULES ON A NUMBER PERCENT BASIS

Optical Microscopy		Wet Micromesh Sieve		Coulter Counter **		Sedimentation	
Size (μ)*	Percent	Size (μ)*	Percent	Size (μ)*	Percent	Size (μ)*	Percent
3.0	16.2	3.5	26.9	0.90	56.7	0.35	52.0
7.5	35.1	6.5	68.8	1.13	35.6	0.45	26.9
12.5	22.3	10.5	9.9	1.43	4.4	0.55	13.5
17.5	16.2	16.5	8.7	1.80	2.4	0.70	4.9
22.5	7.6	27.5	0.7	2.26	0.5	0.90	1.7
27.5	1.7			2.85	0.2	1.10	0.9
32.5	0.8			3.59	0.1	1.35	0.1
37.5	0.1					1.75	0.07

* Equivalent Spherical Diameter

** Single Tube Method

TABLE 4-9. PARTICLE SIZE DISTRIBUTION OF SLUDGE PLATELETS ON A NUMBER PERCENT BASIS

Optical Microscopy		Wet Micromesh Sieve		Coulter Counter **		Sedimentation	
Size (μ)*	Percent	Size (μ)*	Percent	Size (μ)*	Percent	Size (μ)*	Percent
1.50	13.9	1.75	4.4	0.90	52.6	0.52	36.5
3.75	36.4	3.25	82.4	1.13	39.0	0.90	27.9
6.25	27.4	5.25	8.5	1.43	5.0	1.10	17.5
8.75	14.9	8.25	4.3	1.80	1.2	1.35	7.9
11.25	8.3	13.75	0.5	2.26	0.3	1.75	4.4
13.75	2.5			2.85	0.1	2.25	2.6
16.25	1.0					2.78	2.0
18.75	0.5					3.50	0.7
						4.50	0.4
						5.50	0.1

* Equivalent Spherical Diameter

** Single Tube Method

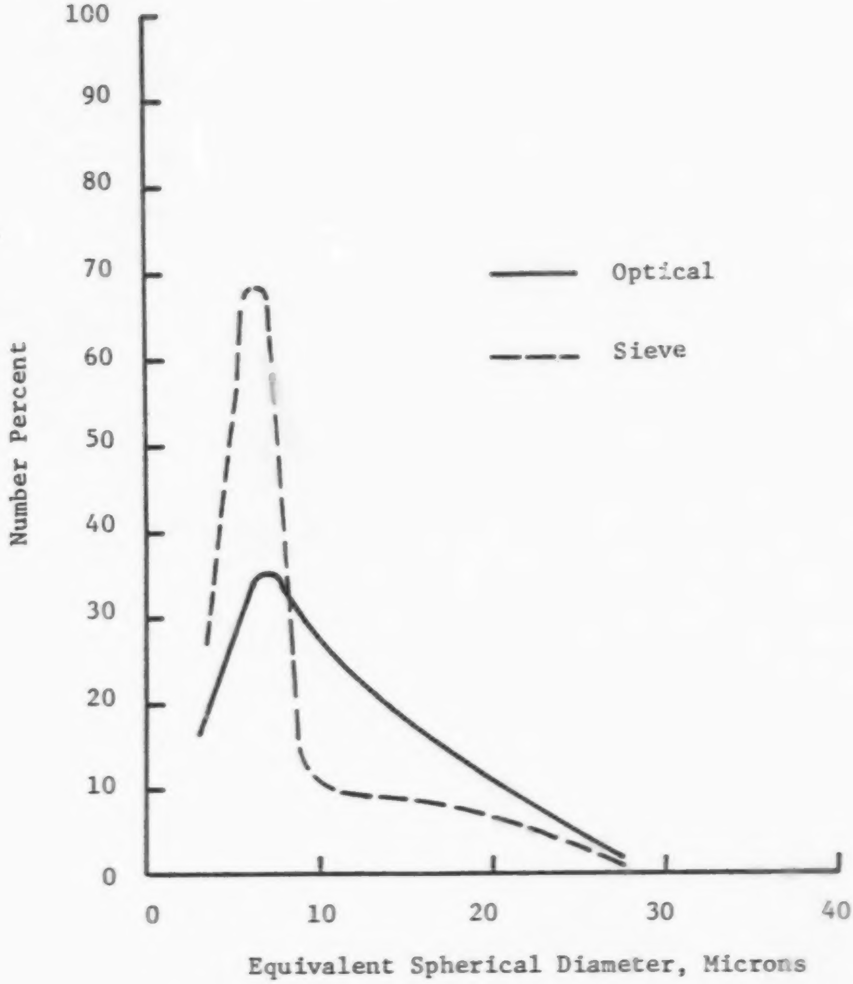

Figure 4-11. Sludge Granules: Number Percent of Particles Versus Equivalent Spherical Diameter Measured by Optical Microscopy and Wet Micromesh Sieve Methods.

02 2561-1

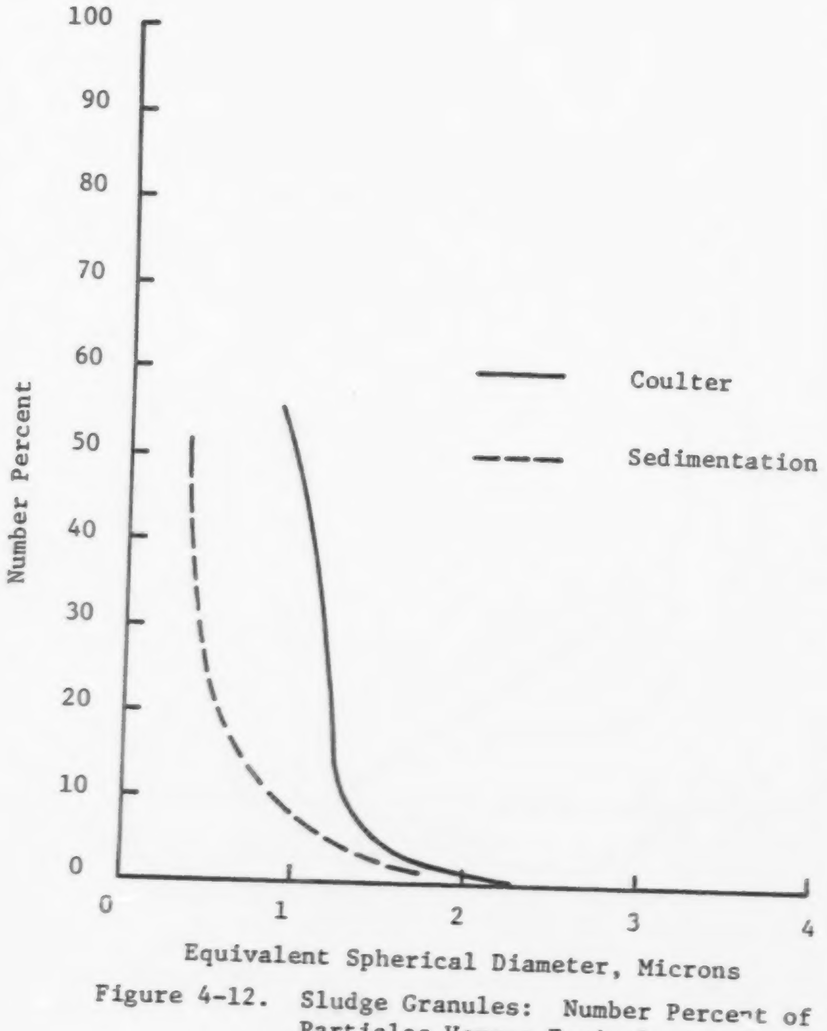

Figure 4-12. Sludge Granules: Number Percent of Particles Versus Equivalent Spherical Diameter Measured by Single Tube Coulter Counter and Sedimentation Methods.

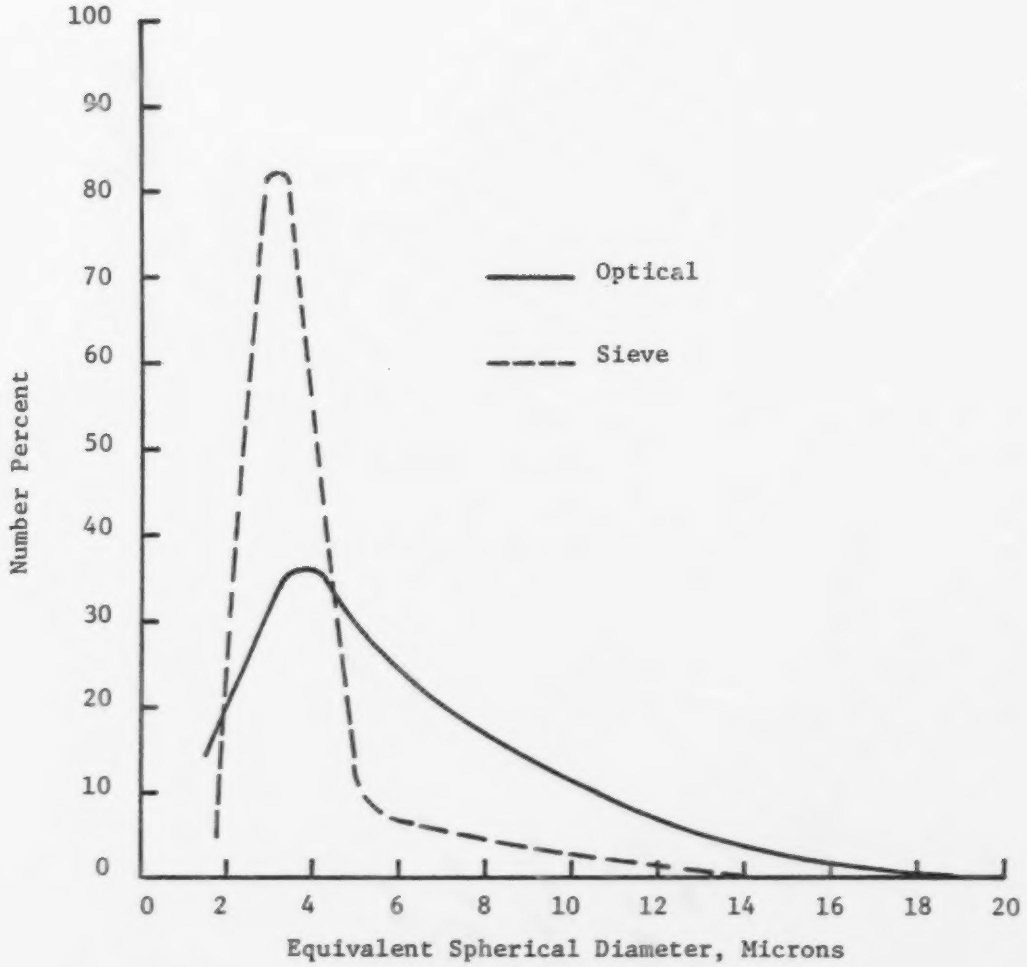

Figure 4-13. Sludge Platelets: Number Percent of Particles Versus Equivalent Spherical Diameter Measured by Optical Microscopy and Wet Micromesh Sieve Methods.

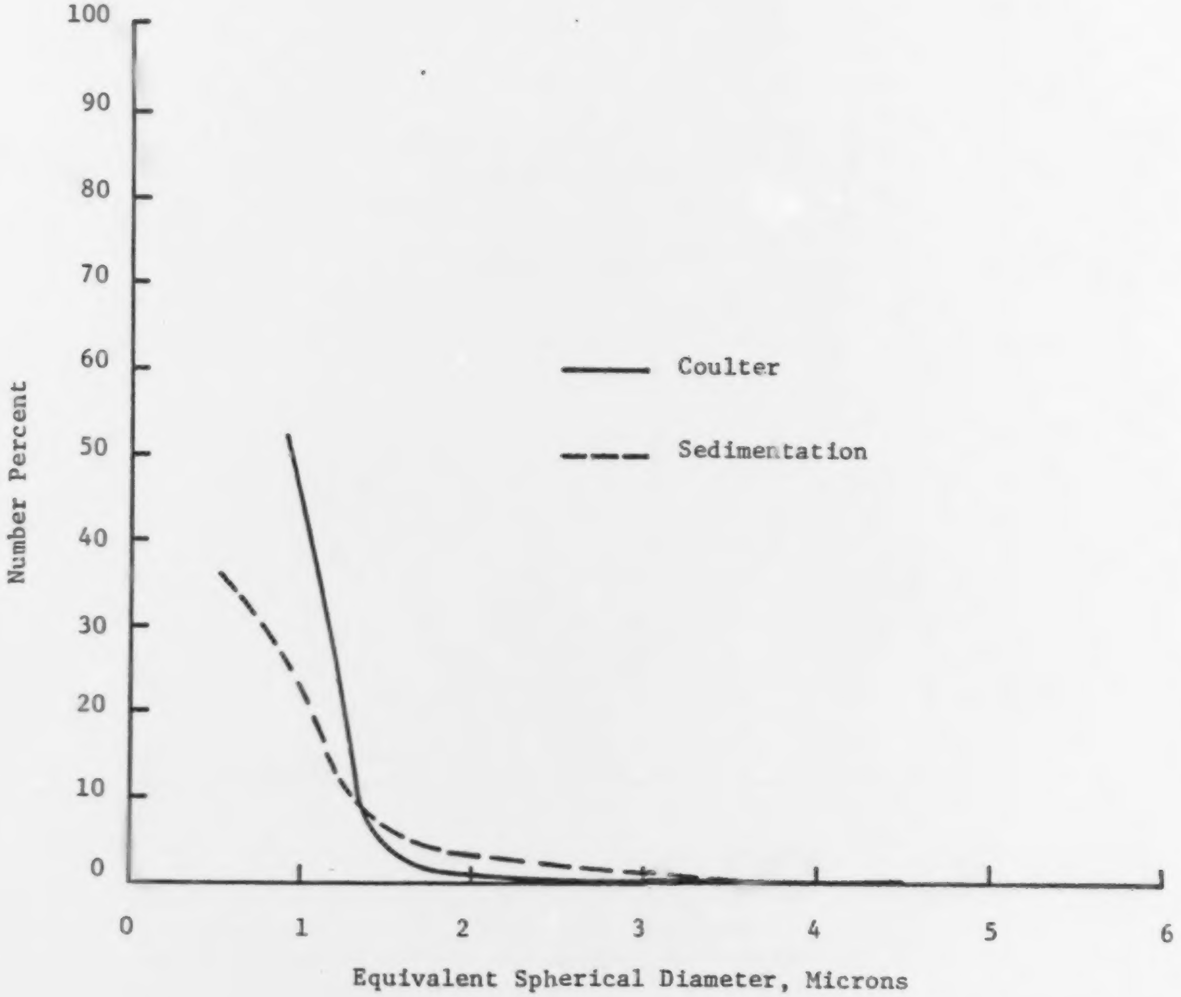

Figure 4-14. Sludge Platelets: Number Percent of Particle Versus Equivalent Spherical Diameter Measured by Single Tube Coulter Counter and Sedimentation Methods.

shows maxima in the particle size distribution curves between 6 and 8 microns for the optical and sieve results. The PSD curves for Coulter Counter and sedimentation data decrease monotonically with increasing particle size and do not show a maximum. A comparison of Figures 4-13 and 4-14 shows maxima in the sieve and optical PSD curves for the platelet sludge sample but no maxima in the sedimentation and Coulter Counter platelet curves. The maxima in the sieve and optical PSD curves for platelets occur between 3 and 4 microns. It will be recalled that the equivalent spherical diameter of the platelets is one half the platelet width. Thus, the 3 to 4 micron maxima for platelets are equivalent to 6 to 8 microns when actual particle shape is considered.

There are a number of different and important interpretations of the differences in the optical and sieve data versus the sedimentation and Coulter Counter data. The maximum in the various optical and sieve PSD curves could indicate that attrition or particle breakage is the major or at least a significant mechanism for new particle generation. This maximum could also be the result of the inherent limitations of optical and sieve methods to measure small particles.

In the case of the optical methods, the smallest particle that can be readily seen at 200X magnification is about 1 to 2 microns. This would appear on a photomicrograph as 0.2 to 0.4 millimeters which is not only difficult to see but is certainly difficult to accurately measure visually against a millimeter ruler. The smallest particle which can be accurately measured at 200X magnification is probably at least 5 microns up to perhaps 10 microns. Thus, the decreased number of particles counted below 5 to 6 microns could simply be a result of not being able to see the smaller particles.

The sieve method also has several inherent problems in the measurement of small particles. One is the rather large tolerance for the sieve openings which significantly limits the accuracy of the smaller mesh sizes compared to the large sizes. Also, the smaller sizes tend to blind more quickly than the larger sizes which could significantly reduce the number of particles reaching the smaller sieve sizes.

It also appears odd that the sludge granule and platelet samples have their PSD curve maxima in essentially the same 6 to 8 micron size range. The granules were produced in a lime scrubber suspected to have very high nucleation rate whereas the platelets were produced in a limestone system. These differences in sludge origin and crystal habit do not seem to support the theory of particle breakage as the source of the maxima in the optical and sieve data PSD curves.

The Coulter Counter and sedimentation PSD curves for granules and platelets do not show maxima. Also, they generally do not measure many, if any, particles above about 3 to 5 microns in size. Thus, one reconciliation of the data is that both types of curves are correct and the methods are mutually exclusive in the size ranges of particles measured. This would indicate that the vast majority of particles are produced through nucleation but a small number of larger particles are produced by particle breakage. This theory breaks down, however, upon close inspection of the actual Coulter Counter particle count data given in Tables 4-4 and 4-5 of Technical Note #200-187-11-02. These data cover the particle size range of 2 to 60 microns and clearly show no maximum in the PSD curve.

The weight of the data presented supports the maxima in the optical and sieve PSD curves being a result of limitations in the methods. The results are not conclusive, however, and more work is needed. Identification of a particle sizing method which could bridge the 1 to 10 micron range with accuracy would greatly clarify which type of PSD curve shape is correct.

The mathematical model for relating sludge PSD to scrubber operating conditions predicts a smooth, monotonic PSD curve as it is currently formulated with constant or linear growth - particle size relations. This type of crystal size distribution is considered normal for crystallization processes and agrees with the predictions of the Coulter Counter and sedimentation methods. If the true PSD curve does contain a maximum due to particle attrition or some other mechanism, then the mathematical model will have to be reformulated to include more complex crystal growth rate functions and perhaps also include the possibility of crystal dissolution in the scrubber.

DCN #77-200-187-11-09

APPENDIX E

TEST PLAN DOCUMENT

Technical Note #200-187-11-04

18 January 1978

Prepared for:
Robert H. Borgwardt
Industrial Environmental Research Laboratory RTP (MD-61)
U. S. Environmental Protection Agency
Research Triangle Park,
North Carolina 27711

Prepared by:
G. P. Behrens

Reviewed by:
P. S. Lowell

TABLE OF CONTENTS

Page

1.0 INTRODUCTION.................................. E-1

2.0 PROCESS DESCRIPTION........................... E-2
- 2.1 Limestone Scrubbing........................ E-4
- 2.2 Lime Scrubbing............................. E-7
- 2.3 Double Alkali Scrubbing.................... E-8

3.0 TEST OBJECTIVES AND APPROACH.................. E-10
- 3.1 Test Objectives............................ E-10
- 3.2 Technical Approach......................... E-11

4.0 TEST PLAN DESCRIPTION......................... E-21
- 4.1 Phase I - Nucleation Site Determination.. E-21
- 4.2 Phase II - Particle Size Distribution Correlation.......................... E-25
- 4.3 Phase III - Sludge Quality Optimization and Model Verification................ E-29

5.0 SAMPLING AND ANALYTICAL MEASUREMENTS.......... E-31
- 5.1 System Characterization Measurements..... E-31
- 5.2 Line-Out Measurements.................... E-34
- 5.3 Sampling Frequency and Timing............ E-36

6.0 PROCESS MEASUREMENTS.......................... E-38
- 6.1 Flow Rates................................. E-38
- 6.2 Pressure Measurements...................... E-38
- 6.3 Temperature Measurements................... E-38
- 6.4 Other Process Data......................... E-40

TABLE OF CONTENTS (Cont'd)

Page

7.0 DATA HANDLING AND ANALYSES PROCEDURES......... E-41
7.1 Chemical Analyses........................ E-41
7.2 Process Measurements..................... E-55
7.3 Process Calculations..................... E-55
7.4 Monthly Progress Reports................. E-69

8.0 POSSIBLE PROBLEM AREAS........................ E-77
8.1 System Operation......................... E-77
8.2 Measurement Problems..................... E-78
8.3 Engineering Analysis..................... E-80

9.0 SUMMARY...................................... E-81

NOMENCLATURE................................. E-82

REFERENCES................................... E-84

LIST OF FIGURES

Figure Page

2-1 RTP Limestone Scrubbing System................ E-5

3-1 Size Distribution Data for Lime and Limestone Scrubber Slurries (Coulter Counter)..... E-16

4-1 Proposed Test Schedule....................... E-22

5-1 Limestone Flow Sheet......................... E-33

7-1 Liquid and Solid Phase Chemical Sample Locations - Characterization Samples.......... E-44

7-2 Proposed Sample Label Format................. E-46

7-3 Sample Collection Schematic Diagram.......... E-48

7-4 RTP Monthly Operating Log.................... E-70

7-5 RTP Scrubbing Liquor Parameters.............. E-71

7-6 RTP Dissolved Solids Concentrations.......... E-72

7-7 Particle Size Distribution................... E-76

LIST OF TABLES

Table Page

4-1 Phase I - Test Schedule.................... E-23

4-2 Phase II - Test Schedule.................... E-26

4-3 Phase III - Test Schedule.................... E-30

5-1 Limestone System Characterization Measurements - Sample Points and Analysis..... E-32

5-2 Limestone Line-Out Measurements............... E-35

5-3 Sample Point Description and Sequence......... E-37

6-1 Process Data Requirements.................... E-39

7-1 Scrubber System Chemical Analyses Required.... E-42

7-2 Sample Handling Flow Sheet.................... E-45

7-3 Proposed Master Log Book Format............... E-49

7-4 Results of Liquid Phase Analyses.............. E-53

7-5 Results of Solid Phase Analyses............... E-54

7-6 Process Measurement Documentation............. E-56

7-7 Typical Equilibrium Program Printout.......... E-58

7-8 Scrubber Rate Calculation Work Sheet.......... E-61

LIST OF TABLES (Cont'd.)

Table		Page
7-9	Hold Tank Rate Calculation Work Sheet.........	E-62
7-10	Particle Calculation Sheet....................	E-63
7-11	Operating Data Summary........................	E-73
7-12	Chemical Reaction Calculation Summary.........	E-75

1.0 INTRODUCTION

Radian Corporation has been contracted by the Environmental Protection Agency to develop a test plan document to evaluate the prospects for improving the physical quality of calcium sulfite sludge without altering its composition. A secondary test objective will be to verify the accuracy of a Radian-developed model for prediction of sludge quality.

The model was developed using present day calcium sulfite crystallization kinetics. Using data produced in EPA Contract 68-02-0223 and others, the model predicts particle size distributions based on nucleation and crystal growth rates of $CaSO_3 \cdot \frac{1}{2}H_2O$. This document presents a series of tests designed to yield useful information on sludge quality due to various scrubber operating parameters.

The test plan information which is presented here is organized into the general categories of: system description, test objectives and approach, test plan description, sampling and analytical measurements, process measurements, process analysis, and problem areas. Each of these subjects is discussed in detail in separate sections of this report.

2.0 PROCESS DESCRIPTION

The overall chemical objective of a scrubbing system is the removal of SO_2 from flue gases. In throwaway wet systems, this SO_2 is reacted with an alkali metal salt, usually calcium carbonate or oxide, to yield calcium sulfite or sulfate sludge. The three processes considered for testing produce a sulfite sludge which has a fraction of sulfate coprecipitated with it. The three FGD processes considered were: limestone scrubbing, lime scrubbing, and double alkali scrubbing. Due to the length of time necessary to test each process, Radian proposes the limestone system first. If significant results are achieved, testing of the other two systems may be implemented.

The decision to test limestone scrubbing is based on several factors:

1) limestone scrubbing has been in existence the longest and most operating problems have been solved,

2) lime will continue to increase in cost as fuel prices rise,

3) double alkali systems in the U.S. have traditionally used lime as an additive, and

4) limestone systems are the simplest in terms of kinetics, precipitation rates and operability.

The EPA Research Triangle Park pilot unit is a three-stage, countercurrent turbulent contractor absorber (TCA). The scrubber has a 23-cm diameter and is approximately 3.7 meters tall. The flow diagram and approximate rates are shown in Figure 2-1.

An oil fired boiler is used to generate 270-510 m^3/hr of flue gas. For this test plan, a gas rate of 510 m^3/hr will be used. SO_2 is spiked into this stream at specified rates to provide the desired concentration. Normal concentration will be 3000 ppm. Oxygen in the flue gas is generally 4-6%. Since the purpose of this test plan is to study calcium sulfite crystals, factors which reduce the oxidation of sulfite to sulfate will be employed. Possibly the biggest factor affecting the oxidation rate is the oxygen concentration in the flue gas. It is recommended that this be kept below 3%. Raising the pickup per pass will also reduce oxidation. A 50-60% removal efficiency should significantly reduce oxidation as compared to a 80-90% SO_2 removal.

The flue gas enters the scrubber below the bottom stage. A 10 wt % scrubbing slurry is introduced at the top of the scrubber. The slurry feed rate is approximately 83 ℓpm. This corresponds to a liquid to gas ratio of 9.8 ℓ/m^3 (73 gal/1000acf). The scrubber feed pH is normally 6, and the scrubber bottoms ranges from 5 to 6. The bottoms stream flows directly into the reaction tank which has a 400 liter volume.

Reaction tank feed streams include:

1) scrubber bottoms

2) clarifier and filter overflows, and

3) limestone additive.

The liquid residence time in the hold tank under these conditions is 5 minutes and the average solids residence time is approximately 10 hours. A bleed stream of 0.5-0.6 liters per minute is taken from the scrubber feed line and sent to the clarifier. The clarifier underflow is sent batchwise to a vacuum filter and the overflow is returned to the hold tank.

Limestone is added to the system from the additive tank. This tank contains a 25% limestone slurry. The slurry is kept well mixed by an agitator and is fed to the hold tank on pH demand. Generally, flow rates will be about 400 milliliters per minute to keep a pH 6 scrubber feed.

The remaining portion of this section describes the process chemistry of each of the three FGD processes. As stated previously, limestone scrubbing will be the only process tested at this time.

2.1 Limestone Scrubbing

The flow diagram for the limestone scrubbing unit at Research Triangle Park is given in Figure 2-1. Average flow rates are also indicated.

The overall reaction in a limestone system is as follows:

$$SO_2(g) + CaCO_3(s) + \tfrac{1}{2}H_2O \rightarrow CaSO_3\cdot\tfrac{1}{2}H_2O(s) + CO_2(g)$$

Some of the sulfite is oxidized to sulfate:

$$SO_2(g) + \tfrac{1}{2}O_2(g) + CaCO_3(s) + 2H_2O \rightarrow$$

$$CaSO_4\cdot 2H_2O(s) + CO_2(g)$$

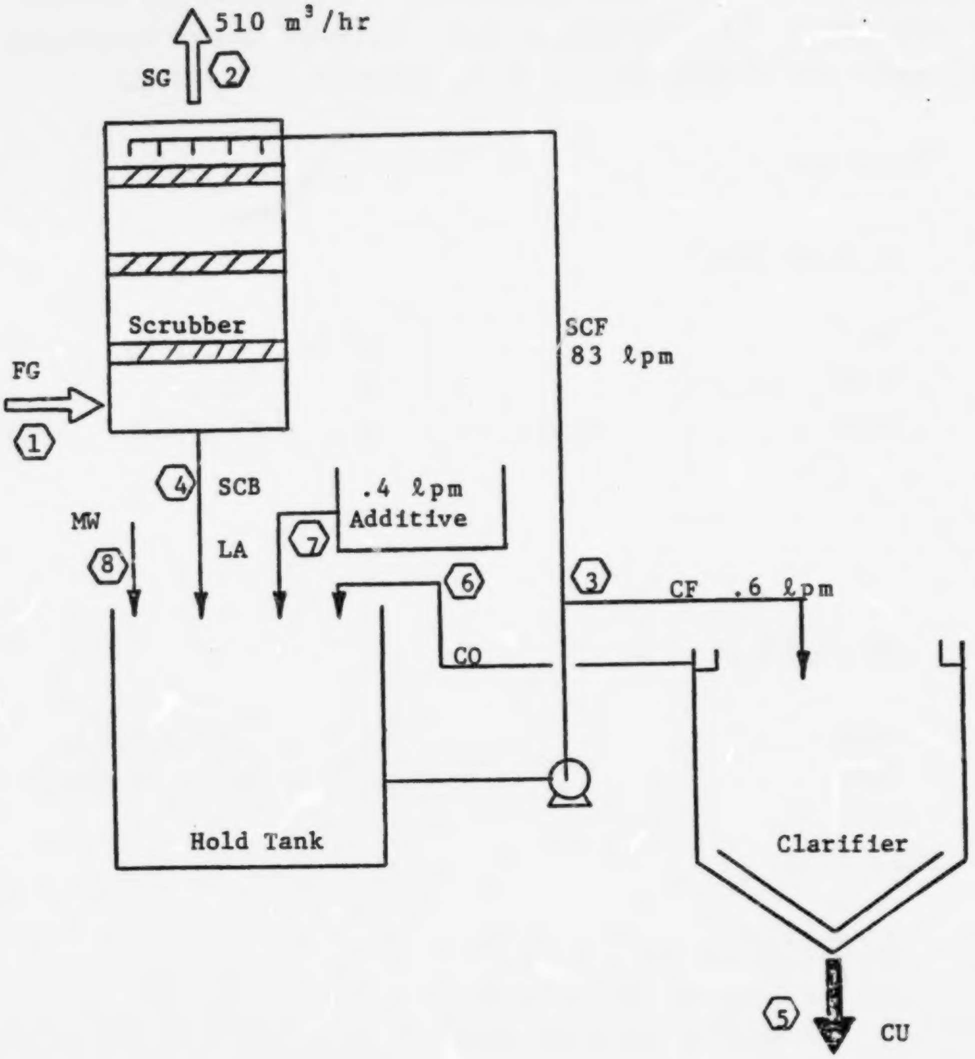
510 m³/hr
SG
2
Scrubber
FG
1
SCF
83 ℓpm
4
SCB
.4 ℓpm
Additive
MW
8
LA
7
6
3
CF .6 ℓpm
CO
Hold Tank
Clarifier
5
CU

Figure 2-1. RTP Limestone Scrubbing System.

The overall reaction may be broken down into sorption (scrubber) and precipitation (hold tank) reactions. The scrubbing slurry has two components: liquid and solid. Both of these components can react with the sorbed SO_2 in its hydrated form, H_2SO_3.

Scrubber:

Liquid Phase

$$\left.\begin{array}{l} SO_3^{=} \\ MgSO_3\ (aq.) \\ MgHCO_3 \\ \quad\vdots \end{array}\right\} + H_2SO_3 \rightleftharpoons \left\{\begin{array}{l} 2HSO_3^- \\ Mg^{++} + 2HSO_3^- \\ Mg^{++} + H^+ + HCO_3^- + HSO_3^- \\ \qquad\qquad\vdots \end{array}\right.$$

Solid Phase

$$\left.\begin{array}{l} CaCO_3 \\ CaSO_3 \cdot \tfrac{1}{2}H_2O \end{array}\right\} + H_2SO_3 \rightleftharpoons \left\{\begin{array}{l} Ca^{++} + SO_3^{=} + H_2CO_3 \\ Ca^{++} + 2HSO_3 + \tfrac{1}{2}H_2O \end{array}\right.$$

Hold Tank:

$$CaCO_3\ (s) \rightleftharpoons Ca^{++} + CO_3^{=}$$
$$CO_3^{=} + HSO_3 \rightleftharpoons HCO_3 + SO_2^{=}$$
$$Ca^{++} + SO_3^{=} + \tfrac{1}{2}H_2O \rightleftharpoons CaSO_3 \cdot \tfrac{1}{2}H_2O\ (s)$$

The base in the limestone system is the carbonate ion produced by limestone dissolution. As a result, there is not a large pH change between the scrubber and the hold tank.

Recent work (JO-R-214) has indicated that as long as the oxidation fraction (specific sulfate/total sulfur-solid phase) is below .15, the coprecipitation phenomena is capable of removing calcium sulfate. Scale-free scrubber operation is then realized. In this test plan, all suldge produced is regarded as calcium sulfite hemihydrate ($CaSO_3 \cdot \frac{1}{2}H_2O$).

Limestone dissolution is a rate controlling factor in this system. It is probable that limestone fines may dissolve in the scrubber to increase the liquid phase alkalinity. This effect will change the particle size distribution in a manner yet to be determined.

2.2 Lime Scrubbing

The overall lime scrubbing reaction is:

$$SO_2(g) + CaO(s) + \tfrac{1}{2}H_2O \rightarrow CaSO_3 \cdot \tfrac{1}{2}H_2O(s)$$

Oxidation of sulfite can also occur:

$$SO_2(g) + \tfrac{1}{2}O_2(g) + CaO + 2H_2O \rightarrow CaSO_4 \cdot 2H_2O(s)$$

Dissolution of lime is extremely fast compared to sulfite precipitation rates or limestone dissolution rates (OT-023). Therefore most of the alkalinity required to sorb SO_2 in the scrubber comes from dissolution of calcium sulfite to form calcium bisulfite. This phase change will have an effect on particle size distribution which could be different from a limestone system. Furthermore, there is a large pH change between the scrubber and hold tank that can effect the nucleation rate.

2.3 Double Alkali Scrubbing

The double alkali process utilizes a soluble sodium-based alkali (NaOH and Na_2SO_3) to absorb SO_2. The sulfur-oxide rich effluent is then reacted with lime ($Ca[OH]_2$) to produce calcium sulfite solids and regenerate the scrubbing liquor. The principle reactions are as follows:

Absorption:

$$2NaOH + SO_2 \rightarrow Na_2SO_3 + H_2O$$

$$Na_2SO_3 + SO_3 + H_2O \rightarrow 2NaHSO_3$$

Oxidation of sulfite also occurs:

$$Na_2SO_3 + \tfrac{1}{2}O_2 \rightarrow Na_2SO_4$$

Regeneration:

$$Ca(OH)_2 + 2NaHSO_3 \rightarrow Na_2SO_3 + CaSO_3 \cdot \tfrac{1}{2}H_2O\downarrow + 3/2\ H_2O$$

$$Ca(OH)_2 + Na_2SO_3 + \tfrac{1}{2}H_2O \rightarrow NaOH + CaSO_3 \cdot \tfrac{1}{2}H_2O\downarrow$$

$$Ca(OH)_2 + Na_2SO_4 + 2H_2O \rightarrow 2NaOH + CaSO_4 \cdot 2H_2O$$

$$CaCO_3 + 2NaHSO_3 + \tfrac{1}{2}H_2O \rightarrow Na_2SO_3 + CO_2 + H_2O + CaSO_3 \cdot \tfrac{1}{2}H_2O$$

By using sodium compounds to absorb SO_2, higher alkalinity levels can be used than in lime/limestone scrubbers. This results in lower L/G ratios. Also scrubber scaling is avoided due to the high sulfite concentration present. With the lime added in a special hold tank, greater utilization is realized. Since the system uses a clear scrubbing liquor, calcium sulfite solids are not pumped around the scrubbing loop. Particle size distribution will therefore be different from lime or limestone systems. Historically, this process produces a sludge which has worse characteristics than lime or limestone systems.

3.0 TEST OBJECTIVES AND APPROACH

The sludge quality/model verification test program will be conducted using a limestone scrubbing system. Three phases of tests are planned for the process. The objectives of each test phase are discussed in this section. The technical approach required to meet these objectives is also outlined.

3.1 Test Objectives

The test phases proposed for the limestone FGD process are listed below:

1) nucleation site determination,

2) particle size distribution correlation, and

3) sludge quality optimization and model verification.

The objectives of each of these test phases are discussed in the following subsections.

3.1.1 Nucleation Site Determination

Phase I testing is intended to locate the major source of nucleation in the scrubbing system. The three possible sites for nucleation are the scrubber, the hold tank, and the pumps. Single parameter tests are planned in this phase. Coulter counter analysis will be used to determine the particle size distribution of hold tank slurry. By observing changes in the number of small particles, varied operating conditions should reveal the nucleation source.

A major portion of the initial phase will be spent studying the effect of equipment on nucleation. Such mechanical nucleation will interfere with nucleation from other changes. It will therefore be eliminated from Phase II and III testing as much as possible once its causes have been identified.

3.1.2 Particle Size Distribution Correlation

The second phase of testing will provide data to correlate the particle size distribution with operational parameters. Particle size distribution is the result of the interaction between nucleation, crystal growth, equipment arrangement, and operational conditions. Four series of tests are planned to generate results for the model. These are percent solids changes, scrubbing liquor quality, residence time variations, and slurry grinding. The data obtained from these parametric studies will be compared with results predicted by the model. Modifications to the model will be made where necessary to reach agreement between predictions and observations.

3.1.3 Sludge Quality Optimization and Model Verification

The final phase will utilize tests proposed by the developed correlation. Multi-parameter tests will be used to check the model's accuracy to predict sludge quality. Further tests will attempt to produce the highest quality sludge possible by changing the most influential process conditions.

3.2 Technical Approach

Radian believes the most important parameter affecting sludge quality is the particle size distribution. Large particles settle and dewater better than small ones. However, larger crystals have smaller area to mass ratios. This can cause a rise in supersaturation. At certain "critical" supersaturation levels, homogenous nucleation occurs, resulting in the formation of many new particles. This showering of solids can result in scale formation in certain circumstances. By using the tests outlined in Section 4, an understanding of nucleation and crystal growth will be obtained. The desired result of this test plan is the production of a high quality sludge obtained by controlling the particle size distribution.

At steady state, several balances must hold true in scrubbing systems. By relating these balances to one another, an understanding of the importance of particle size distribution can be realized. Since no calcium sulfite crystals enter the system, those generated within the system must equal the number of particles leaving the system. This can be expressed as:

$$\dot{n}_o = CF\int_0^\infty n(L)dL \quad , \qquad (3\text{-}1)$$

where $\dot{n}_o$ ≡ nucleation rate (particles/ℓ-second),

CF ≡ clarifier feed rate (ℓ/second),

n ≡ number of particles of size L per unit particle length and per unit volume (ℓ^{-1}-m^{-1}), and

L ≡ characteristic length of particle (meters).

The function of n(L) is usually referred to as the particle size distribution function. The quantitative description of this function is the heart of the problem. Several other pieces of information are also important. Some of these are: the total number of particles, the nucleation rate, and the size distribution function evaluated at zero size.

The value of the integral in equation (3-1) is N, the total number of particles per unit volume. As the length approaches zero, the initial distribution function, n_o, is defined.

$$n_o = \lim_{L \to o} n(L) \quad . \tag{3-2}$$

This initial value is important because it is fundamentally related to the nucleation rate as shown in equation (3-3).

$$\dot{n}_o = \lim_{L \to o} (nR) = n_o R_o \quad . \tag{3-3}$$

It is expected that the nucleation rate is dependent upon relative saturation, solids content, the number average crystal size, and energy dissipation rate in the solution, especially in pumps and mixers. These parameters have been included in an empirical correlation:

$$\dot{n}_o = k_1 (r-1)^h m_s^i \bar{L}_n^j + k_2 \exp[-k_3/\ln r] \,, \tag{3-4}$$

where $r \equiv$ relative saturation,

$m_s \equiv$ slurry solids content,

$\bar{L}_n \equiv$ number average crystal size,

$h, i, j \equiv$ undetermined exponents, and

$k_1, k_2, k_3 \equiv$ undetermined constants.

No experimental data exists which would help in the determination of the six missing constants. Therefore, Phases I and II will be used to generate these values.

For modeling purposes, the growth function, R, must be known. One form for the growth rate assumes that it is a linear function of size.

$$R(\text{meter/sec}) = k_r(1+\delta L)(r-1)^P \quad , \tag{3-5}$$

where k_r ≡ surface reaction rate constant.

At normal levels of supersaturation, experimental data from PP&L has yielded a k_r of 3×10^{-12} meter/sec and a δ of 5×10^5 meter^{-1}. This correlation does not seem to fit lime crystal growth data.

Once the functional dependence of the nucleation and growth rates have been determined, the computer model should be able to predict the existing particle distribution, given the incoming distribution and process parameters. A simplification of the general particle balance equation will be used by the model:

$$\frac{\partial n}{\partial t} = \left[\frac{-\partial}{\partial X}(\bar{u}_X n) + \frac{\partial}{\partial Y}(\bar{u}_Y n) + \frac{\partial}{\partial Z}(\bar{u}_Z n)\right] - \frac{\partial}{\partial L} nR(L) + G(L,X,Y,Z) \quad . \tag{3-6}$$

Basically, the equation says; the change in the number of size L particles with respect to time is equal to the net number of particles of size L convected into a volume (first three terms) plus the number in the volume which grow to size L, (nR(L)), plus particles of size L generated by other mechanisms(G). The nucleation rate is not included in the equation per se. It is actually a boundary condition for the growth term:

$$\dot{n}_o = \Big(n(L)R(L)\Big)\Big|\text{evaluated as } L \to o \quad . \tag{3-7}$$

Several assumptions can be made to simplify equation (3-6). First, steady-state conditions should apply to the number of particles in an operating system. Therefore, $\frac{\partial n}{\partial t} = 0$. The convection terms can be considered as entering and exiting streams when a system component volume is used. Therefore, the final working form of the particle balance equation becomes:

$$\Sigma Q_{out} n_{out} - \Sigma Q_{in} n_{in} = \int_V \left[\frac{-\partial}{\partial L}(nR\{L\}) + G\right] dV \quad , \tag{3-8}$$

where Q = volumetric flow rate (liters/second), and

G = particle generation term other than growth and nucleation (ℓ^{-1}-sec^{-1}).

This equation predicts the change in the particle size distribution, given expressions for the growth, nucleation, and other particle size changing rates. Obtaining these expressions for n(L), R(L) and G is therefore part of the objective of this test plan.

Graphs for n(L) will take the form of Figure 3-1. The distribution will be plotted as the characteristic length L. versus the log of the number of particles having that dimension.

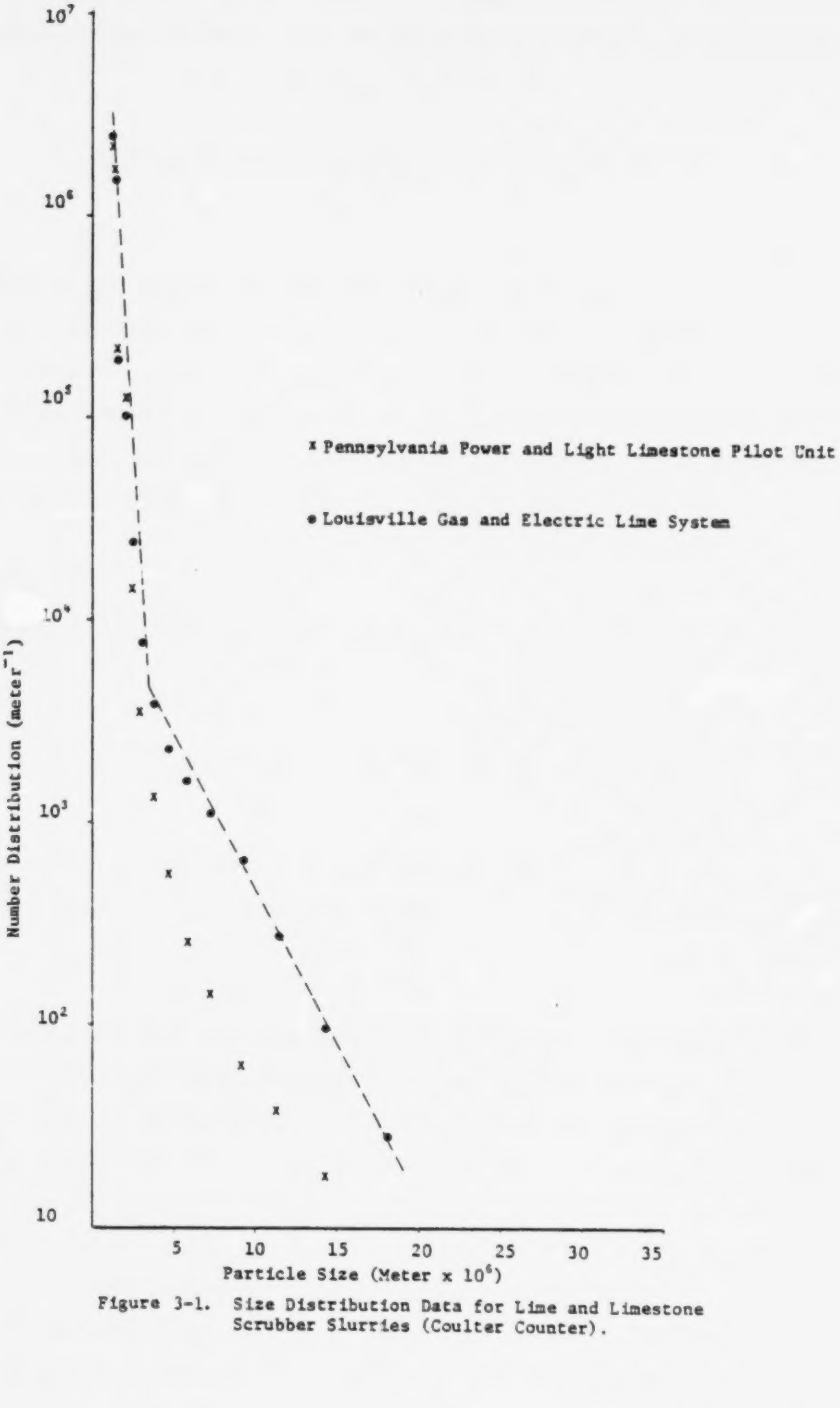

Figure 3-1. Size Distribution Data for Lime and Limestone Scrubber Slurries (Coulter Counter).

The nucleation rate at steady state will simply be the total number of particles in the PSD sample times the clarifier under flow rate. Since the number of particles increases as L approaches zero, and the technique for measuring sub-micron particles is not fully developed, changes in the nucleation rate will be difficult to separate from experimental error unless extreme care is taken in their analyses. A worksheet for PSD calculations is given in Table 7-10, based on the results generated in completion of Figure 7-7.

An alternate method of generating a nucleation rate can also be used. For a scrubbing system, the material balance must also be solved. For every mole of SO_2 absorbed a mole of sludge is formed. Actually, a small amount of sulfur leaves dissolved in the adherent water. Since the sludge consists of calcium sulfite crystals, the material balance is connected to the particle balance.

For limestone systems, the average length to width to thickness ratio is generally 25μ x 20μ x 1μ. Since all of the equations developed here are based on a characteristic length L, definition of a shape factor, k_v is necessary.

$$k_v = \frac{V}{L^3} \quad , \qquad (3\text{-}9)$$

where V = crystal volume (meters^3). A mass balance between the SO_2 pickup and the particle volume change can now be made.

$$\Delta SO_2 = \frac{CF\ k_v\ \rho_s}{MW} \int_0^\infty n(L)L^3dL \quad , \qquad (3\text{-}10)$$

where $\Delta SO_2 \equiv$ SO_2 pickup (gram mol/second),

$CF \equiv$ clarifier feed rate (liters/second),

$\rho_s \equiv$ particle density (grams/cm^3), and

$MW \equiv$ molecular weight (grams/gram mol)

if we define a mass average length $\bar{L}_m$ (meters) such that:

$$\bar{L}_m^3 \equiv \int_0^\infty n(L)L^3\,dL \Big/ \int_0^\infty n(L)\,dL \quad , \qquad (3\text{-}11)$$

then equation (3-10) can be rewritten as:

$$\Delta SO_2 = CF\ k_v\ \rho_s\ N\ \bar{L}_m^3/MW \qquad (3\text{-}12a)$$

$$= k_v\ \rho_s\ \dot{N}\ \bar{L}_m^3/MW \quad , \qquad (3\text{-}12b)$$

where N is the total number of crystals per volume of slurry and $\dot{N}$ is the total number of crystals leaving the system.

In a steady-state situation, $\dot{N}$ should equal $\dot{n}_o$, the nucleation rate. Equation (3-12) shows that for a change in the SO_2 removal rate, the product of $\dot{N}\bar{L}_m^3$ must change. Consequently, if the pickup is constant, and the mass average length increases, the nucleation rate decreases to the third power.

Determination of the net nucleation rate can be done by either Coulter Counter analysis or sedimentation techniques. Both methods can analyze to below .5μ. By counting the total number of particles in a sample, calculations can be made to determine the number of particles leaving the system. This net rate includes generation of particles by methods other than nucleation. In order to obtain useful results, it will be necessary to closely maintain steady-state conditions.

The growth rate function R(L) must also be calculated for input into the computer model. If the scrubbing system approximates mixed suspension, mixed product removal (MSMPR) crystallizer conditions, the particle balance for a well mixed vessel can be simplified to yield:

$$-\frac{d(nR)}{dL} = \frac{n}{\tau} , \tag{3-13}$$

where τ is the mean solids residence time in the system. This equation can be expanded and solved for the size derivatives of the distribution n(L). Thus,

$$\frac{d(\ln n)}{dL} = -\frac{d \ln R}{dL} - \frac{1}{R\tau} . \tag{3-14}$$

If the linear growth rate is constant, $(\frac{d\ln(R)}{dL}) = 0$, then a plot of ln n(L) versus L should be a straight line with slope equal to $-\frac{1}{R\tau}$. If the growth rate increases with size, $(\frac{d\ln(R)}{dL}) > 0$, then the curve will be concave upward.

Figure 3-1 shows size distributions for product crystals from the LG&E lime and PP&L limestone scrubbing systems calculated from Coulter Counter data. Both distributions are clearly concave upward, indicating an increasing growth rate with increasing size.

Equation 3-14 can be rearranged to calculate the growth rate R using the slope of the size distribution:

$$R = -\frac{\frac{1}{\tau} - \frac{dR}{dL}}{\frac{d(\ln n)}{dL}} \quad . \qquad (3\text{-}15)$$

The change in growth rates with crystal size indicated by the data in Figure 3-1 can be estimated by approximating the size distribution with the straight lines indicated on the figure. Along these lines, dR/dL = 0, and

$$R = -\frac{1}{\frac{\tau d \ln n}{dL}} \quad . \qquad (3\text{-}16)$$

For the lime data from LG&E, τ was approximately 1300 minutes. Using this number and the slopes of the indicated lines:

$$R_{small} = 2.4 \times 10^{-10} \text{ meter/min}$$

$$R_{large} = 2.2 \times 10^{-9} \text{ meter/min} \quad .$$

Thus, the larger crystals grow about ten times faster than the smaller crystals.

Once the particle size distribution is plotted, a decision can be made as to how many segments are necessary to model the growth function accurately.

4.0 TEST PLAN DESCRIPTION

In this section, the strategy and sequencing of individual tests to be conducted during each of the three planned test phases are discussed. Operating conditions which are proposed for each specific test run are summarized in Tables 4-1, 4-2, and 4-3. The estimated time duration of each test is also shown in that set of tables.

The overall test schedule shown in Figure 4-1 is based upon individual test duration figures given in Tables 4-1 through 4-3 and an estimate of the necessary analytical and operating manhours required.

4.1 Phase I - Nucleation Site Determination

The eight tests proposed for Phase I are presented in Table 4-1. The suggested flow arrangement is shown in Figure 4-2. In this configuration, the solids retention time is approximately 10 hours. Allowing three or four residence times for the solid phase to line out after a change in operation was instituted would require two days of steady-state operation. After this time, full characterization sample sets could be taken. Allowing for three replicates would make each test run approximately one week in length. As soon as results confirm a reliable set of data, the next test parameter will be implemented to minimize total project length.

The first test will be used as a base case for comparison with further tests. The desired operating and mechanical parameters are given on Table 4-1. It should be noted that unless specifically stated, all variables return to base case conditions after a test run. This is to insure that results

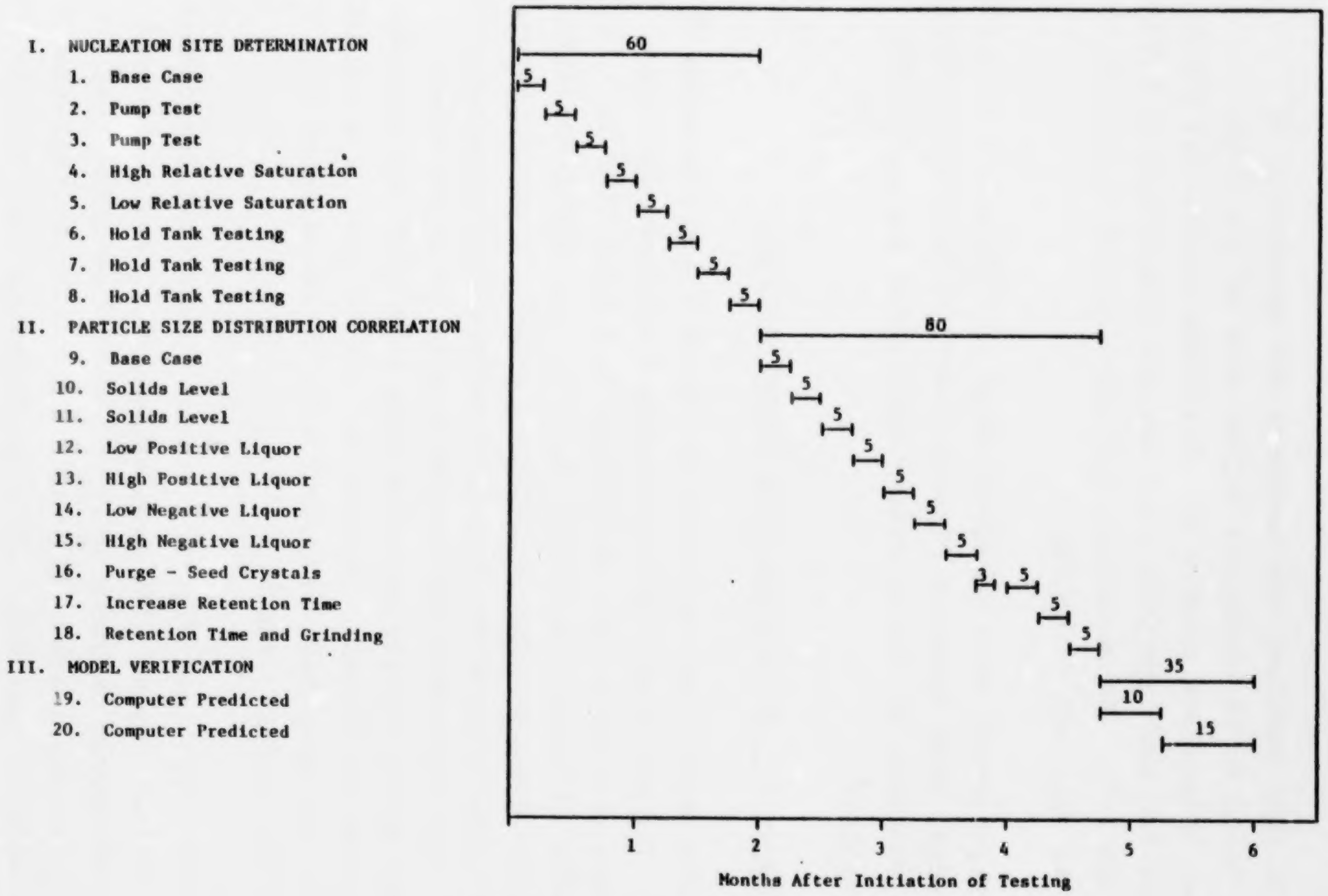

Figure 4-1. Proposed Test Schedule

TABLE 4-1. PHASE I - TEST SCHEDULE

Test #	Days	Objective	Variable Changed	Reason
1	5	Obtain base case[(1)] system operation	None	Basis for further comparison
2	5	Observe effect of impeller material	Switch to steel impeller	Determine effect of pump energy on P.S.D.
3	5	Observe effect of pump speed	Reduce pump RPM's, maintain constant L/G, residence times.	
4	5	Observe higher scrubber supersaturation	Reduce scrubber feed flow, raise SO_2 inlet, (constant SO_2 pickup)	Determine effects of scrubber conditions on P.S.D.
5	5	Observe scrubber subsaturated operation	Scrubber feed pH 4.5	
6	5	Observe mechanical features of hold tank	Switch to steel agitator	Determine effect of hold tank conditions on P.S.D.
7	5	Same as #6	Lower agitator speed	
8	5	Same as #6	Mix additive, clarifier overflow and scrubber bottoms together	
	40			

(1) Base Case - Low oxygen content in flue gas (<3%), 3000 PPM SO_2, feed rate 83 ℓpm, 10% solids, 10 hour solids retention time. Valve positions and nozzles are not to be changed during the study.

generated will have a common basis for comparison. The purpose of Phase I testing will be to determine the source of nucleation. Three possible areas exist where nucleation occurs: the feed pump, the scrubber and the hold tank. Hopefully, only one area contributes significantly, so its location can be determined.

Tests two and three will determine the effect of the feed pump on the particle size distribution. In large pumps, the tip speed can approach 90-100 fps. The pump tip speed at RTP should be about 30 fps. At this low speed, changes might not have a great effect. Test two will use a steel impeller in place of the rubber-tipped one and Test three will operate the pump at a lower speed while maintaining the same flow rate to the scrubber. A Variac or similar device is envisioned to slow down the pump.

Tests four and five are planned to observe changes due to scrubber conditions. Test four will attempt to operate in a higher supersaturated mode than previously. This will be done by reducing the scrubber feed flow (bypass) and raising the inlet SO_2 concentration to a point where the pickup per pass is the same as in the base case. Test five will be run at a scrubber feed of pH 4.5. This will cause the scrubber liquor to be subsaturated with respect to calcium sulfite due to the shift to bisulfite. The pickup rate should be the same as previously. If not, the inlet SO_2 concentration can be changed to increase the driving force.

Tests six and seven will examine some of the effects of the hold tank. In line with the reasoning behind Tests two and three, Test six will use an agitator of steel rather than polypropylene. Test seven will reduce the agitator speed, again with a Variac.

The final test in Phase I, test eight will determine the effect of adding the scrubber bottoms, limestone additive and clarifier overflow at the same location. Recent work at LG&E with lime additive has shown a difference in crystal shape due to additive point changes. However, due to the size of the LG&E system, tight control of other variables was not possible.

After these tests are completed, the nucleation site should be defined. Based on the results obtained, the base case for Phase II (Test Nine) will consist of the operating conditions and variables which have yielded the lowest nucleation rate. This will enable changes in the particle size distribution to be more easily recognized in Phase II.

4.2 Phase II - Particle Size Distribution Correlation

Tests proposed for Phase II are given in Table 4-2 along with variable changes and estimated durations of each test.

At this point, analysis of Phase I data should indicate the major source of nucleation. The thrust of Phase II will be to correlate changes in process variables with the nucleation and growth rates. The equipment configuration and operating conditions for Phase II should reflect the lowest nucleation rate features of Phase I testing. An initial estimate on the equipment arrangement based on previous research (TI-006, KH-034) could be: polypropylene agitator, low mixing speed, rubber impellers, slow pump speed, and medium-high L/G ratio. This or another set of conditions, will form the base case for further testing. It can be seen that these conditions should tend to eliminate the mechanical sources of nucleation. This will improve the observation of different nucleation rates and simplify correlation of these changes with process variations. Four areas of testing are planned for Phase II:

TABLE 4-2. PHASE II - TEST SCHEDULE

Test #	Days	Objective	Variable Changed	Reason
9	5	Base Case[1]	'Best' configuration from Phase I	Future reference
10	5	Change number of crystals in system	5% solids, keep SO_2 pickup constant by raising inlet concentration	Determine effect of solids level on nucleation
11	5	Same as # 10	15% solids, keep SO_2 pickup constant by lowering inlet concentration	
12	5	Change scrubbing liquor quality	Low positive scrubbing liquor ($2M_g$ + Na - Cl)	Determine effect of liquor quality and nucleation and growth rates
13	5	Same as # 12	High positive liquor	
14	5	Same as # 12	Low negative liquor	
15	5	Same as # 12	High negative liquor	
	3	System purge		Eliminate high soluble species concentration
16	5	Add seed crystals	Grind 1% of clarifier underflow stream	Increase number of growth sites
17	5	Increase solids retention time to 16 hours	Increase hold tank size	Longer time for crystal growth
18	5 53	16-hour S.R.T. and grinding	Same as #16 and #17	Same as #16 and #17

(1) Base Case - Configuration from Phase I yielding lowest amount of mechanical nucleation.

1) percent slurry solids changes,

2) scrubbing liquor quality changes,

3) residence time variations, and

4) slurry grinding.

Slurry grinding is a proprietary Radian process which has been patented, stemming from work at the Sunbury SO_2 pilot unit (R/J-074-03).

Test 9 will be used as a base case for Phase II. As stated previously, the configuration will be the combination of parameters which produced the lowest nucleation rate in Phase I. Tests 9 and 11 will use 5 and 15% slurry solids levels, respectively. Changing the solids level will change the number of crystals in the system and also the supersaturation. By changing both of these parameters, the new size distribution is not easily predictable.

Tests 12 through 15 will examine the effect of scrubbing liquor quality on crystal size. In an equilibrium mixture, the anions and cations will balance leaving no residual electronegatively. By rearranging into sets of soluble and insoluble ion pairs, the following liquid phase groupings at pH 6 can be made: very soluble; magnesium, sodium and chloride, and slightly soluble;calcium, sulfite, sulfate, bicarbonate, and carbonate. If the net charge of the very soluble group is negative, i.e., high chloride levels, the other group must balance; i.e., high calcium level. This is a poor scrubbing liquor as the sulfite level is low, due to solubility constraints. If, on the other handthe very soluble group is positive, (e.g. high magnesium levels), the other grouping must have a net charge. This means higher sulfite levels. This sulfite provides extra alkalinity for scrubbing, hence, it is a good liquor. In order to determine quality, the sum of twice the magnesium level plus the sodium minus the chloride is evaluated in terms of moles per liter. The range of +.6 to -.6 is the proposed test band. Examples of these liquors could be 7300 ppm Mg^{++}, 0 ppm Na^{+} and Cl^{-} and 0 ppm Mg^{++} and Na^{+} and 21,000 ppm Cl^{-}. Many other possibilities also exist. Test 12 will have a low positive reading, Test 13 - high positive, Test 14 - low negative and Test 15 - high negative. Tests 14 and 15 may cause scaling in the scrubber. Frequent inspections should be made during these two tests. Following this set of tests, the system should be operated in an open loop configuration to purge the soluble species until their levels return to normal.

Test 16 will observe the effect of grinding a small portion of the clarifier underflow and returning these crystals to the hold tank. Mature sulfite crystals range from 15-50 microns. The grinder will process about one milliliter per minute of underflow. The grinder may produce new crystals by two mechanisms. The first is breakage of existing crystals. The second is production of secondary nuclei because of the extremely high energy dissapation rates. Levins et. al. (LE-305) has shown that as particle size decreases, the mass transfer coefficient between the liquid phase and solid surface increases. Other observations show larger particles growing faster than smaller ones. Further work in this area is needed to resolve this discrepancy.

Test 17 will utilize a longer residence time, approximately 16 hours. The longer residence time will provide more crystal growth opportunity, but will tend to decrease the supersaturation. Test 18 will combine the 16-hour residence time and ground crystals.

4.3 Phase III - Sludge Quality Optimization and Model Verification

Phase III of this test program will be based on analysis of the results from Phases I and II. The primary objective is to improve the quality of the sludge produced in limestone scrubbing systems. The other objective of this phase is to check the accuracy of the model developed by Radian for prediction of sludge quality.

Analysis of data from Phase II should show relationships between operational variations and sludge quality. Hopefully, these changes will fit a correlation. Phase III will use these correlations to produce a sludge of predetermined characteristics. By intermeshing chemical and process options, a scan of scrubber operations can be made. Ideally, the correlation will predict the resulting sludge product.

Obviously, at this time, a detailed description of Phase III tests is not possible. Analysis of Phase II data will show the effects of variables changed in that phase. The extent of variation will determine each parameter's importance to overall sludge quality.

Two months of testing are scheduled for Phase III. It is recommended that sufficient analysis be given to Phase II analysis before the system is restarted. A detailed list of parameter changes for each test should also be made prior to startup.

TABLE 4-3. PHASE III - TEST SCHEDULE

Test #	Days	Objective	Variable Changed	Reason
19,20	37	Optimize sludge quality	??	Primary objective of test plan

5.0 SAMPLING AND ANALYTICAL MEASUREMENTS

Proposed chemical analysis and sampling schedules are presented in this section. Two types of sample sets will be necessary for this test program. Line-out measurements will be taken to determine system stability after a change in operation has been made. After three or four solids residence times have elapsed and the line-out samples indicate steady-state has been reached, a full set of system characterization samples will be taken.

In this section, the two schedules are discussed and related to the test program objectives of Section 4.0. In addition, the sampling techniques required to obtain meaningful test results will be discussed.

5.1 System Characterization Measurements

A listing of system characterization sample points and required analysis is presented in Table 5-1. This table specifies the complete set of sample points and analyses required to perform an in-depth engineering evaluation of the tested scrubbing system. These samples will be gathered once the system has reached steady-state with respect to both solid and liquid phases. Base case testing will be duplicated to insure a reliable source of comparison with subsequent perturbations. In other cases, the operating conditions will be altered immediately after repeatable characterization sampling has occurred.

It should be noted that some deviation from the sampling schedule is expected during the test program. Not all of the analyses listed in the table will be performed for every sample point during every sampling period. Some of these deviations

TABLE 5-1. LIMESTONE SYSTEM CHARACTERIZATION MEASUREMENTS-SAMPLE POINTS AND ANALYSIS

Stream Name	Designation	#	Gas Analyses				Liquid Analyses							Solids Analyses							
			SO_2	O_2	CO_2	H_2O	Ca^{++}	Mg^{++}	Na^{++}	Cl^-	CO_2	SO_2	T.S.	% Solids	Ca	Mg	CO_2	SO_2	SO_3	PSD	Settling
Flue Gas	FG	1	x	x	x	x															
Stack Gas	SG	2	x			x															
Scrubber Feed	SCF	3					x	x	x	x	x	x	x	x	x	x	x	x	x	x	x
Scrubber Bottoms	SCB	4					x	x	x	x	x	x	x							$x^{(1)}$	
Clarifier Underflow	CLU	5					x	x	x	x	x	x	x	x	x	x	x	x	x	$x^{(1)}$	x
Clarifier Overflow	CLO	6					x	x	x	x	x	x	$x^{(2)}$	x						$x^{(2)}$	
Limestone (3) Additive	LA	7					x	x			x			x	x	x	x				
Makeup (3) Water	MW	8					x	x	x	x	x	x	x								

(1) PSD test will be discontinued if no difference is observed with SCF.

(2) Necessary only if % solids >.1%.

(3) Periodic sample sufficient.

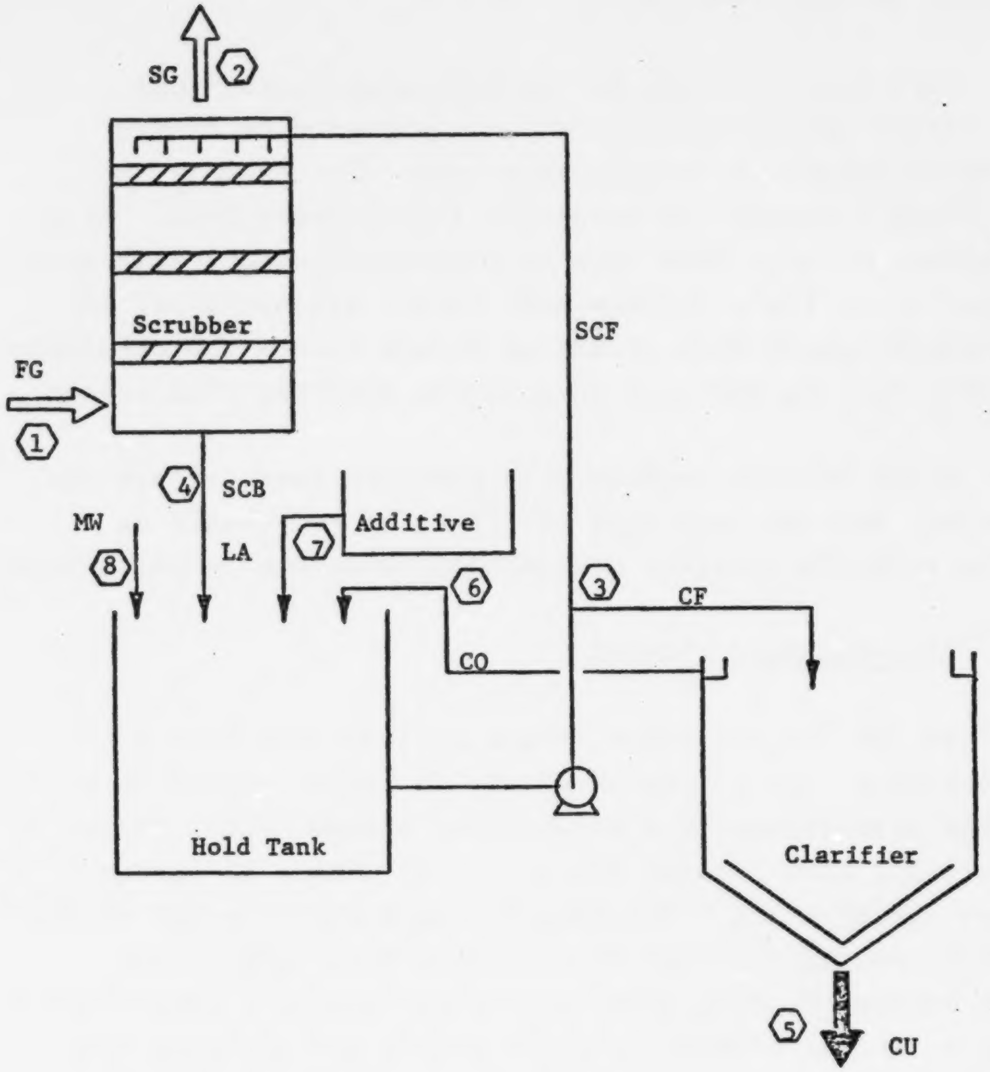
SG
2
Scrubber
SCF
FG
1
4
SCB
MW
Additive
8
LA
7
6
3
CF
CO
Hold Tank
Clarifier
5
CU

Figure 5-1. Limestone Flow Sheet.

are mentioned in the notes attached to the sampling schedules. Other cases are discussed below.

Some species, such as the magnesium, sodium and chloride liquor concentrations, are not expected to change significantly except in certain test runs. For example, no tests in Phase I should significantly affect these ions. As a result, these analyses need only be performed periodically during this phase. Also, these soluble salt levels are not expected to vary significantly from stream to stream within the scrubbing loop so they will be measured only in the scrubber feed stream.

Other streams needing only periodic sampling are the makeup water, and the limestone additive. These should be checked so accurate additive consumption rates can be calculated.

5.2 Line-Out Measurements

In the initial phase, these systems will have a solids residence time of approximately 10 hours. Based on a step change disturbance in a first order system, after three residence times have passed, the system is within 95 percent of its new steady-state. Allowing two days for line-out should therefore be sufficient with the original hold tank volume. Since the nature of these measurements is that of a monitoring function, a minimal number of sample points and analyses will be performed. The primary sample points will be the scrubber feed and the clarifier underflow. The liquid and solid phases from each stream should be similar in composition at steady-state. Table 5-2 lists the tests required for line-out of the limestone system.

TABLE 5-2. LIMESTONE LINE-OUT MEASUREMENTS

			Liquid Analyses							Solids Analyses						
Stream	Designation	#	Ca	Mg	Na	Cl	CO_2	SO_2	TS	Ca	Mg	CO_2	SO_2	TS	PSD	% Solids
Scrubber Feed	SCF	3	x	x				x	x	x	x		x	x	x	x
Clarifier Underflow	CLU	5	x	x				x	x	x	x		x	x	x	x

5.3 Sampling Frequency and Timing

With the original system volume, a test period should last three or four days. After a system perturbation, two days will be allowed for line-out. At the end of the second day (35-40 hours after start-up), a set of line-out samples will be taken. Upon analyzing the results, a decision will be made to take a characterization set the next day. If the results of the full set are judged satisfactory, change to a new test condition will be made. If not, the system will be reanalyzed the next day.

The recommended sampling sequence is given in Table 5-3. It should be noted that sample points 2, 3, and 4 are to be taken simultaneously. Ideally, the whole system should be sampled at the same time. Due to the volumes involved in the tanks, sequential sampling is acceptable. However, comparison between gas and liquid phase SO_2 depletion/pickup valves are meaningless if they are not taken at about the same time.

Once scrubber sampling is completed, the rest of the system can be sampled. A complete sample set should be collectable in 15-20 minutes. In this amount of time, minor process variations should not affect conditions in the various tanks.

TABLE 5-3. SAMPLE POINT DESCRIPTION AND SEQUENCE
(Limestone Systems)

Sample-Sequence	Sample Points Number	Sample Points Description
1	1	Flue Gas Inlet
2	2	Stack Gas Outlet
	3	Scrubber Feed
	4	Scrubber Bottoms
3	5	Clarifier Bottoms
4	6	Clarifier Overflow
5	(7)	Alkaline Additive
6	(8)	Makeup Water

( ) Indicates periodic sampling point

6.0 PROCESS MEASUREMENTS

In order to properly characterize scrubber systems, certain process measurements must be gathered in conjunction with the chemical analyses discussed in the previous section. These process measurements include such variables as slurry and liquor flow rates, gas flow rates, various tank levels and stream temperatures and pH's. Table 6-1 indicates which process measurements will be required for system characterization.

6.1 Flow Rates

Measurement of the scrubber feed rate is necessary for testing purposes. At present, this is done by measuring a tank level change over a time interval. Installation and calibration of a rotameter would simplify controlling the feed rate.

The gas flow is measured by a differential pressure cell attached to an orifice plate. Measurement of the SO_2 addition rate is performed by hourly weighing of supply gas cylinders. Due to the small flows involved, the remaining streams (limestone additive, clarifier feed, overflow and bottoms and makeup water) can be measured with a graduated cylinder.

6.2 Pressure Measurements

The pressure measurement required will be taken by the D.P. cell for gas flow determination.

6.3 Temperature Measurements

Table 6-1 indicates that every sampled stream should have a temperature measurement. Temperature is a required input to the equilibrium program. After continuous operation has

TABLE 6-1. PROCESS DATA REQUIREMENTS

Stream Name	Flow Rate	Pressure	SO_2 Conc.	pH	Temp
Gas					
Flue Gas (FG)	x	x	x		
Stack Gas (SG)			x		x
Liquid					
Scrubber Feed (SCF)	x	x		x	x
Scrubber Bottoms (SCB)				x	x
Clarifier Feed (CF)	x			x	x
Clarifier Overflow (CO)	x			x	x
Clarifier Underflow (CU)	x			x	x
Limestone Additive (LA)	x			x	x
Makeup Water (MW)	x			x	x

Vessel Level Data

Vessel	Level
Hold Tank	x
Additive Tank	x

been established, the variation in temperature may be deemed minor and readings taken only periodically.

6.4 Other Process Data

Various process data will be gathered on a routine basis during the test runs. Among these are gas inlet and outlet SO_2 concentrations (DuPont on-line analyzer readings), pH's and tank slurry levels. The DuPont readings should be checked manually occasionally to maintain reliability.

During sampling, the pH's of all the sampled streams will be recorded. This measurement will be taken: 1) to check on-line pH instrumentation for calibration purposes and 2) for use in the equilibrium program.

Tank levels will be recorded routinely. In combination with the water makeup rate, the slurry level will determine the magnitude of the system's water requirement. It is desirable from a system operation documentation standpoint for the water rate and tank levels to remain reasonably constant. With constant slurry volume conditions, changes in liquid or solid phase chemistry can be attributed to intended changes in system operation.

7.0 DATA HANDLING AND ANALYSES PROCEDURES

This section provides documentation of the data handling and analyses procedures that will be used during the test program. It includes specifications of chemical analyses to be performed, various sample and process log book formats, instructions for sample handling and computational formats for engineering calculations.

7.1 Chemical Analyses

Table 7-1 lists the analyses which need to be performed on the scrubbing systems. In order to generate all of the analyses listed in Table 7-1, as many as five different sample bottles may be needed at each sample point. One sample bottle will be used to collect slurry for a weight percent solids determination. The dry solids obtained will be used for further solids analyses. A second bottle (∿2 liters) will collect slurry for the settling test. The remaining three bottles will be used for filtered liquid phase analyses. Sulfite analyses will require a 125 ml bottle containing (1) a known volume of a standard iodine solution and (2) a sodium acetate buffer solution. Another filtrate sample (∿100 ml) will be collected in a sample bottle containing an EDTA-ammonium hydroxide buffer solution whenever liquid carbonate analyses are desired. The third filtrate sample (∿100 ml) will be caught in a sample bottle containing ∿50 mls of a dilute hydrogen perioxide solution. This sample will be used for the remaining liquid phase analyses.

Naturally, not all of the five sample bottles discussed above need to be filled for each sampling port. Only those sample which are required to obtain the data listed in Table 5-1 will be taken during a given test run.

TABLE 7-1. SCRUBBER SYSTEM CHEMICAL ANALYSES REQUIRED

Gas	Liquid	Solid
Sulfur Dioxide	Calcium	Calcium
Carbon Dioxide	Magnesium	Magnesium
Oxygen	Sodium	Carbonate
Water Vapor	Chloride	Sulfite
	Carbonate	Total Sulfur
	Sulfite	% Solids
	Total Sulfur	Particle Size Distribution
	Temperature	
	pH	Settling Tests

Using the analytical data specifications shown in Table 5-1 and the sample bottle requirements discussed above, Figure 7-1 was prepared to illustrate which sample bottles are required at each sample location. The requirements shown in Figure 7-1 are representative of full characterization sets. Sampling requirements for system line-out are obviously less severe than those indicated.

Generation of usable chemical analysis data requires (1) the use of proper sampling procedures, (2) the employment of accurate analytical methods, and (3) the evaluation and presentation of the resulting data. Each of these phases is detailed in subsections 7.1.1, 7.1.2, and 7.1.3 respectively.

7.1.1 Sample Handling Procedure

Considering the large volume of samples to be handled and analyzed after each test run, a variety of problems may arise if proper sample handling procedures are not followed. As many as thirty separate sample bottles may be needed for one characterization set alone. In this section, Radian's proposed approach to sample preparation, labeling, actual sample technique, and sampling logging is outlined.

7.1.1.1 Sample Bottle Preparation

Bottle preparation will depend on the type of sampling required (line-out, or characterization). For line-out samples, fewer bottles need preparing. The five different types of sample bottles will be processed according to the steps outlined in Table 7-2. In general, bottle "prep" will consist of attaching a label, adding the necessary reagents, and/or deionized water, weighing the bottle and recording necessary information. An example of the proposed label format is shown in Figure 7-2.

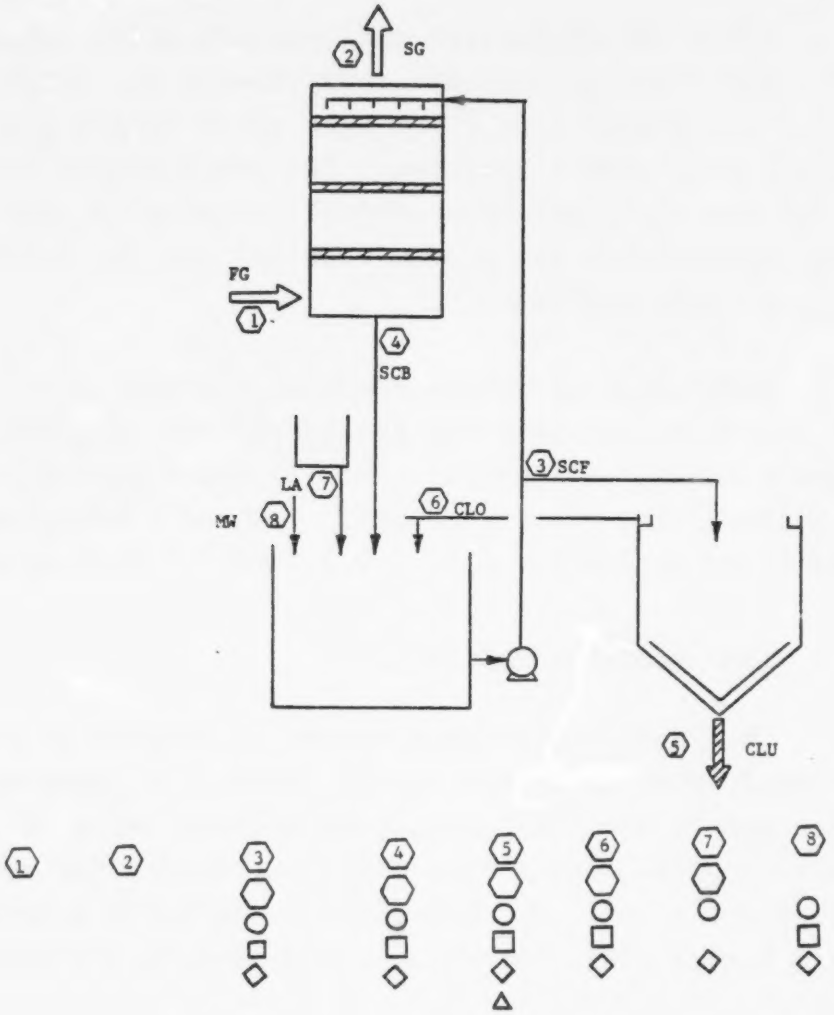
2
SG
FG
1
4
SCB
LA
7
MW
8
6
CLO
3
SCF
5
CLU
1
2
3
4
5
6
7
8

KEY:

⬡ Slurry (250 mls); Wt % Solids, Particle Size Distribution

○ Filtrate (100 mls); Ca, Mg, Na, Cl, T.S.

□ Filtrate (125 mls); SO$_3^=$

◇ Filtrate (100 mls); CO$_3^=$

△ Slurry (2 liters); Settling Test

Figure 7-1. Liquid and Solid Phase Chemical Sample Locations - Characterization Samples.

TABLE 7-2. SAMPLE HANDLING FLOW SHEET

Sample Description		Prepare Sample Bottles →	Sampling →	Log Collected Samples →	Sample Check
Slurry	Weight % Solids, P.S.D. -⬡-	(1) Attach proper label (2) Tare flask	(1) Collect 250 ml slurry (2) Record pH, temperature	(1) Log in master log book	Check to see that all required samples have been collected.
	Settling Test -△-	(1) Attach proper label	(1) Collect two liters slurry	(1) Log in master log book	
Filtrate	Liquid Species -○-	(1) Attach proper label (2) Tare bottle (3) Add Dilute H_2O_2 (4) Reweigh bottle	(1) Collect ~100 ml filtrate (2) Record time	(1) Log in master log book	
	Liquid Sulfite -□-	(1) Attach proper label (2) Add buffer (3) Add I_2 solution (4) Weight bottle with solution	(1) Collect filtrate until color change noted (do not pass end point).	(1) Log in master log book	
	Liquid Carbonate -◇-	(1) Attach proper label (2) Tare bottle (3) Add buffer (4) Reweigh bottle	(1) Collect 100 ml filtrate	(1) Log in master log book	

I.D. # x

Sample Type x

Dilution Factor o

Time ✓

pH ✓

Temperature ✓

Date x

Prepared by: x

o Full Weight

x Added Weight

x Tare Weight

x	Denotes information to be recorded during bottle prep
✓	Denotes information to be recorded during sampling
o	Denotes information to be recorded after sampling

Figure 7-2. Proposed Sample Label Format.

The designated symbols for the various types of sample bottles used in Table 7-2 are related to the required sample schedule shown in Figure 7-1. The total number of sample bottles prepared will be sufficient to fulfill the sampling requirements. A suitable number of spares should also be prepared.

7.1.1.2 Sampling Procedure

After the sample bottles have been prepared, the required samples must be gathered. A schematic of the sample collection apparatus is presented in Figure 7-3.

Once the apparatus has been set up, the sample port will be purged. The slurry sample and pH and temperature will then be taken. Purging of the filter will then be done, allowing ∿50 mls of filtrate to pass through. The liquid species, sulfite, and carbonate samples will then be taken. Finally, two liters of slurry will be collected for the settling test if necessary.

7.1.1.3 Sample Logging

Upon completion of the sample gathering, all samples will be taken to the laboratory for logging into the master log book. To keep a logical sequence of numbers, the following identification scheme is proposed. The I.D. number will contain the sample location point, month and date. As an example, the abbreviation for the scrubber feed is SCF. A sample taken on April 27th would then be identified by, SCF0427. If a second scrubber feed sample were taken, an additional letter could be added, SCF0427A. This method will simplify both labeling and log in procedures. A suggested format for the master log book is shown in Table 7-3. Other information deemed useful by on-site personnel may be incorporated in the master log book.

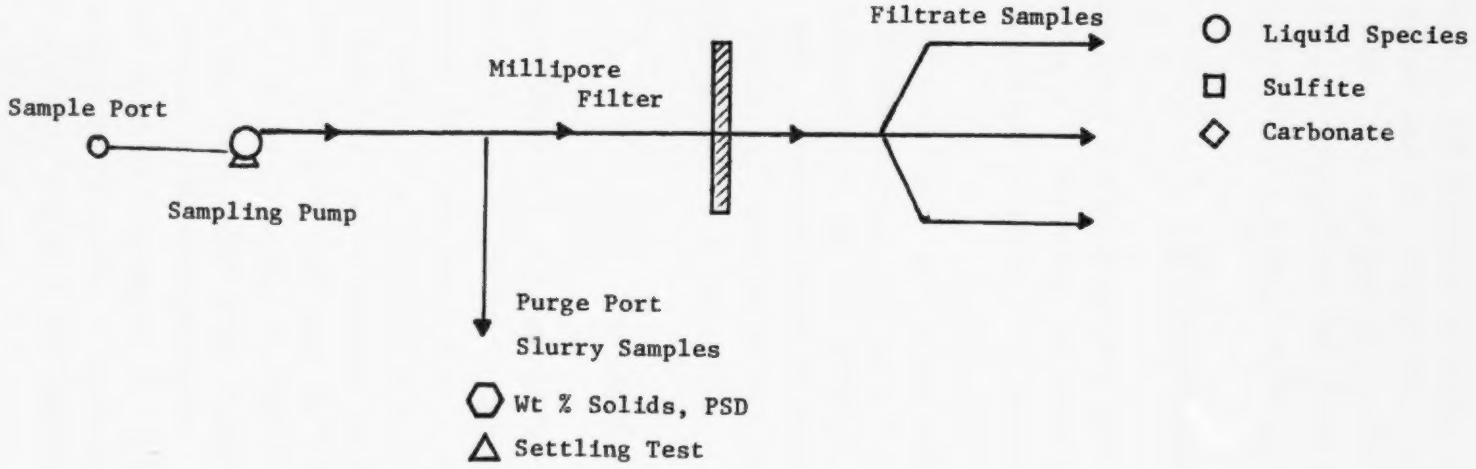
Sample Port
Sampling Pump
Millipore
Filter
Filtrate Samples
○ Liquid Species
□ Sulfite
◇ Carbonate
Purge Port
Slurry Samples
⬡ Wt % Solids, PSD
△ Settling Test

Figure 7-3. Sample Collection Schematic Diagram.

TABLE 7-3. PROPOSED MASTER LOG BOOK FORMAT

							Liquid Analyses (mmoles/ℓ)							Solid Analyses (mmoles/g)					Gas Analyses		
ID#	Description	Date	Time	pH	T°C	Dil. F.	Ca^{+2}	Mg^{+2}	Na^{+}	Cl^{-1}	CO_3^{-2}	SO_3^{-2}	T.S.	Ca^{+2}	Mg^{+2}	CO_3^{-2}	SO_4^{-2}	T.S.	SO_2 (ppm)	O_2 (%)	CO_2 (%)
SCF0427	FIL, SL	4/27/78	9:00	6.0	50																
SCB0427	FIL	4/27/78	9:05	4.5	52																
CLO0427	FIL	4/27/78	9:10	6.0	48																
CLU0427	FIL, SL	4/27/78	9:15	5.8	48																
LA0427	FIL, SL	4/27/78	9:20	10.0	25																
MW0427	FIL	4/27/78	9:20	7.0	25																

FIL - Filtrate

SL - Solids

Dil. F. - Dilution Factor

7.1.2 Analytical Procedures

Once the samples have been logged in, sample analyses will begin. This subsection deals with the recommended analysis procedures and the order of sample analysis. An introduction to proposed methods of checking data consistency is also furnished.

7.1.2.1 Gas Analyses

Gas phase analyses will use the following procedures. Sulfur dioxide determination will be made using the DuPont analyzer. Weekly calibration should be done by the Reich method. Oxygen and carbon dioxide will employ an Orsat apparatus and water vapor can be determined by either condensation or wet bulb/dry bulb procedure.

7.1.2.2 Liquid Analysis

⬡- Solids Content (Wt % Solids) Particle Size Distribution, Solids Analyses)....

The weight percent solids content of the circulating slurry will be monitored hourly by tracking the slurry density (weighing a known volume of slurry). Daily slurry samples will be filtered and the solids dried at 60°C. The dry solids will be further used for solid phase analyses. Using the weights of the bottle, slurry sample, and dried solids, the weight percent solids content of the slurry will be calculated to confirm the accuracy of the slurry density method.

○- Liquid Species....

Calcium, magnesium, and sodium will be determined by atomic absorption analyses. Chloride and total sulfur will be analyzed by a Dionex ion chromatograph.

◇ - Liquid Carbonate....

A nondispersive infrared technique will be employed for liquid phase carbonate determination. The samples are acidified and the carbonate is determined in the gas phase.

△ - Slurry Text....

Qualitative observations of sludge behaviour can be quickly determined by settling tests. By using a constant 3 percent slurry for all tests, comparison between test conditions can be made. This test should also be done at the same temperature each time. The dilutant should be filtered slurry liquor.

7.1.2.3 Solids Analyses

Chemical analyses of the solids will use the same methods as liquid analyses. The sample will first be dissolved in peroxide. To obtain a specific sulfate analysis, a sample will be purged with carbon dioxide in a hydrochloric acid mixture, and then analyzed on the Dionex. Solid carbonate will be analyzed by nondispersive I.R. techniques.

Particle size determinations will be done by either Coulter counter analysis, sedimentation methods, or some other technique which gives accurate results.

Also scanning electron micrographs (SEM) should be taken for each test condition. At magnifications of 500X, 1000X, and 3000X, these provide a method for quick qualitative comparison of crystal sizes and shapes.

7.1.2.4 Analytical Consistency Checks

As a routine procedure, the data for each sample location will be checked for analytical consistency. Liquid phase results will be checked by performing equilibrium calculations. The Radian aqueous ionic equilibrium program is capable of generating relative saturations and a percent residual electronegativity. Past Radian experience has indicated that data which show errors of less than 5% are characteristic of a consistent set of chemical analyses. Certainly a residual electronegativity in excess of 20% is unreasonable. Repeat analyses will be performed on any sample when this is felt to be justified. These calculations and their implications to the test program will be discussed in more detail in Section 7.3.

Periodic repetition of different analyses will be performed as a general rule throughout the test program. This duplication of analyses will document the reproducibility of the analytical results.

7.1.3 Data Handling and Presentation

Analytical results will be reported in formats similar to those shown in Table 7-4 (Liquid Anaytical Results) and 7-5 (Solid Phase Analytical Results). These results will be presented in this manner so that engineering evaluations and calculations can be easily performed.

The results sheets, in combination with the sample log book entries, will allow on-site personnel to determine which samples need further processing and which analyses are complete.

TABLE 7-4. RESULTS OF LIQUID PHASE ANALYSES

Scrubber System ____________

Test # ________

Date ________

			Total Concentration (mmol/liter)										
Sample Designation	Temp. (C°)	pH	Ca	Mg	Na	Sulfite	Sulfate	Total S	Carbonate	Chloride	$CaSO_3$ RS	$CaSO_4$ RS	% Charge Imbalance

Prepared by: ______

TABLE 7-5. RESULTS OF SOLID PHASE ANALYSES

Scrubber System____________________

Test #________________________ Date___________

				Total Concentration (mmol/gram)			
Sample Designation	% Solids in Slurry	Ca	Mg	Carbonate	Specific Sulfite	Specific Sulfate	Total Sulfur

Prepared by:___________

7.2 Process Measurements

Enough process measurements will be taken to fulfill the requirements discussed in Section 6.0 and listed in Table 6-1. Process measurement data for each sample set will be documented on forms similar to those shown in Table 7-6. While the pH and temperature of all sampled streams are considered process measurements, they will not be listed on this form. Temperature and pH data will be gathered at the time of sampling, and convenience dictates that they be recorded on the appropriate diluted filtrate sample bottle.

The process data gathered at the time of sampling will be checked to insure that the data are sufficient (1) to document system performance and (2) to enable important process rates to be quantified. The process measurement documentation table (Table 7-6) should facilitate this procedure.

7.3 Process Calculations

In this section the procedures which will be used to interpret the analytical and process performance data gathered by the techniques just discussed are reviewed. Two general types of activities are covered here. The first level of analysis which is required will be primarily concerned with a confirmation of the consistency of the analytical results. This activity, and a proposed method is discussed in Section 7.3.1.

The second level of data analysis is concerned with the interpretation of test results. This activity will be the responsibility of the on-site personnel. It will include all computational activities required (1) to monitor the day to day test conditions and (2) to interpret overall test results. This aspect is discussed in Section 7.3.2.

TABLE 7-6. PROCESS MEASUREMENT DOCUMENTATION

Scrubber System_______________ Date____________

Test #

FLOW RATE DATA

Stream	Flow Rate	Units
Flue Gas (FG)		Nm^3/sec
Scrubber Feed (SCF)		LPM
Scrubber Bottoms (SCB)		LPM
Clarifier Feed (CLF)		LPM
Clarifier Overflow (CLO)		LPM
Clarifier Underflow (CLU)		KGPM
Limestone Additive (LA)		LPM
Makeup Water (MW)		LPM

PRESSURE DATA

Stream	Pressure	Units
Flue Gas (FG)		Centimeters H_2O vacuum
Stack Gas (SG)		Centimeters H_2O vacuum

LEVEL MEASUREMENT DATA

Vessel	Level (Centimeters from Reference)
Scrubber Bottoms	
Hold Tank	
Additive Tank	

OTHER MEASUREMENTS

Inlet SO_2 Concentration = _______________ppm

Outlet SO_2 Concentration = _______________ppm

Hold Tank pH = _______________

Slurry Density = _______________Wt % Solid

Underflow Density = ____________Wt % Solid

7.3.1. Analytical Consistency Confirmation

Vapor-liquid and liquid-solid mass transfer reactions in an SO_2 scrubbing system are generally very slow compared to the rates at which ionic reactions in the liquid phase take place. It is therefore reasonable to treat the liquid phase in an SO_2 scrubber as an equilibrium mixture.

Analysis of liquid phase equilibrium data involves many interacting equations which can best be solved by computer. Radian has developed an aqueous ionic equilibrium program which is capable of predicting liquid phase activities of the various ionic species found in a typical scrubber liquor. Inputs required by the program include total liquid phase concentrations of sodium, calcium, magnesium, sulfite, sulfate, carbonate, and chloride, and also the solution pH and temperature. Program outputs include (1) liquid phase activities and activity coefficients, (2) equilibrium partial pressures of SO_2 and CO_2 above the liquid phase, (3) relative saturations of potential precipitating species, and (4) a calculated value for residual electroneutrality, a measure of the solution charge imbalance which is indicative of the consistency of the analytical input data. A typical equilibrium program output sheet is shown in Table 7-7. The interpretation and utilization of these output results are discussed below.

After all of the required liquid phase analyses for a given sample are completed, the solution pH and temperature (determined at the time that the samples are taken) and its composition will be input to the Radian equilibrium program. The program output sheet will then be examined to determine whether the residual electroneutrality figure is within tolerable limits. They will be done by dividing the charge imbalance

TABLE 7-7. TYPICAL EQUILIBRIUM PROGRAM PRINTOUT

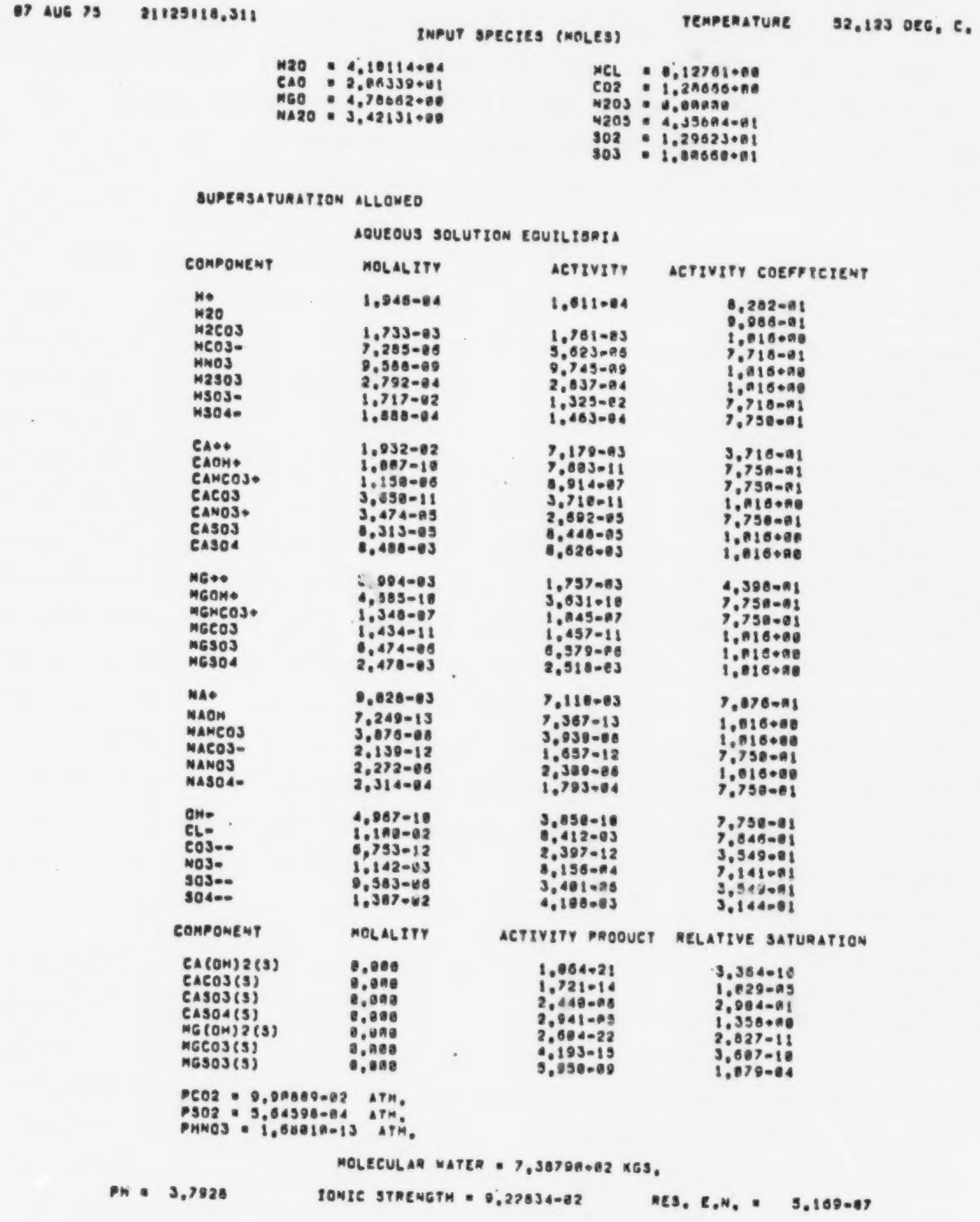

```
07 AUG 75    21:25:18,311                                    TEMPERATURE    52,123 DEG. C.
                                     INPUT SPECIES (MOLES)

                     H2O  = 4,10114+04                   HCL  = 0,12761+00
                     CAO  = 2,06339+01                   CO2  = 1,20656+00
                     MGO  = 4,78662+00                   N2O3 = 0,00000
                     NA2O = 3,42131+00                   N2O5 = 4,35604-01
                                                         SO2  = 1,29623+01
                                                         SO3  = 1,80660+01

              SUPERSATURATION ALLOWED

                             AQUEOUS SOLUTION EQUILIBRIA

             COMPONENT             MOLALITY             ACTIVITY     ACTIVITY COEFFICIENT

              H+                   1,946-04             1,611-04          8,282-01
              H2O                                                         9,986-01
              H2CO3                1,733-03             1,761-03          1,016+00
              HCO3-                7,285-06             5,623-06          7,718-01
              HNO3                 9,588-09             9,745-09          1,016+00
              H2SO3                2,792-04             2,837-04          1,016+00
              HSO3-                1,717-02             1,325-02          7,718-01
              HSO4-                1,888-04             1,463-04          7,750-01

              CA++                 1,932-02             7,179-03          3,716-01
              CAOH+                1,007-10             7,803-11          7,750-01
              CAHCO3+              1,150-06             8,914-07          7,750-01
              CACO3                3,650-11             3,710-11          1,016+00
              CANO3+               3,474-05             2,692-05          7,750-01
              CASO3                8,313-05             8,446-05          1,016+00
              CASO4                8,488-03             8,626-03          1,016+00

              MG++                 3,994-03             1,757-03          4,398-01
              MGOH+                4,685-10             3,631-10          7,750-01
              MGHCO3+              1,348-07             1,045-07          7,750-01
              MGCO3                1,434-11             1,457-11          1,016+00
              MGSO3                6,474-06             6,579-06          1,016+00
              MGSO4                2,478-03             2,518-03          1,016+00

              NA+                  9,028-03             7,110-03          7,876-01
              NAOH                 7,249-13             7,367-13          1,016+00
              NAHCO3               3,876-08             3,939-08          1,016+00
              NACO3-               2,139-12             1,657-12          7,750-01
              NANO3                2,272-06             2,309-06          1,016+00
              NASO4-               2,314-04             1,793-04          7,750-01

              OH-                  4,967-10             3,850-10          7,750-01
              CL-                  1,100-02             8,412-03          7,646-01
              CO3--                6,753-12             2,397-12          3,549-01
              NO3-                 1,142-03             8,156-04          7,141-01
              SO3--                9,583-06             3,401-06          3,549-01
              SO4--                1,307-02             4,108-03          3,144-01
             COMPONENT             MOLALITY        ACTIVITY PRODUCT  RELATIVE SATURATION

              CA(OH)2(S)           0,000                1,064-21          3,364-10
              CACO3(S)             0,000                1,721-14          1,029-05
              CASO3(S)             0,000                2,440-06          2,904-01
              CASO4(S)             0,000                2,941-05          1,358+00
              MG(OH)2(S)           0,000                2,604-22          2,827-11
              MGCO3(S)             0,000                4,193-15          3,607-10
              MGSO3(S)             0,000                5,950-09          1,079-04
              PCO2 = 9,00889-02  ATM.
              PSO2 = 5,64598-04  ATM.
              PHNO3 = 1,60010-13  ATM.

                             MOLECULAR WATER = 7,38790+02 KGS.

        PH =  3,7928         IONIC STRENGTH = 9,27834-02       RES. E.N. =   5,169-07
```

by the total ionic strength in the analyzed sample. From previous Radian experience, a 5% or less error indicates reasonable analytical consistency. If the error is judged to be too great, some of the analyses may be repeated.

A second analytical consistency check may be used for the scrubber effluent streams. The equilibrium SO_2 pressure above the exiting slurry effluent streams will be compared to the measured SO_2 partial pressure in the stack gas. If the measured stack gas SO_2 concentration does not exceed the calculated SO_2 equilibrium partial pressure above the upper bed downcomer, a gas phase or liquid phase analytical error is indicated, and the analytical data will be re-examined.

The equilibrium printout also specifies relative saturations (r) for the various solids which may form in a scrubbing [illegible]ids of major interest are calcium sulfite and [illegible] The relative saturations calculated from the most recently gathered data will provide the basis for quick estimations of current relative saturations during on-site testing. (A method of quick relative saturation estimation is discussed in detail in Section 7.3.2.) System relative saturation levels can be used as a measure of the scaling potential of a given scrubbing liquor. Since previously untried operating conditions will be attempted during the test program, reasonably accurate relative saturation estimation procedures are vital to the conduct of the tests. Should critical supersaturation levels be approached in the scrubbing loop system, operating parameters must be altered as necessary. Calculated relative saturations will be compared to both estimated relative saturations and to information obtained from periodic visual scrubber inspections.

The liquid phase activities computed by the equilibrium program will be useful in the detailed evaluations to be performed at the conclusion of the on-site testing. For example, it may be possible to correlate sulfate ion activity with the sulfate to sulfite ratio of the coprecipitated solids. Also, the activities of chloride and magnesium may provide insight into the effects of these ions on the coprecipitation phenomenon.

7.3.2 On-Site Calculations

The on-site engineering staff will be responsible for all calculations required to interpret the test results and to monitor the daily performance of the system. At a minimum, this function will include process rate determinations, calcium sulfite and sulfate relative saturation estimates, and process variable tracking. Any additional calculations required for results interpretation or for determination of test program direction will also be performed on-site.

7.3.2.1 Process Rate Calculations

A detailed discussion of proposed methods and assumptions involved in calculating the important process rates is presented in Section 3.0. Basicially, the significant chemical reactions include the vapor-liquid and solid liquid reactions in the scrubber and the solid-liquid reactions in the holding tank system. By employing the assumptions and calculation procedures presented in Section 3.0, typical worksheets have been prepared for determination of the hold tank and scrubber chemical reaction rates as well as the particle distribution and the crystal growth rate. These example worksheets are shown in Tables 7-8, 7-9, and 7-10. The calculations will be made as soon as the necessary data become available.

TABLE 7-8. SCRUBBER RATE CALCULATION WORK SHEET

Gas Streams	Flow Rate (acfm) (G)	Temp. (°F) (T)	SO_2 Concentration (ppm) (y)	SO_2 Flow Rate (g-moles/min)$^{(1)}$
Inlet:				
Flue Gas (FG)				
Outlet:				
Stack Gas (SG)				

		Aqueous Species Concentrations (mg/ℓ)				Species Flow Rates (g-moles/min)			
Liquor Streams	Flow Rate (ℓ/min) (L)	(C_{Ca})	(C_{SO_2})	(C_{SO_3})	(C_{CO_2})	$Ca^{(2)}$	$SO_2^{(3)}$	$SO_3^{(4)}$	$CO_2^{(5)}$
Inlet:									
Scrubber Feed (SCF)									
Outlet:									
Scrubber Bottoms (SB)									

$$SO_2 \text{ Sorption Rate} = \sum_{in} SO_2(g) - \sum_{out} SO_2(g)$$

$$\text{Sulfite Oxidation Rate*} = \left[\frac{SO_3(s)}{SO_3(s) + SO_2(s)}\right]_{\text{Leaving System}} \times SO_2 \text{ Sorption Rate}$$

$$CaSO_3 \text{ Dissolution Rate} = \sum_{out} SO_2(aq) - \sum_{in} SO_2(aq) + \text{Sulfite Oxidation Rate*} - SO_2 \text{ Sorption Rate}$$

$$CaSO_4 \text{ Dissolution Rate} = \sum_{out} SO_3(aq) - \sum_{in} SO_3(aq) - \text{Sulfite Oxidation Rate*}$$

$$CaCO_3 \text{ Dissolution Rate**} = \sum_{out} Ca(aq) - \sum_{in} Ca(aq) - CaSO_3 \text{ Dissolution} - CaSO_4 \text{ Dissolution}$$

---

(1) SO_2 Gas Flow Rate (g-moles/min) $= \left\{(G) \times \left[\frac{520}{(T) + 460}\right] \times \frac{454 \text{ g-moles}}{379 \text{ scf}} \times \frac{y}{10^6}\right\}$

(2) Aqueous Ca Flow Rate (g-moles/min) $= \left\{(L)(C_{Ca}) \times \left(\frac{\text{g-moles Ca}}{4\text{x}10^4 \text{ mg Ca}}\right)\right\}$

(3) Aqueous SO_2 Flow Rate (g-moles/min) $= \left\{(L) \times (C_{SO_2}) \times \left(\frac{\text{g-moles } SO_2}{6.4\text{x}10^4 \text{ mg } SO_2}\right)\right\}$

(4) Aqueous SO_3 Flow Rate (g-moles/min) $= \left\{(L) \times (C_{SO_3}) \times \left(\frac{\text{g-moles } SO_3}{8.0\text{x}10^4 \text{ mg } SO_3}\right)\right\}$

(5) Aqueous CO_2 Flow Rate (g-moles/min) $= \left\{(L) \times (C_{CO_2}) \times \left(\frac{\text{g-moles } CO_2}{4.4\text{x}10^4 \text{ mg } CO_2}\right)\right\}$

* During early phases of the test program all system oxidation will be assumed to occur in the scrubber. If the actual scrubber oxidation can be quantified in later tests, this difference will be accounted for.

** Calcium carbonate dissolution rate will be calculated assuming all of the $Ca(OH)_2$ dissolves in the hold tank.

TABLE 7-9. HOLD TANK RATE CALCULATION WORK SHEET

Liquor Streams	Flow Rate (ℓ/min) (L)	Aqueous Species Concentrations (mg/ℓ)				Species Flow Rates (g-moles/min)			
		(C_{Ca})	(C_{SO_2})	(C_{SO_3})	(C_{CO_2})	$Ca^{(1)}$	$SO_2^{(2)}$	$SO_3^{(3)}$	$CO_2^{(4)}$
Inlet:									
Scrubber Bottoms (SB)									
Outlet:									
Scrubber Feed (SCF)									

$$CaSO_3 \text{ Precipitation Rate}^* = \sum_{in} SO_2(aq) - \sum_{out} SO_2(aq)$$

$$CaSO_4 \text{ Precipitation Rate}^* = \sum_{in} SO_3(aq) - \sum_{out} SO_3(aq)$$

$$CaCO_3 \text{ Precipitation Rate}^{**} = \sum_{in} CO_2(aq) - \sum_{out} CO_2(aq)$$

$$Ca(OH)_2 \text{ Dissolution} = \sum_{out} Ca - \sum_{in} + CaSO_3 \text{ Precipitation Rate} + CaSO_4 \text{ Precipitation Rate} + CaCO_3 \text{ Precipitation Rate}$$

NOTE: Several small streams (clarifier and filter effluents for example) may be neglected when performing hold tank balances because the liquid species flow rates for these are insignificant compared to the stream flows listed above.

---

(1) Aqueous Ca Flow Rate (g-moles/min) $= \left\{(L) \times (C_{Ca}) \times \left(\frac{\text{g-moles Ca}}{4\text{x}10^4 \text{ mg Ca}}\right)\right\}$

(2) Aqueous SO_2 Flow Rate (g-moles/min) $= \left\{(L) \times (C_{SO_2}) \times \left(\frac{\text{g-moles } SO_2}{6.4\text{x}10^4 \text{ mg } SO_2}\right)\right\}$

(3) Aqueous SO_3 Flow Rate (g-moles/min) $= \left\{(L) \times (C_{SO_3}) \times \left(\frac{\text{g-moles } SO_3}{8.0\text{x}10^4 \text{ mg } SO_3}\right)\right\}$

(4) Aqueous CO_2 Flow Rate (g-moles/min) $= \left\{(L) \times (C_{CO_2}) \times \left(\frac{\text{g-moles } CO_2}{4.4\text{x}10^4 \text{ mg } CO_2}\right)\right\}$

* These balances are made assuming negligible oxidation in the hold tank. The balances will be modified should the hold tank oxidation be quantified.

** The carbonate precipitation rate is made assuming no desorption of CO_2 from the hold tank liquor.

TABLE 7-10. PARTICLE CALCULATION SHEET

$$\dot{N} = CU \times N \cong \dot{n}_o$$

$$R_{small} = \frac{-1}{\tau \frac{\Delta \log n}{\Delta L (2.303)}} \qquad (<4\mu)$$

$$= \frac{-1}{\frac{600 \text{ min } (3.3-9.4)}{4\text{x}10^{-6}(2.303)}} = 2.5\text{x}10^{-9} \text{ meter/min}$$

$$R_{large} = \frac{-1}{\frac{600(1-3.3)}{36\text{x}10^{-6}(2.303)}} = 6.0\text{x}10^{-8} \text{ meter/min} \qquad (>4\mu)$$

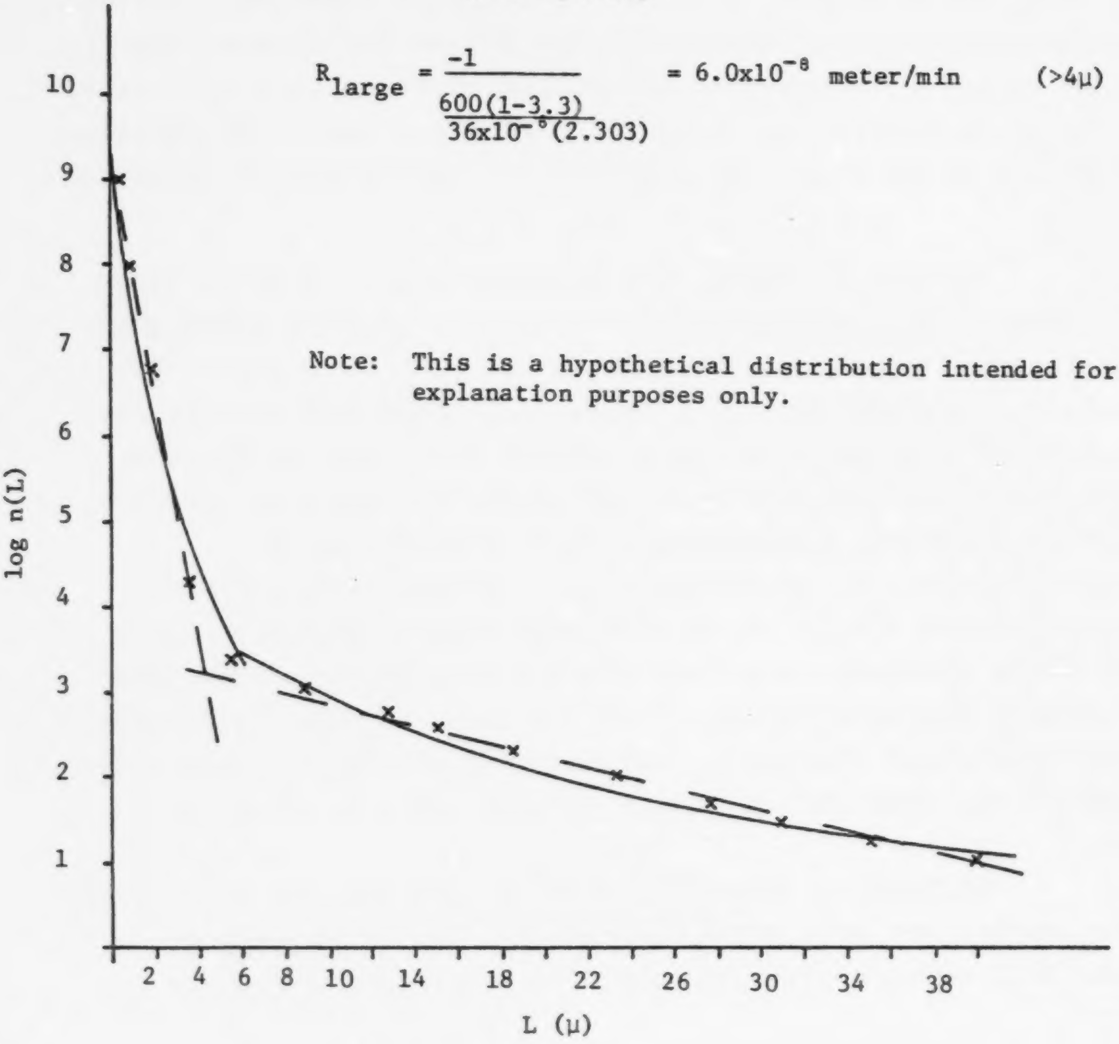

Note: This is a hypothetical distribution intended for explanation purposes only.

7.3.2.2 Relative Saturation Estimates

Relative saturation levels are important parameters influencing crystal growth. For most tests, a constant level will be desired. Therefore, a quick method of estimation or daily computer predictions will be required. The following is a method for estimation using liquid species analyses. A quick turnaround on the chemical analyses for this determination (calcium, total sulfur, sulfite, temperature, and ionic strength) will be required. An approximate technique for determining system relative saturations should therefore be developed prior to the start of the test program by making a series of equilibrium runs which cover the regions of expected system operation.

On-site estimates for supersaturation will be based on a simplified treatment of perturbations about a given solution to the full set of chemical equilibrium equations. Periodically, complete sets of process data could be input to the equilibrium computer routine at Radian or a similar program. These data will include the temperature, pH, calcium, sulfite, sulfate, chloride, magnesium, sodium, and carbonate concentrations. Since the magnesium, sodium, and chloride, concentrations should normally change very slowly with time, reasonably accurate estimates of supersaturation can be made based upon measured values of pH, calcium, sulfite, and sulfate. These quantities can all be conveniently obtained within a few hours of the time that a sample is taken at a given point.

Estimating techniques for calcium sulfate and sulfite supersaturations will differ somewhat. The solubility of $CaSO_4 \cdot 2H_2O$ depends primarily on the temperature and ionic strength of the liquor as well as the amount of magnesium present. Its solubility is not very sensitive to pH changes which can occur in a limestone scrubbing unit. In most cases, it should be possible to estimate the sulfate supersaturation by simply using the ratio of the measured and "base case" concentration products for total calcium (Ca) and total sulfate (SO_3). That is,

$$\underset{CaSO_4(s)}{r(\text{estimated})} \approx \underset{CaSO_4(s)}{r(\text{base case})} \times \frac{m_{Ca}m_{SO_3}(\text{measured})}{m_{Ca}m_{SO_3}(\text{base case})} \qquad (7\text{-}1)$$

Base case calculations should be run at several temperatures to provide a basis for interpolation. Temperatures in the system should not vary substantially with time, however.

Estimates of calcium sulfite supersaturations may prove more difficult. These will be quite sensitive to pH in addition to temperature, ionic strength, and magnesium content. The fraction of total sulfite that is in the form of sulfite ion may change by several orders of magnitude over the pH range 5-7.

A semi-empirical form for estimating calcium sulfite supersaturations may be developed by considering the equilibria involving the sulfite ion. The most important of these are:

$$K_1 = \frac{a^2_{H^+}\, a_{SO_3^=}}{a_{H_2SO_3(\ell)}} \qquad (7\text{-}2)$$

$$K_2 = \frac{a_{H^+} \, a_{SO_3^=}}{a_{HSO_3^-}} \qquad (7\text{-}3)$$

$$K_3 = \frac{a_{Ca^{++}} \, a_{SO_3^=}}{a_{CaSO_3(\ell)}} \qquad (7\text{-}4)$$

$$K_4 = \frac{a_{Mg^{++}} \, a_{SO_3^=}}{a_{MgSO_3(\ell)}} \qquad (7\text{-}5)$$

An additional relationship is the total sulfite (SO_2) material balance for the liquid phase given by Equation 7-6.

$$m_{SO_2} = m_{H_2SO_3(\ell)} + m_{HSO_3^-} + m_{CaSO_3(\ell)} + m_{MgSO_3(\ell)} + m_{SO_3^=} \qquad (7\text{-}6)$$

A simultaneous solution to Equations 7-2 through 7-5 yields an approximate expression for the sulfite ion activity in terms of the measured quantities of total SO_2 and pH. Some simplifications are needed to arrive at this expression, however. First, the activity coefficients of all species in Equations 7-2 through 7-5 will be held constant over the range of solution composition covered by the approximation. These equations can then be written in terms of concentrations:

$$K_1' = \frac{a_{H^+}^2 \, m_{SO_3^=}}{m_{H_2SO_3(\ell)}} \qquad (7\text{-}7)$$

$$K_2' = \frac{a_{H^+} \, m_{SO_3^=}}{m_{HSO_3^-}} \qquad (7\text{-}8)$$

$$K_3' = \frac{m_{Ca^{++}} \, m_{SO_3^=}}{m_{CaSO_3(\ell)}} \tag{7-9}$$

$$K_4' = \frac{m_{Mg^{++}} \, m_{SO_3^=}}{m_{MgSO_3(\ell)}} \tag{7-10}$$

Two additional variables may be eliminated by treating the calcium and magnesium ion concentrations as constants. This should be a reasonable approximation since percentage variations in calcium and magnesium concentrations in the system are known to be quite small compared to changes in total SO_2 concentration. Thus,

$$K_3'' = \frac{m_{SO_3^=}}{m_{CaSO_3(\ell)}} \tag{7-11}$$

$$K_4'' = \frac{m_{SO_3^=}}{m_{MgSO_3(\ell)}} \tag{7-12}$$

Equations 7-6, 7-7, 7-8, 7-11, and 7-12 can now be combined to yield the final expression.

$$m_{SO_3^=} = \frac{m_{SO_2}}{\frac{1}{K_1'} a_{H^+}^2 + \frac{1}{K_2'} a_{H^+} + (1 + \frac{1}{K_3''} + \frac{1}{K_4''})} \tag{7-13}$$

Equation 7-13 may be used to compare the sulfite concentration (or activity if the activity coefficient is assumed constant) at one level of pH and total SO_2 to that at another. The constants must be evaluated from the base case computer solutions. The following terms are included:

$$K_1' = \frac{K_{H_2SO_3(\ell)}\ \gamma_{H_2SO_3}}{\gamma_{SO_3^=}} \qquad (7\text{-}14)$$

$$K_2' = \frac{K_{HSO_3^-}\ \gamma_{HSO_3^-}}{\gamma_{SO_3^=}} \qquad (7\text{-}15)$$

$$K_3'' = \frac{K_{CaSO_3(\ell)}\ \gamma_{CaSO_3(\ell)}}{a_{Ca^{++}}\ \gamma_{SO_3^=}} \qquad (7\text{-}16)$$

$$K_4'' = \frac{K_{MgSO_3(\ell)}\ \gamma_{MgSO_3(\ell)}}{a_{Mg^{++}}\ \gamma_{SO_3^=}} \qquad (7\text{-}17)$$

where $K_{H_2SO_3(\ell)}$, $K_{HSO_3^-}$, $K_{CaSO_3(\ell)}$, and $K_{MgSO_3(\ell)}$ are functions of temperature.

Finally the estimated calcium sulfite supersaturation may be taken as the base case supersaturation times the ratio of the measured and base case concentration products:

$$\underset{CaSO_3(s)}{r(\text{estimated})} = \underset{CaSO_3(s)}{r(\text{base case})}\ \frac{m_{Ca}m_{SO_3^=}(\text{measured})}{m_{Ca}m_{SO_3^=}(\text{base case})} \qquad (7\text{-}18)$$

In Equation 7-18, the total calcium concentration, m_{Ca}, is measured directly and the sulfite ion concentration,

$m_{SO_3^=}$, is obtained using Equation 7-13 along with measured values for m_{SO_2} and pH. The base case values for input to these equations will be periodically updated. It should be noted here that this estimation will not be adequate during certain tests when the magnesium and chloride levels are changed. Rapid analytical turnaround with subsequent use of the Radian equilibrium program will probably be required to track relative saturation during this phase.

7.3.2.3 Process Variable Monitoring

Various system parameters will be monitored to assess scrubbing system operation on a day-to-day basis. At a minimum, pH's, flows, and circulating solids density will be tracked. Gas flows and SO_2 concentrations should be monitored hourly to insure steady-state operation. By monitoring these and possibly other variables, their impact upon test results can be properly interpreted.

7.4 Monthly Progress Reports

Once a month a detailed report should be submitted to describing the status of the project and to report the findings of the previous month's tests. A monthly operations summary will involve the preparation of figures similar to those shown in Figure 7-4, 7-5, and 7-6. Included in this graphical summary will be (1) test performed and date, (2) daily average SO_2 concentrations and ranges, (3) average SO_2 removal efficiency, (4) scrubber feed and scrubber bottoms pH, (5) slurry solids concentration and (6) dissolved solids concentration.

In addition, Table 7-11 will be presented in the monthly progress report. This sheet specifies process condi-

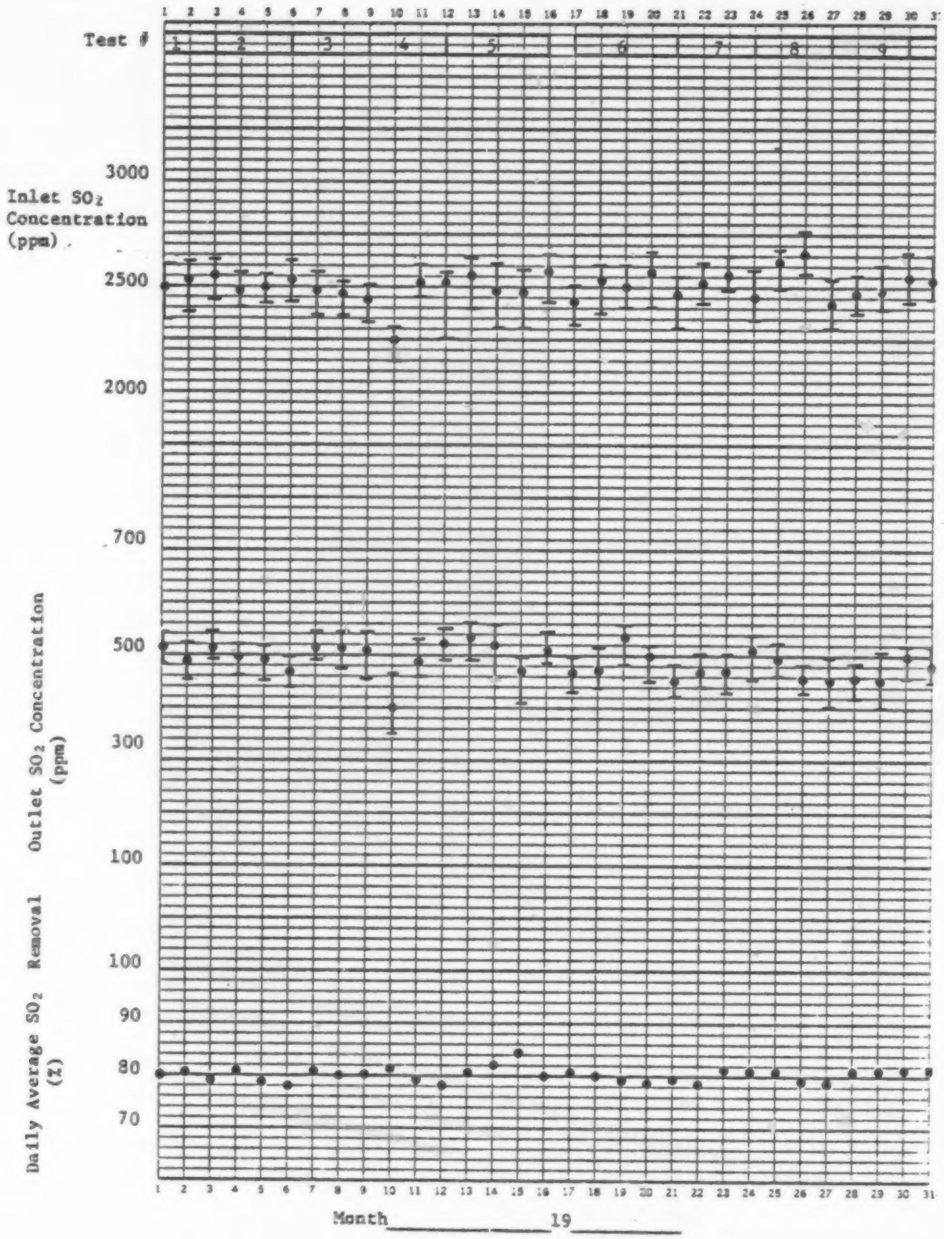

Figure 7-4. RTP Monthly Operating Log.

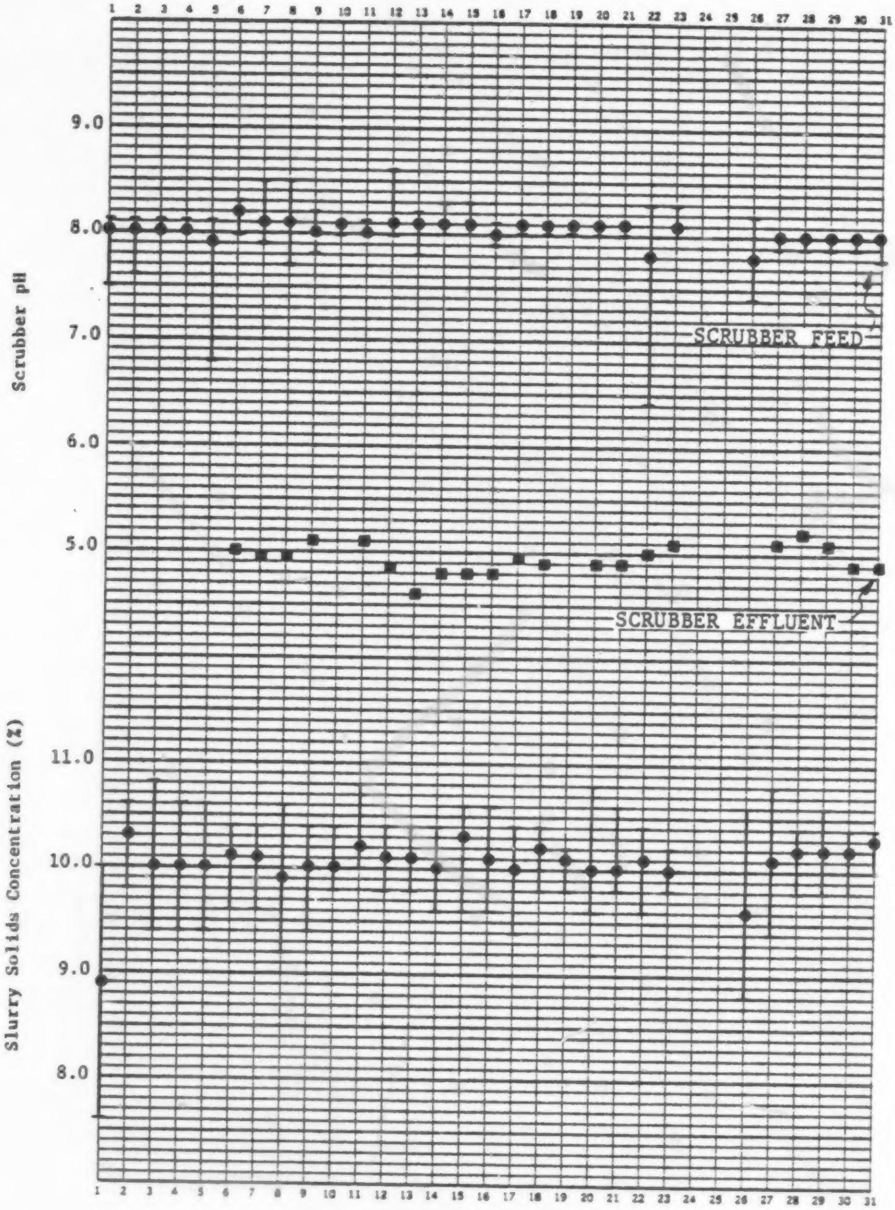

Month ________ 19________

Figure 7-5. RTP Scrubbing Liquor Parameters.

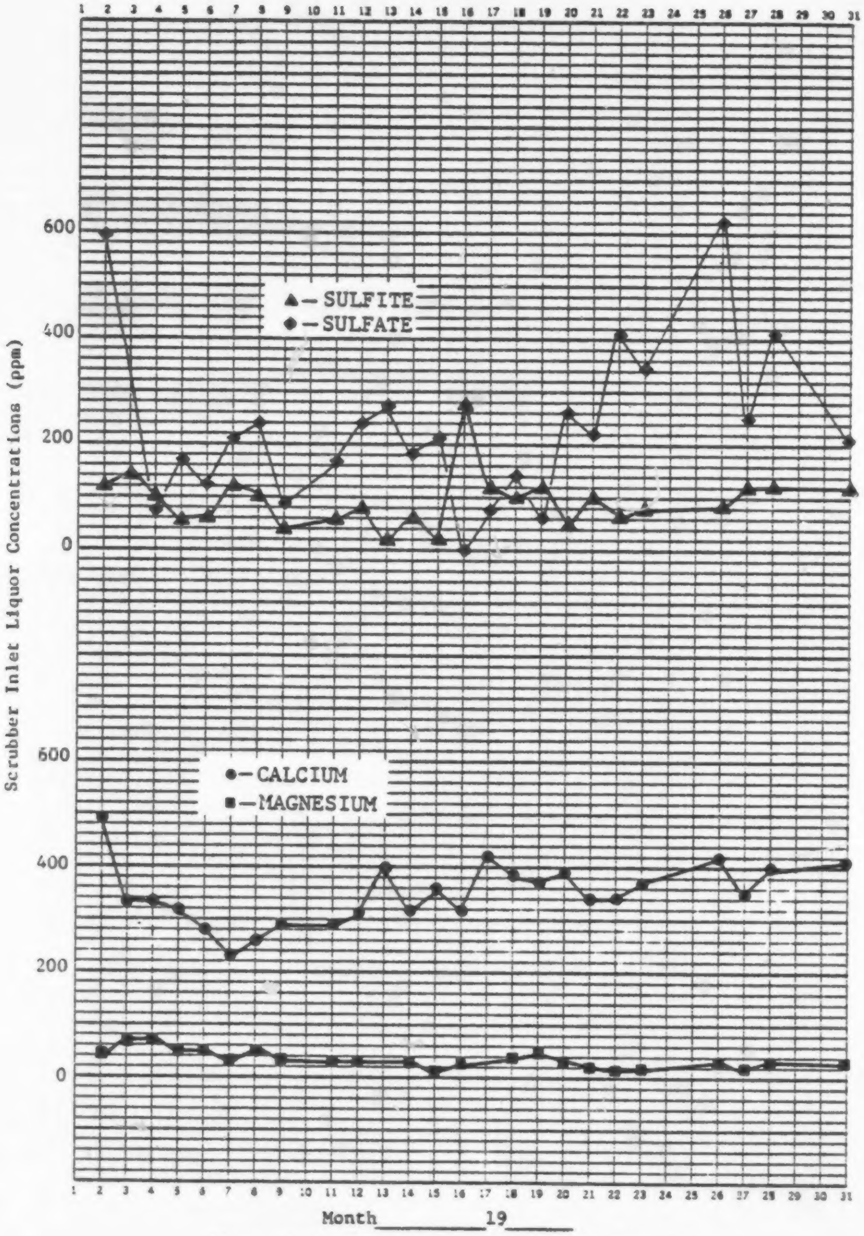

Figure 7-6. RTP Dissolved Solids Concentrations.

TABLE 7-11. OPERATING DATA SUMMARY

Prepared by______________

Date:								
Time:								
Test No.:								
Sample Set No.:								
System Operating Time (hrs):								
GAS PHASE MEASUREMENTS								
Gas Flow Rate (10^3 acfm)								
ΔP Across Scrubber (inches H_2O)								
Inlet SO_2 Concentration (ppm):	DuPont Analyzer							
	Manual Analyzer							
Outlet SO_2 Concentration (ppm):	DuPont Analyzer							
	Manual Analyzer							
SO_2 Removal Efficiency (%)								
LIQUID/SOLID PHASE MEASUREMENTS								
Flow Rates (gpm):	Scrubber Feed							
	Scrubber Bottoms							
	Clarifier Feed							
	Combined Clarifier and Filter Overflows							
	Filter Bottoms							
	Limestone Additive							
	Make-Up Water							
Level Measurements:	Scrubber Bottoms							
	Additive Tank							
	Reaction Tank							
Circulating Slurry Solids Content (% weight)								
Filter Bottoms Solids Content (% weight)								
Percent Oxidation								
Hold Tank Effluent (pH)								
STOICHIOMETRY [Moles $CaCO_3$ Added/Moles SO_2 Sorbed]								
L/G (gal/scf)								

COMMENTS:

tions at the time of each characterization test. Comments on operating anomalies or difficulties will be noted as they occur. The more significant operating problems will be discussed in detail in the progress report.

Completed chemical analysis results will also be presented in monthly progress letters. The resulting data will be compiled on forms similar to Table 7-4 and 7-5. These results should include the computed electroneutrality imbalance generated by an equilibrium program.

A calculations summary will be furnished for each characterization set. A proposed format is shown in Table 7-12. In addition, the relative saturations data will also be documented in this table. Figure 7-7 will be used to plot the particle size distribution analysis for the various tests. Transparent overlays could be made to provide easy comparison of different test results.

Brief discussions of each test will be given in these reports among with an interpretation of the results. Should the results of one test affect the scope of the program or suggest possible test program alterations, these options will be documented.

TABLE 7-12. CHEMICAL REACTION CALCULATION SUMMARY

Scrubber System____________ Date____________

Test No.__________ Prepared by____________

	Scrubber	Hold Tank
Reaction Rate (g-moles/min):		
SO_2 Sorption		
Oxidation		
Calcium Sulfite Precipitation		
Calcium Sulfate Precipitation		
Calcium Carbonate Precipitation		
Calcium Hydroxide Dissolution		
Effluent Relative Saturations*:		
$CaSO_3$		
$CaSO_4$		

Particle Size Distribution:

Nucleation Rate (#/sec)	
Growth Rate (Large)(M/sec)	
Growth Rate (Small)(M/sec)	

---

* Based on equilibrium program output data.

FIGURE 7-7

PARTICLE SIZE DISTRIBUTION

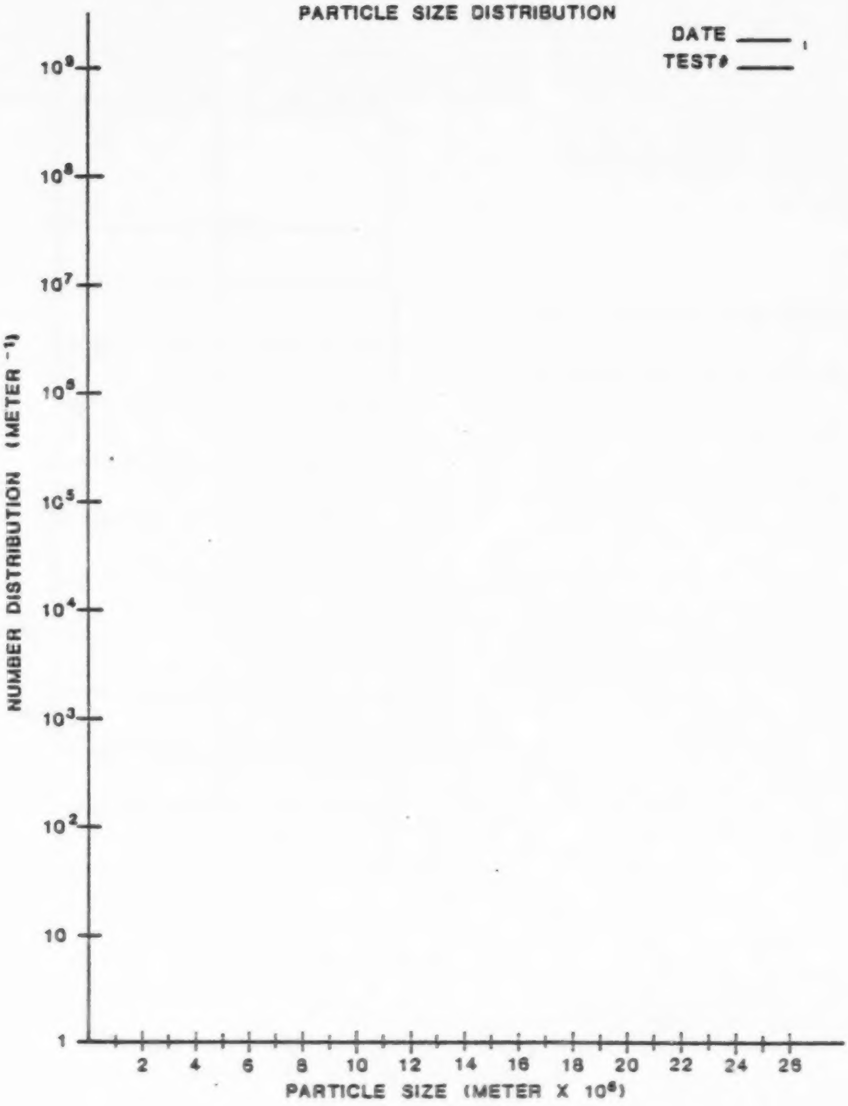

DATE ____

TEST# ____

02-2346-1

8.0 POSSIBLE PROBLEM AREAS

This section furnishes a discussion of several areas in which difficulties may be encountered during the execution of the test program. Three general areas where problems may be discovered are addressed: 1) system operation, 2) process and analytical measurements, and 3) engineering analysis.

8.1 System Operation

Several aspects of system operation which may have an impact upon test results are discussed in this section.

8.1.1 Effect of Unsteady-State Operation

It would be ideal if each of the proposed system tests could be conducted under specified "steady-state" conditions. Realistically, it is reasonable to expect that fluctuations in process conditions will occur.

One possible fluctuation is in the SO_2 inlet concentration. Small changes will not seriously affect scrubber conditions, however, if a large change is noted, the rate should be readjusted and two hours allowed for the scrubber chemistry to stabilize.

The reason for allowing a stabilization period, is that for a change in the SO_2 concentration will change the system pH. This will affect the limestone additive and alter the chemical composition of the scrubbing liquor. Any sample taken during this period would not be representative of the overall test conditions.

If significant changes are observed in the SO_2 concentration or slurry tank levels during sampling, a repeat sample should be taken to insure accurate results are obtained.

8.1.2 Recommended Operating Conditions

Several system configurations and operating conditions have been proposed in the test plan that are different from the base case arrangement. Operation in these modes should not be difficult, however, some potential sources of problems are discussed in general below.

8.1.2.1 Solids Concentration Changes

Several tests are planned at varied solids levels or concentration. At the lower level, the clarifier will have to settle particles faster in order to remove the same amount of solids. No major problem is envisioned, due to the small size of the pilot unit and the available extra capacity of the vacuum filter.

The higher solids level should not provide any major problems either. Over a longer term, erosion might increase, but for a week long test, no difficulty is foreseen.

8.1.2.2 Hold Tank Modifications

Various modifications to the hold tank system have been proposed. Different agitator materials and speeds are planned along with moving the additive location. Increased residence time is also planned. None of these changes should cause any operational problems.

8.2 Measurement Problems

Readily apparent problems with the required measurements for the test plan are discussed in this section.

8.2.1 Analytical Problems

Standard chemical analyses of scrubber streams has been done for quite some time. Accurate, reliable, and quick methods of chemical analysis are fairly well standardized. At the present time, the particle size distribution measurement is the least developed. Reproducibility between microscopic, scanning electron microscopy and Coulter counter analysis has not been fully demonstrated. Please see Technical Note #200-187-11-02 for a description of Radian's recommended method for determination of the particle size distribution.

8.2.2 Process Measurements

No major problem is seen in the obtaining of process measurements. The scrubbing facility has been operated for several years, and as a research facility, accurate measurement recording procedures were incorporated in its design.

8.2.3 Steady-State Determination

System steady-state determinations are a key to obtaining reliable test results in a minimum amount of time. Due to the nature of the tests in this document, solid phase line-out is essential for meaningful results. By assuming that the hold tank is a continuous stirred tank reactor, the solid phase residence time can be modeled as a first order system. For a step change in a process variable in a first order system, 95% of the new effect is attained within three residence times. Based on a ten-hour solids residence time, two days of continuous operation should be sufficient to insure steady-state conditions. Analytical tests required to insure steady-state conditions are given in Section 5.2.

8.3 Engineering Analysis

As part of the overall engineering analysis effort, rates of important chemical reactions, crystal growth and nucleation will be calculated. A discussion of the methods of calculation is presented in Section 3.0. These rates will be used in relating the particle size distribution to operating parameters. In any correlation effort, exact agreement between the assumed function and experimental data is unexpected. Hopefully with accurate process and analytical measurements, the derived correlations will closely model the physical situation.

9.0 SUMMARY

The basic objectives of the test program are to:

- develop quantitative relationships between calcium sulfite particle size distribution and process variables, and
- using the computer model developed by Radian, determine conditions for producing an optimum sludge product.

To accomplish these objectives, tests will be conducted to:

- locate the source of nucleation in the scrubbing system,
- correlate growth and nucleation rates with process parameters, and
- determine if computer predicted test conditions produce the optimum sludge.

NOMENCLATURE

a - Chemical Activity

CF - Clarifier Feed (liters/sec)

cm - Centimeters

CLO - Clarifier

CLU - Clarifier Underflow (liters/sec)

FG - Flue Gas Rate (m^3/hr)

G - Particle Generation Term other than growth and convection (ℓ^{-1} sec^{-1})

g - gram

h - Experimental Exponent

i - Experimental Exponent

j - Experimental Exponent

k_1, k_2, k_3 - Undetermined exponents

K_1, K_2, K_3, K_4 - equilibrium constants

kg - Kilogram

k_r - Surface Reaction Rate Constant (m^2/sec)

k_v - Shape Factor

L - Characteristic Particle Length (m)

ℓ - Liters

LA - Limestone Additive Rate (ℓ/sec)

$\bar{L}_m$ - Mass Average Length (m)

$\bar{L}_n$ - Number Average Length (m)

m - Meters

m_i - moles of specie i

m_s - Calcium Sulfite Coprecipitate Solids Concentration (g/ℓ)

MW - Molecular Weight (g/mole)

N - Number of Particles per Slurry Volume (ℓ^{-1})

n - Number of Particles of Size L per Volume (ℓ^{-1} m^{-1})

$\dot{N}$ - Number of Particles of Size L per Volume Leaving System ($\ell^{-1}m^{-}$ sec^{-1})

n_o - Nuclei Concentration (ℓ^{-1})

$\dot{n}_o$ - Nucleation Rate (ℓ^{-1} sec^{-1})

p - Experimental Exponent

Q - Volumetric Flow Rate (ℓ/sec)

R - Linear Crystal Growth Rate (m/sec)

R_o - Crystal Growth Rate at Zero Size (m/sec)

r - Relative Saturation

SCB - Scrubber Bottoms Flow Rate (ℓ/sec)

SCF - Scrubber Feed Flow Rate (ℓ/sec)

SG - Stack Gas Flow Rate (m^3/hr)

ΔSO_2 - SO_2 Pickup (moles/sec)

T - Temperature (K°)

$\bar{u}_i$ - Slurry Velocity in the ith direction (m/sec)

V - Slurry Volume (ℓ)

X - Length Dimension (m)

Y - Length Dimension (m)

Z - Length Dimension (m)

γ - activity coefficient

δ - Growth Constant (m^{-1})

ρ_s - Particle Density (g/cm)

τ - Mean Solids Residence Time (sec)

μ - Micron (10^{-6}m)

REFERENCES

JO-R-214 Jones, Benjamin F., Philip S. Lowell, and Frank B. Meserole, *Experimental and Theoretical Studies of Solid Solution Formation in Lime and Limestone SO_2 Scrubbers*, final report, EPA 600/2-76-273a EPA Contract No. 68-02-1883, Radian Project No. 200-144, Austin, Texas, Radian Corp., Oct. 1976.

KH-034 Khamskii, Evgenii V., *Crystallization from solutions*, New York, Consultants Bureau, 1969.

LE-305 Levins, D.M., and J.R. Glastonbury, "Particle-liquid hydrodynamics and mass transfer in a stirred vessel", 2 pts, *Trans. Inst. Chem. Engrs.* 50, 32 (1972), pt.1; *Trans. Inst. Chem. Engrs.* 50, 132 (1972), pt. 2.

LO-R-170 Lowell, Philip S., "Process Removing Sulfur Dioxide from Gases", *U.S. Patent 3,972,980* (Aug. 1976).

OT-023 Ottmers, D. M., Jr., et al., *A Theoretical and Experimental Study of the Lime/Limestone Wet Scrubbing Process*. PB 243-399/AS, EPA 650/2-75-006. Contract No. 68-02-0023. Austin, Tx., Radian Corp., 1974.

TI-006 Ting, H.H. and W.L. McCabe, "Supersaturation and Crystal Formation in Seeded Solutions", *I&EC 26, 1201-7 (1934)*.